Tarabay Antoun

Currently, nuclear explosion monitoring relies on semi empirical models to discriminate explosions from earthquakes and to estimate key parameters, such as explosive yield. While these models have been highly successful in monitoring established test sites, there is concern that future tests could occur in media and at scaled depths of burial outside of the domain of empirical observations. The goal of SPE is to replace these semi empirical relationships with numerical techniques that are grounded in a physical basis and thus applicable to any geologic setting or depth of burial. The LLNL efforts are focused on developing source-to-sensor modeling capabilities and on elucidating the physical mechanisms responsible for the observed behavior. This is accomplished through the development and application of 3D fully coupled near field and far field modeling capabilities, and analysis and interpretation of multivariate SPE shock and seismic data.

Souheil Ezzedine

We have performed 3D simulations of underground explosions conducted recently in granitic outcrop as part of the Source Physics Experiment (SPE) campaign. The main goal of these simulations is to understand the nature of the shear motions recorded in the near field under condition of uncertainties in a) the geological characterization of the joints, such as density, orientation and persistency and b) the geomechanical material properties, such as friction angle, bulk sonic speed, poro-elasticity etc. The approach is probabilistic; joints are depicted using a Boolean stochastic representation of inclusions conditional to their probability density functions inferred from borehole data. Then, using a novel continuum approach, joints and faults are painted into the continuum host material, granite. To insure the fidelity of the painted joints we have conducted a sensitivity study on the numerical depiction of joints. Simulating wave propagation into heterogeneous discontinuous rock mass is highly non-linear problem and uncertainty propagation via intrusive methods is practically forbidden. Therefore, using a series of nested Monte Carlo simulations, we have explored and propagated both the geological and the geomechanical uncertainty parameters using a Bayesian sampling approach. We have probabilistically shown that significant shear motions can be generated by sliding on the joints caused by spherical wave propagation. Polarity of the shear motion may change during unloading when the stress state may favor joint sliding on a different joint set. Although this study focuses on understanding shear wave generation in the near field, the overall goal of our investigation is to understand the far field seismic signatures associated with shear waves generated in the immediate vicinity of an underground explosion. Using a filtering technique, we have abstracted the near field behavior into a probabilistic source-zone model that can be used in the far field wave propagation study.

Sean Ford

Comparison of two standard explosion models with each other and with new results from the Source Physics Experiments (SPE) demonstrate that the models are in substantial agreement for large and normally buried explosions, consistent with much of the historic data collected during American and Soviet nuclear testing. However for small and/or deeply buried explosions like SPE, the predictions of the two models can differ significantly.

Analysis of the low-frequency seismic data for a simple model of the SPE explosions, known as a seismic moment tensor, reveal the size and character of the events. The events easily identify as explosions, though the shear energy is inconsistent with the model of a simple explosion. We find no single non-explosive source that can fit the observed shear energy, which is consistent with a more complicated source.

Small changes in the near-source medium can be monitored with an interferometric technique using observations of the seismic coda. This technique is suited for investigations of the damage due to SPE-2 and illuminated by SPE-3. The coda-wave observations of SPE-2 and -3 show that any damage was limited to a small region less than 5 meters in radius, consistent with direct observation from drillback operations.

Spall is the heaving of near-surface material during an explosion and can offer insight to late-time damage, a phenomenon that may have implications for yield estimation. We analyze the spall records of SPE and compare them with standard models. The SPE observations compare favorably and confirm that the spall contribution to observations is small compared to the explosion component.

Rob Mellors

Three aspects of the Source Physics Experiment are presented: electromagnetic measurements (EM), body wave amplitudes at local distances, and velocity model estimates using correlation methods. The EM measurements were made near the shot point at distances of 60 and 90 m for SPE2 using three-component magnetometers and at closer distances for SPE3. A possible EM signal was recorded for SPE3 at a distance of 25 m. These measurements, as well as future measurements, may serve to illuminate the EM signals associated with chemical explosions.

The use of high-frequency body wave amplitudes at local distances is explored as a tool to distinguish between the SPE explosions and local earthquakes. The method appears effective, but some nearby stations show anomalous effects that may be due to lateral variations in seismic velocities.

Correlation methods are used to construct velocity models of the subsurface centered on the SPE source point. The analysis yields results that are comparable to velocity models developed using alternate methods such as active source, surface wave dispersion, and borehole measurements. A shallow low velocity zone is evident on all models on the granite bedrock but the thickness and velocity variations vary laterally. A large effort using ambient noise correlation is underway to characterize the SPE testbed and involves approximately 8000 paths between station pairs. This will yield a high resolution 3D model.

Arben Pitarka

The objective of our work is the improvement of our understanding of the excitation and propagation of seismic waves, from underground explosions and shallow earthquakes. The main subjects of our ongoing investigation are the generation of shear-waves, propagation of seismic energy at local and regional distances, and development of numerical techniques for simulating ground motion from underground explosions using physics based source models for different emplacement conditions.

We performed analysis using SPE3 synthetics and observed far-field waveforms recorded by five linear arrays of stations within 10 km of the shot point, and a small array of stations located in the Yucca Flat, with a 2km epicentral distance. Analysis of the small array data in the frequency-wave number domain, and investigation of particle motion in the complex domain allowed us to determine the origin and the kind of far-field waves recorded during the explosion.

We presented an overview of our investigation results. We tested the efficiency of our local three-dimensional velocity model and our numerical scheme that uses threeâ€“dimensional hydrodynamic methods, coupled with an anelastic wave propagation finite-difference method to model the explosion source and ground motion recorded at far-field stations. The best source models that fit the recorded shear and compressional near-field motion, and a calibrated 3D local velocity model, were used to evaluate the sensitivity of wave propagation near the source region to source process, including spall and source-region fracture network, underground structure, high frequency wave scattering, and surface topography. In particular, we focused on the contribution of these effects to S-wave generation and P/S amplitude ratio in the modeled frequency range of 0.1-8Hz.

Oleg Vorobiev

This work is focused on analysis of near-field measurements (up to 100 m from the source) recorded during Source Physics Experiments in a granitic formation (the Climax Stock) at the Nevada National Security Site (NNSS). One of the main goals of these experiments is to investigate the possible mechanisms of shear wave generation in the nonlinear source region. SPE experiments revealed significant tangential motion (up to 30 % of the radial) at many locations as well as azimuthal variations in radial velocities which cannot be generated by a spherical source in isotropic materials.

Understanding the nature of this non-radial motion is important for discriminating between the natural seismicity and underground explosions signatures. Possible mechanisms leading to such motion include, but not limited to, heterogeneities in the rock such as joints, faults and geologic layers as well as surface topography and vertical motion at the surface caused by material spall and gravity. We have performed a three dimensional computational studies considering all these effects. Both discrete and continuum methods have been employed to model heterogeneities. In the discrete method, the joints and faults were represented by cohesive contact elements. This enables us to examine various friction laws at the joints which include softening, dilatancy, water saturation and rate-dependent friction. Yet this approach requires the mesh to be aligned with joints, which may present technical difficulties in 3D when multiple non-persistent joints are present. In addition, the discrete method is more computationally expensive since the contact faces may move and create new contacts while encountering new opposite faces.

When the joints are stiff and other effects such dilatancy, softening, rate-dependency etc.) can be neglected, the continuum method can be applied. In this approach, the joints are treated as plane material weaknesses and are imbedded into the computational elements. The advantage of this approach is that it does not require either sophisticated meshing algorithms or contact detection algorithm, thus alleviating the computational burden. It is also suitable for evaluating the bounds of possible shear motion due to uncertainties in the joints distribution. Details of this uncertainty quantification study are presented in a separate abstract.

In the present work using both the continuum and the discrete approaches we study the effects of the surface spall, in-situ stress and joint orientation on the observed near-field motion. Three dimensional numerical simulations are performed for different burial depths and yields to investigate scalability of both radial and shear motions. The motion calculated in the near-field is then propagated into a far field. Results of the far field study are presented in an accompanied work (Pitarka et al.).

Overview of the LLNL SPE R&D and Analysis Activities

Tarabay Antoun

William R. Walter, Sean R. Ford, Stephen C. Myers, Michael E. Pasyanos, Arben Pitarka, Oleg Vorobiev, Lew Glenn, Souheil Ezzedine, Robert J. Mellors, Arthur J. Rodgers, Stanley D. Ruppert, Teresa Hauk, Eric Matzel, Moira Pyle and Doug Dodge

Lawrence Livermore National Laboratory

State of Analysis Review

22 August, 2013

This work was performed under the auspices of the U.S. Department of Energy by Lawrence Livermore National Laboratory under Contract DE-AC52-07NA27344. Lawrence Livermore National Security, LLC

Seismic monitoring is currently a semi empirical science

- The best monitoring is where there are regional calibrations
  - Capability degrades to teleseismic level away from the calibrations
  - Some areas of interest do not have calibration
- NEED: the capability to predict the observed signal from an arbitrary source for an arbitrary receiver
  - Three Dimensional Earth Model
  - Source model that predicts P- and S-wave excitation
- Current numerical simulation capability does not yet explain all the past nuclear data including
  - Generation of S-waves (including Love and reversed Rayleigh waves)
  - Effects of media and emplacement conditions on seismic waves

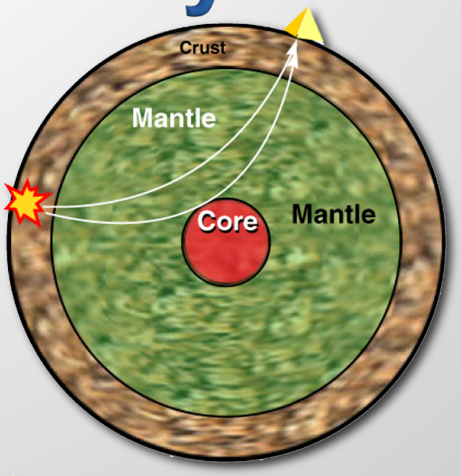

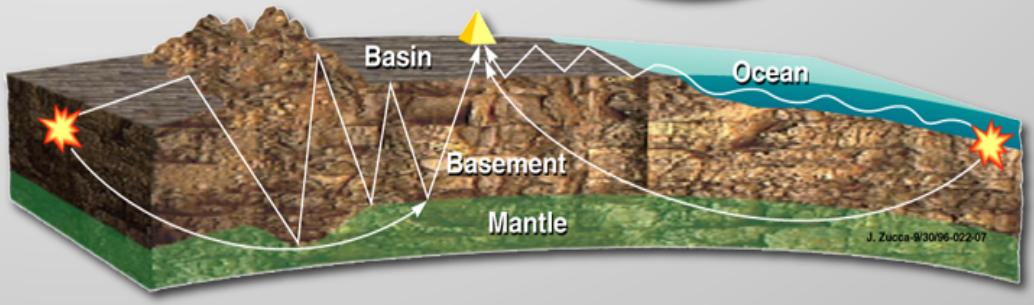

Source Physics Experiments at NNSS will provide critical data to develop predictive capabilities for low-yield nuclear test monitoring

Based on historic testing we have a good empirical understanding of ID algorithms but lack physics-based predictable models

Earthquake

Shear slip on a plane

S-wave energy dominates

Strong Love waves

Rayleigh & P-wave radiation pattern

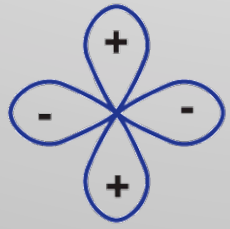

$m_b \sim M_s$

P/S < 1

Double-couple

$$\begin{pmatrix} 0 & 0 & 1 \\ 0 & 0 & 0 \\ 1 & 0 & 0 \end{pmatrix}$$

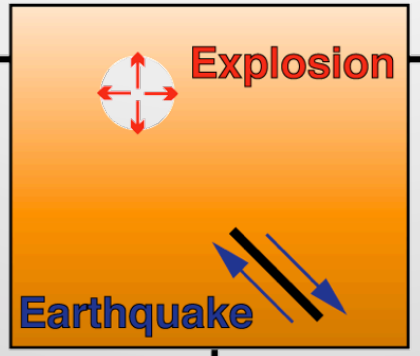

Explosion

Pressure pulse on a sphere

P-wave energy dominates

No Love waves

Constant Rayleigh & P pattern

$m_b > M_s$

P/S > 1

Isotropic

$$\begin{pmatrix} 1 & 0 & 0 \\ 0 & 1 & 0 \\ 0 & 0 & 1 \end{pmatrix}$$

The monitoring community does not currently have an accepted model for explosion S-wave generation

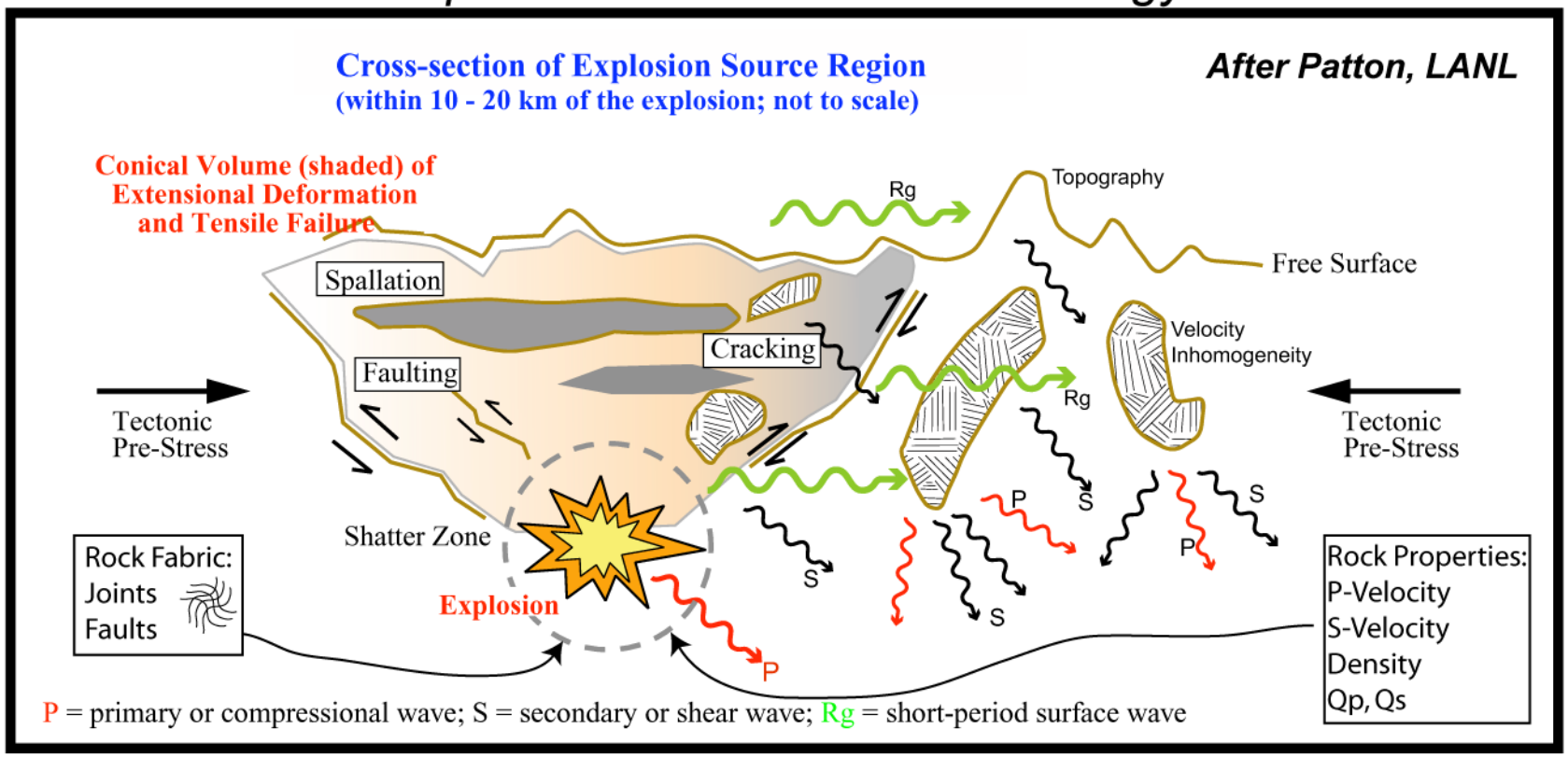

Many potential sources but no quantifiable physics-based model

The SPE is a bridge from current test site empirically-based monitoring to a more worldwide Physics-based Monitoring

Phase I – Granite shots

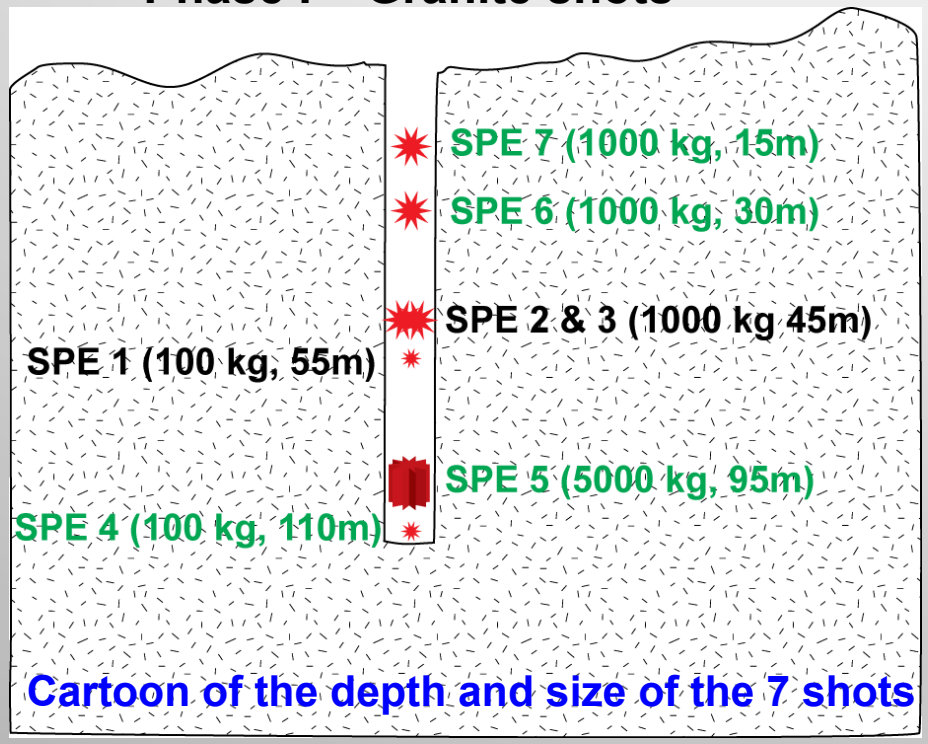

Shot Name	DOB[a] (m)	SDOB[b] (m)	Yield (Kg TNT)	Origin Time	Short Description and Scientific Basis
SPE-1	54.9	991	85	3 May 2011 22:00:00.011	Initial ~Green function (GF) shot in a simple geology. Simulation capability R&D for non-isotropic effects.
SPE-2	45.7	364	992	24 October 2011 19:00:00.012	Increase shot size to record signals to 100km Investigate depth of burial (DOB) effects with SPE5&6
SPE-3	45.8	377	899	24 July 2012 18:00:00.447	Investigate damage zone effects relative to SPE2
SPE-4	110[c]	TBD	TBD	TBD	Minimize spall, ~GF for SPE 5, DOB relative to SPE1
SPE-5	100[c]	TBD	TBD	TBD	Increase shot size to record signals to 300 km
SPE-6	30[c]	TBD	TBD	TBD	DOB investigation with SPE2&7, middle depth
SPE-7	15[c]	TBD	TBD	TBD	Final granite SPE, standard DOB for nuclear test shot

Solution: a series of Source Physics Experiments to provide the necessary physics-based model development and validation data

A fully coupled source-to-sensor modeling capability is being developed and applied to address the major scientific goals of SPE

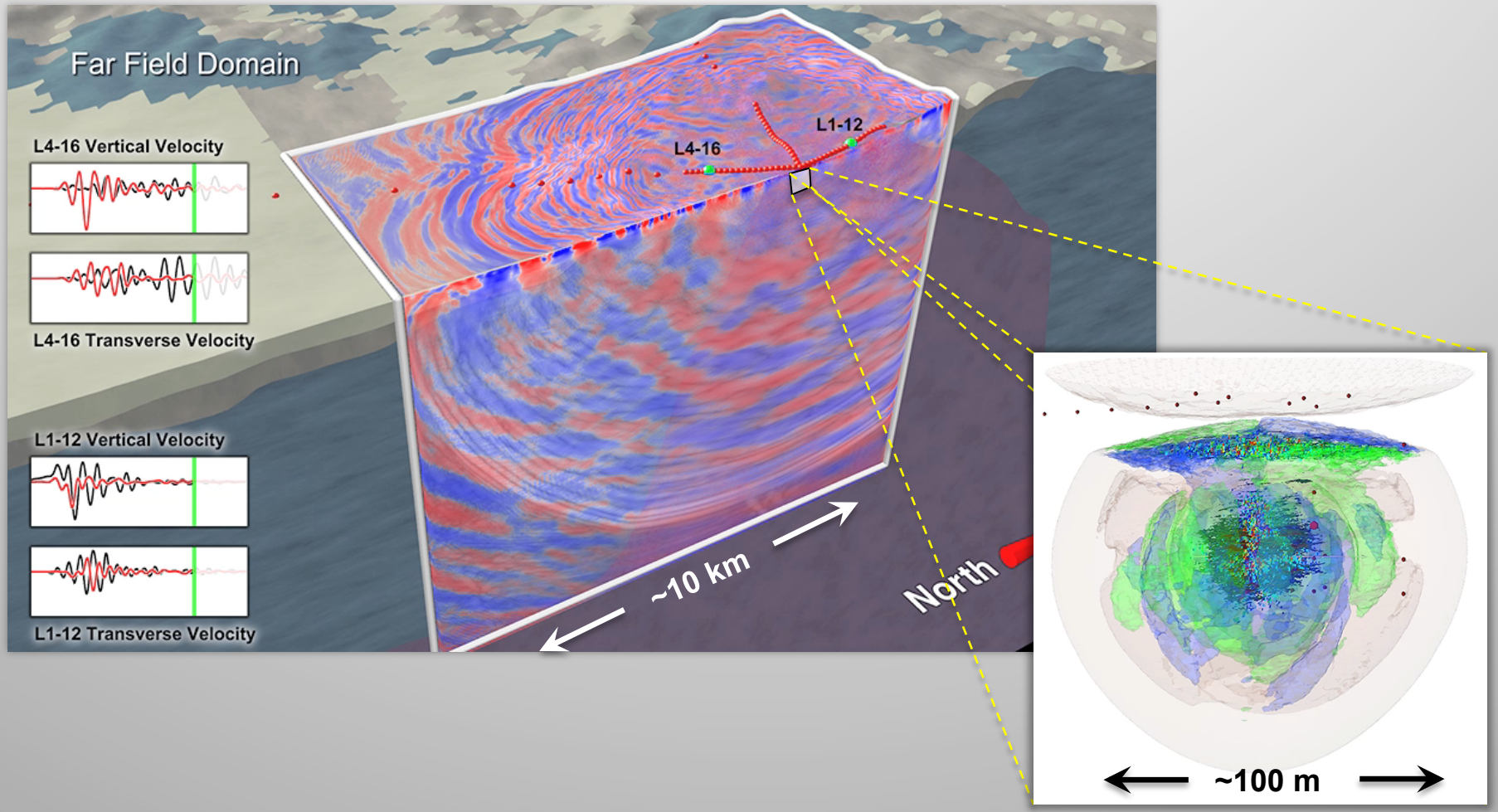

Time	Title	Presenter
8:05	LLNL Overview	Tarabay Antoun
8:20	Discrete and continuum simulations of near-field ground motion from the Source Physics Experiment	Oleg Vorobiev
8:50	Stochastic three-dimensional investigation of near-source motions from an underground explosion	Souheil Ezzedine
9:20	Analysis of recorded and simulated far-field ground motion from the source physics experiment	Arben Pitarka
9:50	SPE Animation	
10:30	Explosion and spall model comparison with the Source Physics Experiment	Sean Ford
11:00	SPE signals and setting: EM, seismic amplitudes and velocity models	Rob Mellors

Stochastic 3D investigation of near-source motions from an underground explosion

S. Ezzedine[1], O. Vorobiev[2], L. Glenn[2],T. Antoun[2] & A. Pitarka[2]

[1]Computational Engineering Division, [2]Earth Sciences Division

Lawrence Livermore National Laboratory

State of Analysis Review
August 21-22, 2013
Las Vegas

LLNL-PRES-643215

This work was performed under the auspices of the U.S. Department of Energy by Lawrence Livermore National Laboratory under contract DE-AC52-07NA27344. Lawrence Livermore National Security, LLC

Uncertainty propagation throughout SPE designs, analyses, monitoring network and yield estimation

Three-tier analysis

Flow chart of UQ propagation and estimation for SPE

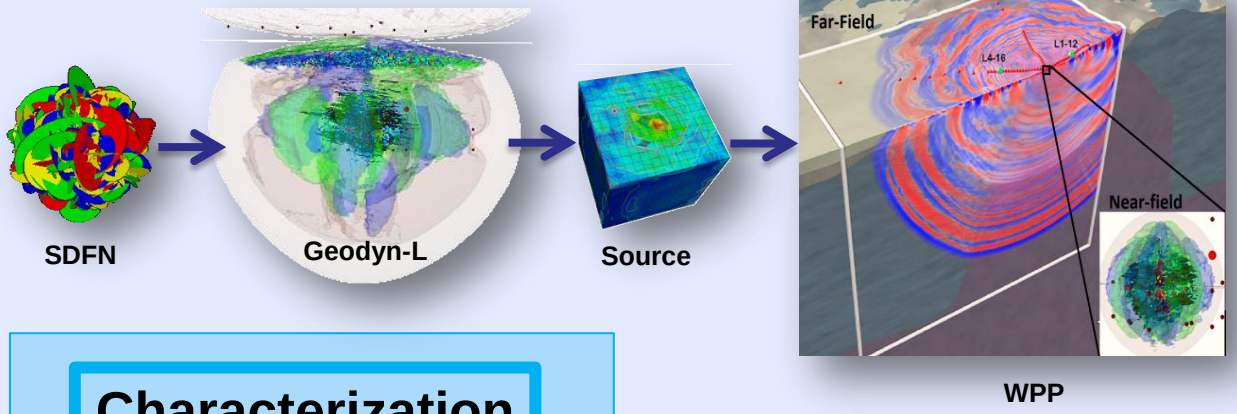

Characterization

SDFN

Geodyn-L

Near Field predictions

observations

Source

Characterization

SDFN

WPP

Far Field predictions

observations

Yield prediction

Monitoring design

Uncertainty Quantification enables us to make decision where /when characterization is limited

- **Uncertainties do exist in every walks of life**
  - It "cannot be eliminated" but minimized
  - Uncertainty is not essentially a "bad thing"
  - It enables make decision with margin of confidence

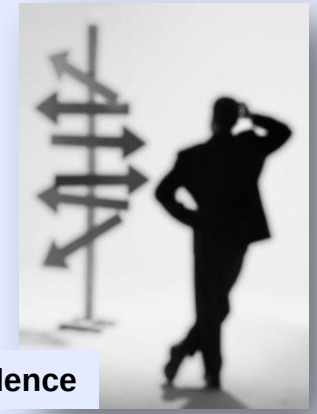

Make decision w/ confidence

- **UQ use to be a very expensive task**
  - UQ is becoming relatively to moderately inexpensive
  - Nowadays, computational tools (hardware & software) are readily available
  - DOE Labs are at the leading-edge in UQ

LLNL's HPC

- **Several sites of interest are of limited access and/or only "remote" characterization is available**
  - Monitoring underground explosion
  - Estimating yield and depth of sources
  - Probabilistic discrimination of explosives from EQs in jointed rock

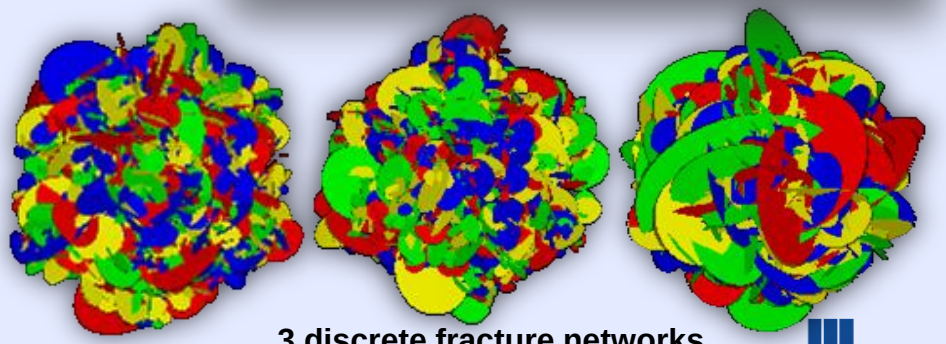

3 discrete fracture networks

Uncertainties exist in SPE from end to end: e.g. in data, conceptual and numerical models

- **Aleatoric**
  - A SDFN is characterized by:
    - e.g. Statistical Models
    - e.g. Set of joints
  - Material properties
    - Scale disparity Measurements at laboratory scale may not be necessarily applicable to large scale
    - Intrinsic properties can vary spatially and temporally
  - Characterization is local but we need to 'extrapolate' between the wells
- **Epistemic**
  - Physics based uncertainty
  - Model "uncertainty"
    - Physics (discrete vs continuum)
    - Different codes ~ different outcomes
- **Measurements (direct or indirect)**

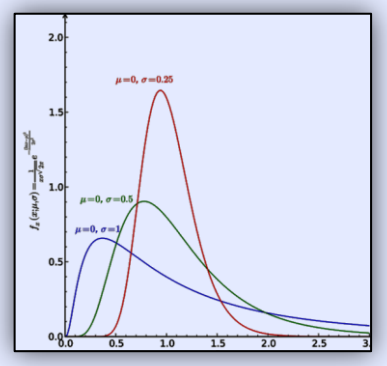

Statistical characterization

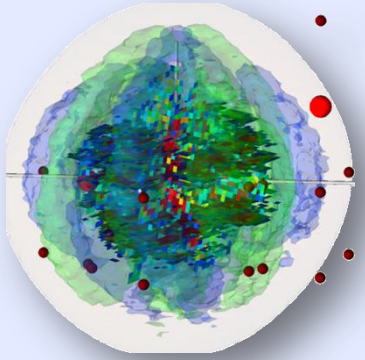

Multi-scale problem

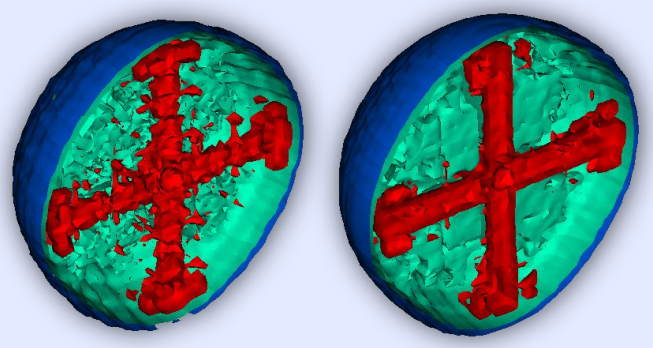

Numerical simulations

There are several approaches for representing joints, DFN is the most appropriate for SPE UQ analyses

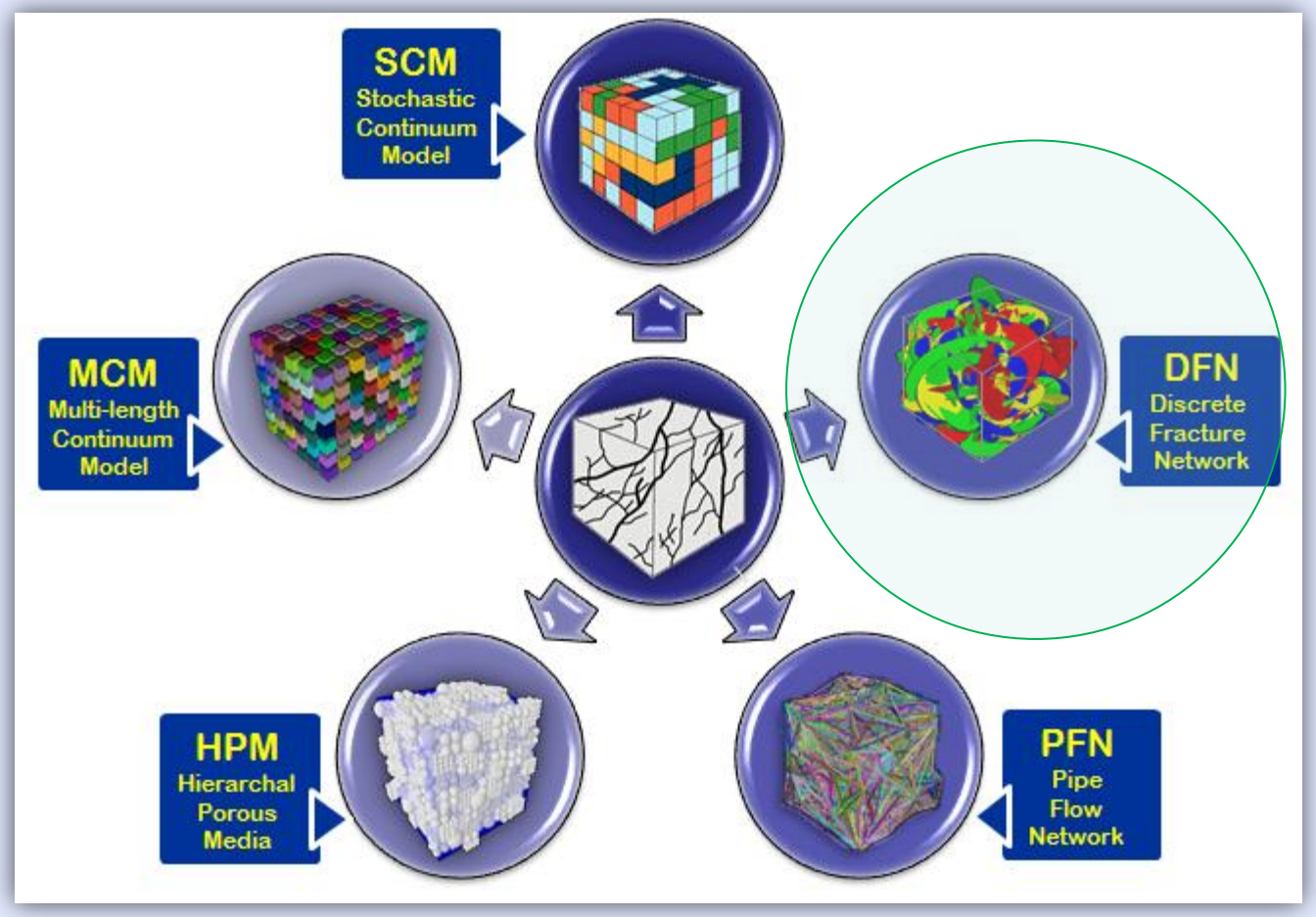

Discrete Fracture Network (DNF) approach offers unique capabilities to not only "mimic" in-situ fracture characterization but also to assess uncertainties, their propagation and quantification

Fracture (Joint) characterization in a stochastic discrete fracture network (SDFN) approach

- **In-Situ fractures are assumed**
  - random with a finite size
  - belong to different (sets) families

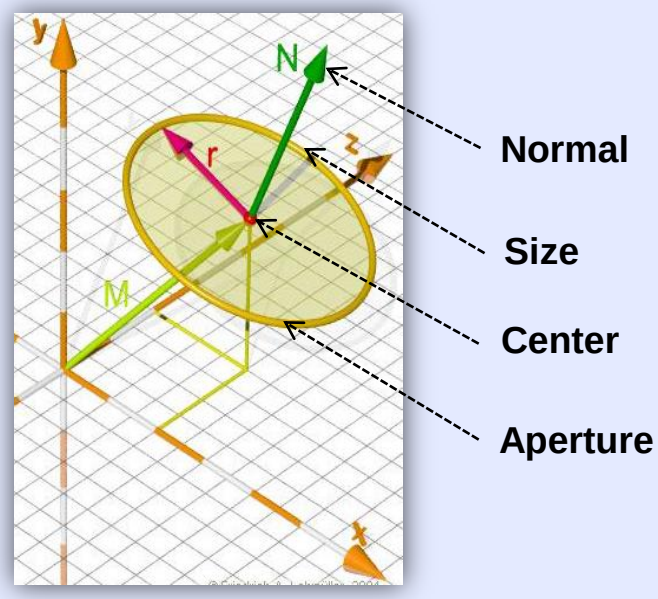

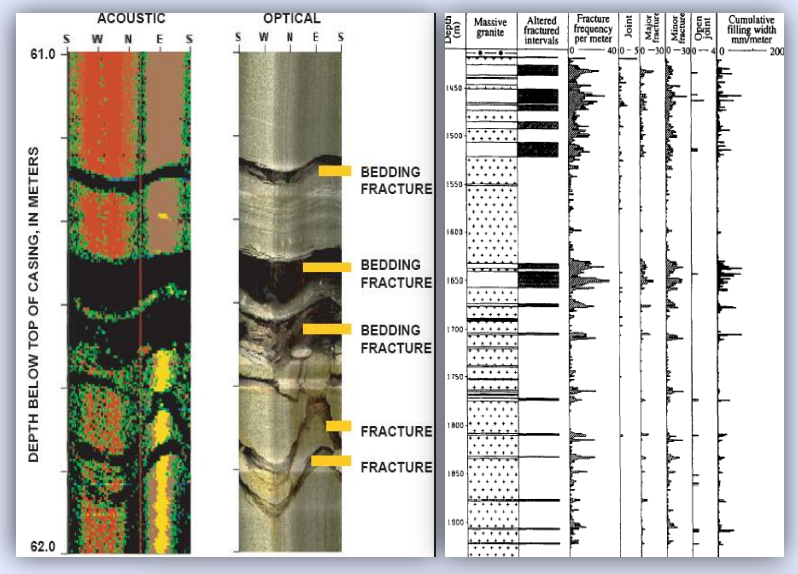

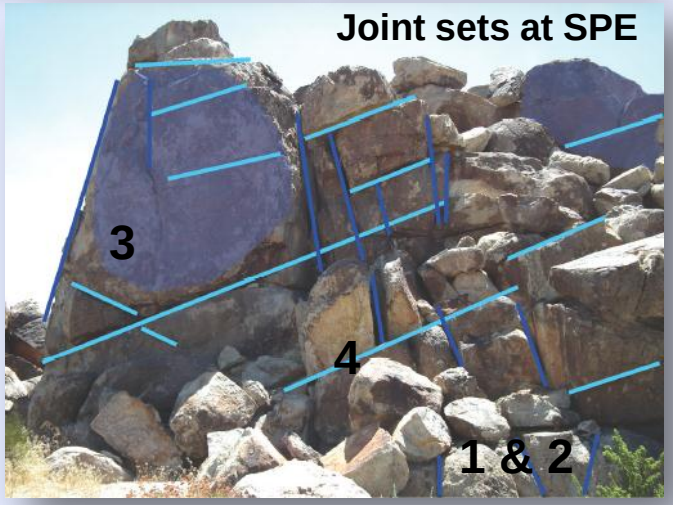

- **Each set of joints is characterized by:**
  - density, location of centers,
  - orientations, aperture & radius PDFs
  - PDFs are inferred from in situ characterization
  - In line with what is been conducted for SPE

Several parameters can be tuned to create equally probable SDFN with same statistics

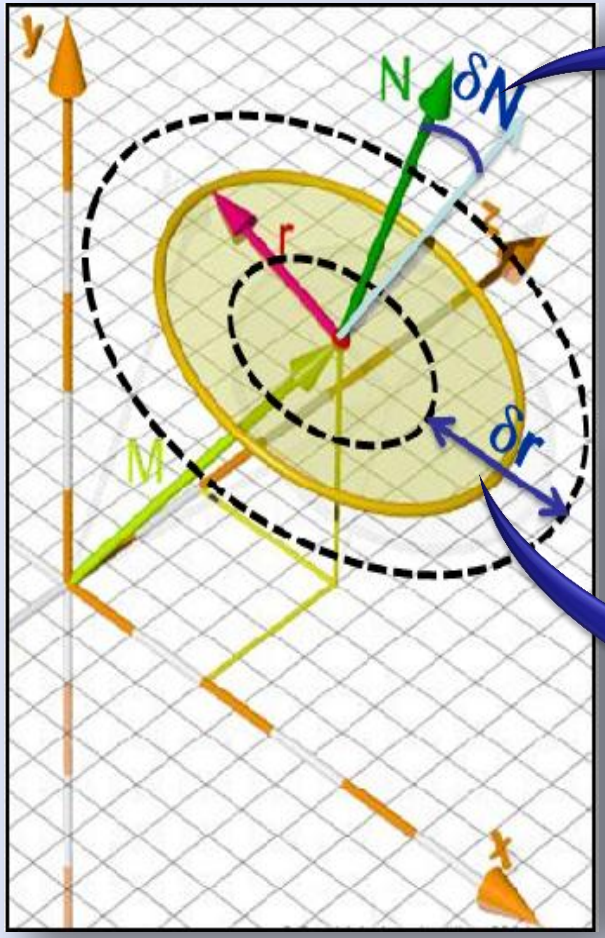

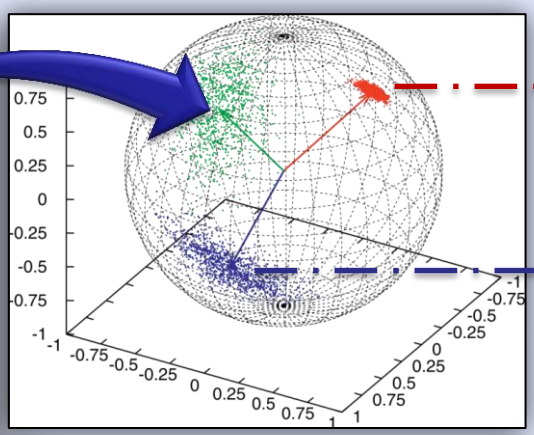

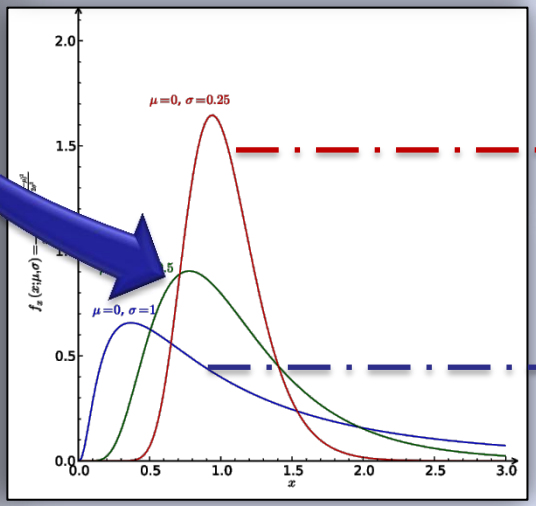

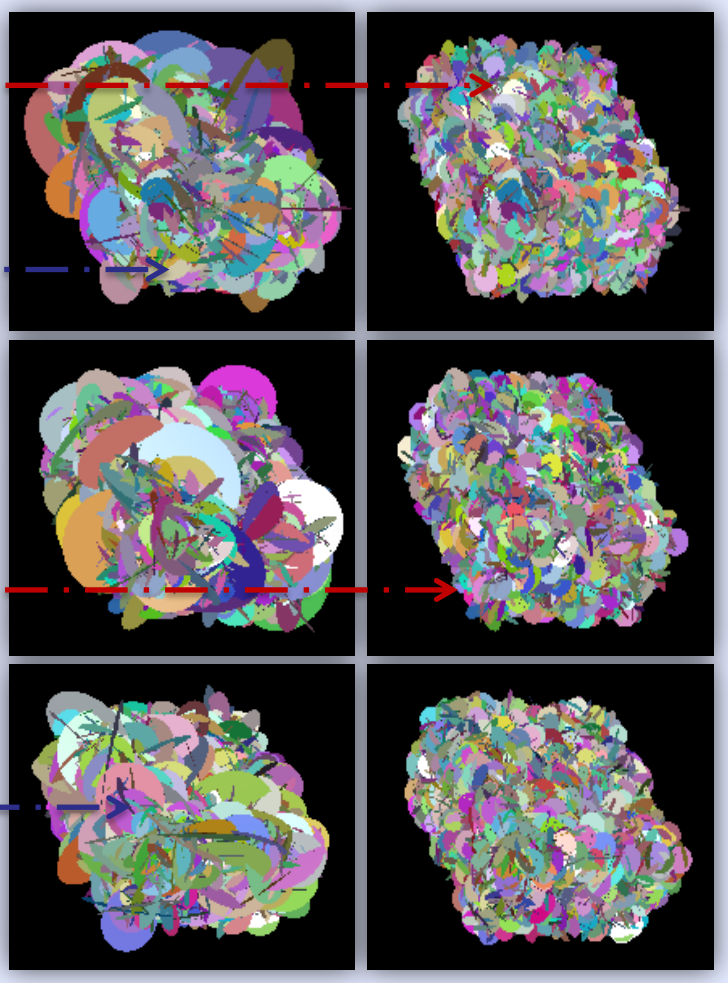

Joint orientation and size can be tuned to create equally probable fracture networks (rock mass)

Example of three equally probable realizations with different statistical control on the size and orientation of the joints

WP in jointed rock mass is a highly non-linear problem, UQ is conducted using brute force Monte Carlo

- **"Geological" uncertainties:**
  - Statistical Models
    - Center Density
    - Orientation Density
    - Aperture Density
    - Radius Density
    - Fracture Geometry
  - Number of Fracture Family
- **"Geomechanical" uncertainties:**
  - Equation of state
    - Density, bulk sound speed..
  - Yield surface model
    - Tensile strength…
  - Porosity model
    - Friction, cohesion, compaction…

Large parameter space

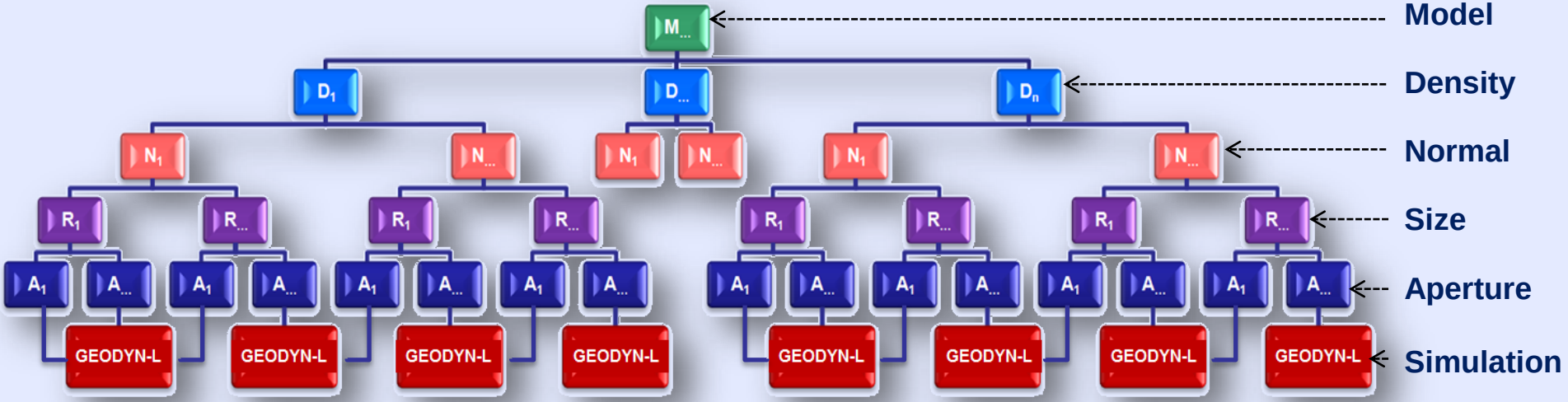

Wave propagation with discrete representation of joints is CPU time cumbersome

Typical physical dimension

joint aperture ~1 mm
joints spacing ~1 m
source size ~1 m
region ~300 m

Computational requirements

~20-50 million elements
~100-200 million zones
~3240 CPU for 12 hours

Uncertainty quantification

~ 40 runs a set
~ 9 parameters
~ 200TB

Judiciously conduct the UQ

sampling effectively
reducing model complexity

A prototype model for SPE3

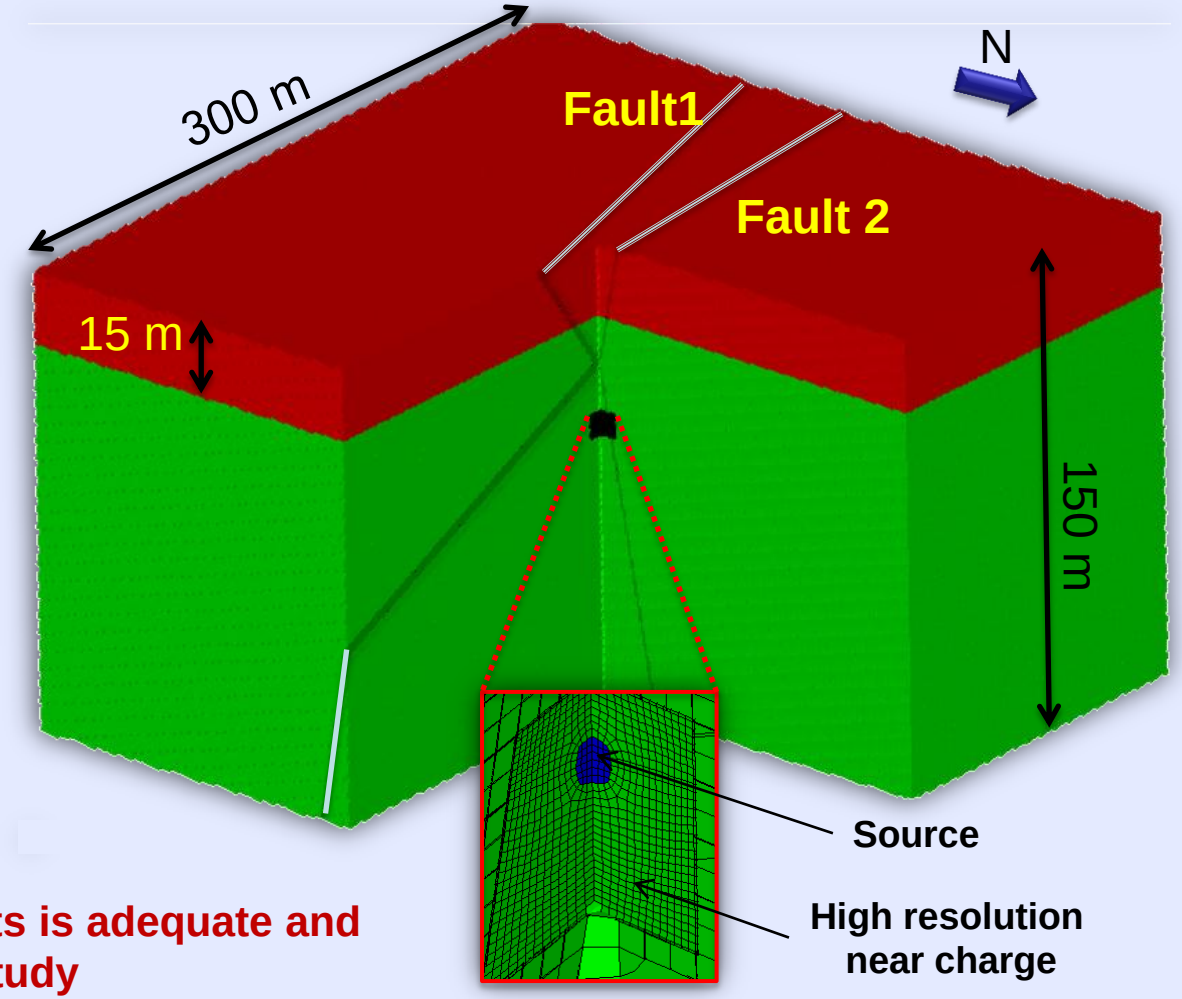

Continuum representation of joints is adequate and accurate for UQ and parametric study

Several cases where solved with discrete & continuum joint representation, both approaches show very similar results

Explosion in hard rock with three Cartesian sets of joints

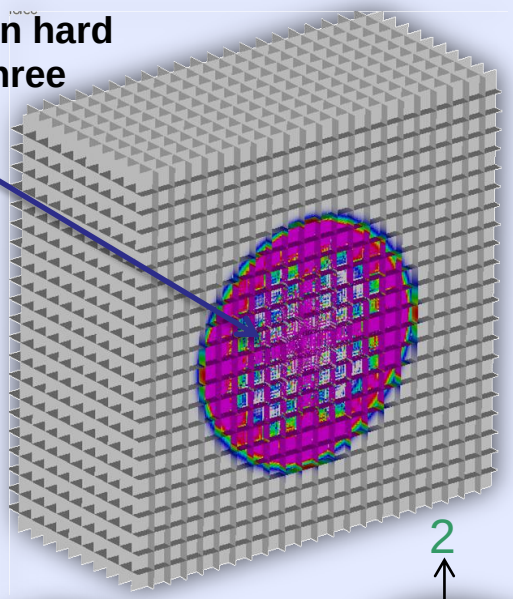

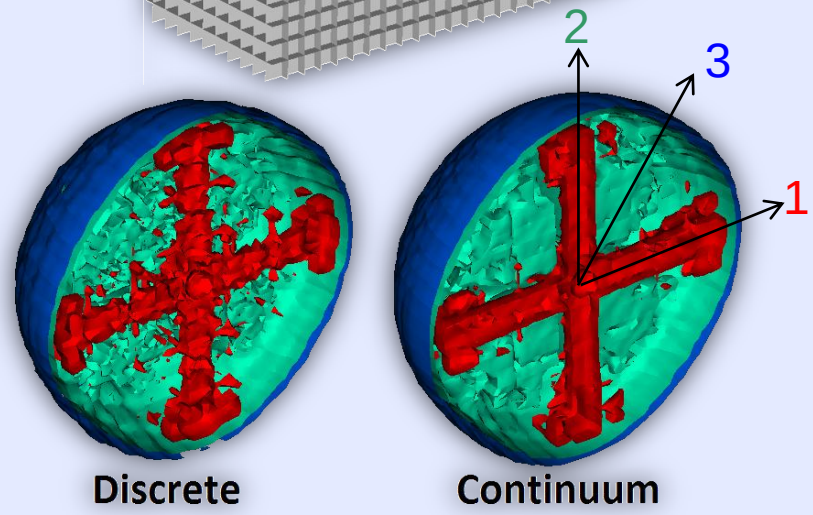

Pressure contours (0-50 MPa)
Joint spacing 1 m, friction ~0.2

Discrete joint representation

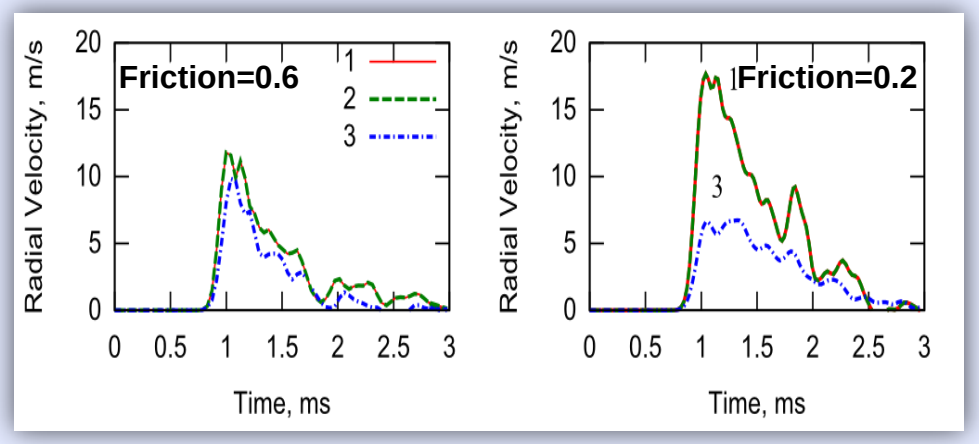

Continuum joint representation

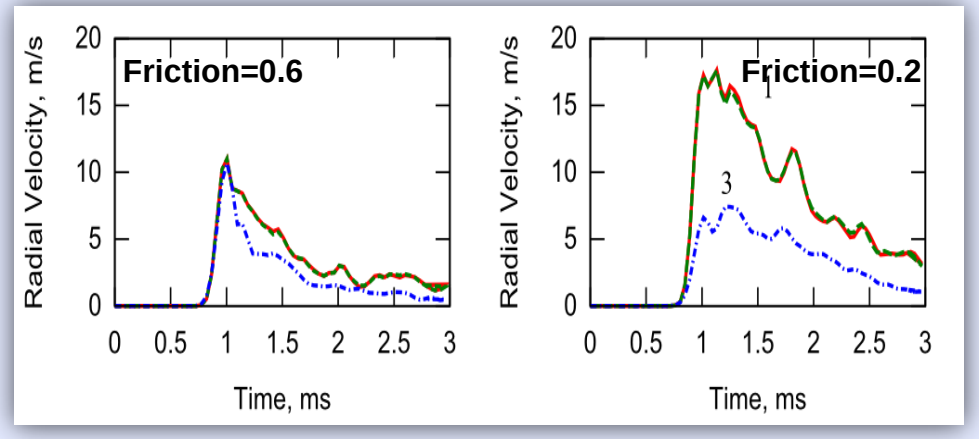

Dependence on joint friction

Continuum approach relies on meshing appropriately the joints, a mesh sensitivity analysis has been conducted

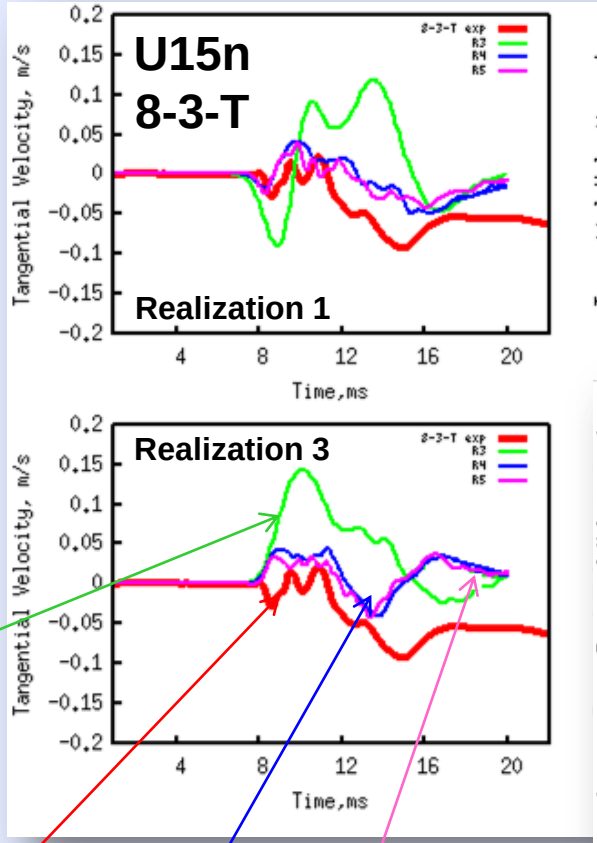

R3: 1-2Hrs 864 CPUs (x1)
R4: 2-4Hrs 864 CPUs (x4)
R5: 6-8Hrs 864 CPUs (x8)

R4 is a balance between accuracy and CPU-Hrs

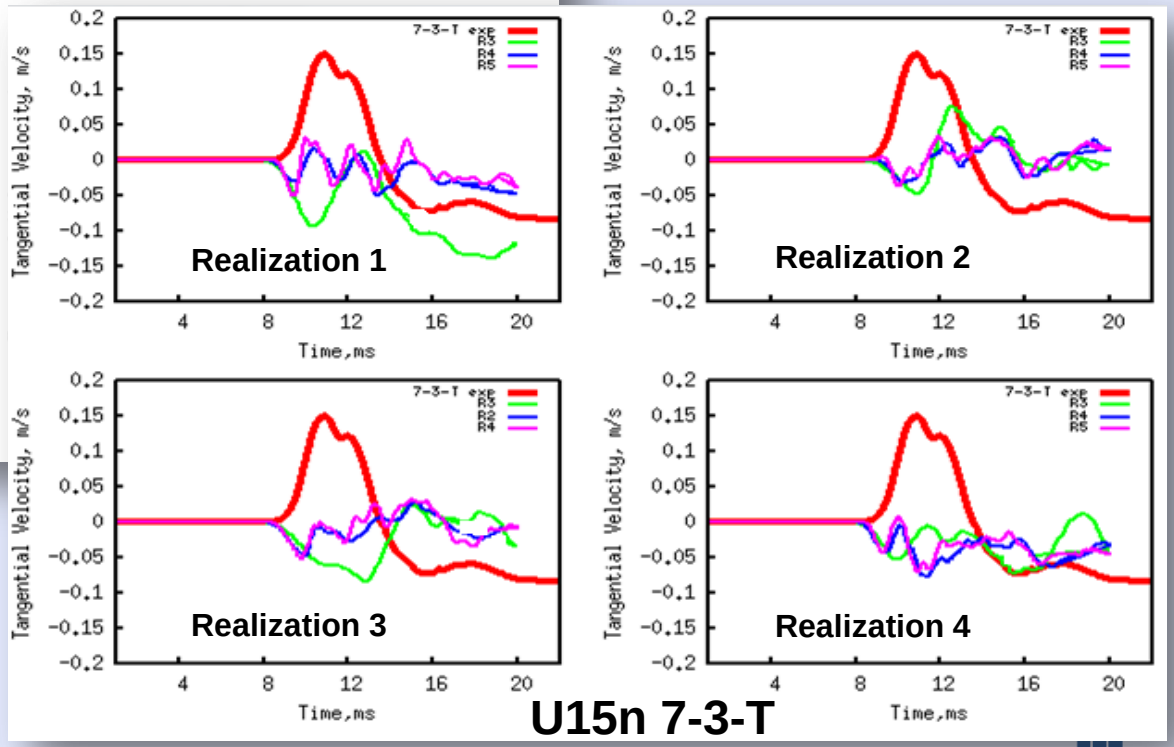

R4 & R5 are very similar and within 2% in average
R3 is distinctly different

UQ analysis: single Layer model -- Radial velocity of 20 Monte Carlo simulations

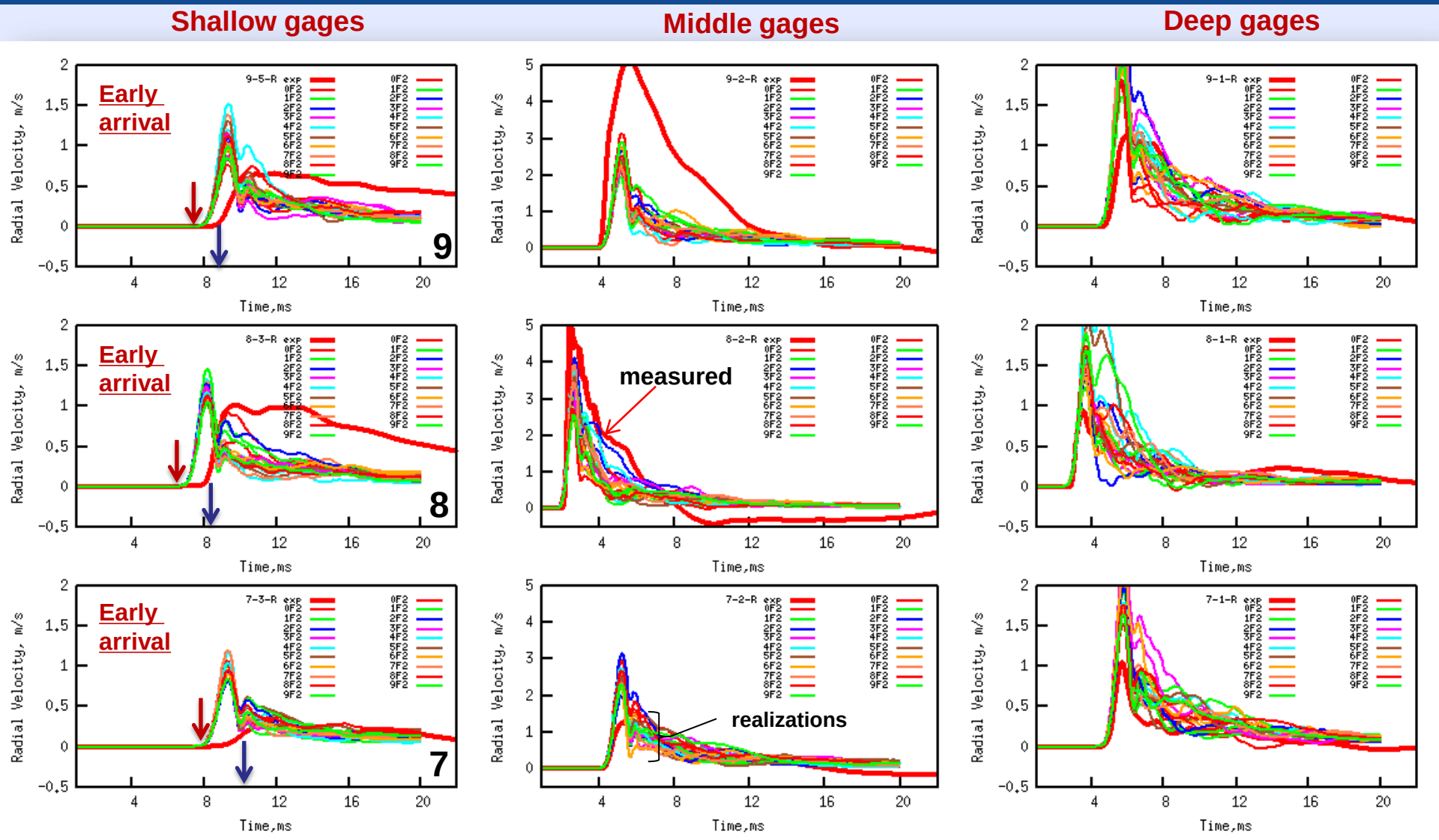

Good coverage of velocities at middle and deep gages – discrepancies in arrival times at shallow gages

UQ analysis: single layer model – Tangential velocity of 20 Monte Carlo simulations

Shallow gages | Middle gages | Deep gages

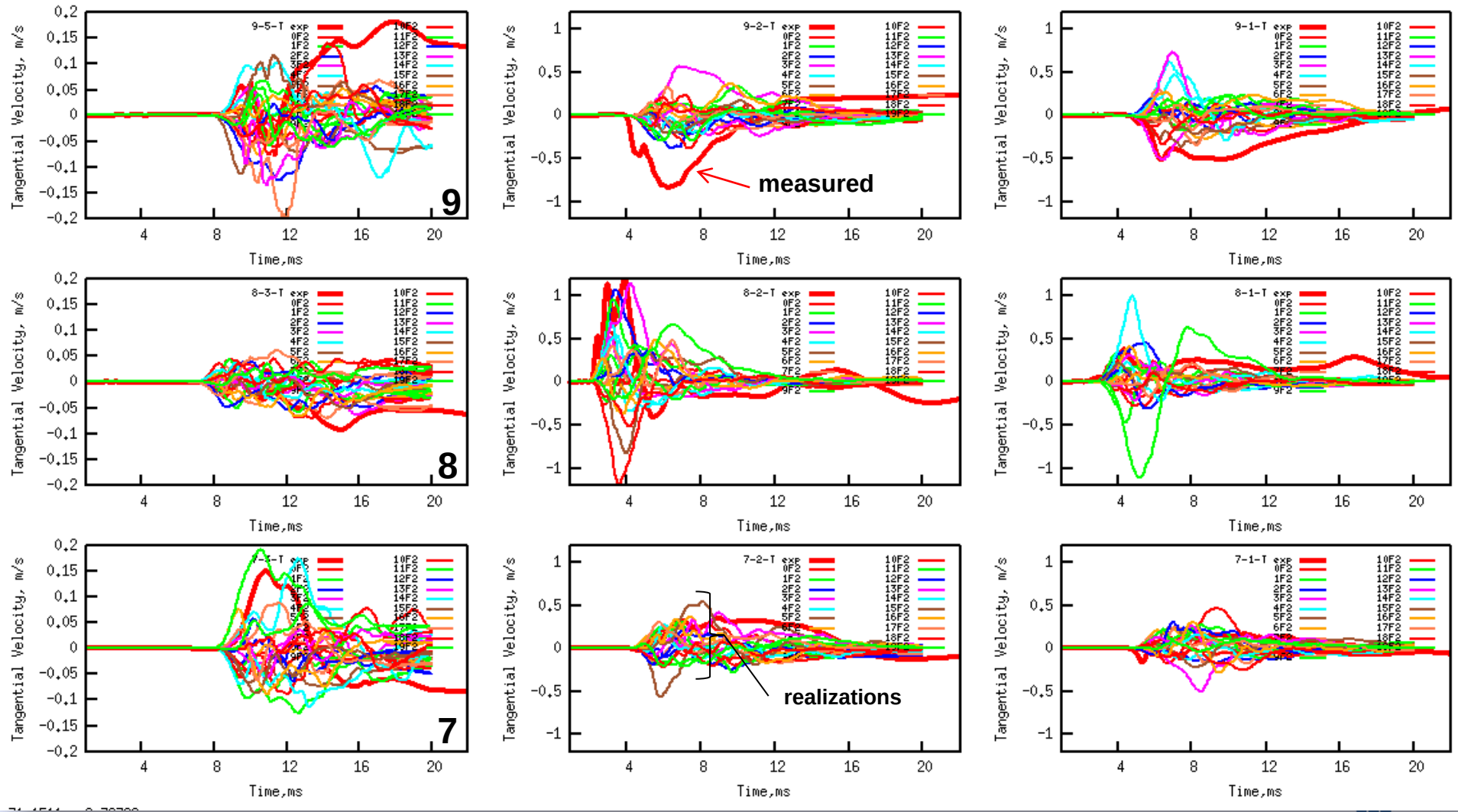

Wide coverage of velocities at all gages – no apparent discrimination on the polarization

UQ analysis: double layer model – Radial velocity statistics based on 40 MCS

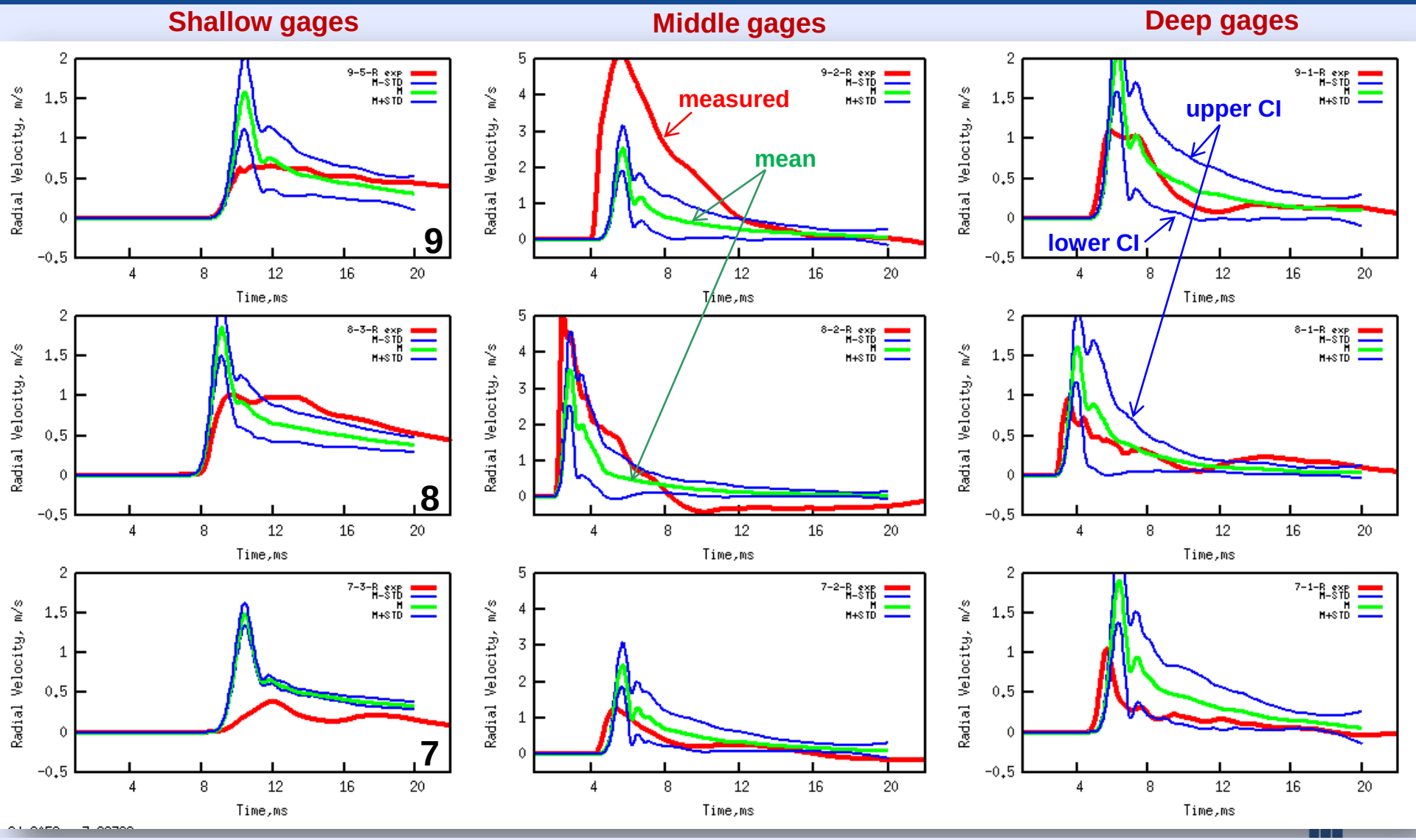

Gage 9-2 is anomalous – Model over predicts peak velocity – we expect attenuation from joint compliances

UQ analysis: double layer model – Tangential velocity statistics based on 40 MCS

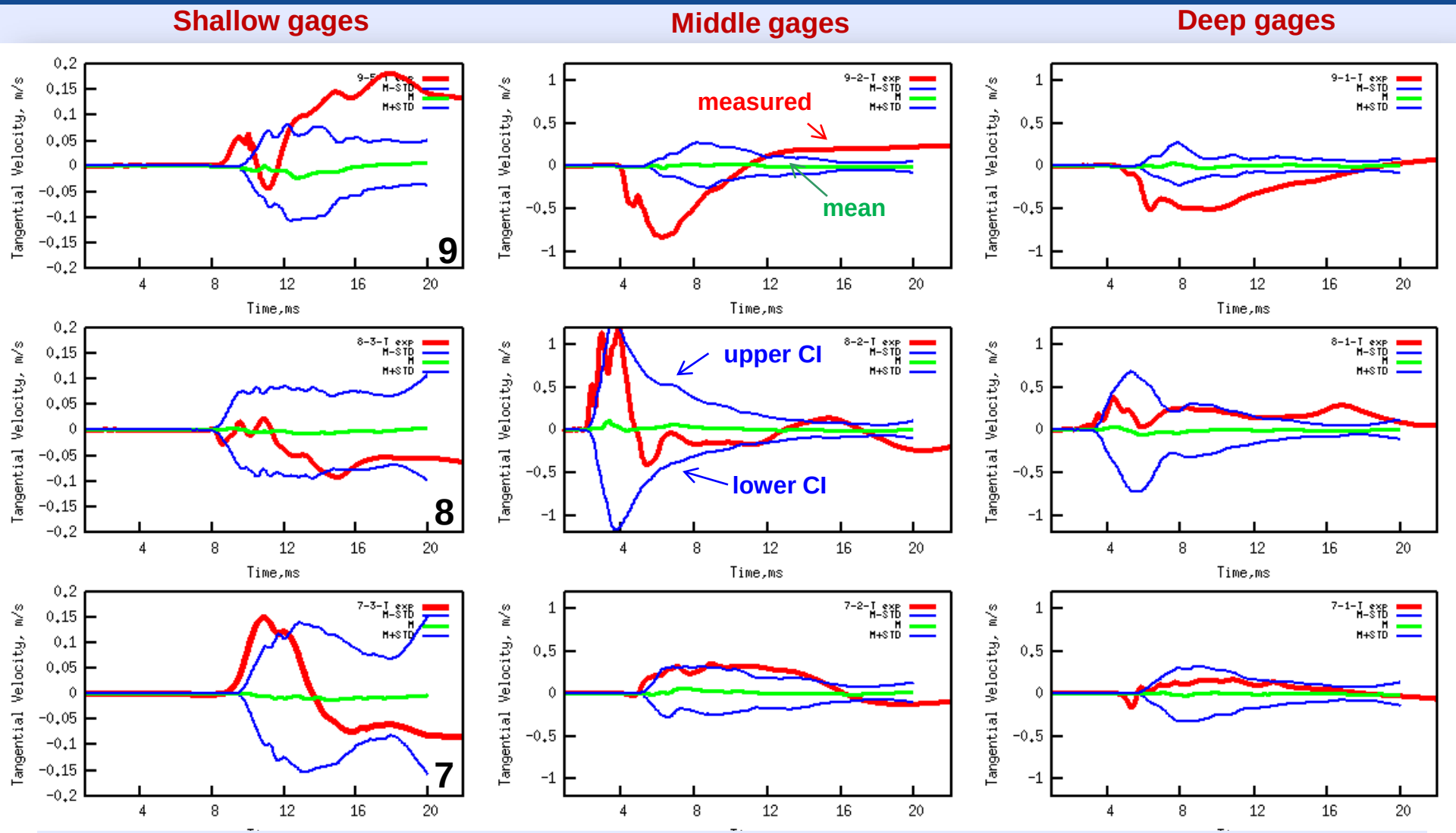

Interestingly observed data lays with 95%CI of the simulations – bias to upper CI – joint compliances will shift the mean thus CI – note that the polarization is captured in several gages

Sensitivity Analysis:
Effect of joint density on velocities

Nominal density | **Nominal density x 10**

Radial

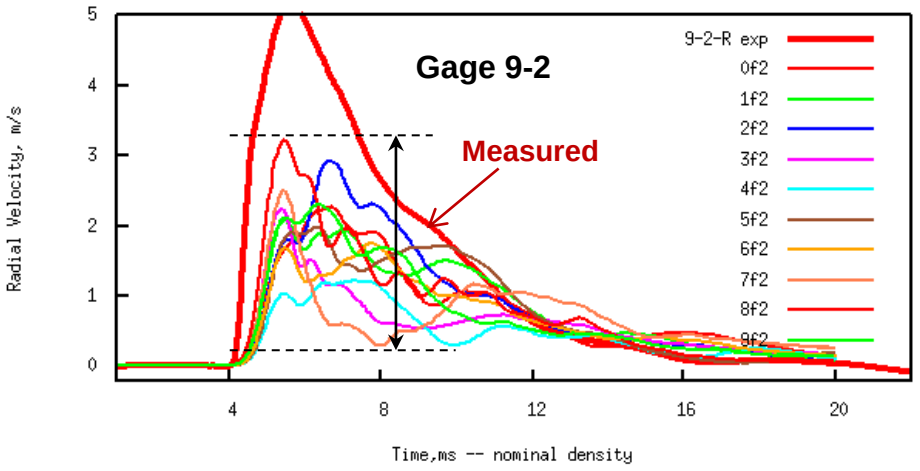

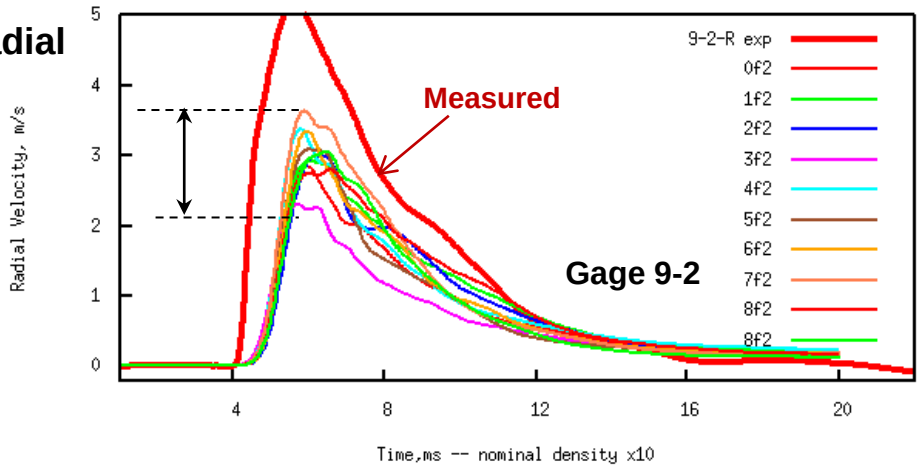

Tangential

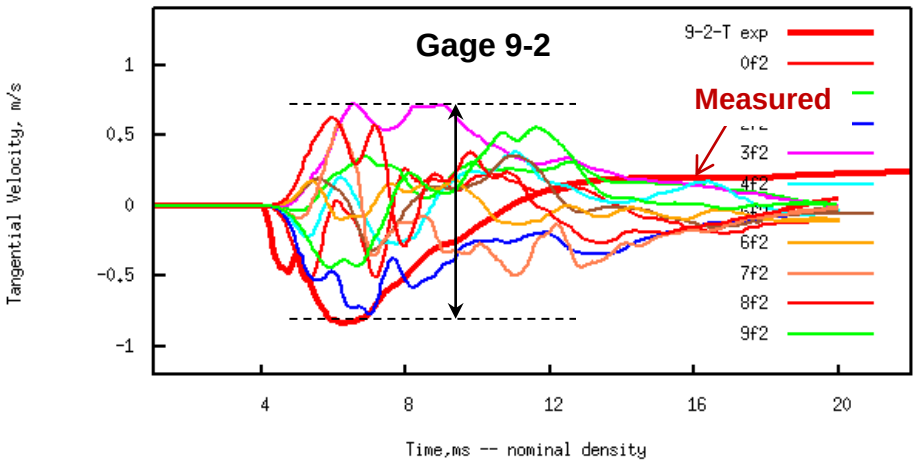

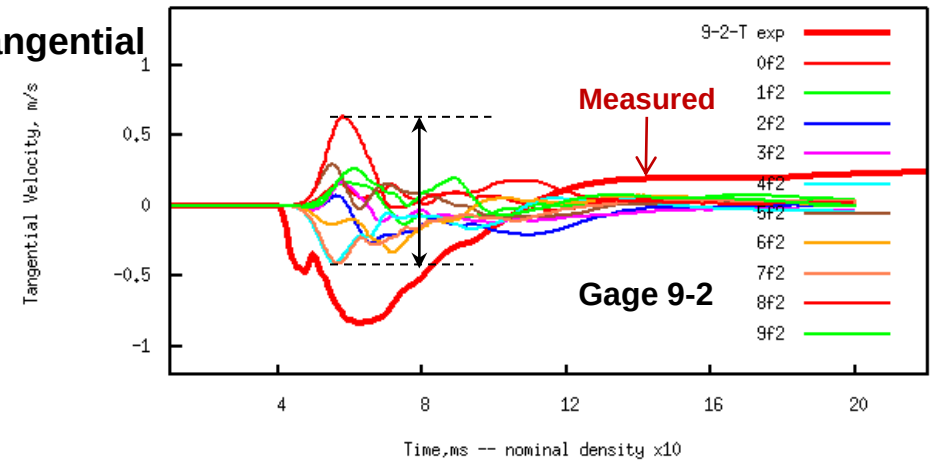

Increasing the density of joints leads to a decrease in velocity fluctuations (spread)

Increasing the density of joints leads to more "homogenized" rock mass

Sensitivity Analysis:
Effect of poro-elasticity of top layer – Radial velocities

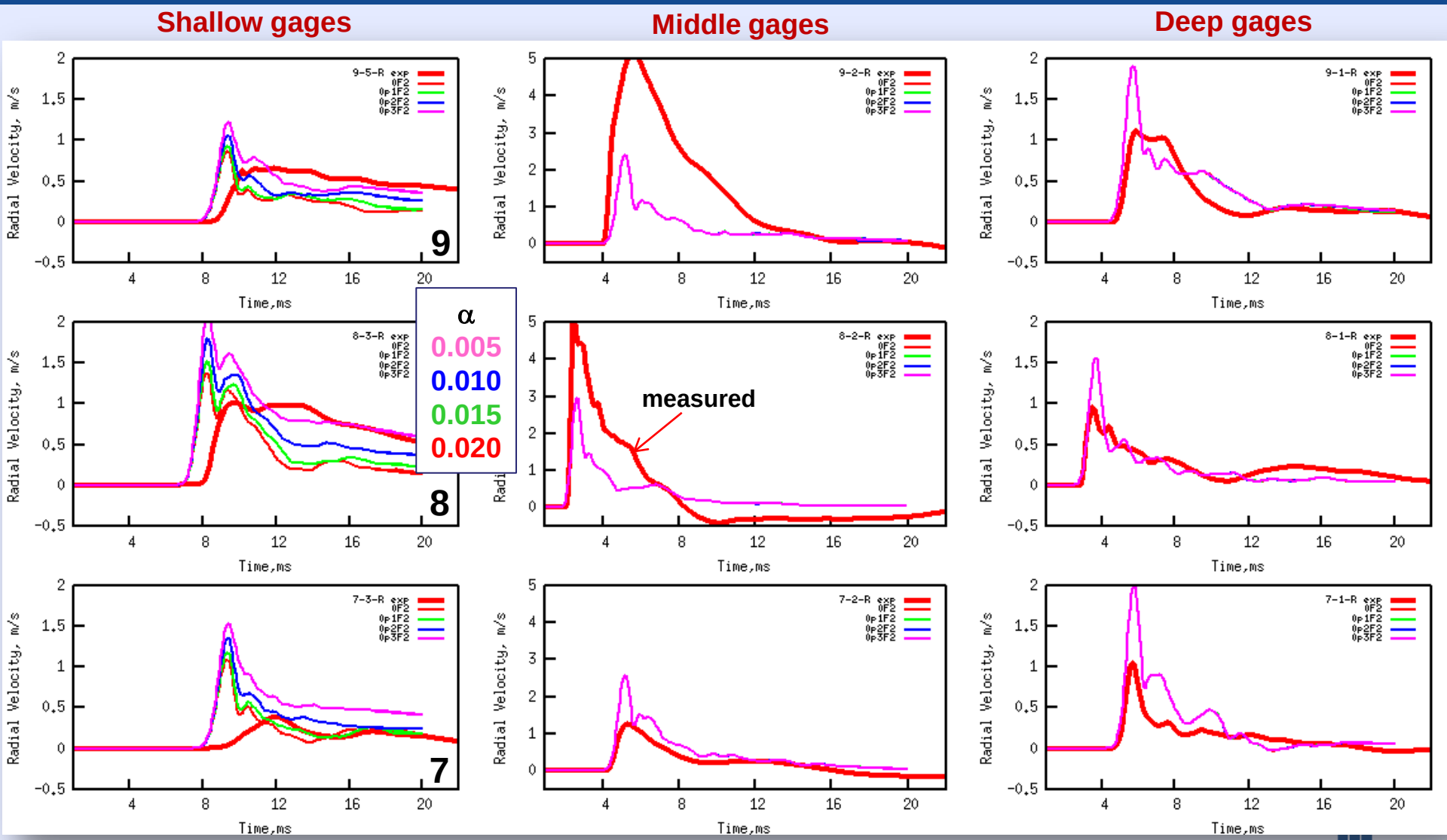

Reducing the top layer poroelastic parameter leads to amplifying the velocities at shallow gages

Sensitivity Analysis:
Effect of poro-elasticity of top layer – Tangential velocities

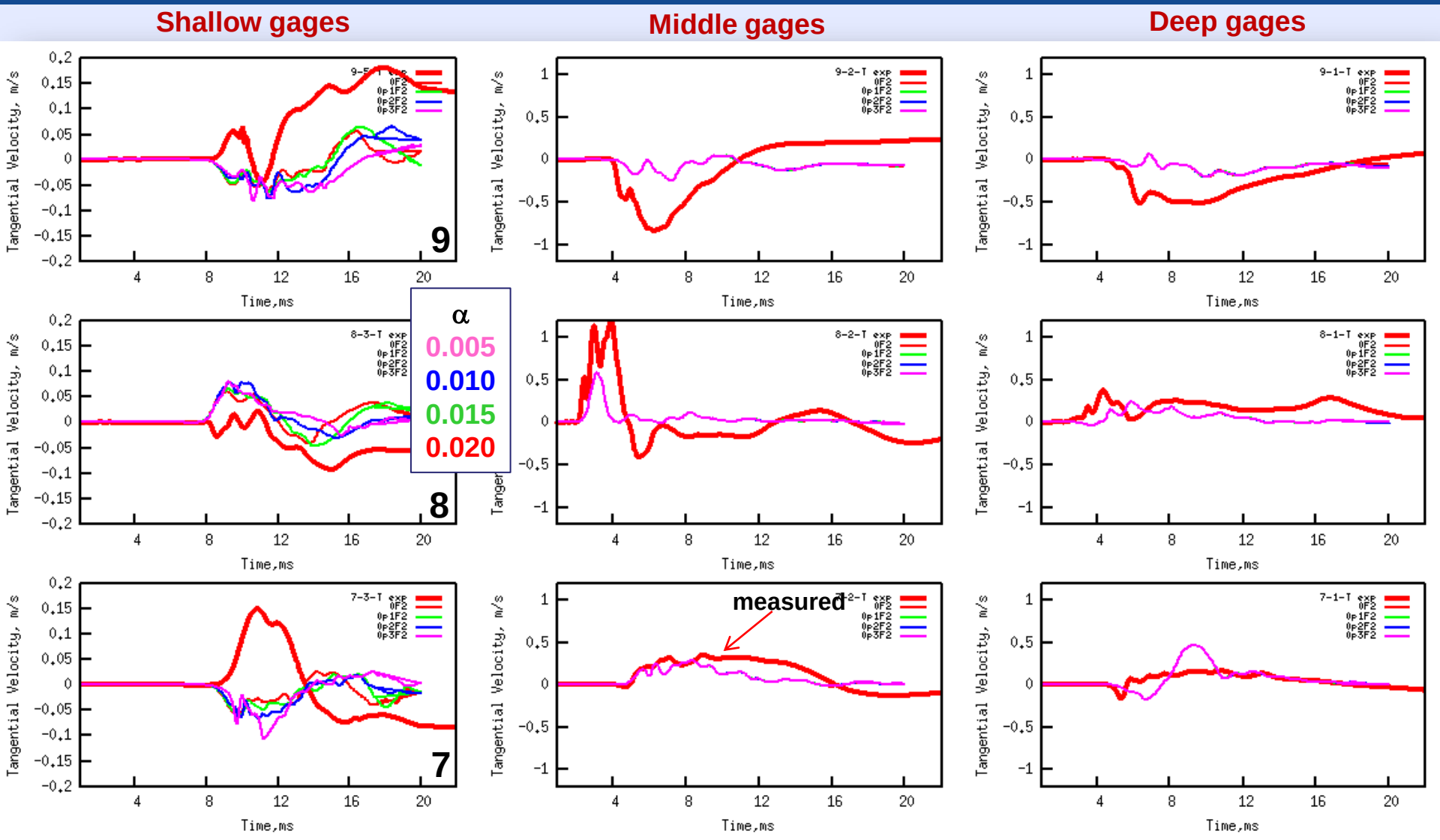

Reducing the top layer poroelastic parameter impacts the velocities at shallow gages

Sensitivity Analysis:
Effect of thickness of top layer – Radial velocity

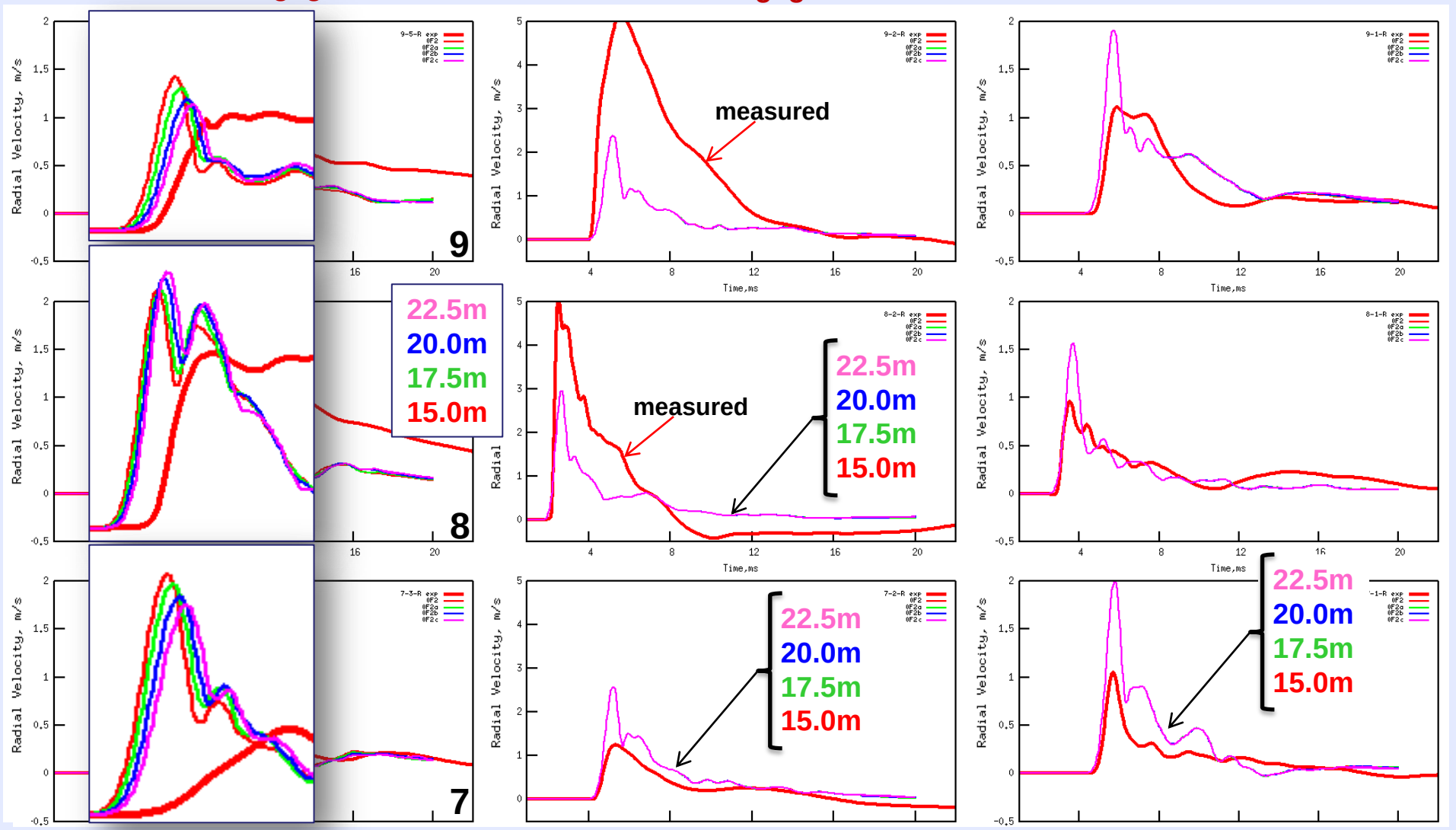

Thickening the top layer impacts arrival times at shallow gages while deeper gages remain unchanged

Sensitivity Analysis:
Effect of thickness of top layer – Tangential velocity

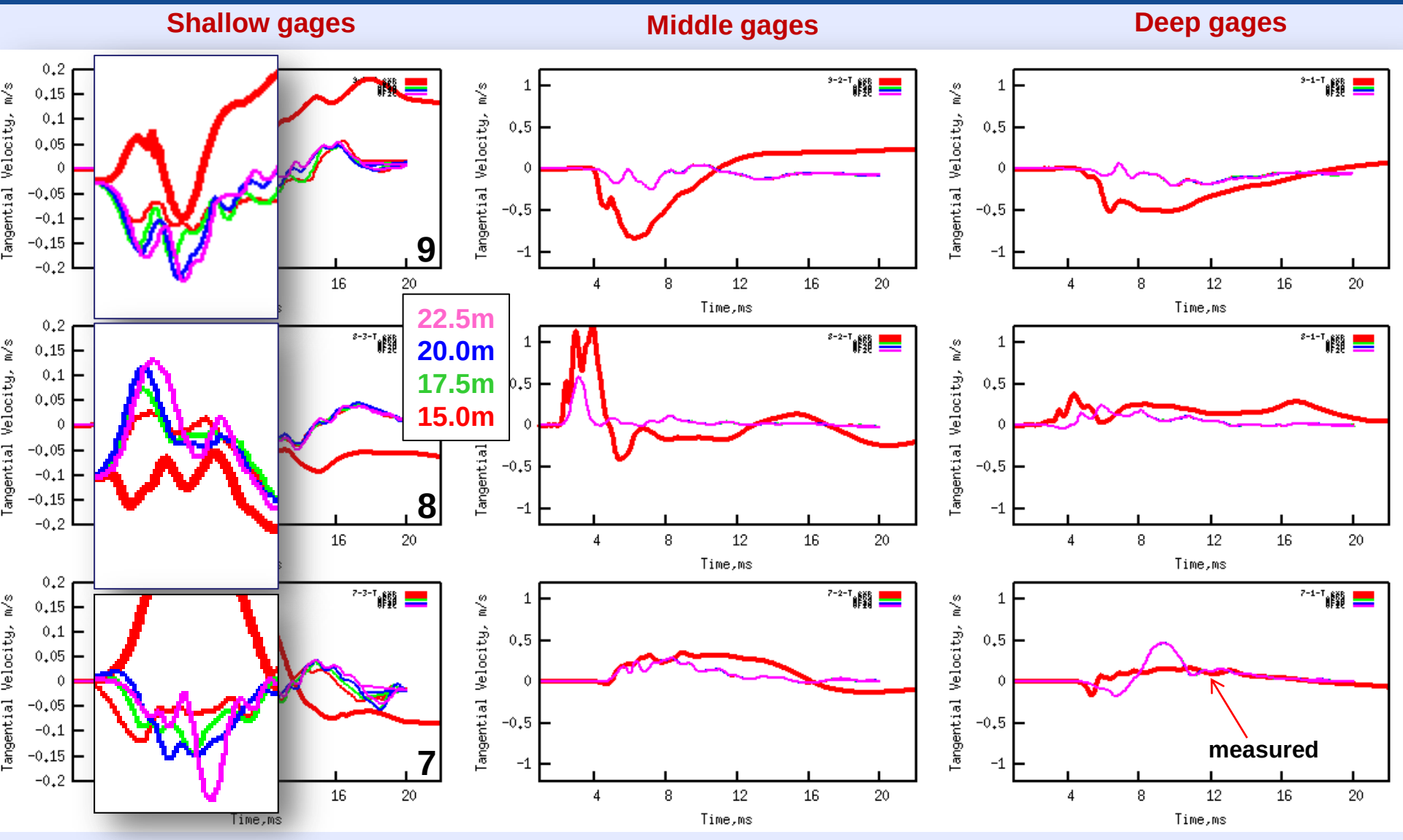

Thickening top layer leads to amplifying the velocities at shallow gages -- deeper ones remain unchanged

Sensitivity Analysis:
Effect of joint orientation on radial velocity

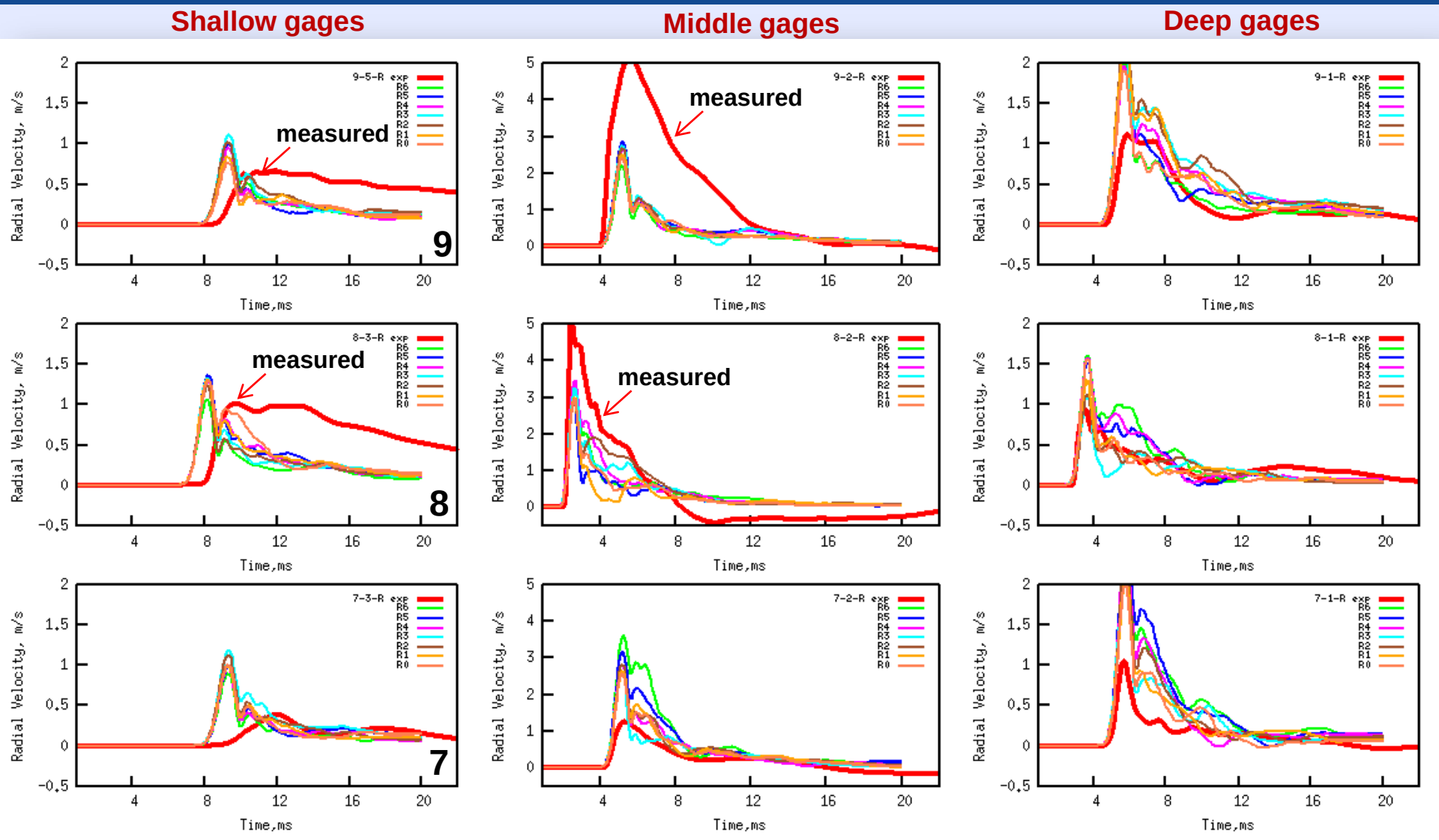

Re-orientation of vertical set of joints can amplify the spread of velocities and their peak magnitude

Sensitivity Analysis:
Effect of joint orientation on tangential velocity

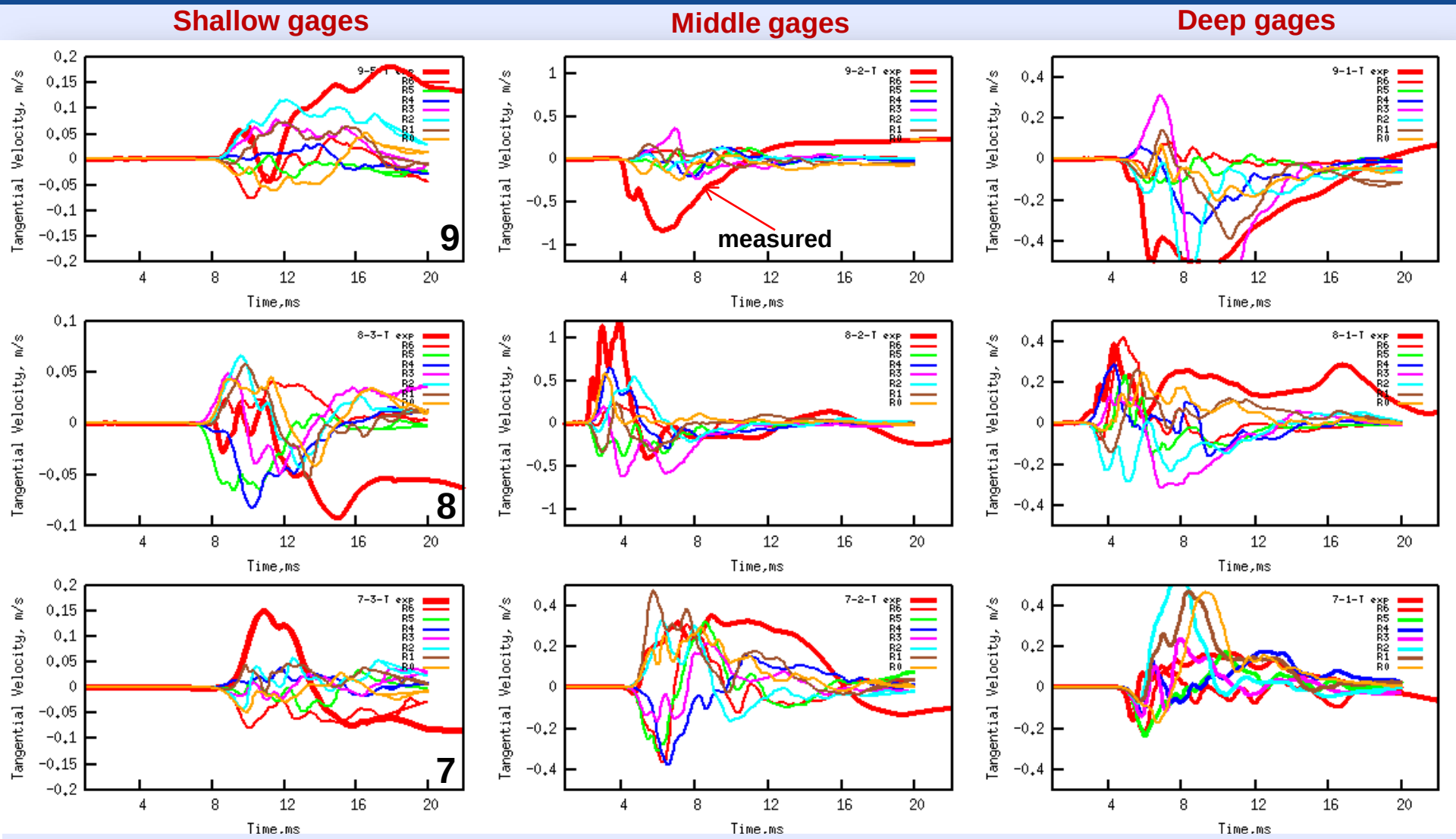

Joint orientation of vertical set of joints leads to polarization switch in tangential velocities – joint compliances may lead to correlation between polarization and rotation angle of joints.

Far Field Monitoring Implications: Do joints nearby the source impact far-field signatures?

- **One-way coupling** between nonlinear, inelastic near-field and linear, visco-elastic far-field regions using a padding mortar space in 3D.
- **Near-field:** 3D Lagrangian hydrodynamics code with non-linear material response (GEODYN-L)
  - Explosion loading
  - Compressional and tensile failure, yielding, porosity, cavity formation
  - source mortar embedded within finite difference model
- **Far-field: 3D-FDM (WPP)**
  - Driven by interpolated time series from GEODYN model
  - Signals propagated through complex 3D velocity model of geology to distances of 10's of kms
  - Coupling verified and validated.

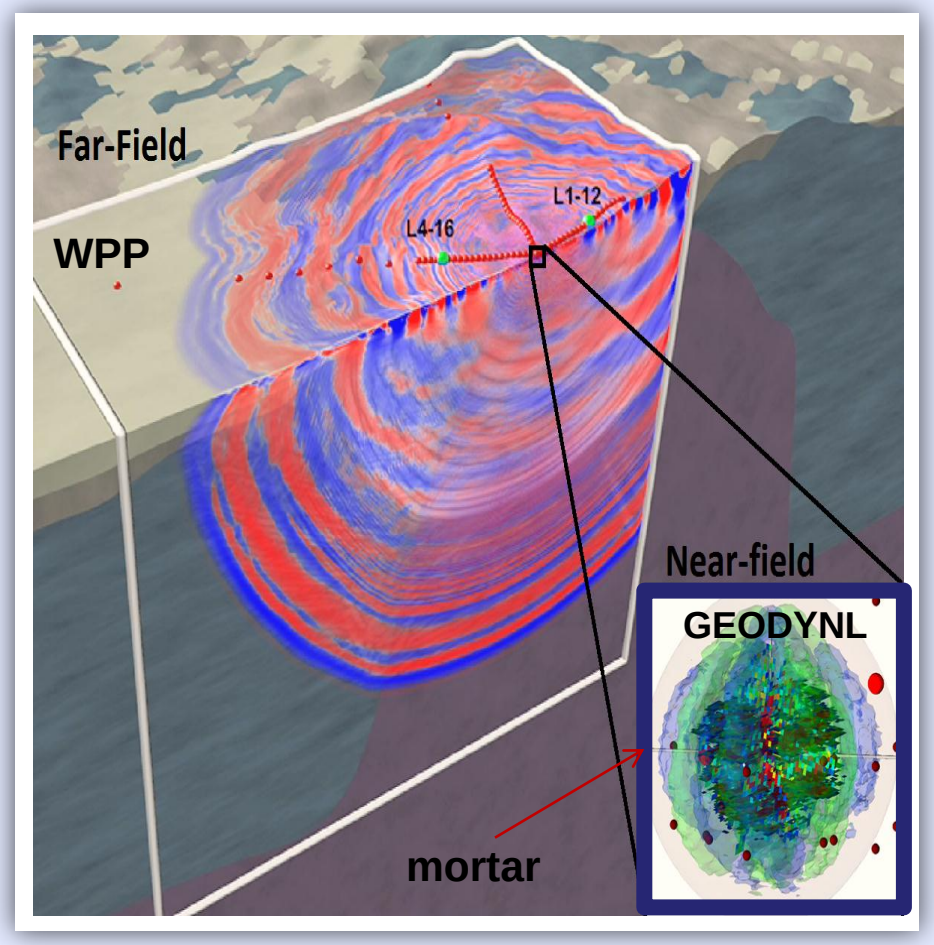

WPP

3D finite-difference code Curvilinear grid for topography, mesh refinement, viscoelastic model .Designed for massively parallel systems

Uncertainty propagation to far field monitoring receivers: source abstraction and WPP simulations

Flow chart of UQ propagation and estimation for SPE

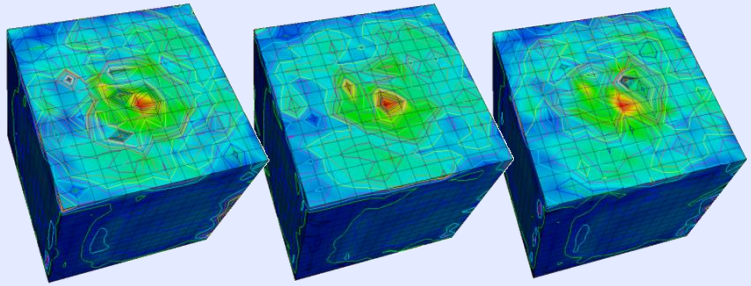

Examples of 3 equally probable sources for far field propagation

Our ultimate goal is to estimate yields and design monitoring networks under conditions of uncertainty

Summary & Path forward

- **Summary:**
  - A UQ framework has been established and streamlined with SPE from end-to-end analyses
  - Several UQ & SA studies have been conducted
  - Joints affects significantly near field motions, impacts on far field motions are been explored
  - Vertical joints can lead to horizontal motion (persistence throughout MCS and their stats)
  - Friction angle and joint density (thus spacing) affect shear motions
  - Joint compliances will attenuate the peak velocity and will increase pulse spread
- **Path forward:**
  - Assess the impact of joint compliances on velocities
  - Propagate UQ to Far Field receivers
  - Help with SPE4 and SPE5 designs
  - Design a monitoring network based on uncertainty
  - Design a yield estimator under conditions of uncertainty
  - Global sensitivity (what does really matter)

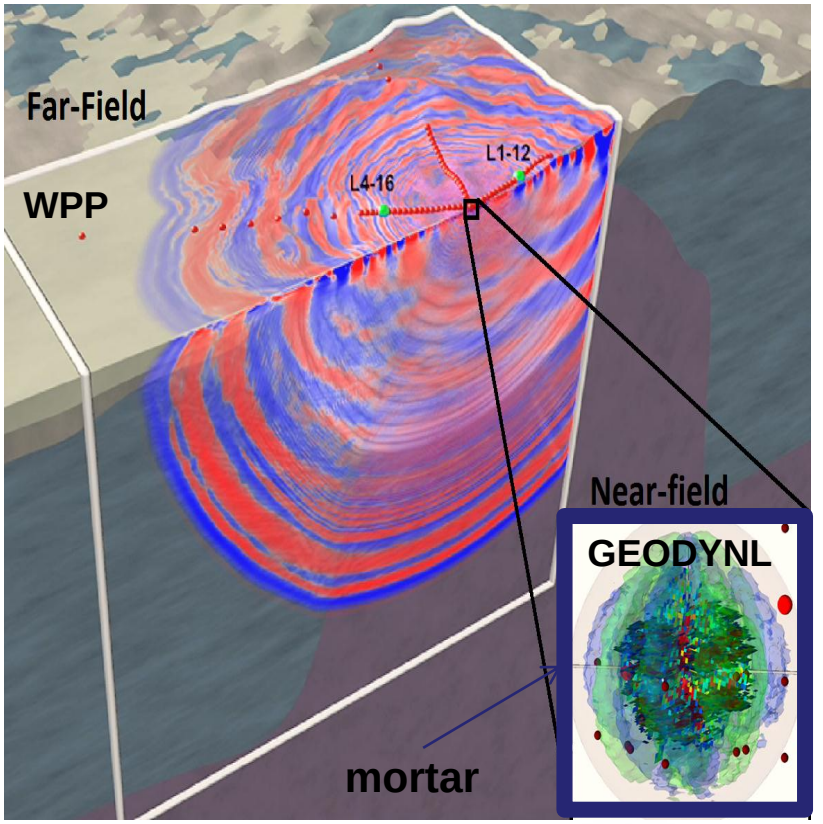

NSTec
NNSA National Nuclear Security Administration
Sandia National Laboratories
Los Alamos NATIONAL LABORATORY EST. 1943

For more information:

Souheil Ezzedine

Ezzedine1@llnl.gov

925-422-0565

Auspices

This work was partially performed under the auspices of the U.S. Department of Energy by Lawrence Livermore National Laboratory under Contract DE-AC52-07NA27344.

Disclaimer

Lawrence Livermore
National Laboratory

SPE SoAR

Sean Ford, Bill Walter, and Rob Mellors, LLNL

- Explosion Model Comparison
  - Canonical explosion models compared to SPE
- Moment Tensor Analysis
  - Inversion for SPE moment tensor solution
- Coda-wave Interferometry
  - Inferences on slowness perturbation due to SPE-2/-3
- Spall
  - Standard spall models compared to SPE

An Explosion Model Comparison with Insights from the Source Physics Experiment

Sean Ford and Bill Walter

SSA 2013

sean@llnl.gov

Lawrence Livermore National Laboratory is operated by Lawrence Livermore National Security, LLC, for the U.S. Department of Energy, National Nuclear Security Administration under Contract DE-AC52-07NA27344.

LLNL-PRES-635238

Motivation & Introduction

- Predict absolute ground motion for explosions using non-standard testing practice (i.e., not NTS or STS media at ~100 m/kT$^{1/3}$)

- Mueller & Murphy (1971) MM71
  - Scaling laws for seismic observables

- Denny & Johnson (1991) DJ91
  - Regression analysis for seismic observables

Previous work

- Denny (1998)
  - DOB
  - DJ91 f_c < observed

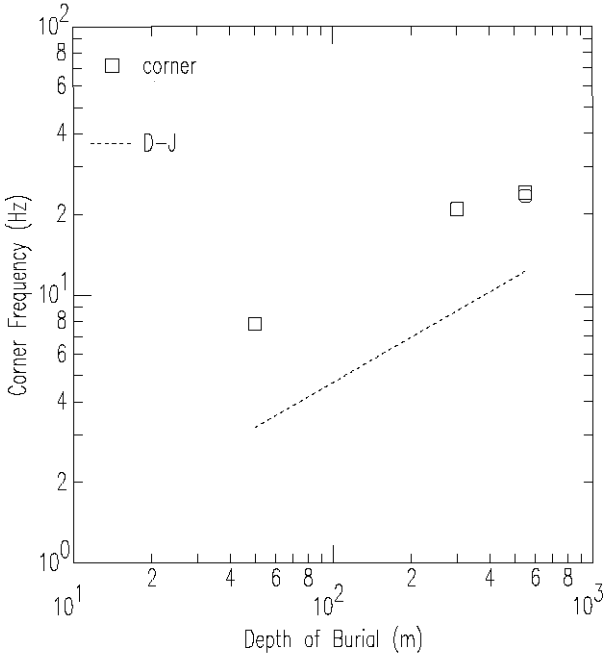

Previous work

- Denny (1998)
  - DOB
  - DJ91 f_c < observed
- Stump et al. (1999)
  - NPE
  - MM71 with $r_c \sim W^{1/3}$

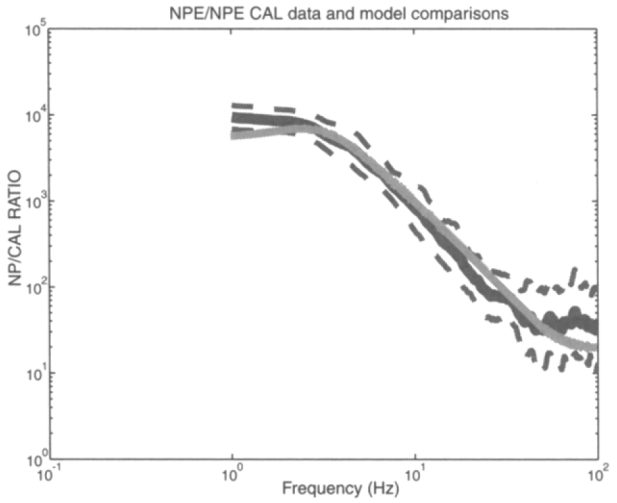

Previous work

- Denny (1998)
  - DOB
  - DJ91 f_c < observed
- Stump et al. (1999)
  - NPE
  - MM71 with $r_c \sim W^{1/3}$
- Rougier et al. (2011)
  - Simulation
  - DJ91 $r_c \cong$ predicted

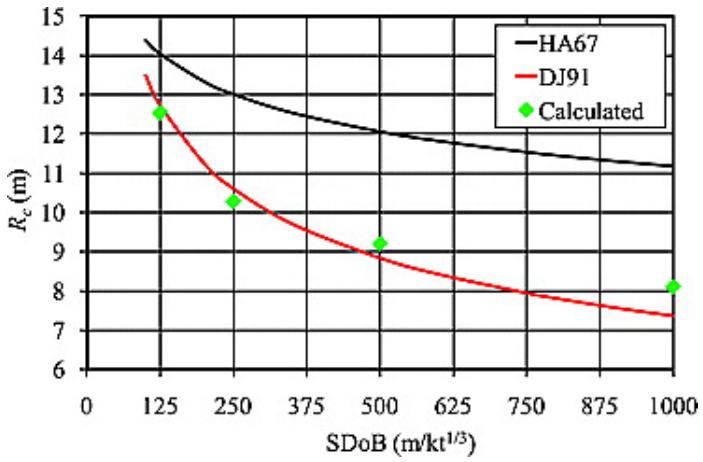

Model comparison (M_0)

- Denny & Johnson (1991) DJ91
  - Combine chem and nuke data in cavity regression where $r_c \sim W^{1/3}$ so $M_0 \sim W$
  - Relate cavity to "measured moment"

$$M_0^{DJ} = 4.2743 \times 10^{10} W \alpha^2 \beta^{-1.1544} P^{-0.4385} 10^{-0.0344 GP} \rho$$

Model comparison (M_0)

- Denny & Johnson (1991) DJ91
  - Combine chem and nuke data in cavity regression where $r_c \sim W^{1/3}$ so $M_0 \sim W$
  - Relate cavity to "measured moment"

$$M_0^{DJ} = 4.2743 \times 10^{10} W \alpha^2 \beta^{-1.1544} P^{-0.4385} 10^{-0.0344 GP} \rho$$

- Mueller & Murphy (1971) MM71
  - Assume scaling in amplitude and yield for nuke data
  - Employ a cavity regression where $r_c \sim W^{0.29}$ so $M_0 \sim W^{0.87}$

$$M_0^{MM} = 3.1416 W^{0.87} \alpha^2 \beta^{-2} R_0^3 P_0 h_0^{1/3} h^{-1/3}$$

Model comparison (f_c)

- DJ91 relate cavity to source radius with $\beta / \pi f_c$

$$f_c^{DJ} = 0.2045 W^{-1/3} \beta^{-0.0642} P^{0.5522} 10^{0.0025 GP} \rho^{-0.7245}$$

Model comparison (f_c)

- DJ91 relate cavity to source radius with $\beta / \pi f_c$

$$f_c^{DJ} = 0.2045 W^{-1/3} \beta^{-0.0642} P^{0.5522} 10^{0.0025 GP} \rho^{-0.7245}$$

- MM71 relate elastic radius to ω_0 with α / f_c

$$f_c^{MM} = 0.1592 W^{-1/3} \alpha R_0^{-1} h_0^{-1/n} h^{1/n}$$

Model comparison (f_c)

- DJ91 relate cavity to source radius with $\beta / \pi f_c$

$$f_c^{DJ} = 0.2045 W^{-1/3} \beta^{-0.0642} P^{0.5522} 10^{0.0025 GP} \rho^{-0.7245}$$

- MM71 relate elastic radius to ω_0 with α / f_c

$$f_c^{MM} = 0.1592 W^{-1/3} \alpha R_0^{-1} h_0^{-1/n} h^{1/n}$$

- DJ91/MM71 ~ f(DOB)
  - Allow for chem/nuke factor

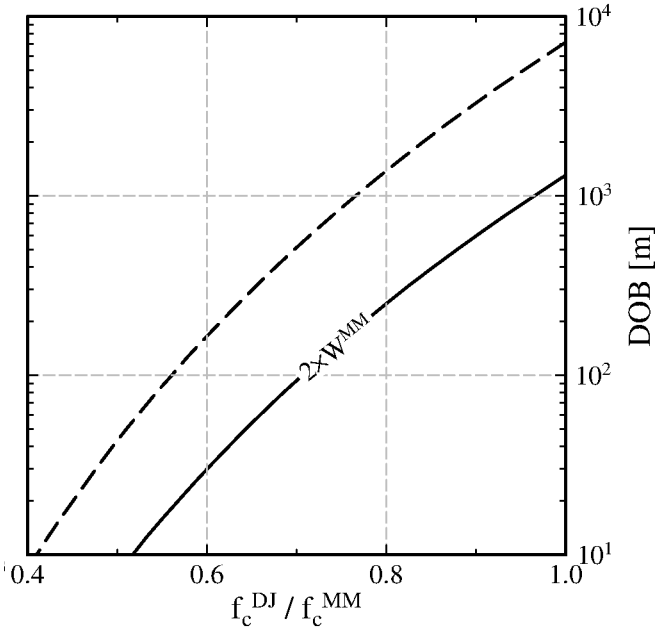

Model comparison (*W*)

- Invert DJ91 and MM71 M_0 relationship for yield

$$W^{DJ} = 2.940 \times 10^{-10} \beta^{1.1544} P^{0.4385} 10^{0.0344 GP} \Psi_{\infty}$$

$$W^{MM} = 4.9207 \rho^{1.1494} \beta^{2.2989} R_0^{-3.4483} P_0^{-1.1494} h_0^{-0.3831} h^{0.3831} \Psi_{\infty}^{1.1494}$$

Model comparison (*W*)

- Invert DJ91 and MM71 M_0 relationship for yield

$$W^{DJ} = 2.940 \times 10^{-10} \beta^{1.1544} P^{0.4385} 10^{0.0344GP} \Psi_\infty$$

$$W^{MM} = 4.9207 \rho^{1.1494} \beta^{2.2989} R_0^{-3.4483} P_0^{-1.1494} h_0^{-0.3831} h^{0.3831} \Psi_\infty^{1.1494}$$

  - Assume shot point ρ ~ overburden ρ $\quad \dfrac{W^{DJ}}{W^{MM}} = F \dfrac{h^{0.0554}}{M_0^{0.1494}}$

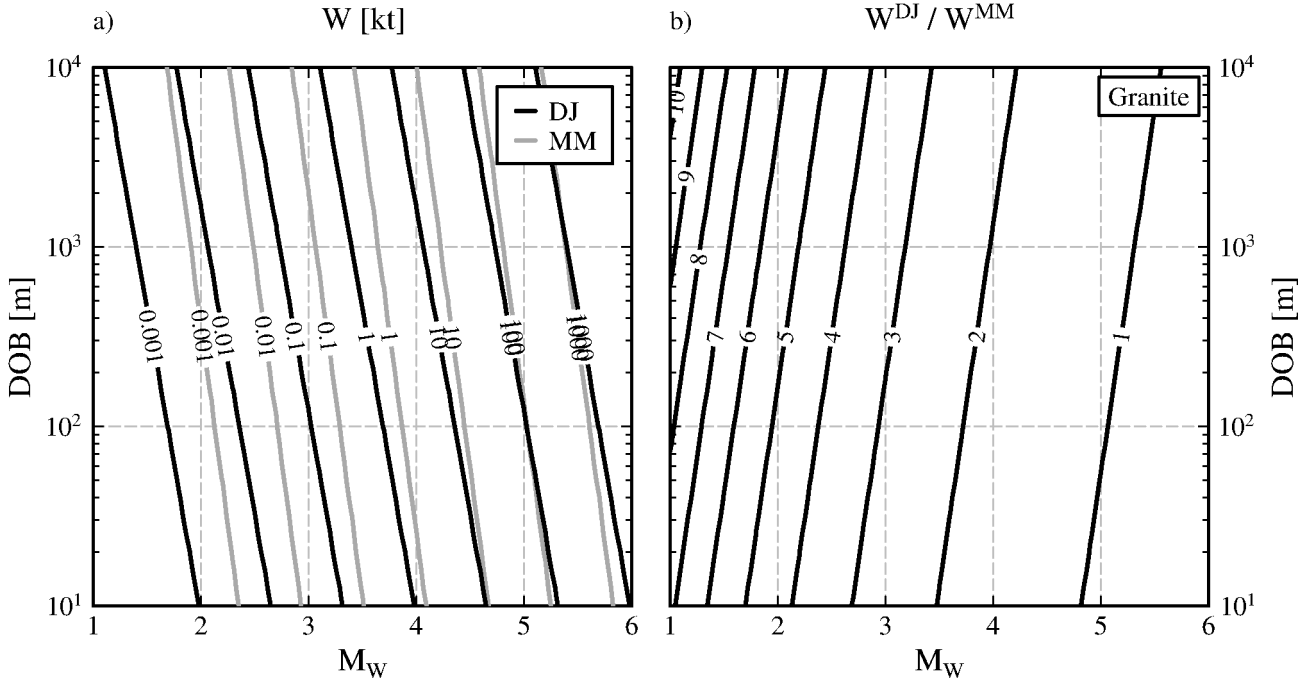

Model comparison (*W*)

- Invert DJ91 and MM71 M_0 relationship for yield

$$W^{DJ} = 2.940 \times 10^{-10} \beta^{1.1544} P^{0.4385} 10^{0.0344GP} \Psi_\infty$$

$$W^{MM} = 4.9207 \rho^{1.1494} \beta^{2.2989} R_0^{-3.4483} P_0^{-1.1494} h_0^{-0.3831} h^{0.3831} \Psi_\infty^{1.1494}$$

  - Assume shot point ρ ~ overburden ρ $\quad \dfrac{W^{DJ}}{W^{MM}} = F \dfrac{h^{0.0554}}{M_0^{0.1494}}$

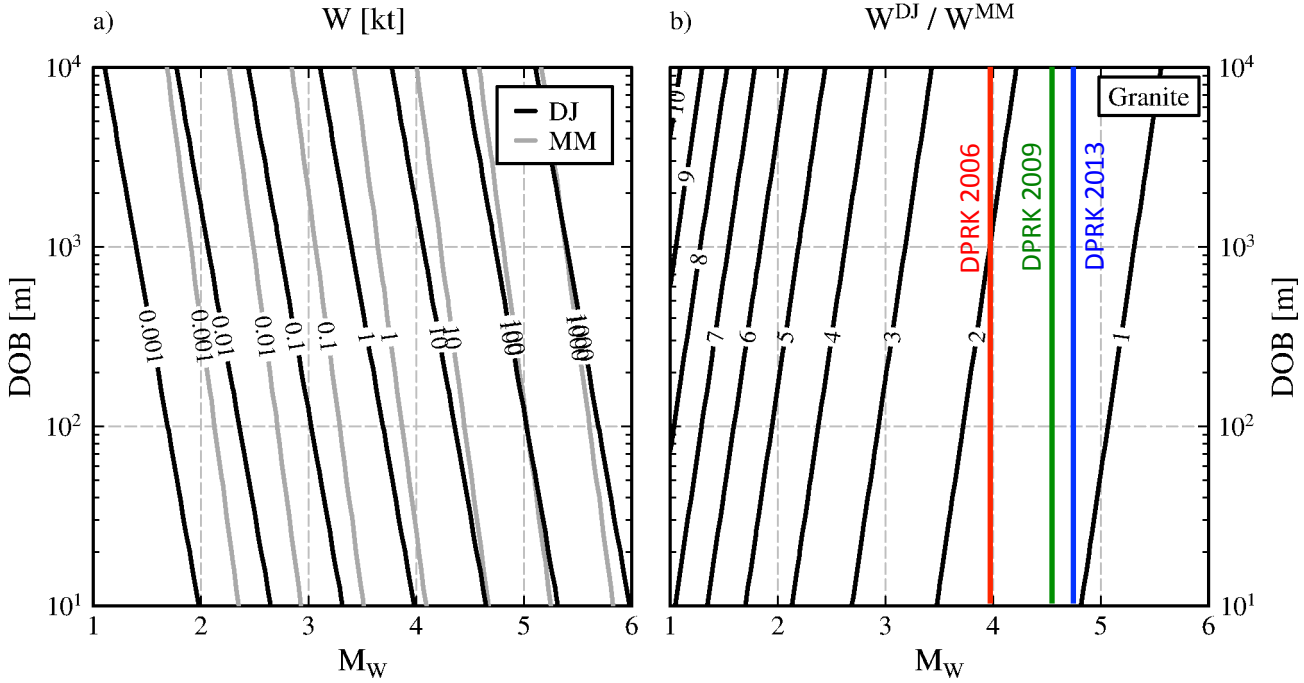

Model comparison (*W*)

- Invert DJ91 and MM71 M_0 relationship for yield

$$W^{DJ} = 2.940 \times 10^{-10} \beta^{1.1544} P^{0.4385} 10^{0.0344GP} \Psi_\infty$$

$$W^{MM} = 4.9207 \rho^{1.1494} \beta^{2.2989} R_0^{-3.4483} P_0^{-1.1494} h_0^{-0.3831} h^{0.3831} \Psi_\infty^{1.1494}$$

  - Assume shot point ρ ~ overburden ρ $\quad \dfrac{W^{DJ}}{W^{MM}} = F \dfrac{h^{0.0554}}{M_0^{0.1494}}$

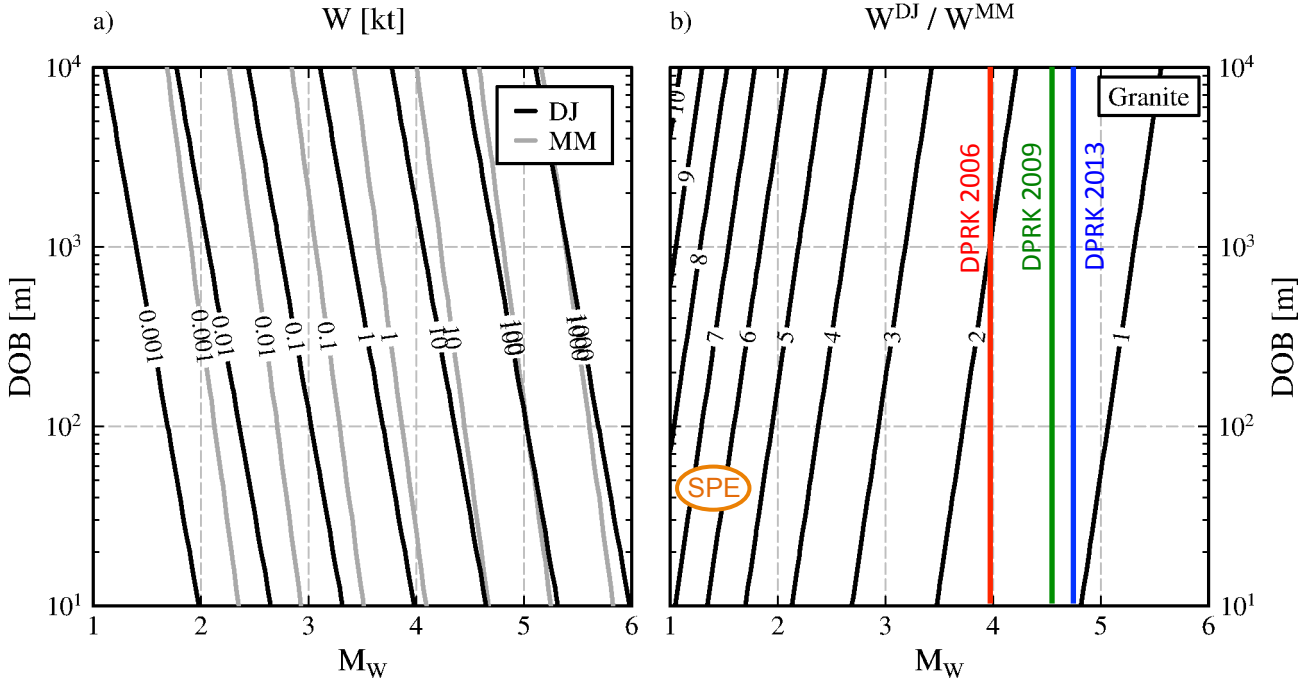

Data: SPE

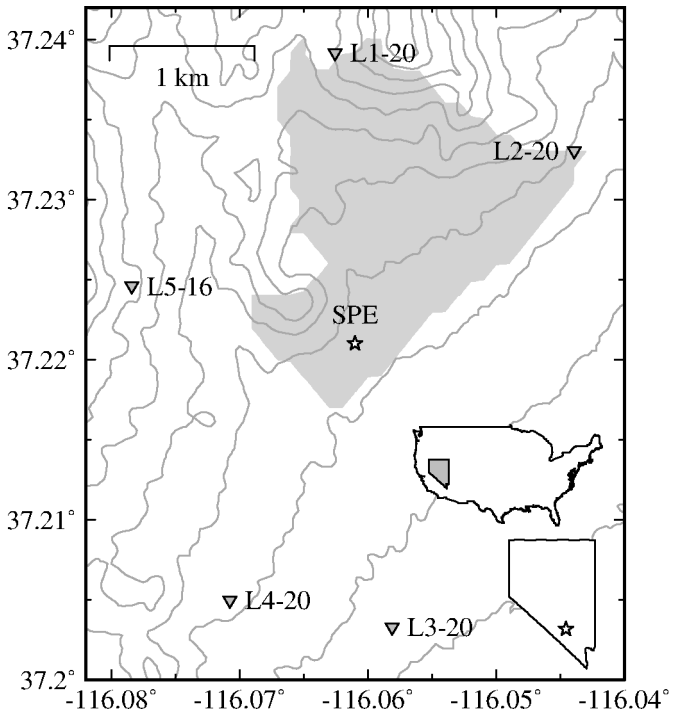

Shot	Yield [kg] (=TNT)	Depth [m]	sDOB [m/kT$^{1/3}$]
SPE-1	85.2	54.9	990
SPE-2	991.6	45.7	364

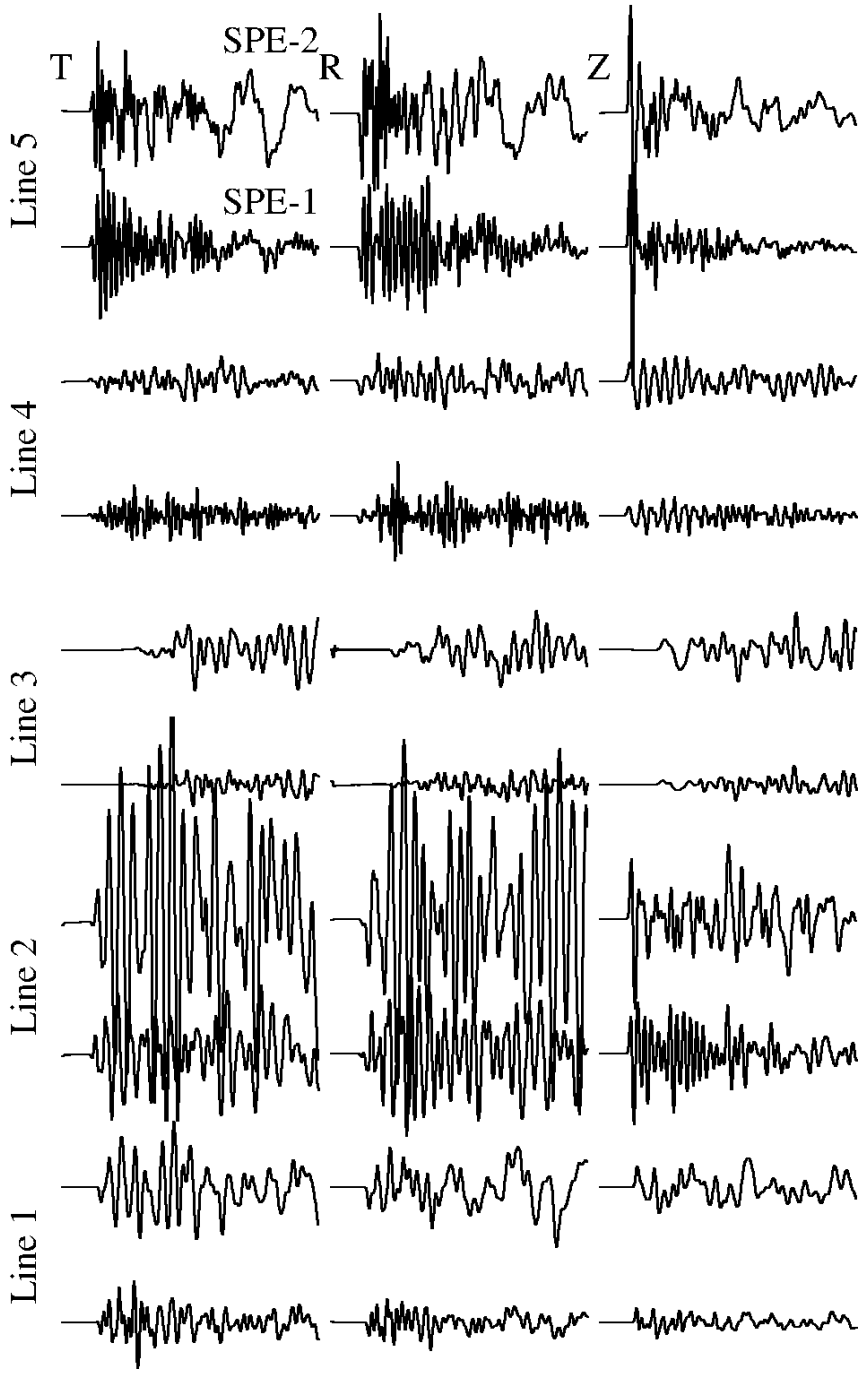

Relative comparison: Spectral ratio

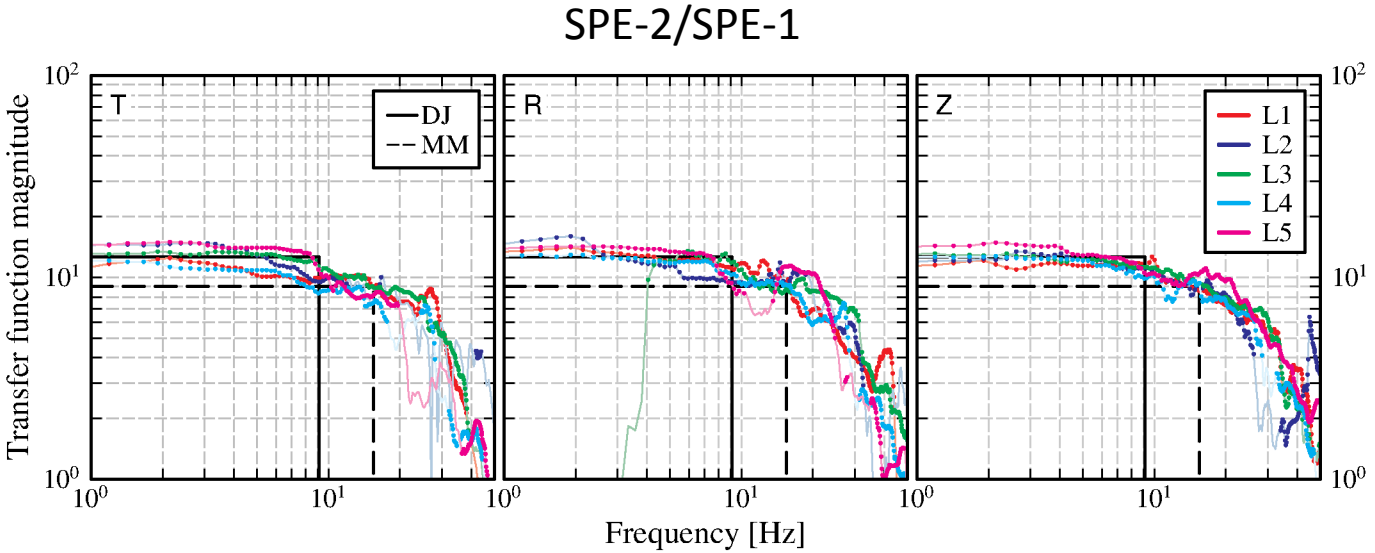

- MM under-predicts long period ratio
- DJ under-predicts corner-frequency

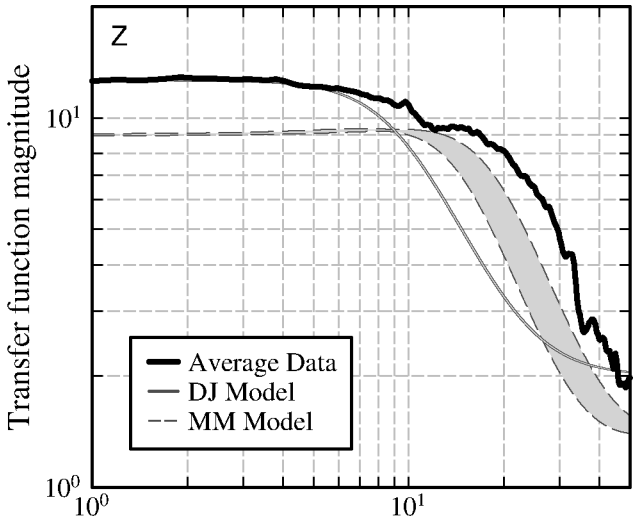

Relative comparison: Spectral ratio

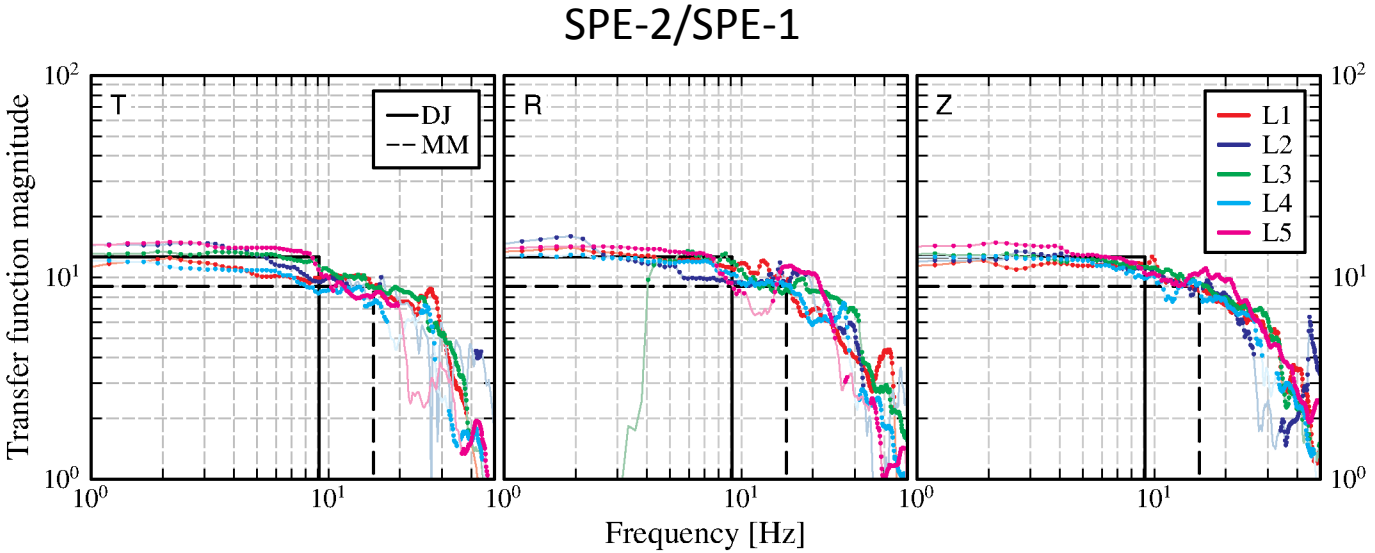

- Altering MM71 so that $r_c \sim W^{1/3}$ (Murphy & Barker, 1994) gives a better fit to the long-period ratio

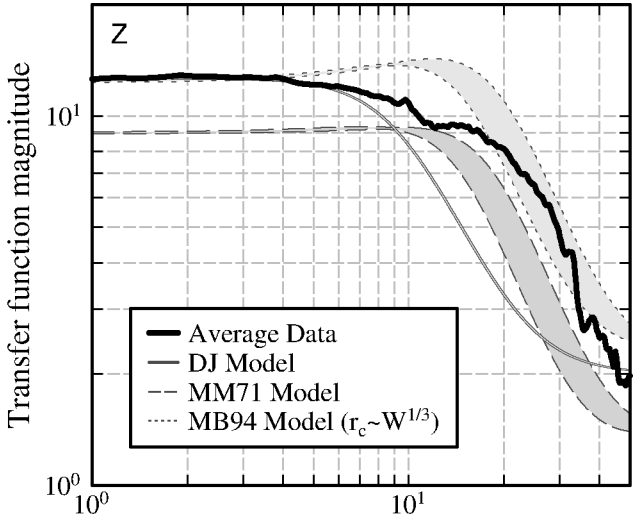

Absolute comparison: MT synthetic

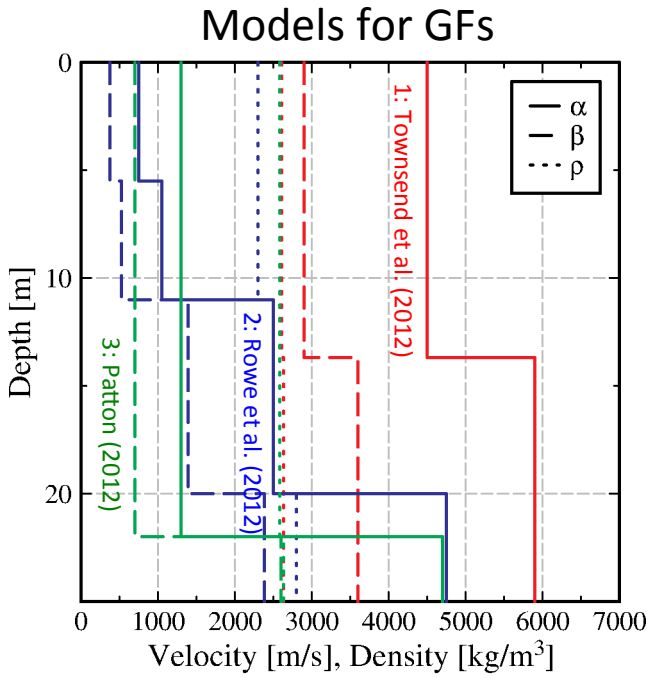

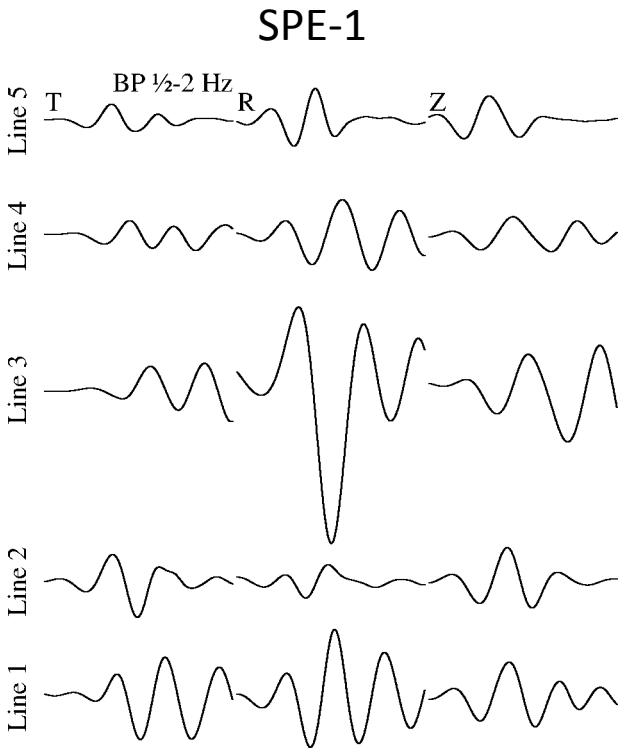

- Energy on tangential component
- Site effects along some lines

Absolute comparison: MT synthetic

Model	M_0^{DJ} [nAk]
1	48.5
2	52.5
3	44.8

Note: 1 Ak = 10^{18} N-m

SPE-1

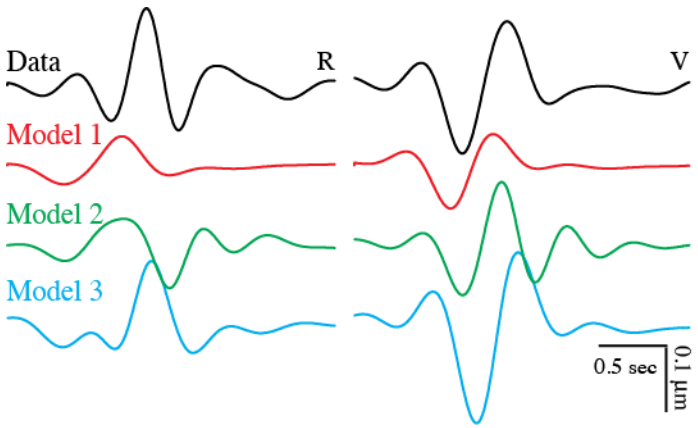

- DJ91 prediction near the observed displacement
- Best phase and amplitude fit by Model 3 (Patton, 2012)

Absolute comparison: MT synthetic

Model	M_0^{DJ} [nAk]	M_0^{MM} [nAk] 1×W	2×W
1	48.5	251.7	460.1
2	52.5	373.3	682.3
3	44.8	306.3	559.7

Note: 1 Ak = 10^{18} N-m

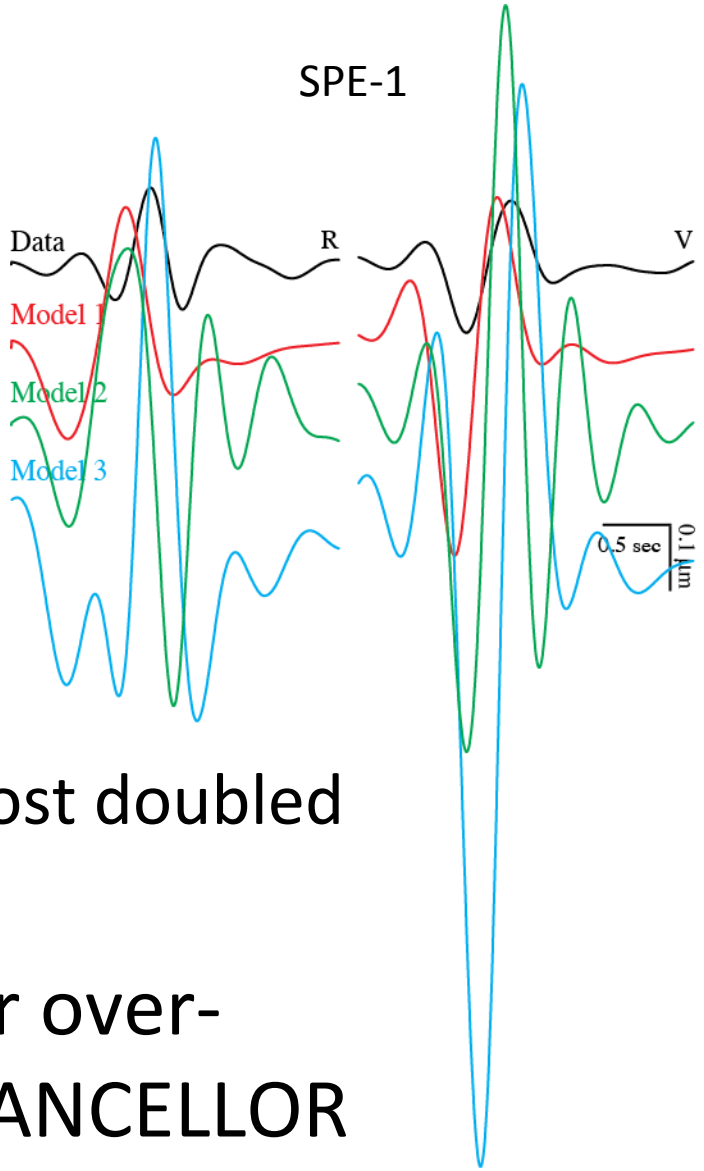

- MM71 over-predicts M_0
  - Synthetic amplitudes are almost doubled for chem/nuke factor = 2
- Johnson (1988) found similar over-prediction for HARZER & CHANCELLOR

Conclusions & Future work

- Differences in yield predictions are greatest for small and/or deeply buried explosions
- SPE is most consistent with D&J-predicted M_0 and M&M-predicted f_c

Conclusions & Future work

- Differences in yield predictions are greatest for small and/or deeply buried explosions
- SPE is most consistent with D&J-predicted M_0 and M&M-predicted f_c

- Future work: Chem/Nuke at depth (Xu et al., '12)

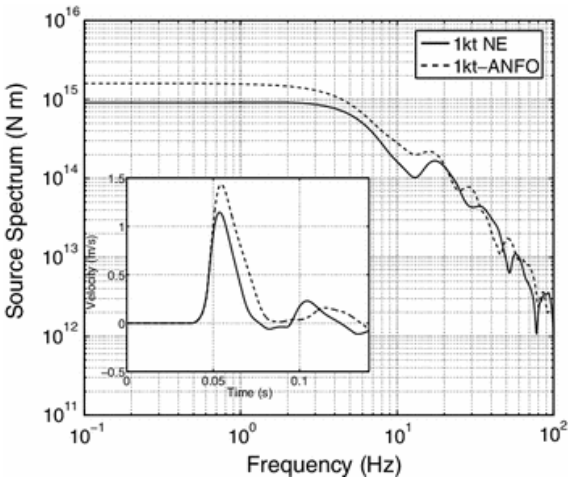

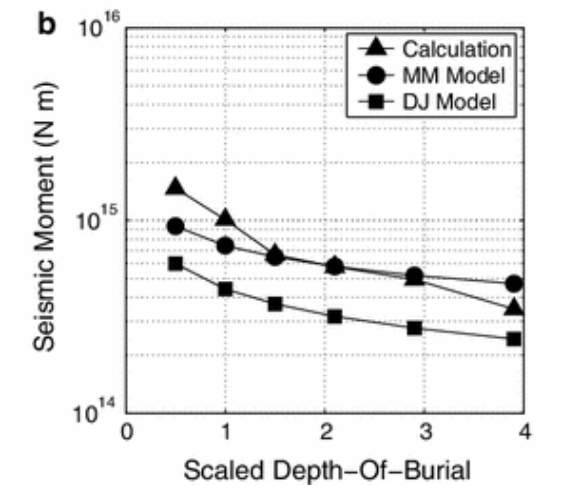

Conclusions & Future work

- Differences in yield predictions are greatest for small and/or deeply buried explosions
- SPE is most consistent with D&J-predicted M_0 and M&M-predicted f_c

- Future work: New model

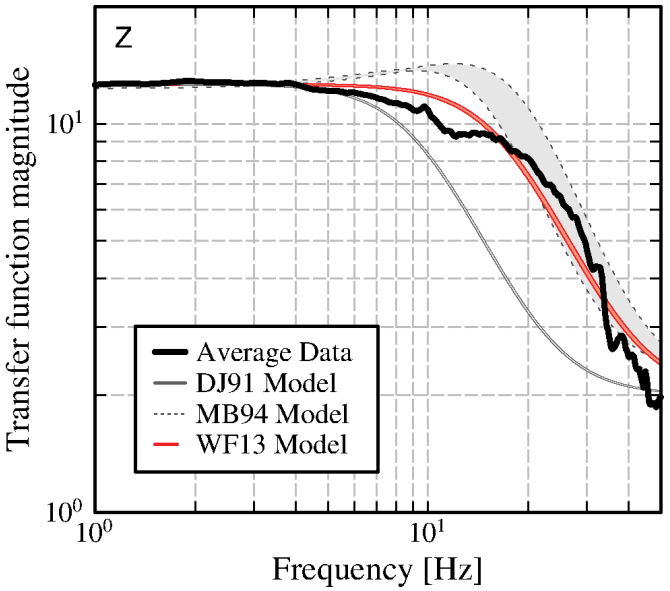

Moment tensor analysis of SPE-1 and -2

Sean Ford, Rob Mellors, and Bill Walter

SSA 2012

sean@llnl.gov

LLNL-PRES-552338

Calibration 1: Response

- H/V ratios of regional events similar between SN and TPNV
  - H/V noise ratio SN=5 TPNV=1¼ (much noisier horizontals)
- Long-period (15-25s) ratio of SN to TPNV teleseismic event provided ground-motion gain corrections
  - CMG-40T = 1, Trillium-120 = 1.5

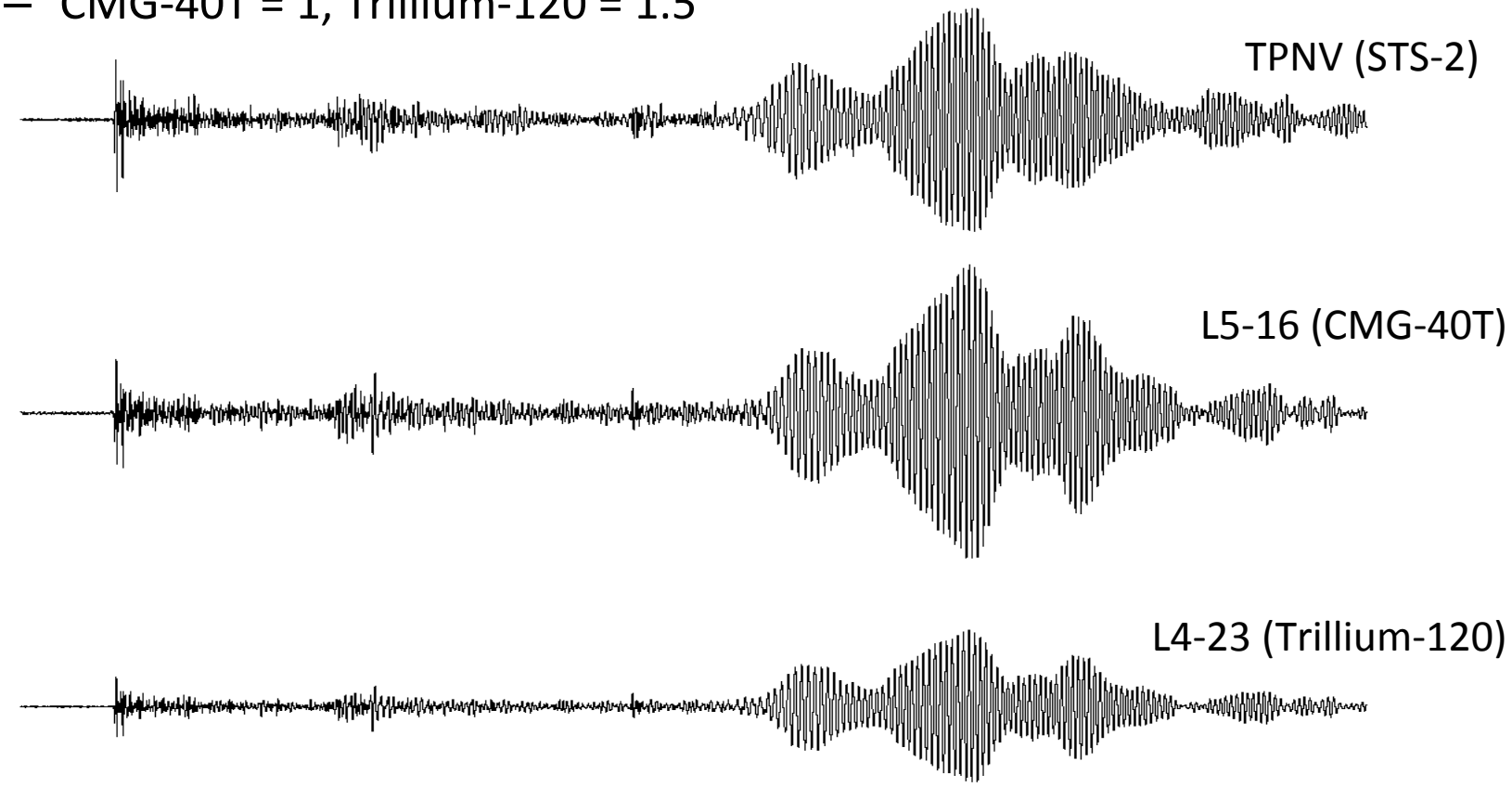

Calibration 2: Orientation

- Horizontal particle motion of teleseismic event
  - L1-20/L2-20/L3-20/L4-20/L5-16 = +5/0/?/0/-1

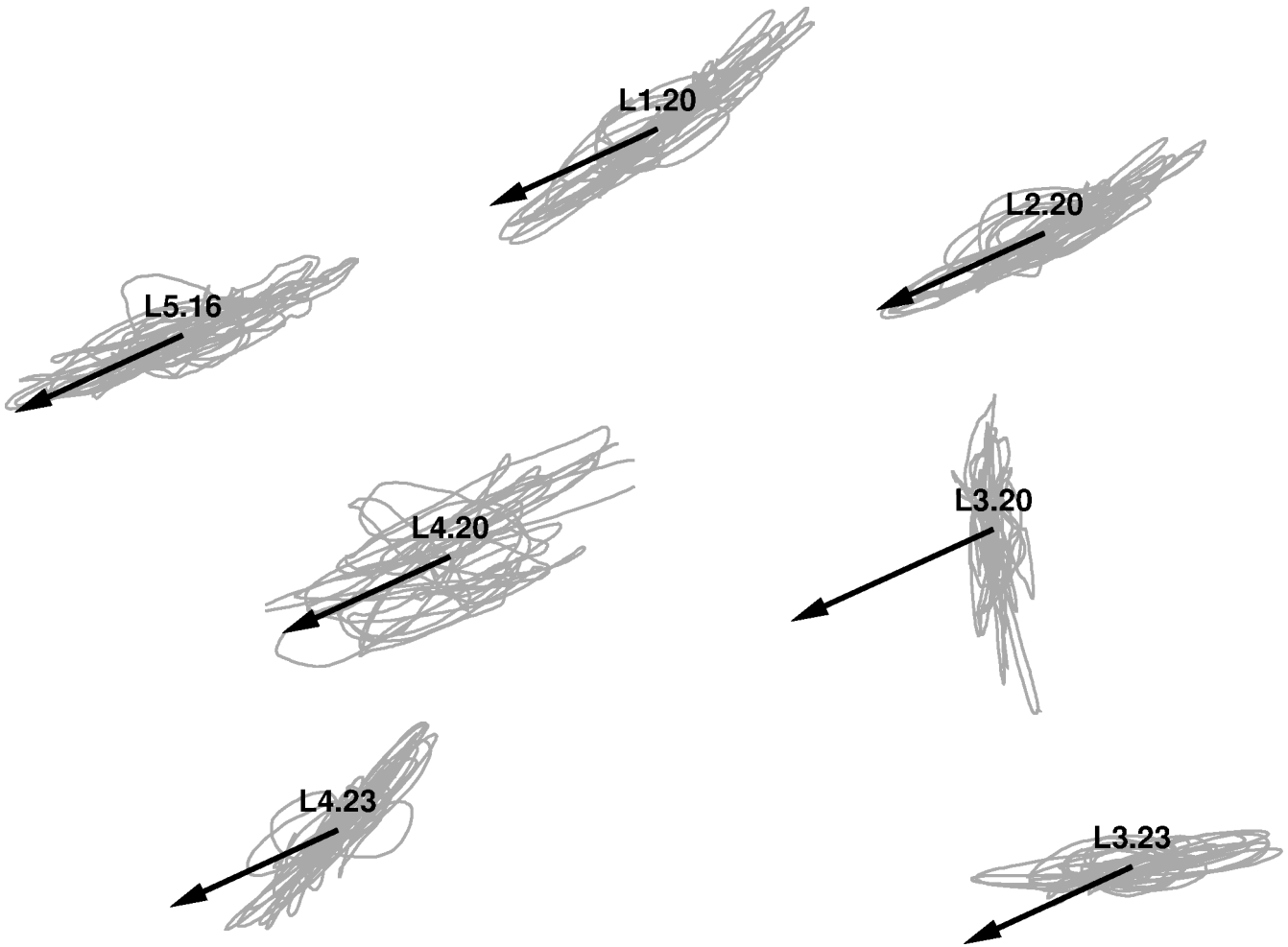

Data

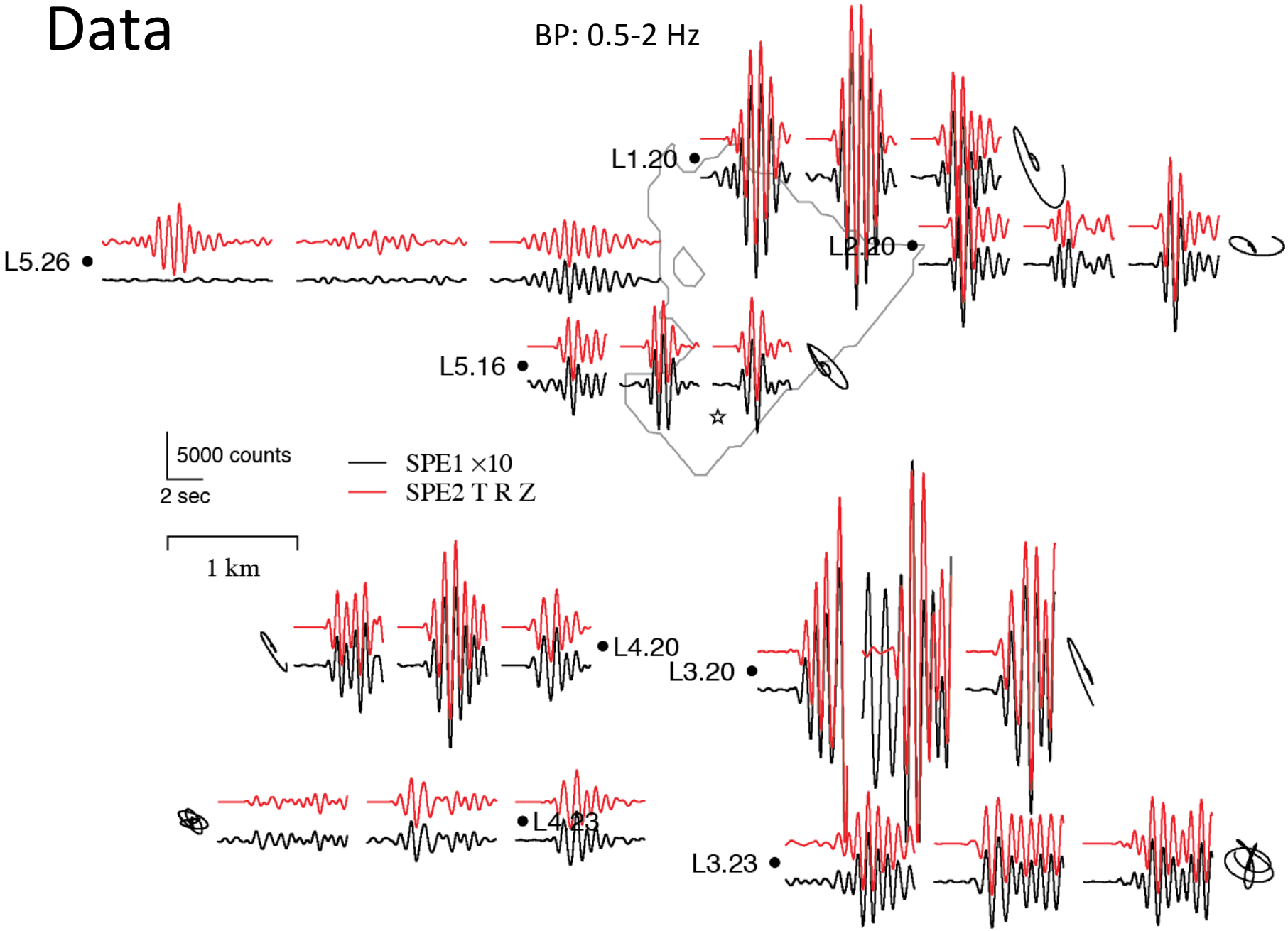
BP: 0.5-2 Hz
L1.20
L2.20
L5.26
L5.16
5000 counts
2 sec
SPE1 ×10
SPE2 T R Z
1 km
L4.20
L3.20
L4.23
L3.23

Velocity model

- V_P/V_S = 5000/2700 [m/s]
  - V_P/V_S = 1.852 v = 0.294
- 20m thick weathered layer
  - V_P/V_S = 2900/1600 [m/s]
- ρ = 2600/2650 kg/m^3
- Q = 600 / 300
- Constant to depth

Well log (Townsend et al., 2012)

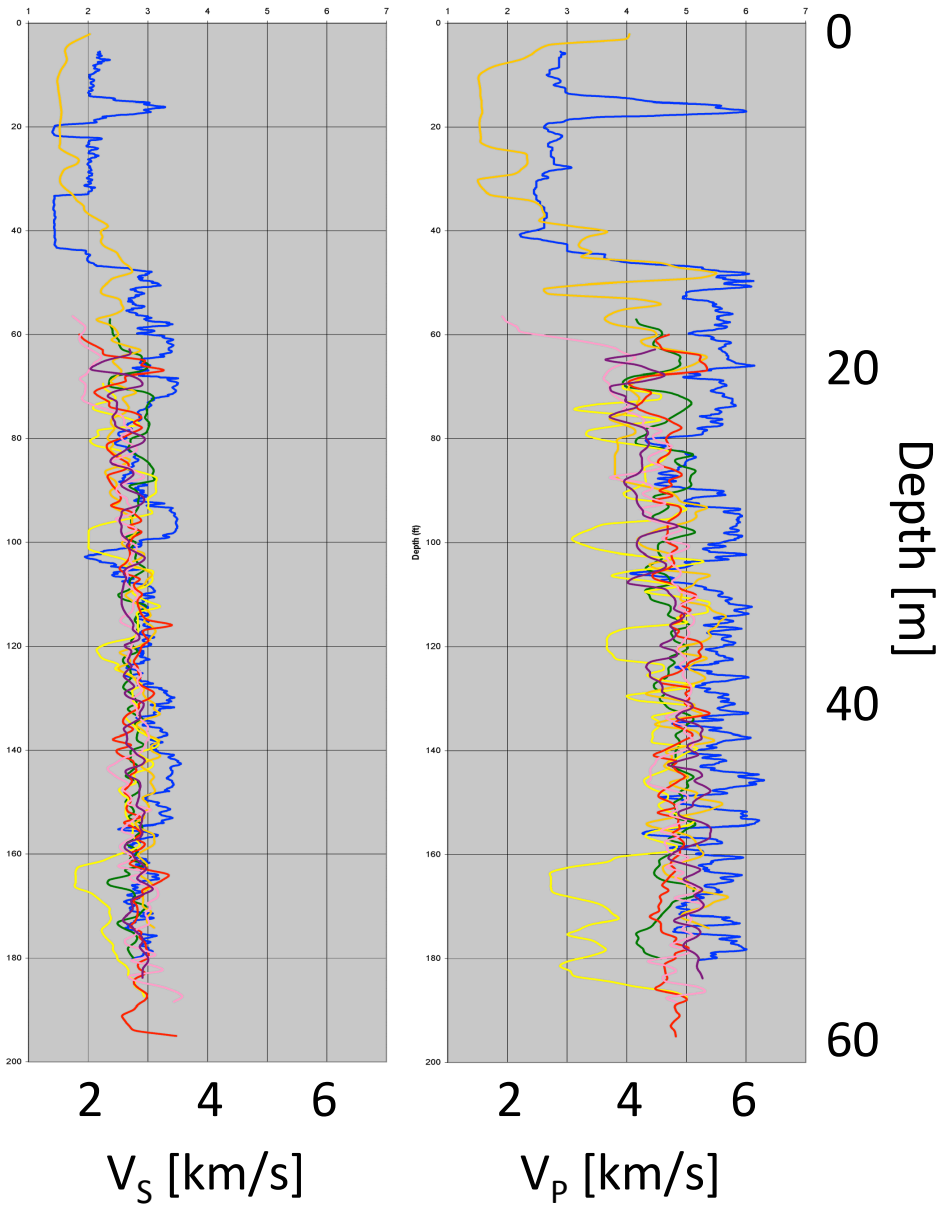

Data

3-component

Displacement

0.5 – 2 Hz

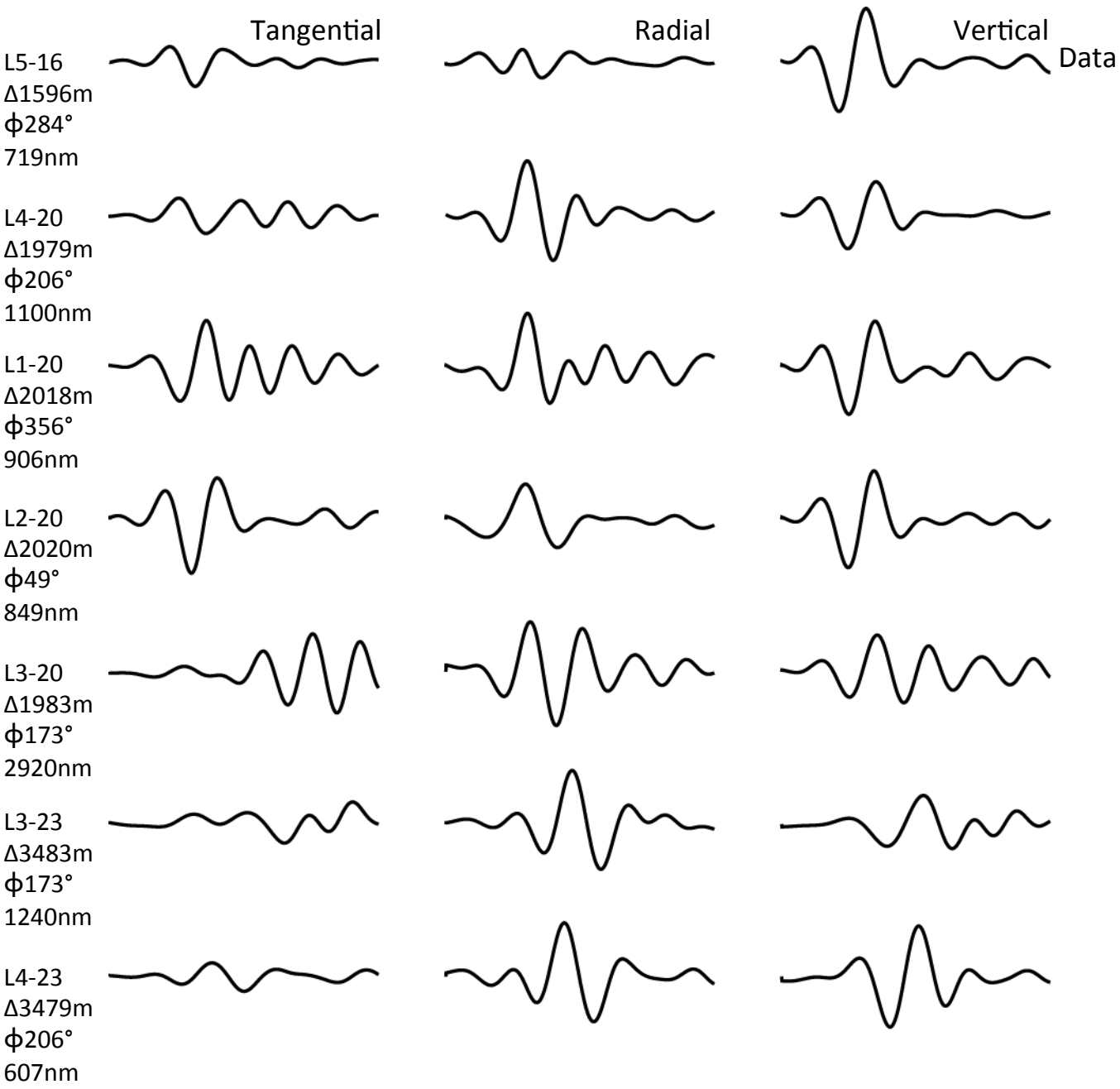

Explosion

$M_0 6.3 \times 10^{11}$ N-m

$M_W 1.8$

VR 44.5%

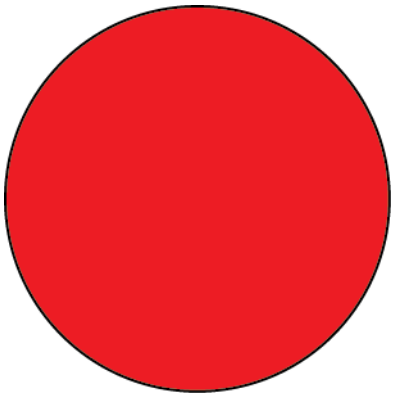

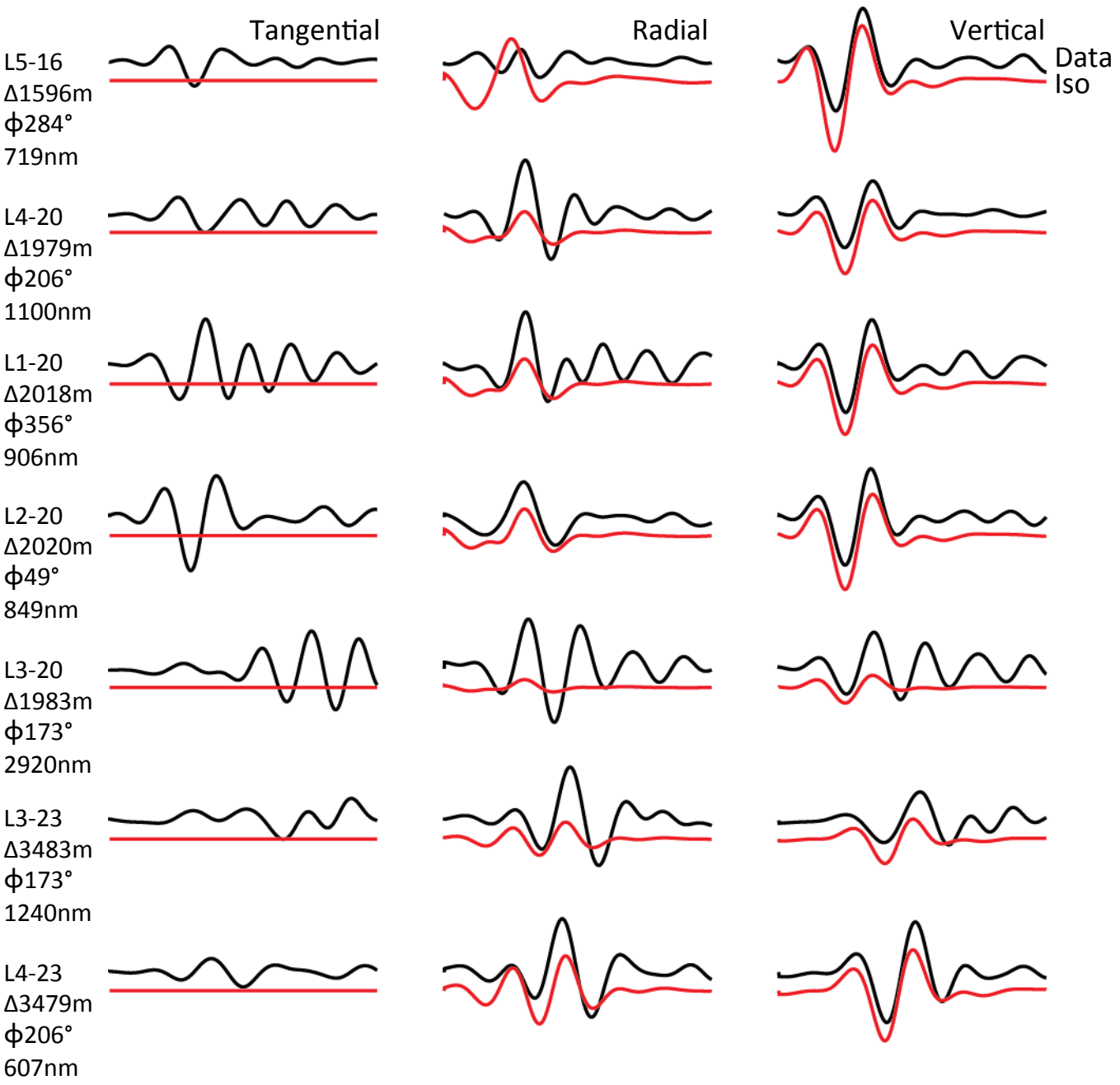

Full MT

$M_0$2.1×10^{12} N-m

M_W2.2

VR 48.4%

ISO/CLVD/DC

75 / 20 / 5

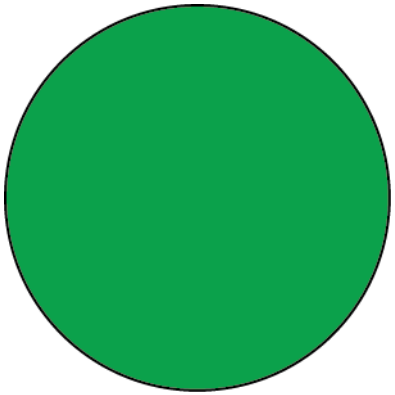

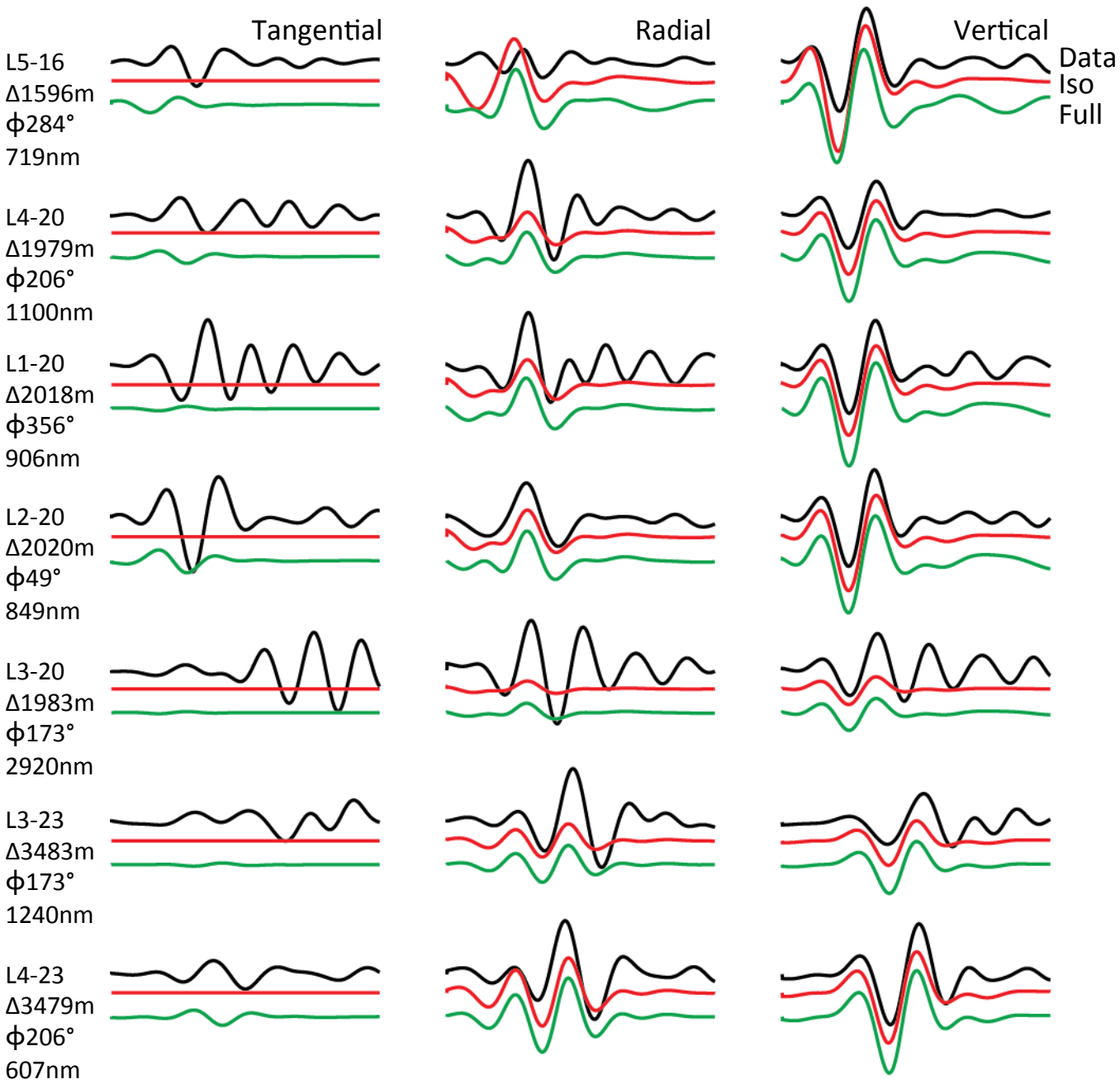

Deviatoric

$M_0 4.1 \times 10^{11}$ N-m

$M_W 1.7$

VR 42.3%

CLVD/DC

68 / 32

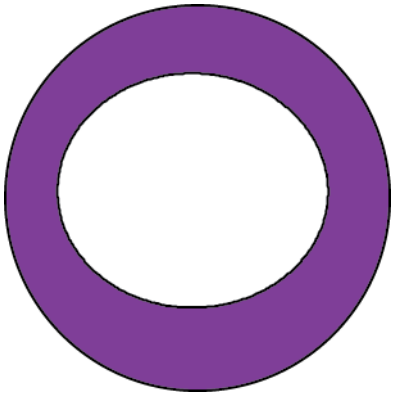

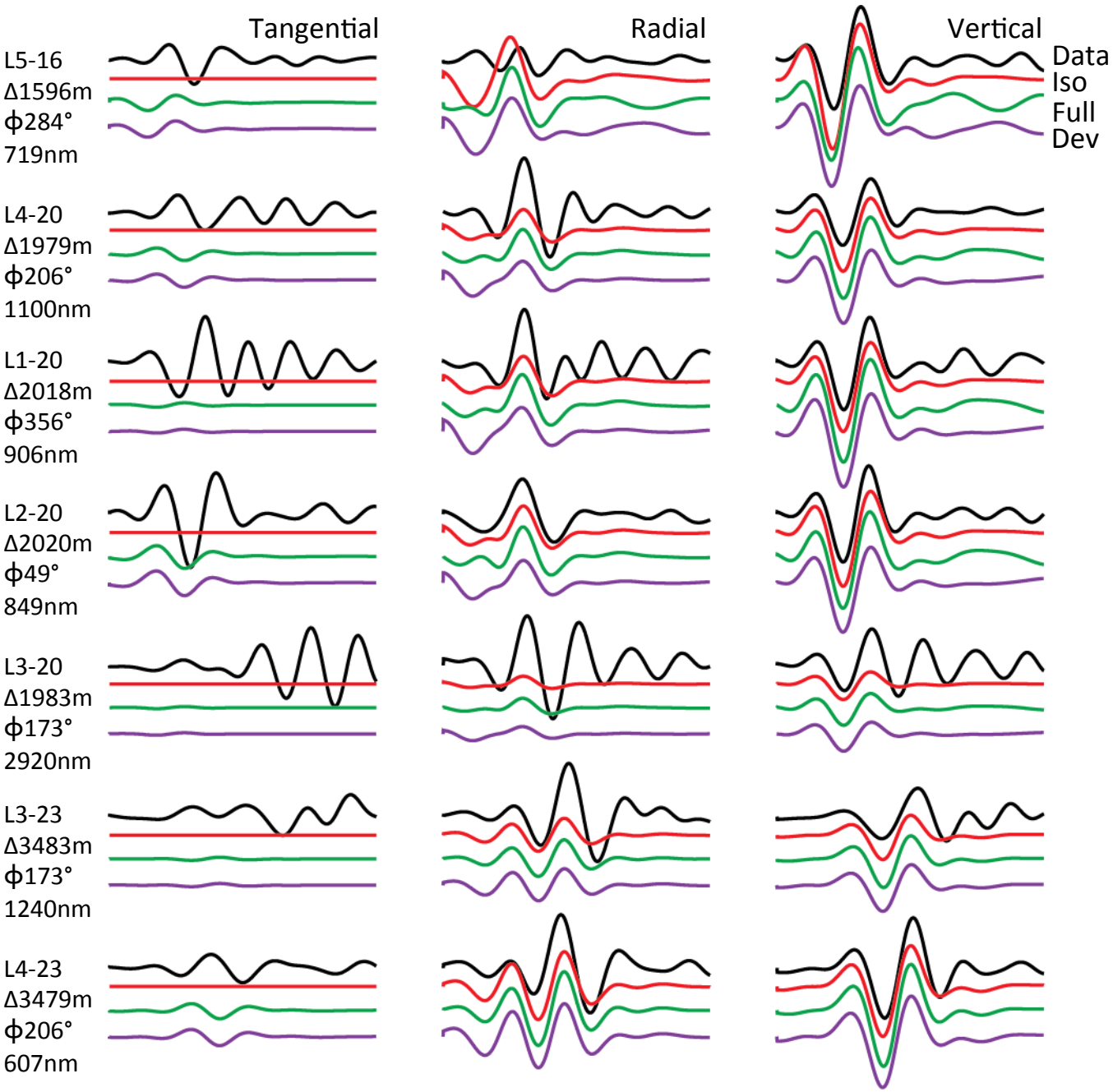

Best-DC

$M_0 3.1 \times 10^{11}$ N-m

$M_W 1.6$

VR 36.7%

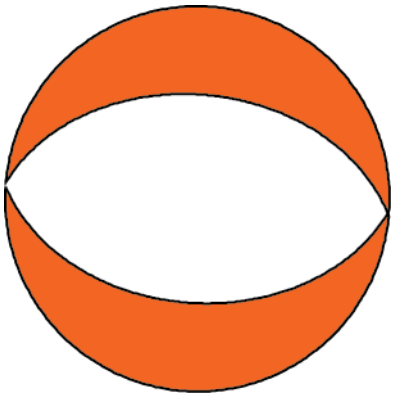

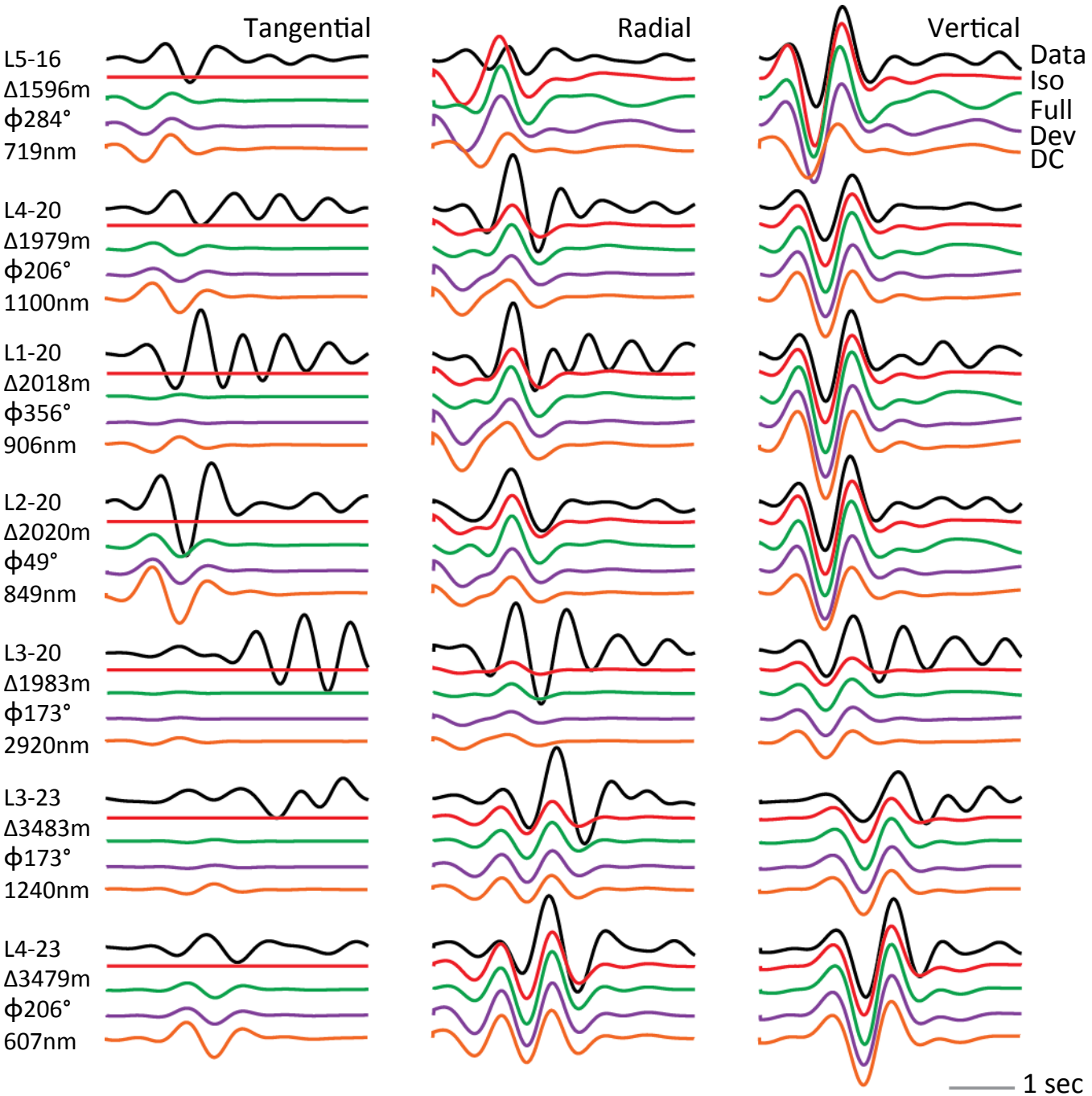

Explosion

$M_0 10.9 \times 10^{11}$ N-m

$M_W 1.9$

60%

+ DC

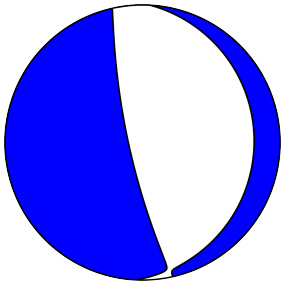

$M_0 8.6 \times 10^{11}$ N-m

$M_W 1.7$

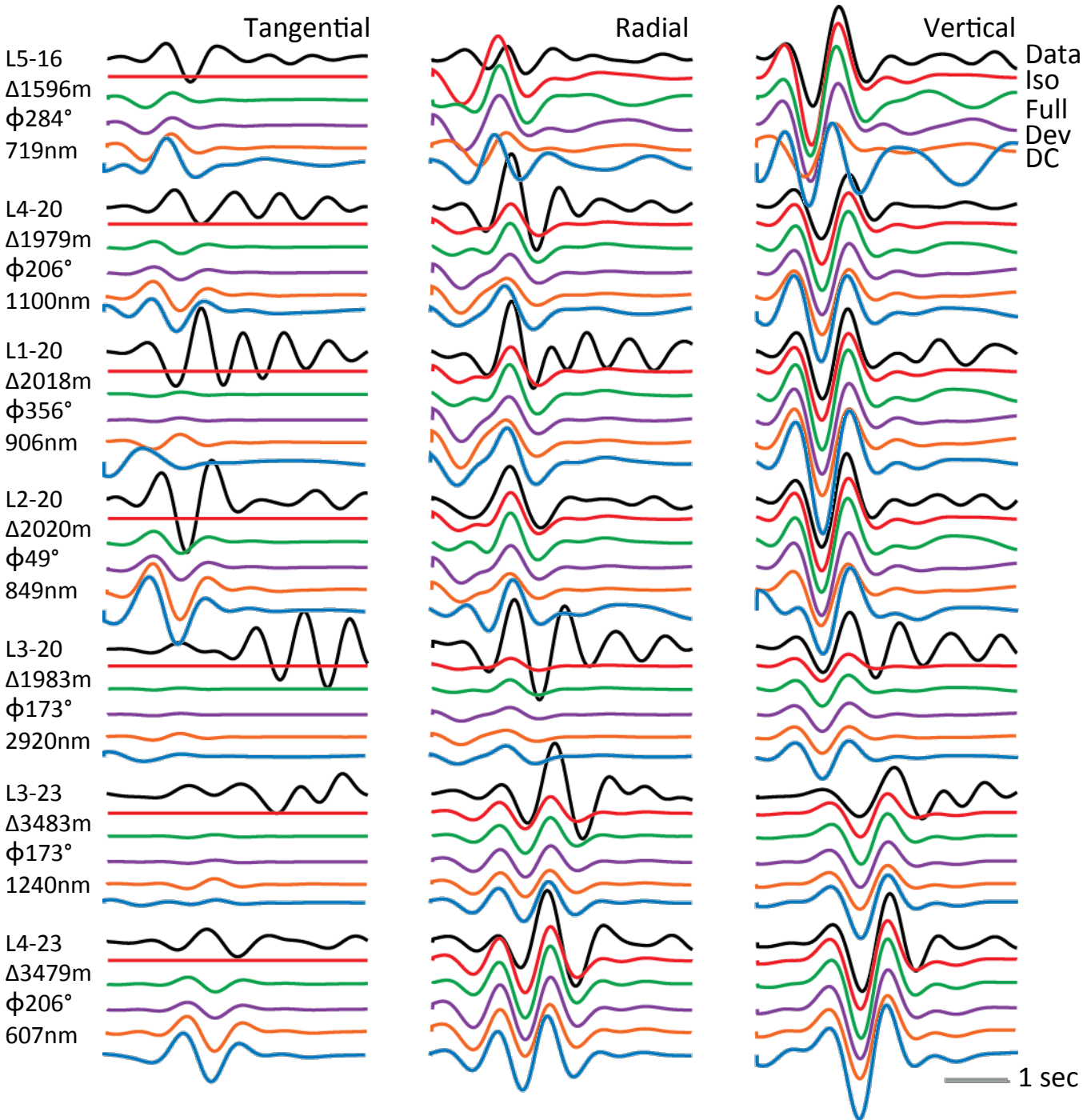

Explosion

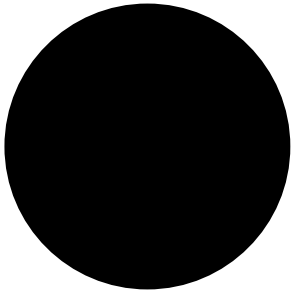

1D GFs

M_0 63×10^{10} N-m

3D GFs

M_0 38×10^{10} N-m

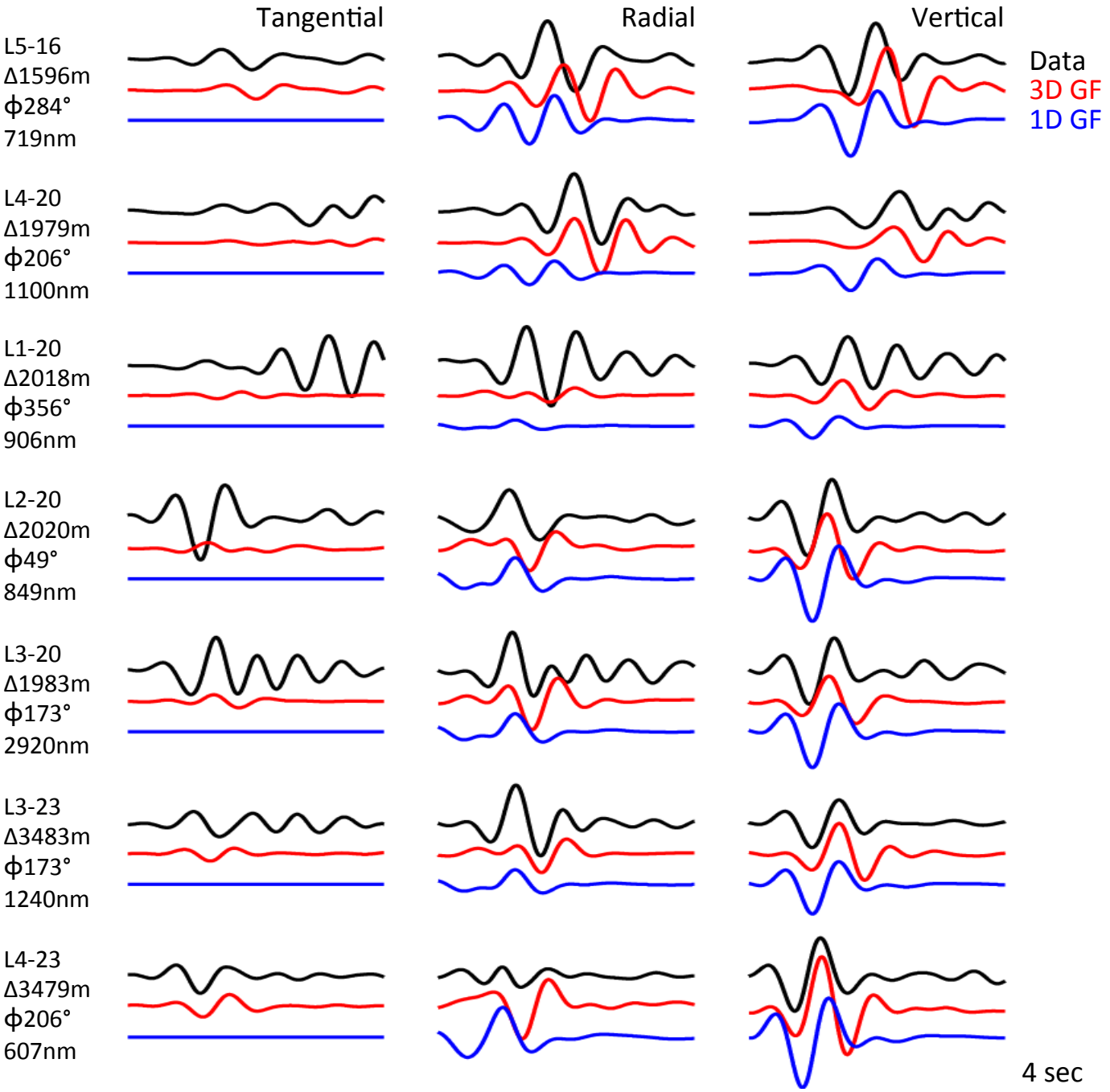

Source-type plot (Hudson et al., 1989)

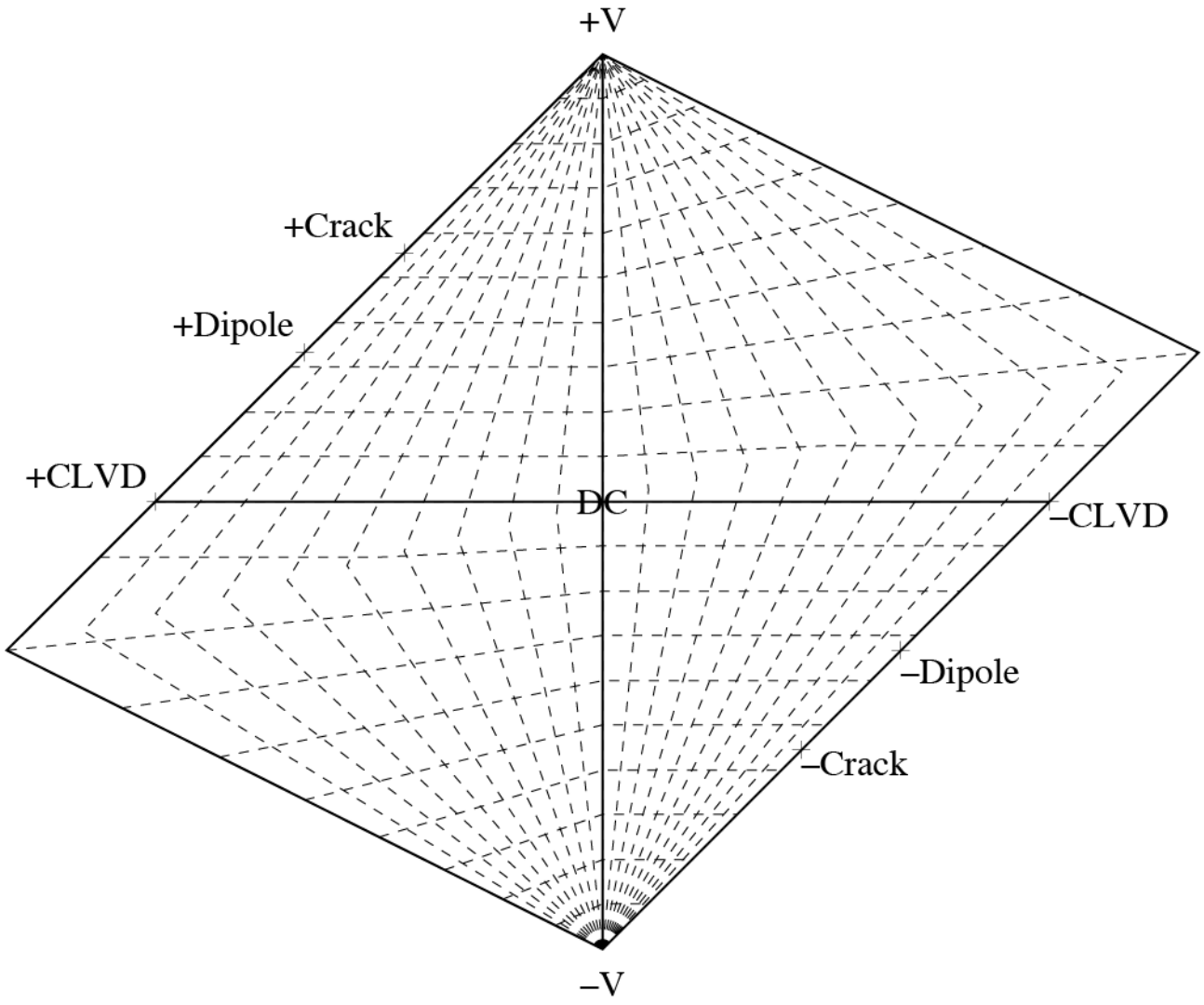

Source-type plot (Hudson et al., 1989)

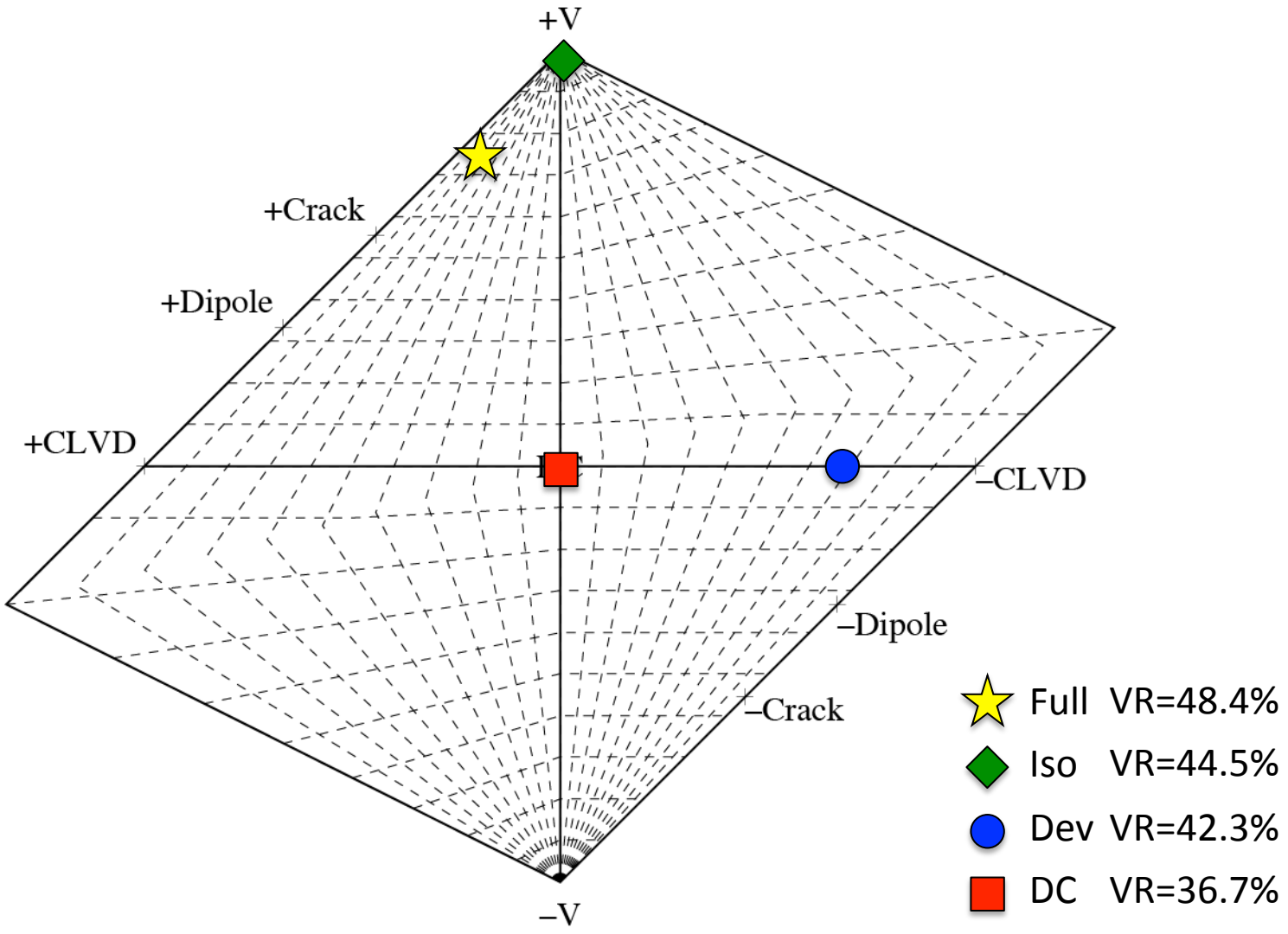

SPE-1

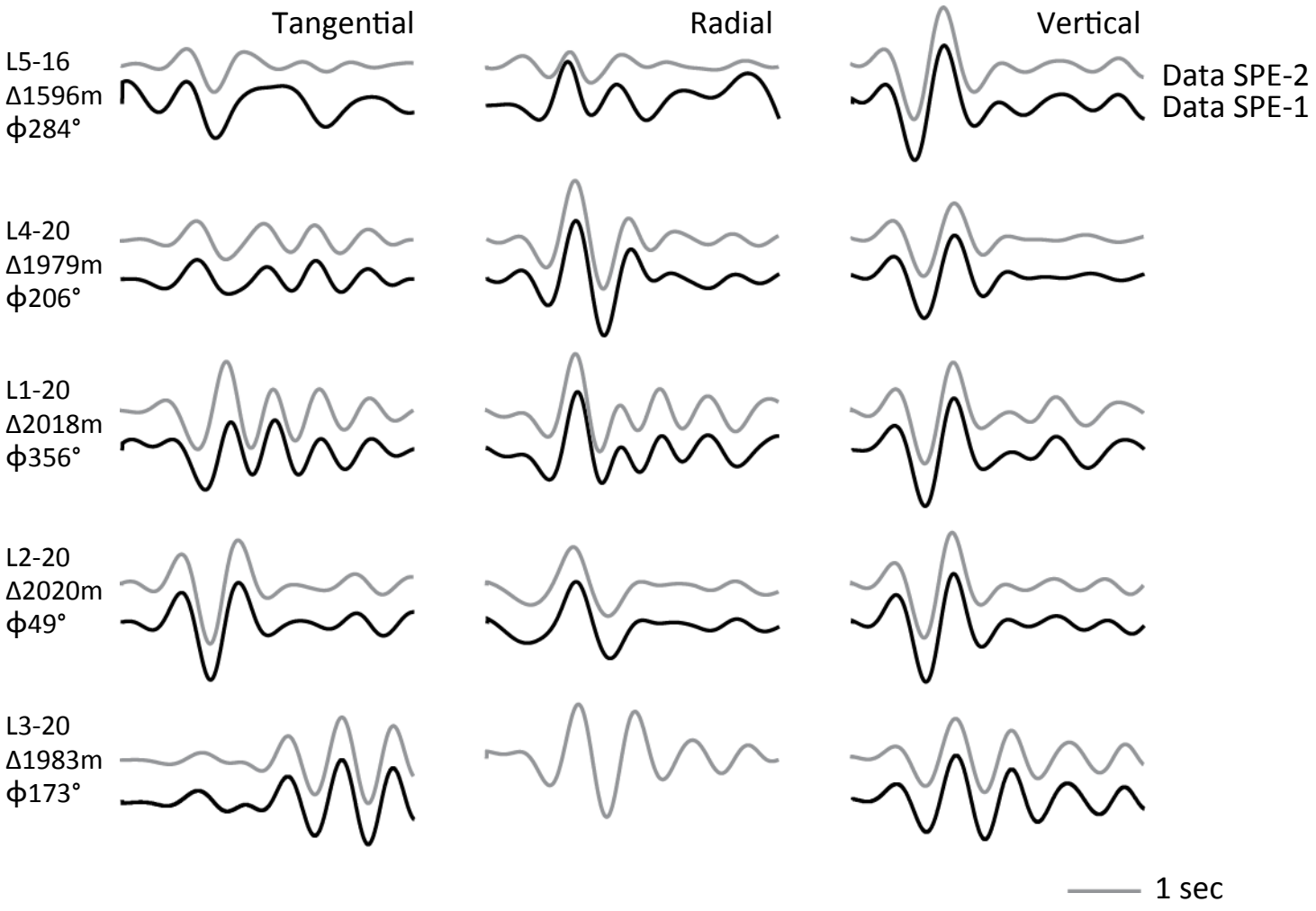
Tangential
Radial
Vertical
Data SPE-2
Data SPE-1
L5-16
Δ1596m
ϕ284°
L4-20
Δ1979m
ϕ206°
L1-20
Δ2018m
ϕ356°
L2-20
Δ2020m
ϕ49°
L3-20
Δ1983m
ϕ173°
1 sec

SPE-1 Explosion - 6×10^{10} N-m (M_W1.2)

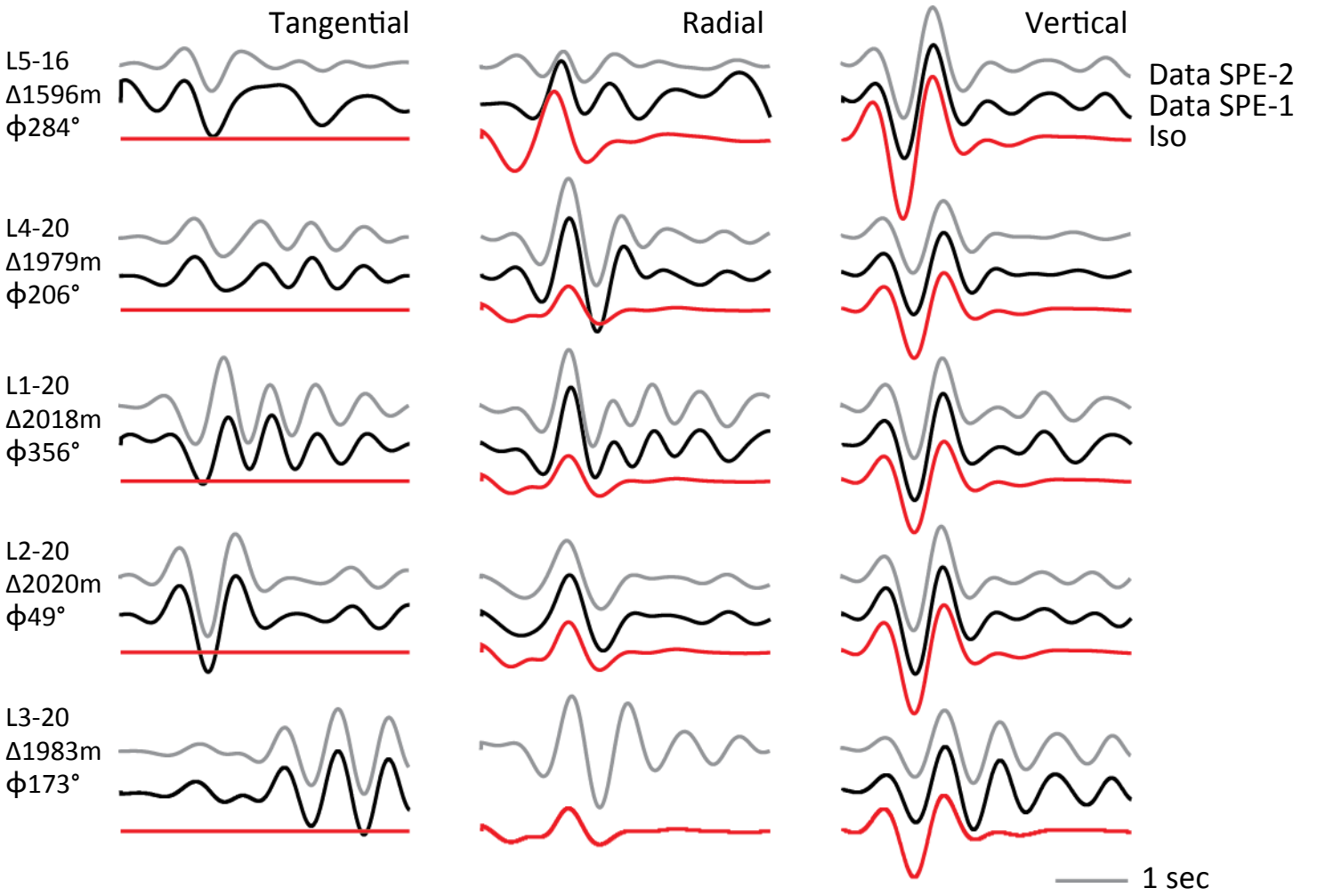

- M_0(SPE-2) ≅ 10 × M_0(SPE-1)

Deconvolution for relative moment-rate

- Deconvolve SPE-1 from SPE-2 on L5-16 vertical at <40 Hz

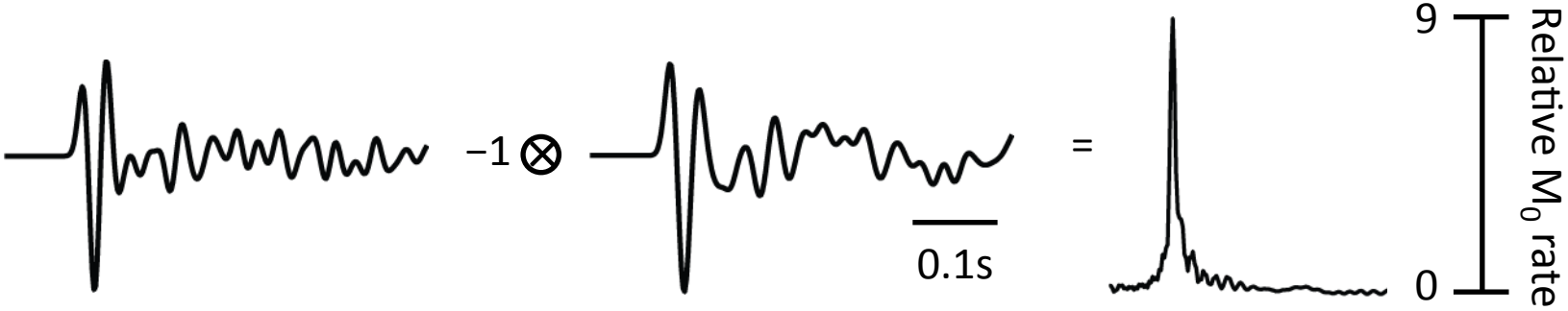

Deconvolution for relative moment-rate

- Deconvolve SPE-1 from SPE-2 on L5-16 vertical at <40 Hz

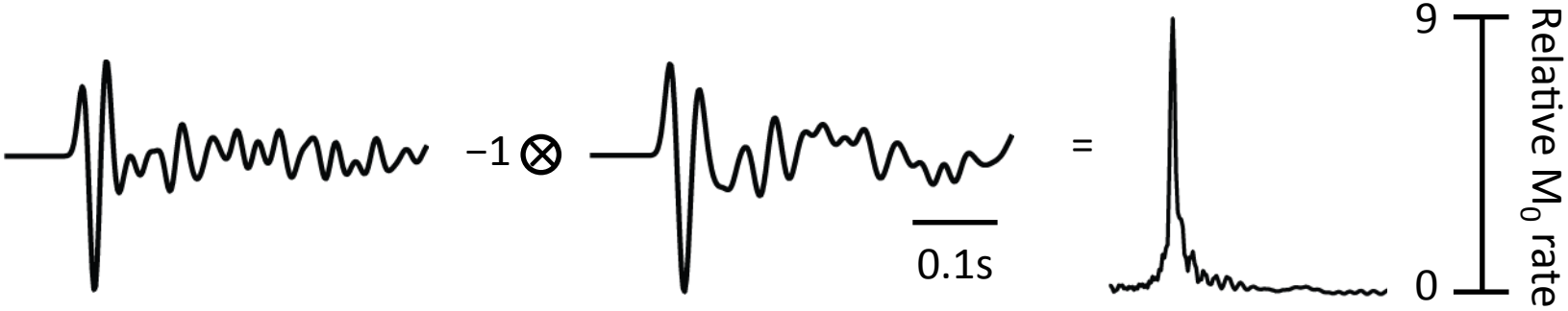

- Convolve moment-rate function with SPE-1 L5-16 all channels

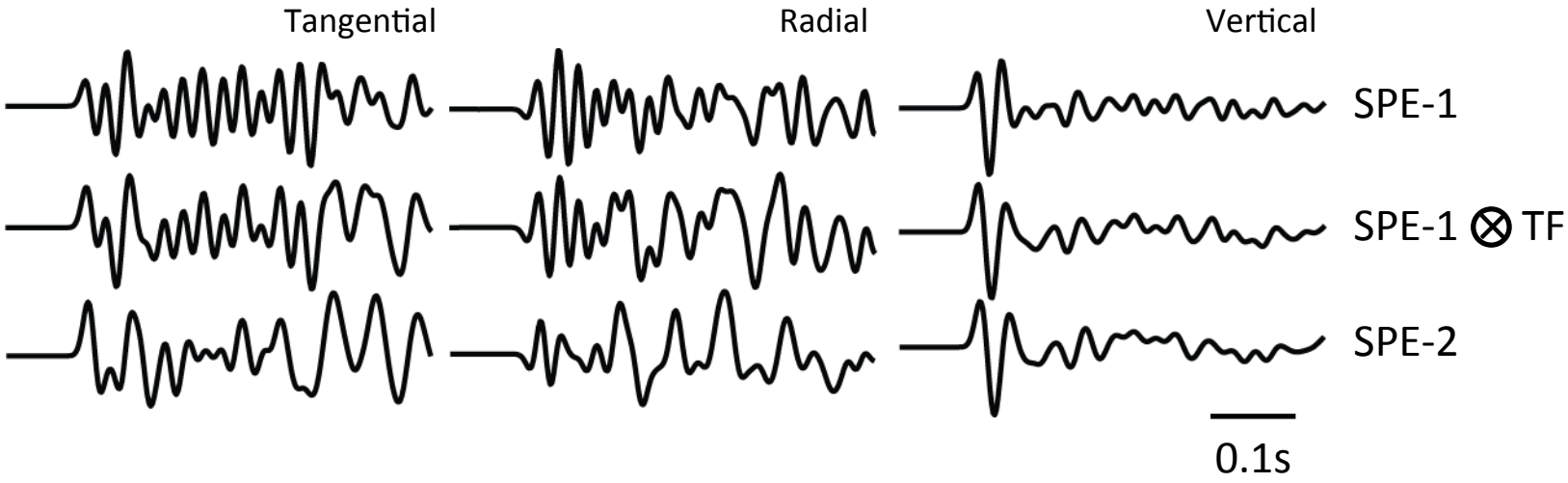

Denny & Johnson (1991) scaling relations

- Regression for cavity radius as a function of yield obtained

$$R_c = \frac{1.47 \times 10^4 W^{1/3}}{\beta^{0.3848} P_0^{0.2625} 10^{0.0025 GP}}$$

- Regression for seismic moment obtained

$$M_0 = \frac{1}{311} M_t P_0^{0.349} 10^{-0.027 GP} \qquad \text{where} \qquad M_t = \frac{4}{3} \pi \rho \alpha^2 R_c^3$$

- Prediction of R_c for SPE-1/-2 = 0.79 / 1.79 m

- Explosion M_0 predicts W for SPE-1/2 = 98 / 945 kg TNT

Preliminary findings

- SPE-2 best-fit isotropic M_0 6.3×10^{11} N-m = 10 × SPE-1 isotropic M_0
- SPE-1/-2 low-frequency waveforms are very similar
- Full MT low-frequency point-source inversion cannot fit tangential displacement
- Evidence for multipathing requires >1D velocity-model

Future work

- Distributed source
- Variable 1D models to capture M_0 error
- Higher frequency and greater bandwidth inversions
- Variable weighting of low-amplitude initial arrivals
- Use of eGF for kinematic source inversion

Coda wave interferometry of SPE-2/-3 for velocity change due to damage

Sean Ford, LLNL

Approach

- GS11D-vertical observations of SPE-2/-3
- Non-overlapping windows of 0.4 s ($10 \times T_{dom}$)
- Damage should change elastic properties leading to velocity change and travel-time perturbation
- Use coda wave interferometry to measure travel-time perturbation [Snieder et al., 2002]

$$\frac{\delta v}{v} = -\frac{\delta t}{t}$$

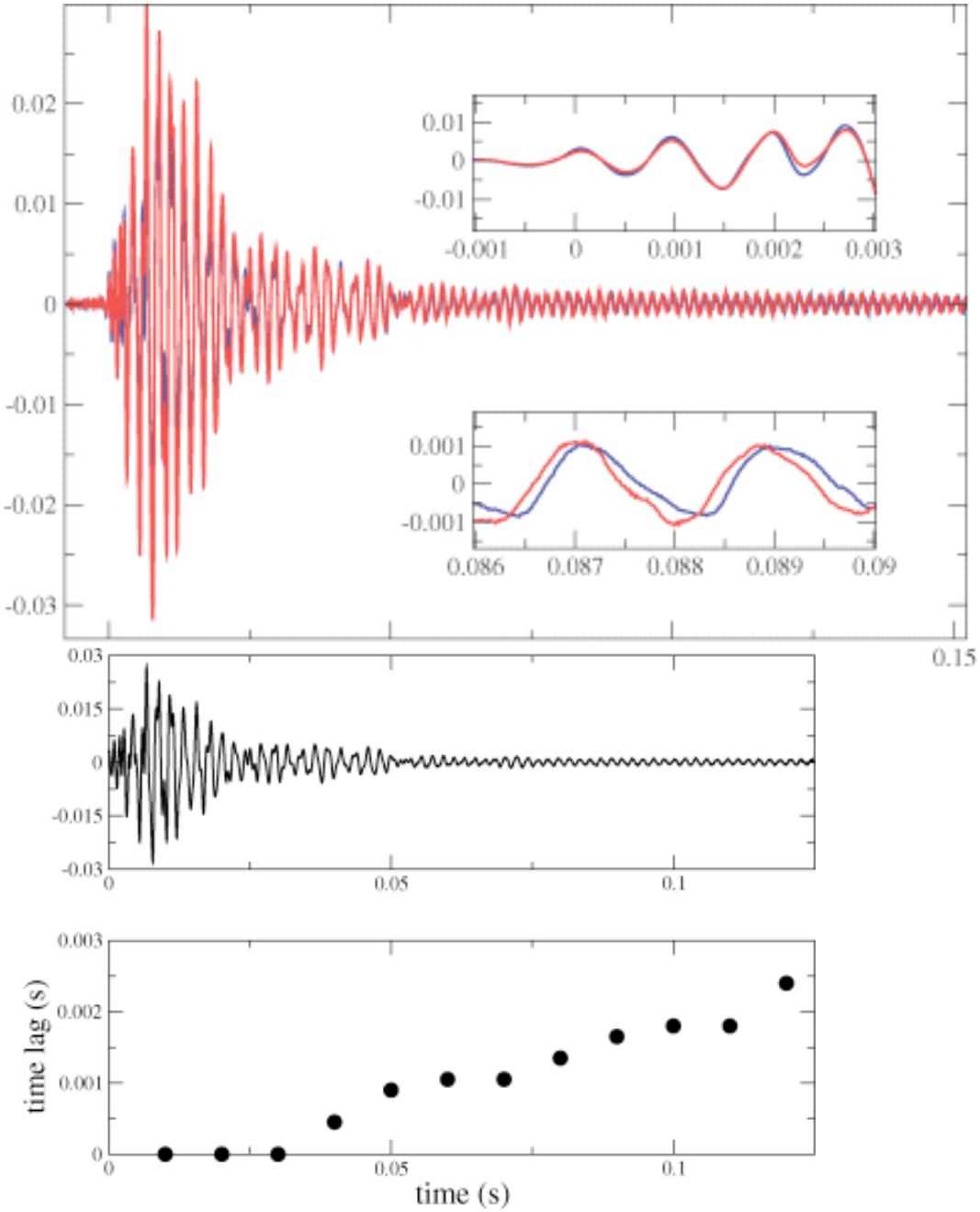

Example from Gret et al. [2006] *Geophys. J. Int.*

Two waveforms, one measured at 4.14 MPa of pressure in the cell (blue) and one measured at 12.41 MPa (red). The upper panel shows the early time window and the lower panel part of the coda.

The seismic record (top panel), and estimates of δt for multiple time-windows (bottom panel). The first three points are computed from the early part of the waveform and are not sufficiently sensitive to detect the velocity change.

Analysis at L4-05 (Δ=500m)

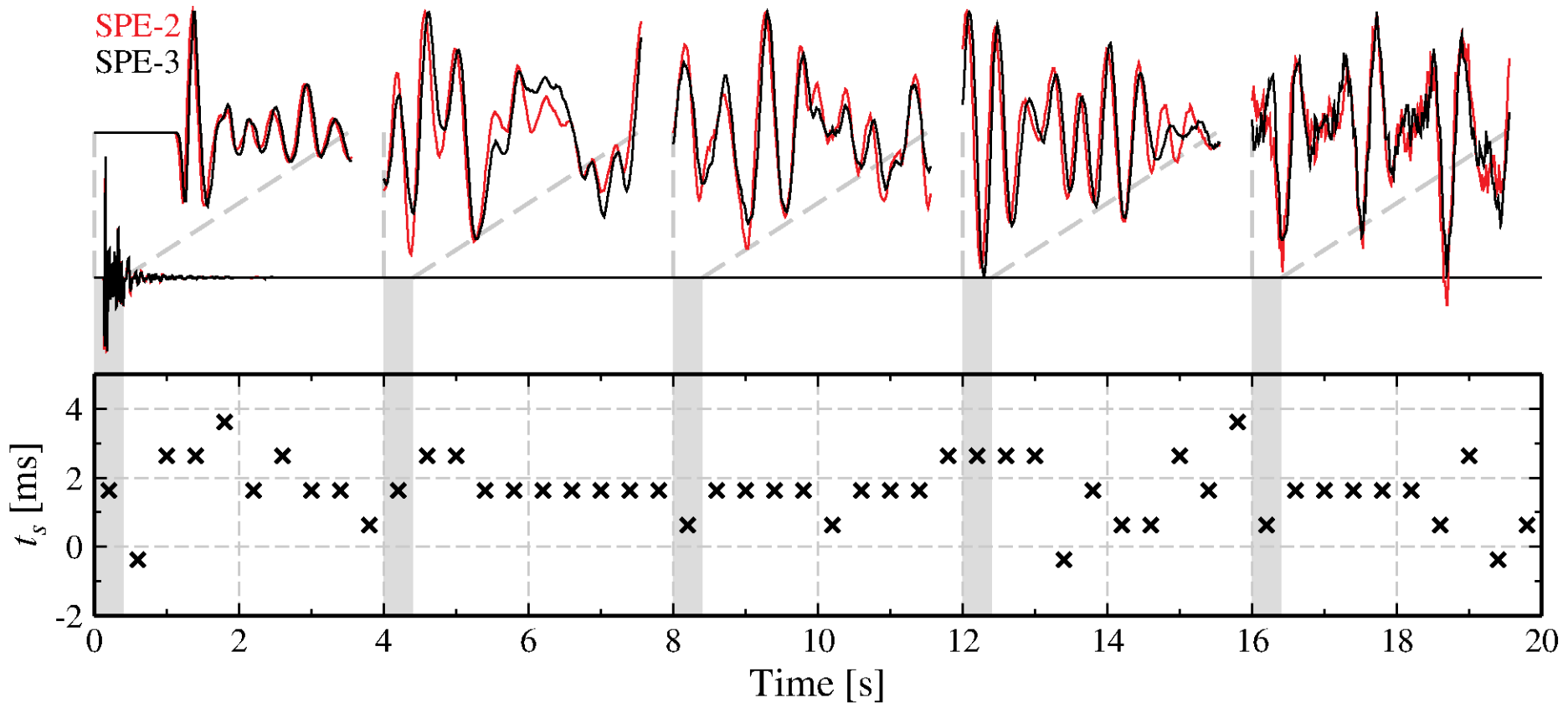

Analysis at all stations

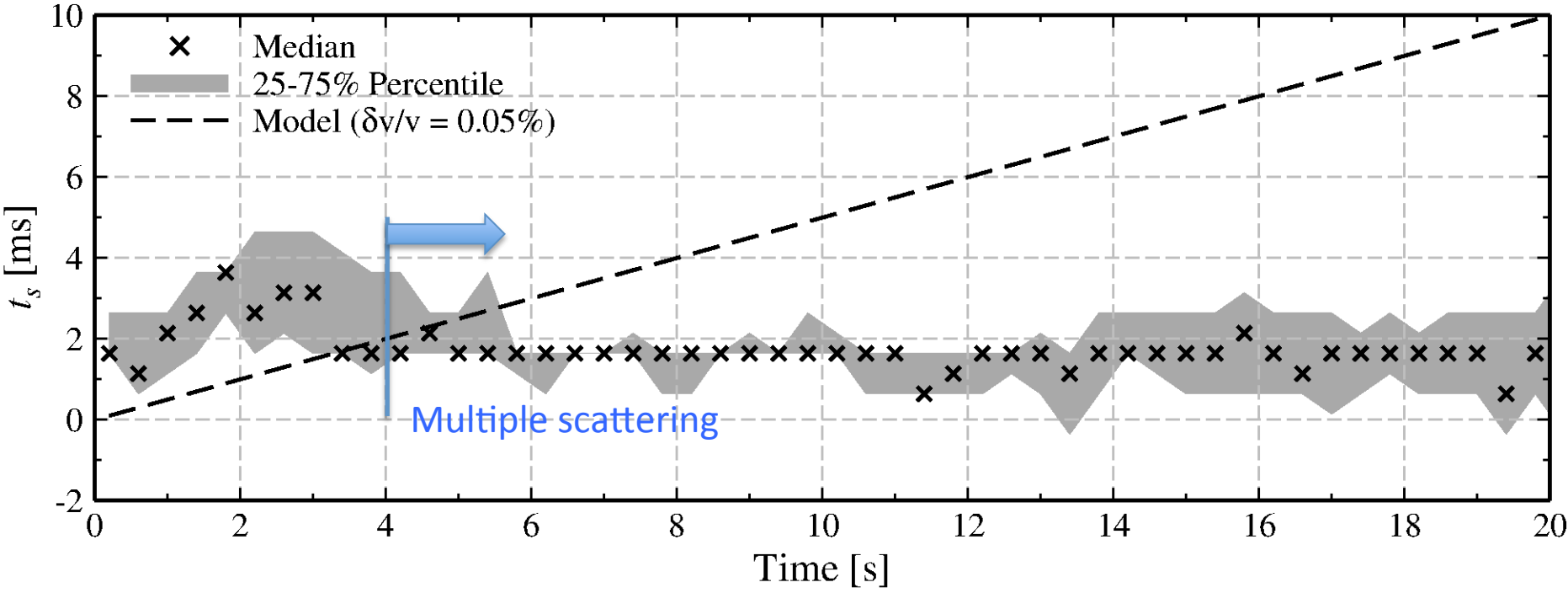

Prediction

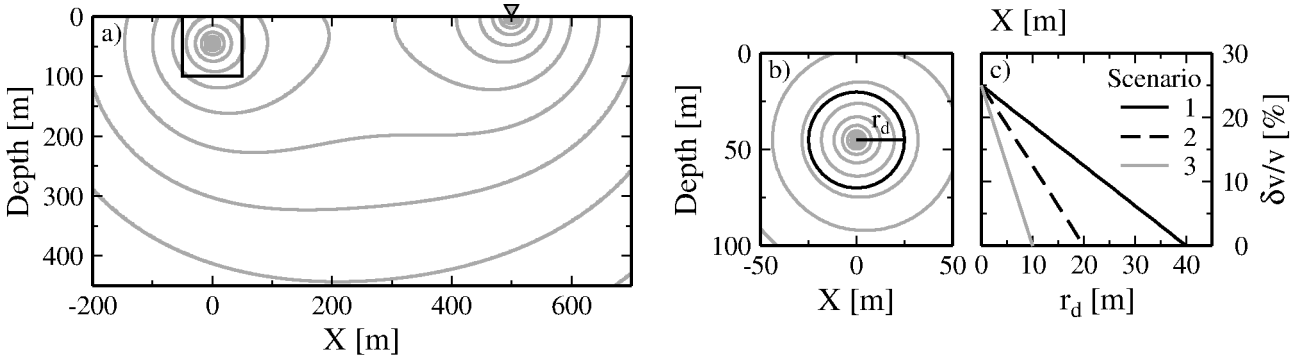
a)
Depth [m]
X [m]
b)
Depth [m]
X [m]
c)
Scenario
1
2
3
δv/v [%]
r_d [m]

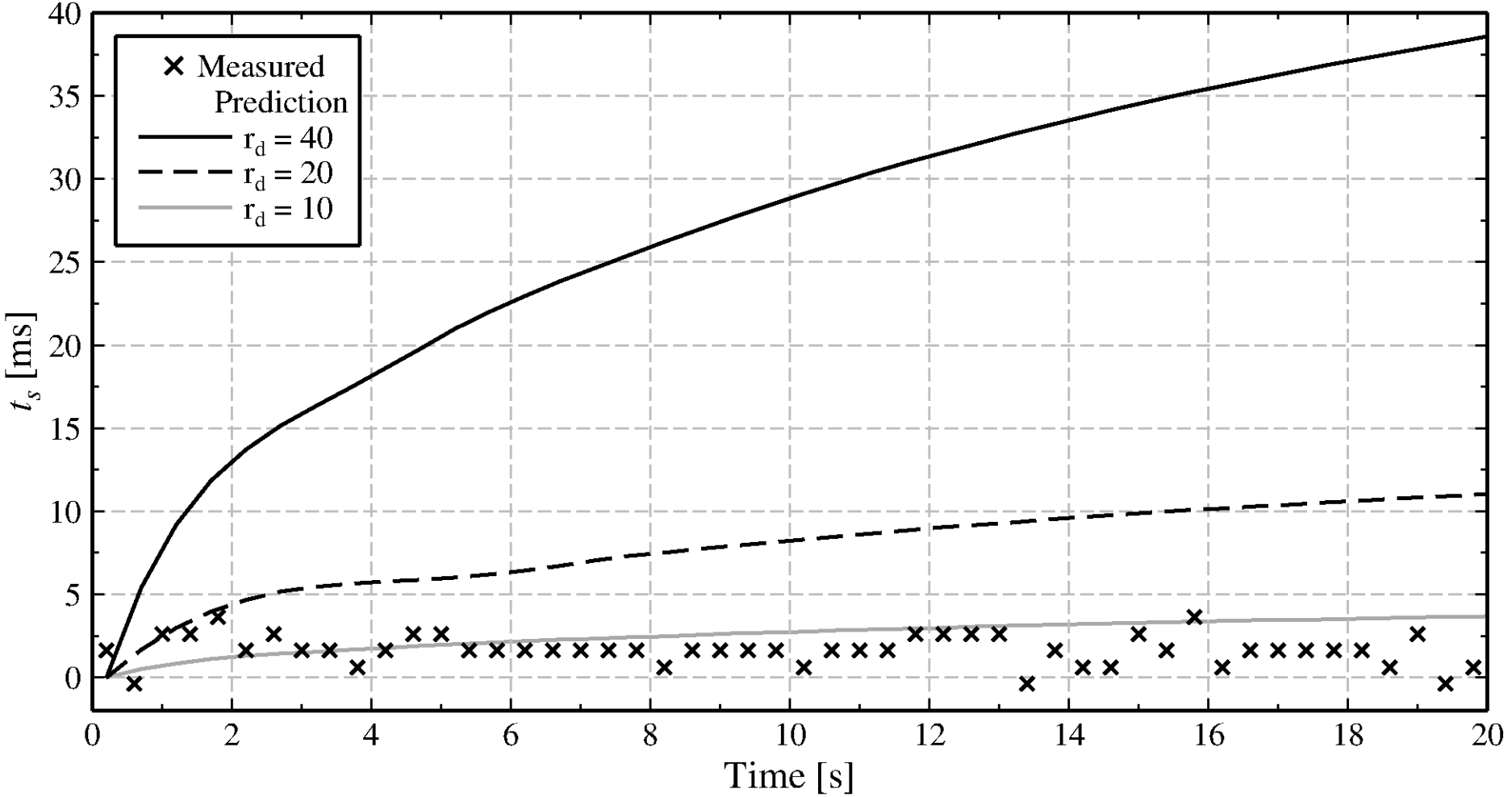
Measured
Prediction
r_d = 40
r_d = 20
r_d = 10
t_s [ms]
Time [s]

Near-field data

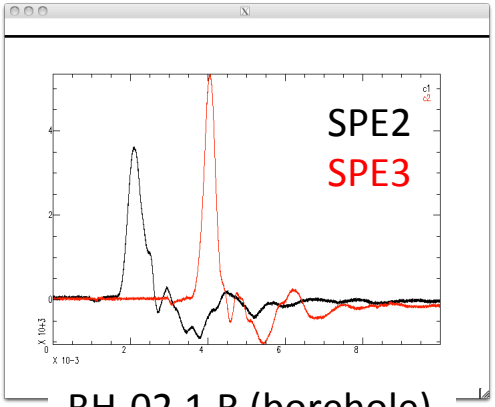

BH-02.1.R (borehole)

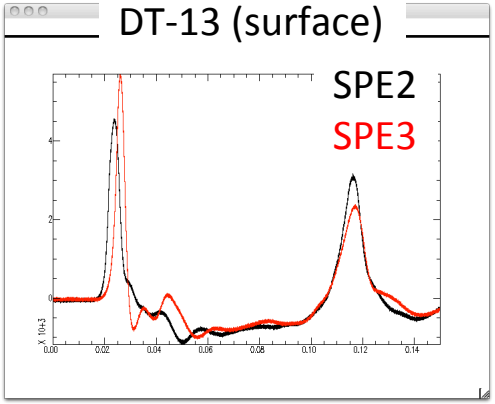

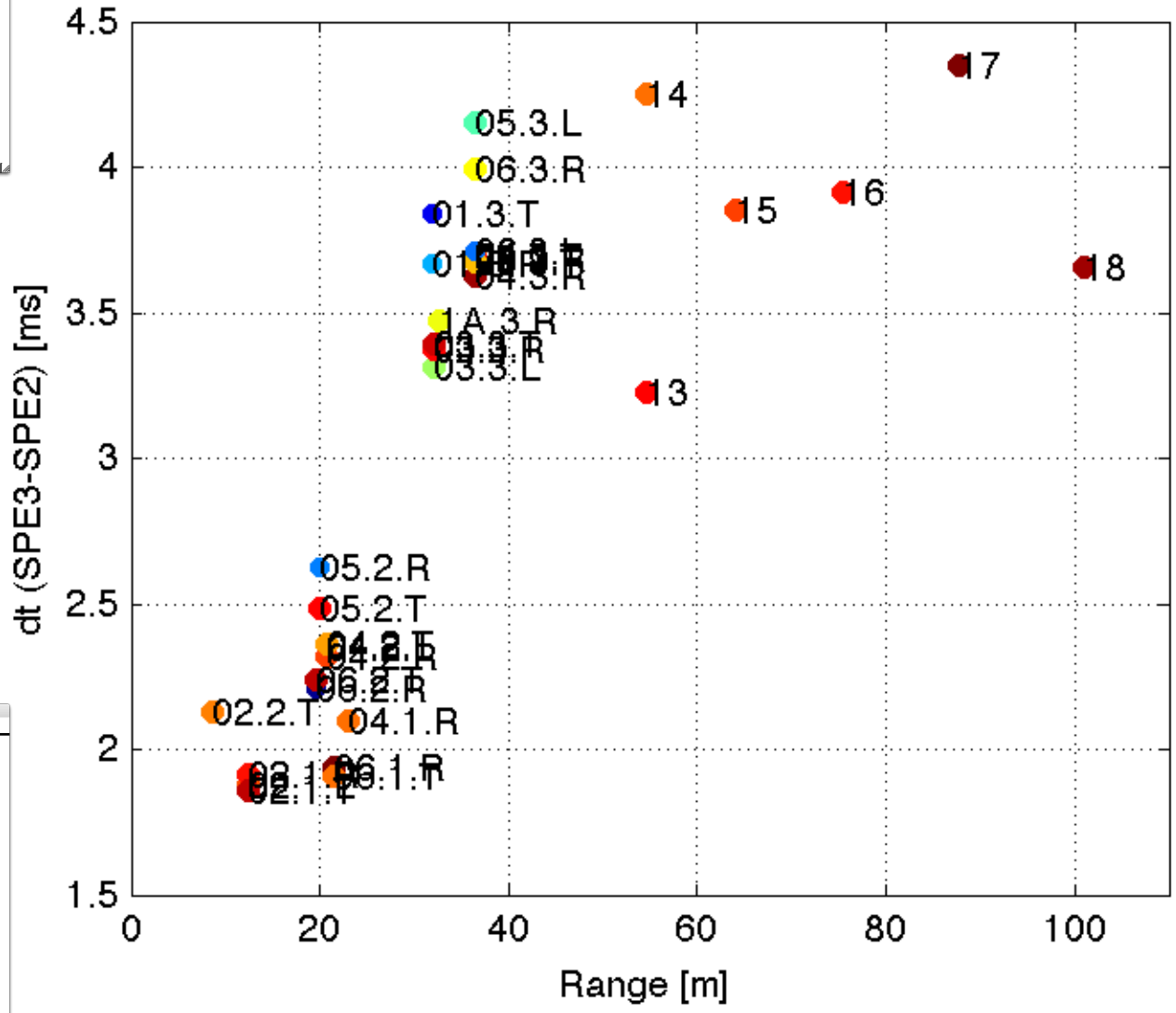

1D inversion for slowness perturbation

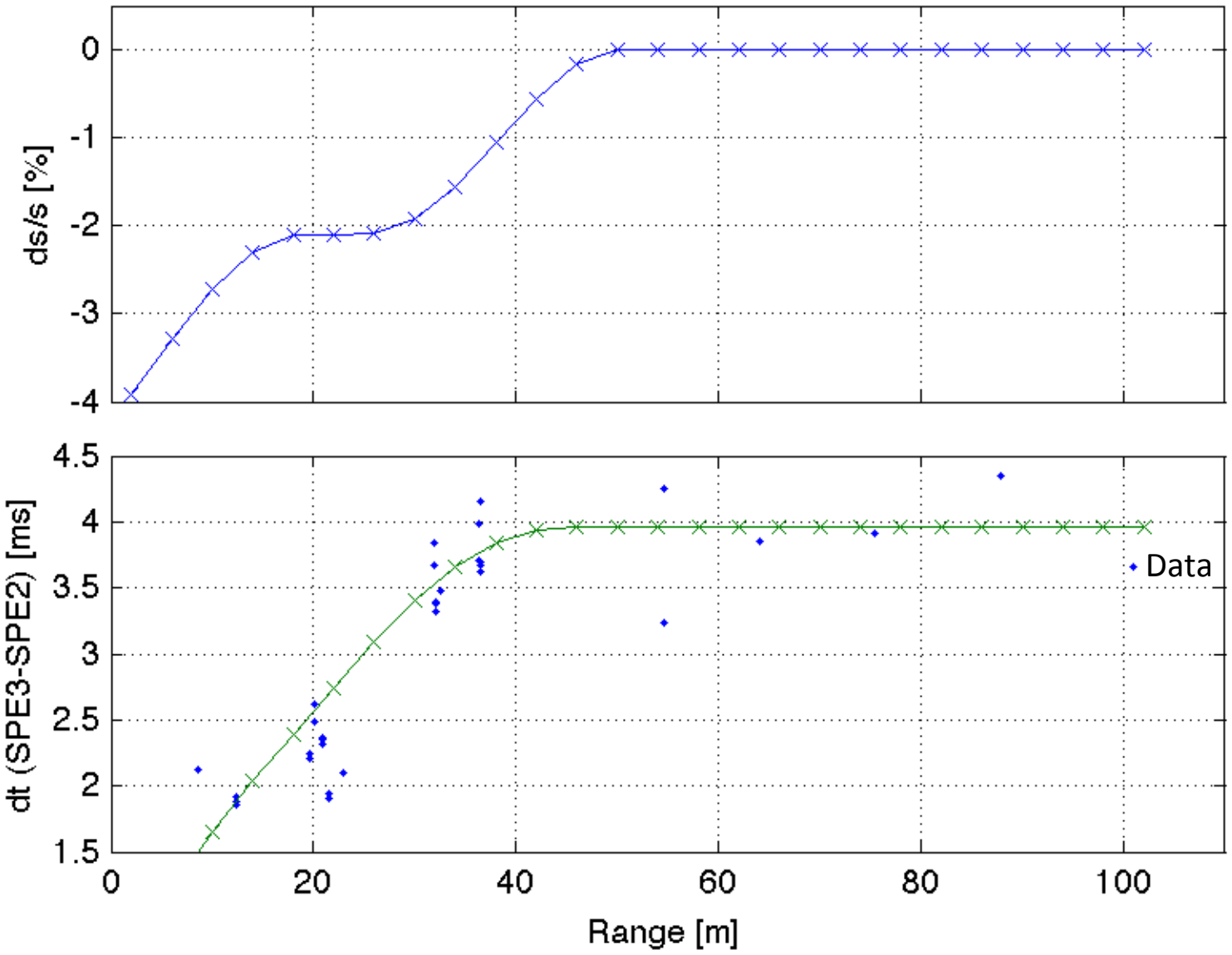

1D inversion for slowness perturbation

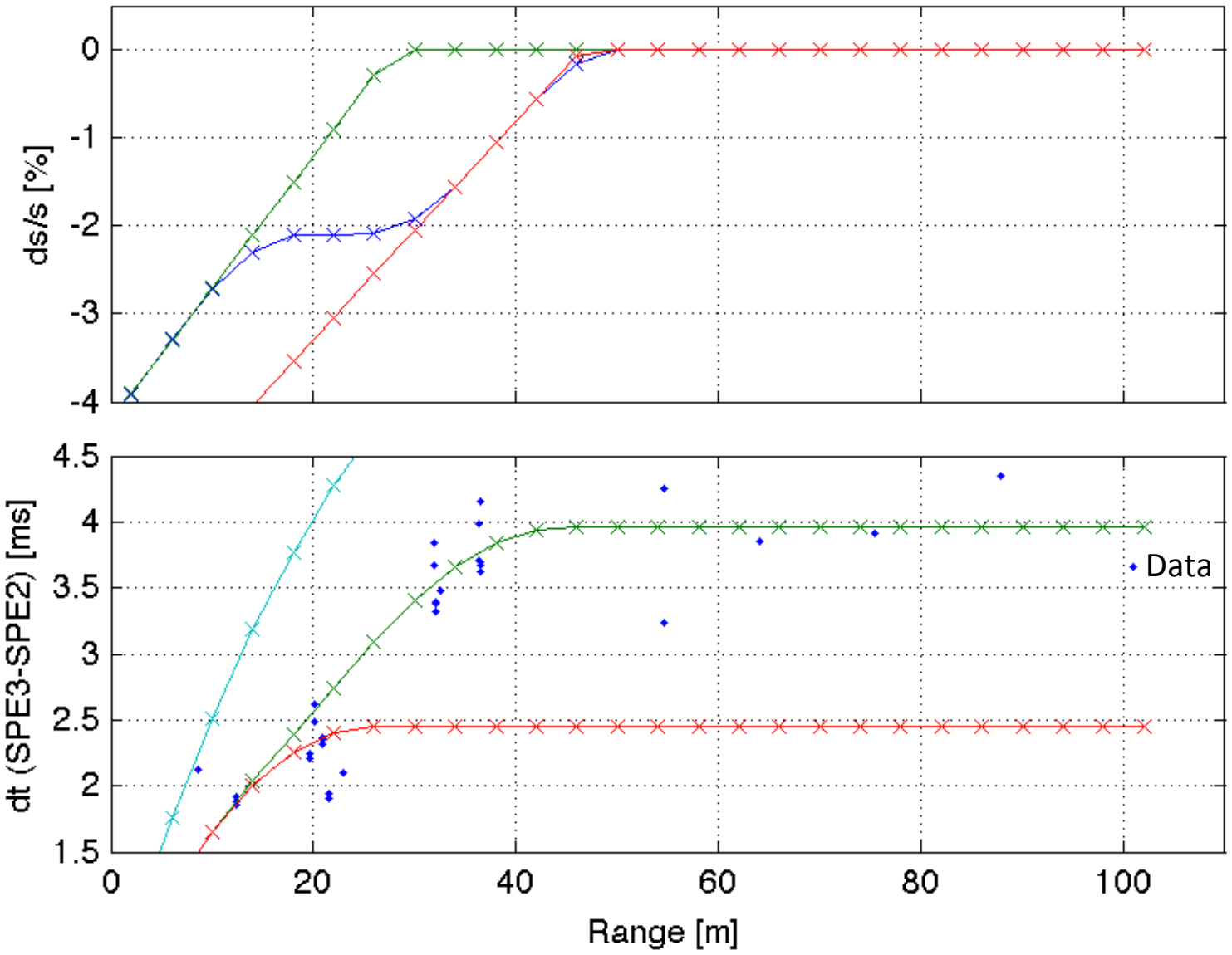

To Do

- Note SPE W and h
- Note historical parameters

A Spall Model Comparison with Insights from the Source Physics Experiment

Sean Ford and Rob Mellors, LLNL

Lawrence Livermore National Laboratory is operated by Lawrence Livermore National Security, LLC, for the U.S. Department of Energy, National Nuclear Security Administration under Contract DE-AC52-07NA27344.

Spall model

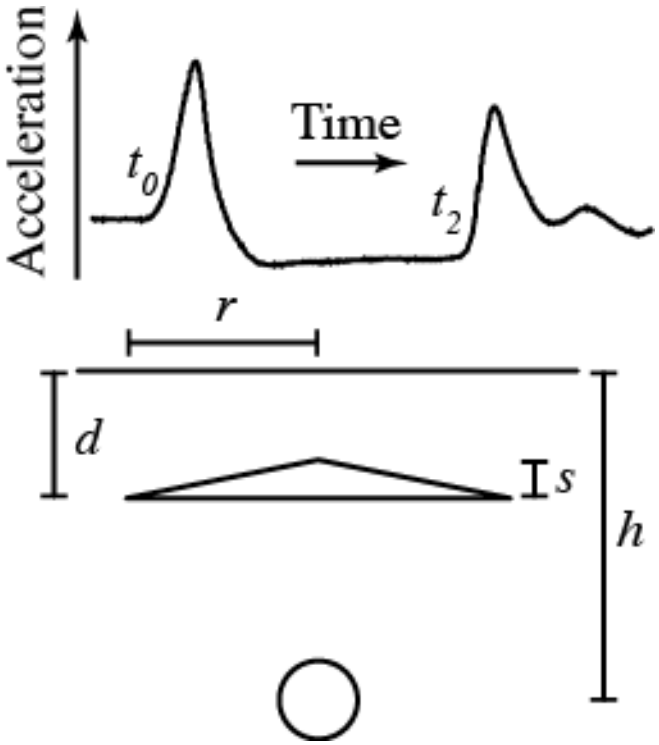

Study	Depth (d) [m]	Lateral extent (r) [m]	Maximum gap (s) [m]	Peak velocity (v) [m/s]
Viecelli (1973)	$10^{3.44}\ W^{2/3}h^{-1}$	$100\ W^{1/3}$	$10^{8.82}\ W^{4/3}h^{-4}$	from s via eq (2)
Sobel (1978)	$22\ W^{1/3}$	$10^{2.84}\ W^{0.37}h^{-0.16}$	$10^{0.57}\ W^{0.52}h^{-0.50}$	from s via eq (2)
Patton (1990)*	$54\ W^{0.25}$	$334\ W^{0.25}$	from v via eq (1)	$10^{4}\ W^{1.61/3}\ h^{-1.61}$

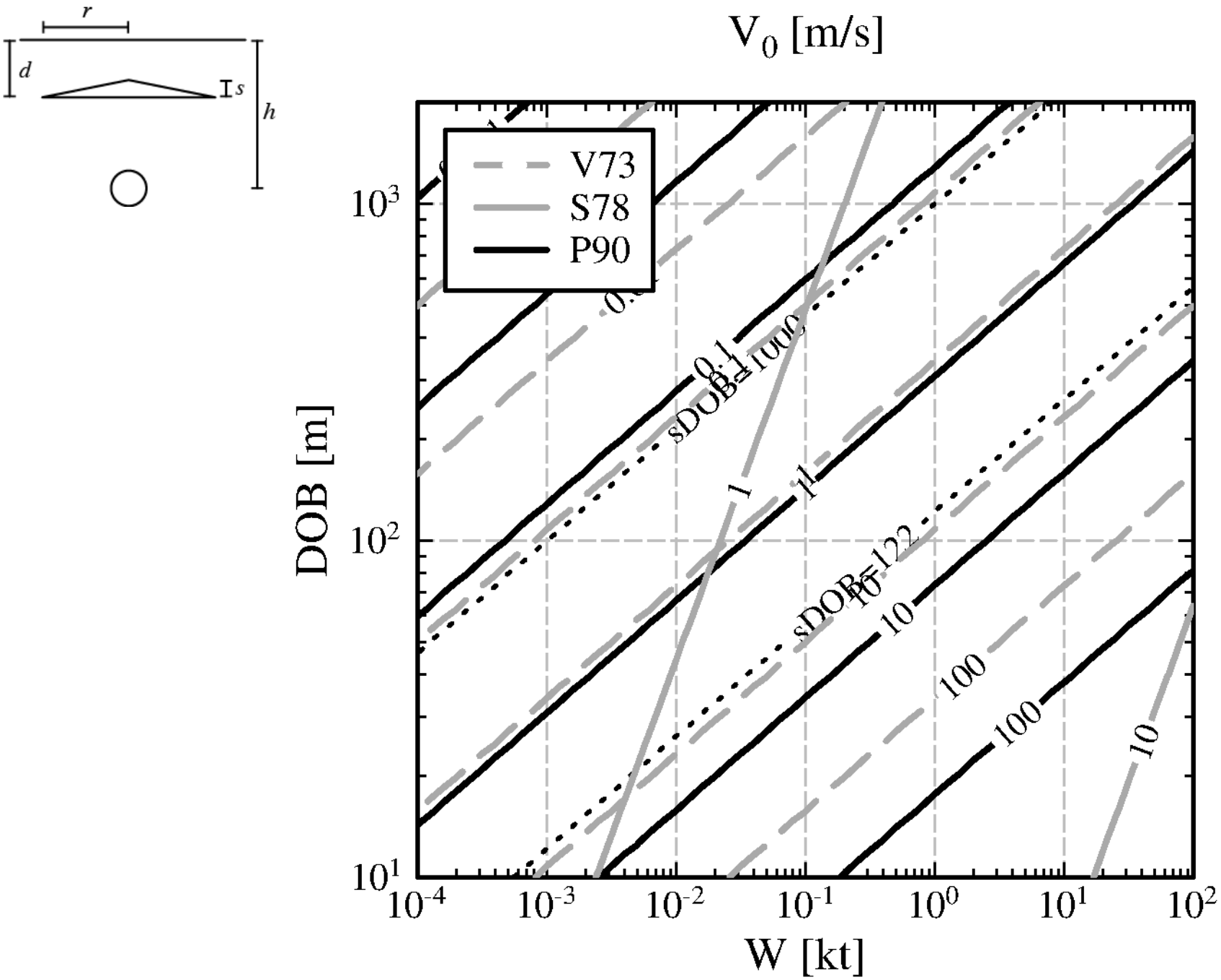
r
d
Is
h
V0 [m/s]
V73
S78
P90
sDOB=100
sDOB=122
DOB [m]
W [kt]
10^3
10^2
10^1
10^-4
10^-3
10^-2
10^-1
10^0
10^1
10^2

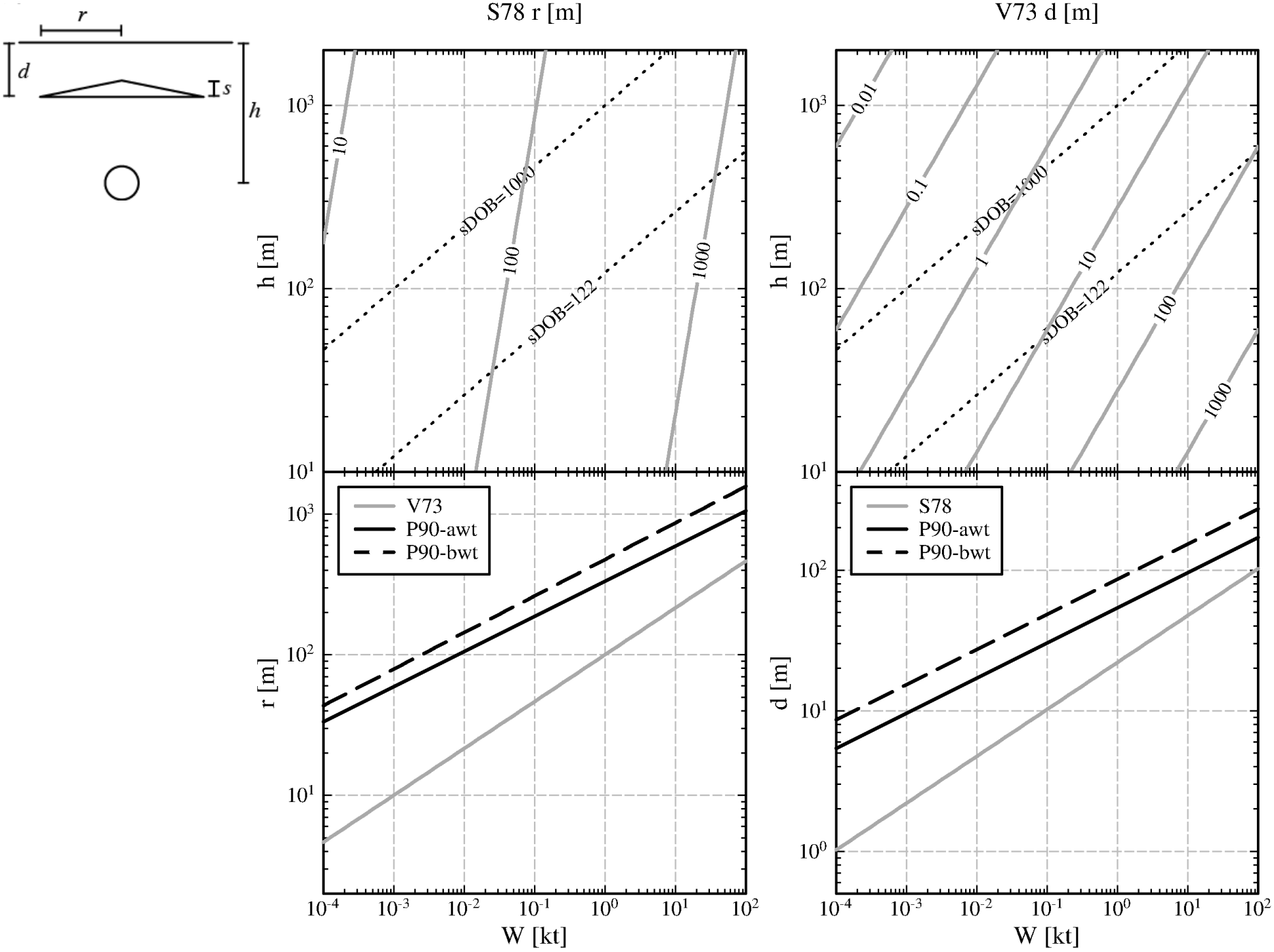
r
d
s
h
S78 r [m]
V73 d [m]
h [m]
10
100
1000
sDOB=1000
sDOB=122
0.01
0.1
1
10
100
1000
sDOB=1000
sDOB=122
V73
P90-awt
P90-bwt
S78
P90-awt
P90-bwt
r [m]
d [m]
W [kt]
W [kt]

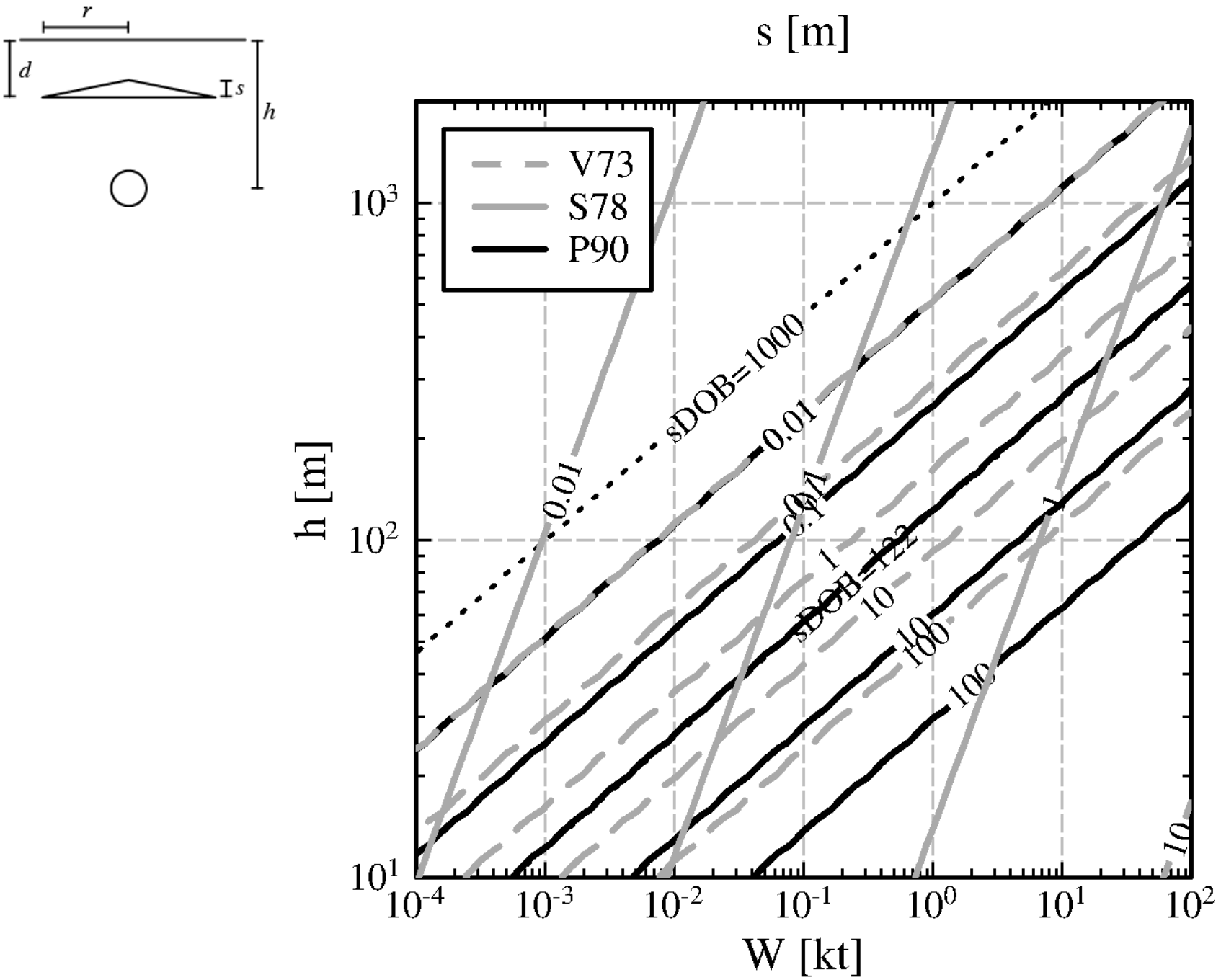
r
d
s
h
s [m]
V73
S78
P90
sDOB=1000
sDOB=122
0.01
0.1
1
10
100
h [m]
W [kt]
10^1
10^2
10^3
10^{-4}
10^{-3}
10^{-2}
10^{-1}
10^0
10^1
10^2

SPE Observations

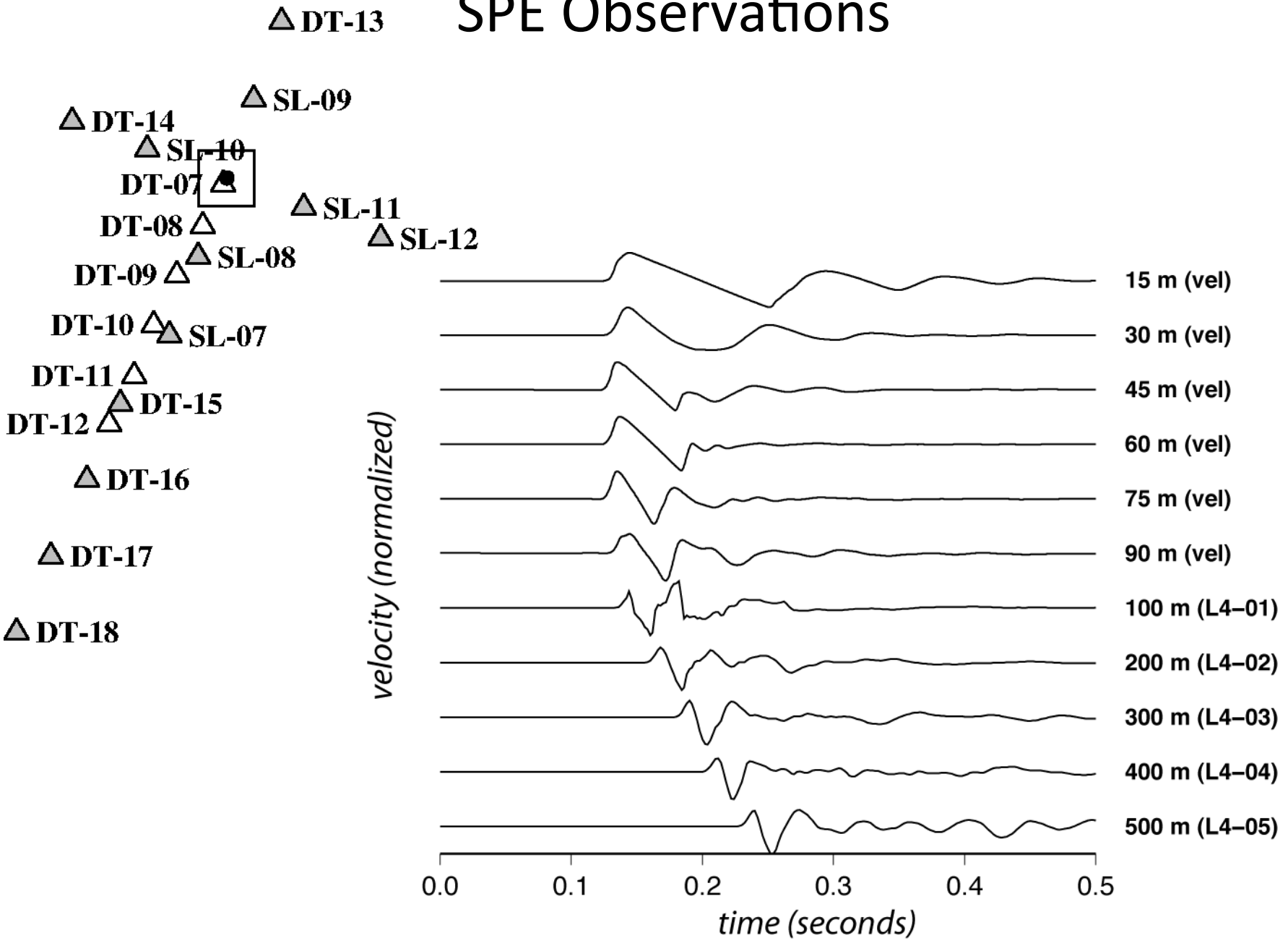

Comparison with PILEDRIVER

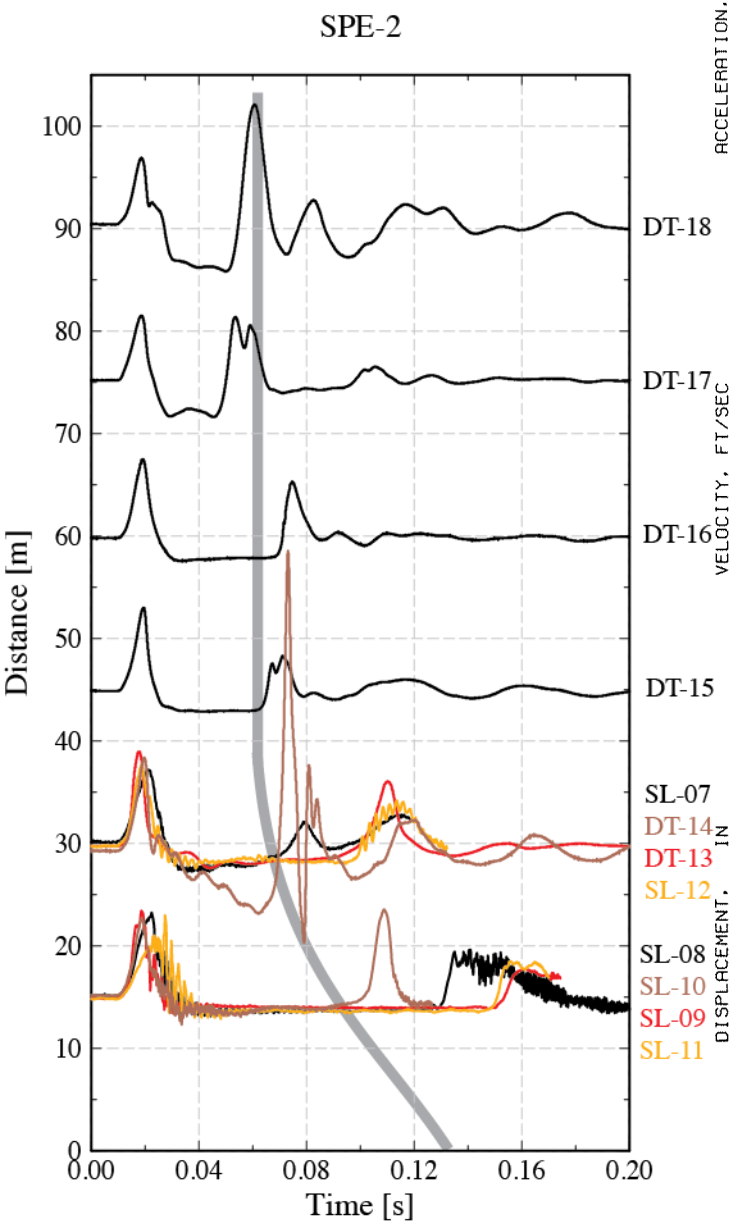

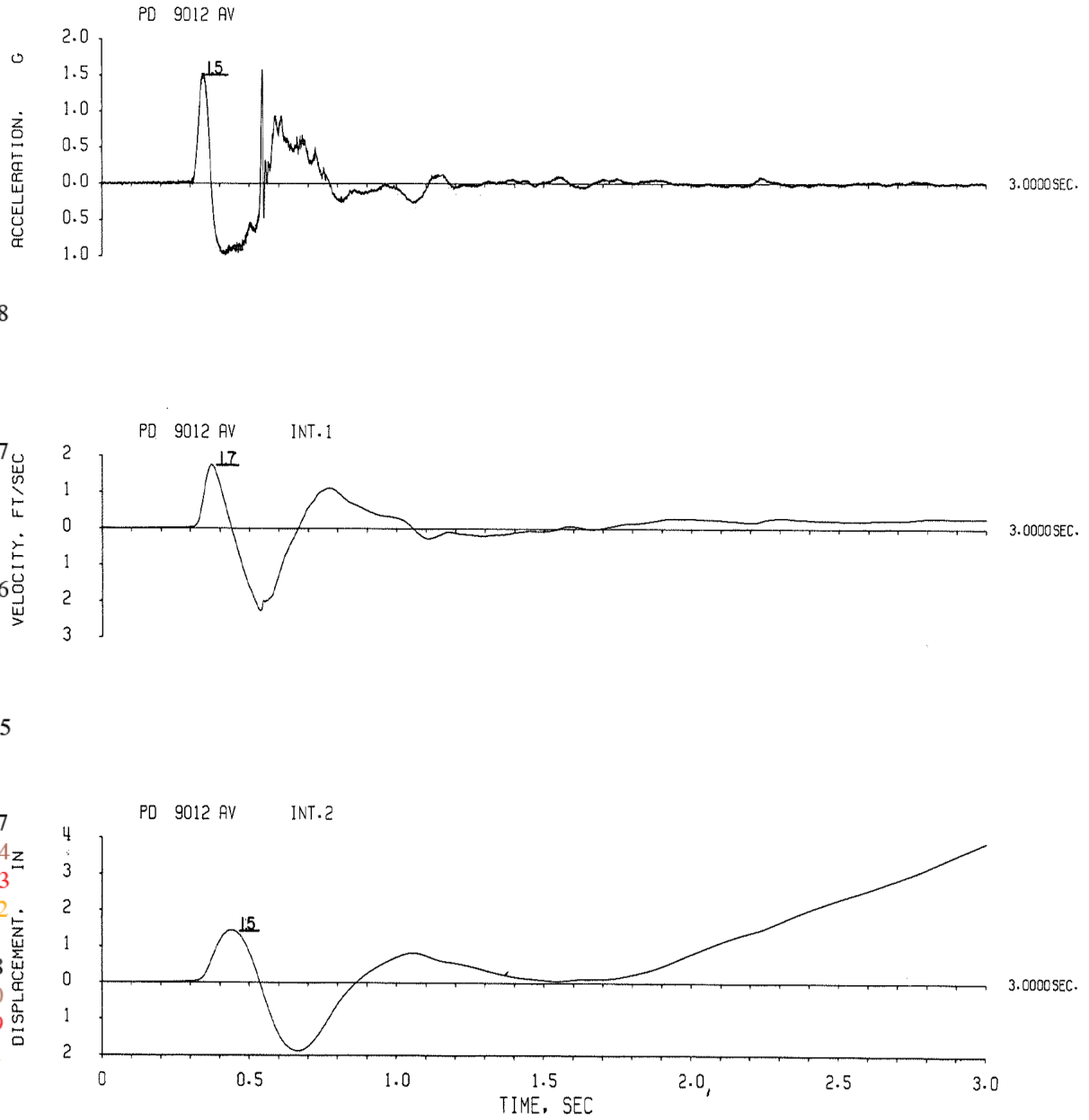

Figure 3.49 Vertical acceleration, velocity, and displacement, 4500 feet horizontal range, 1453 feet above the working point.

Comparison with PILEDRIVER

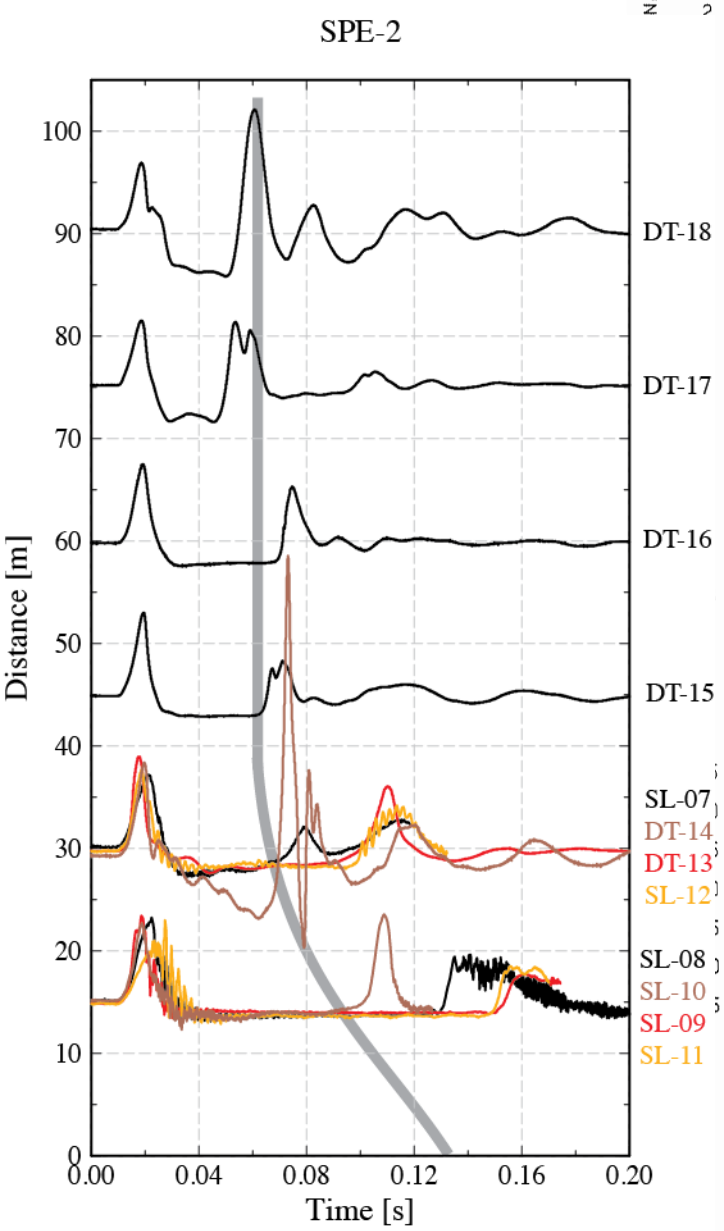

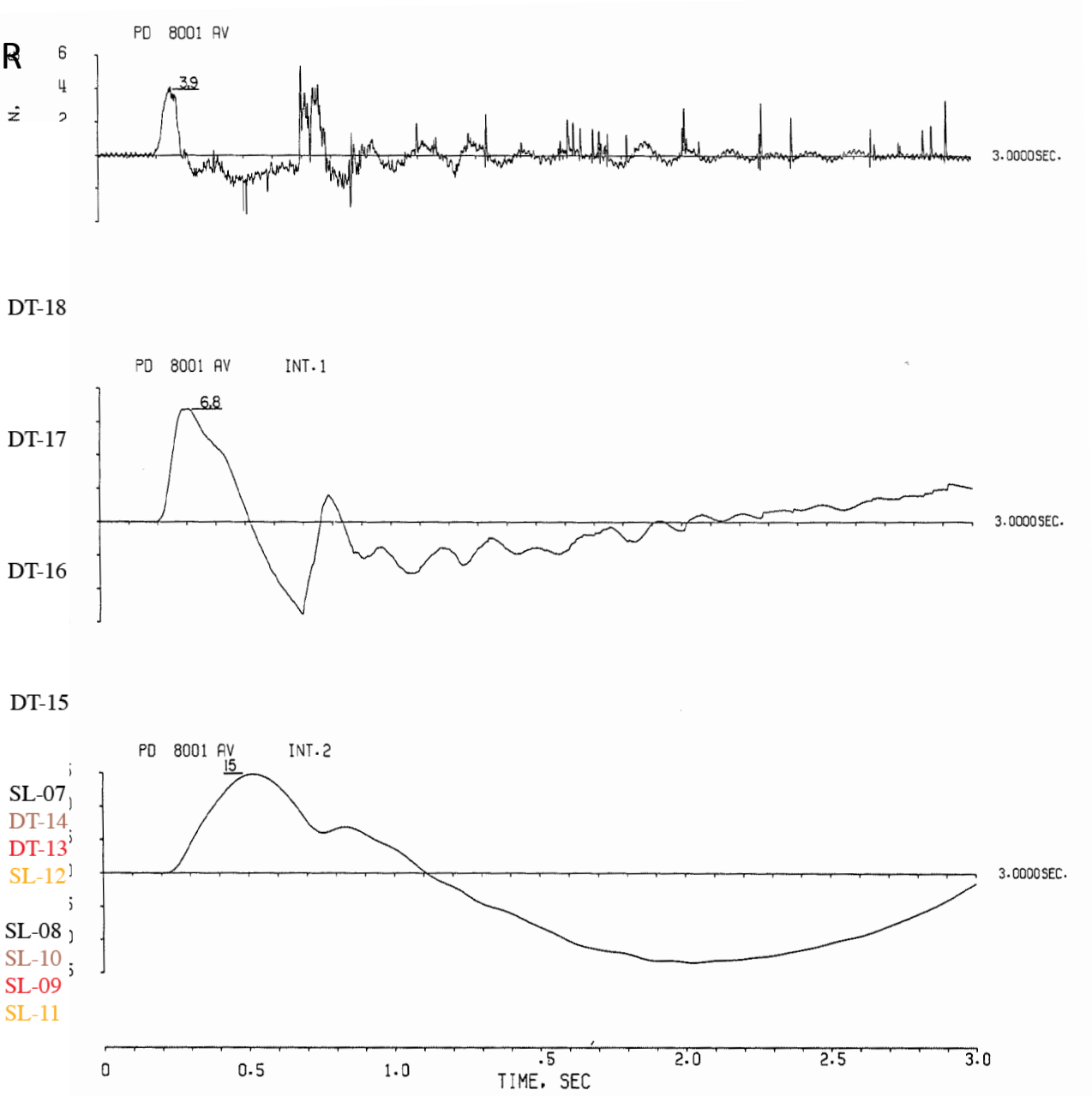

Figure 3.52 Vertical acceleration, velocity, and displacement, C van floor, front.

Comparison with PILEDRIVER

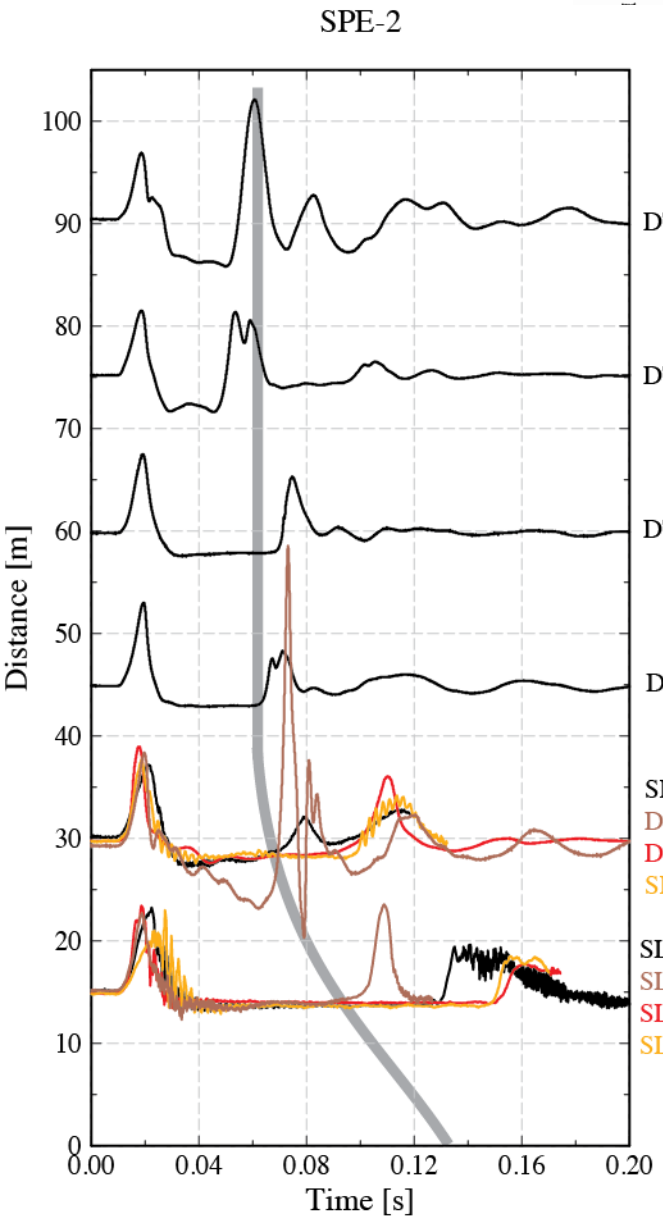

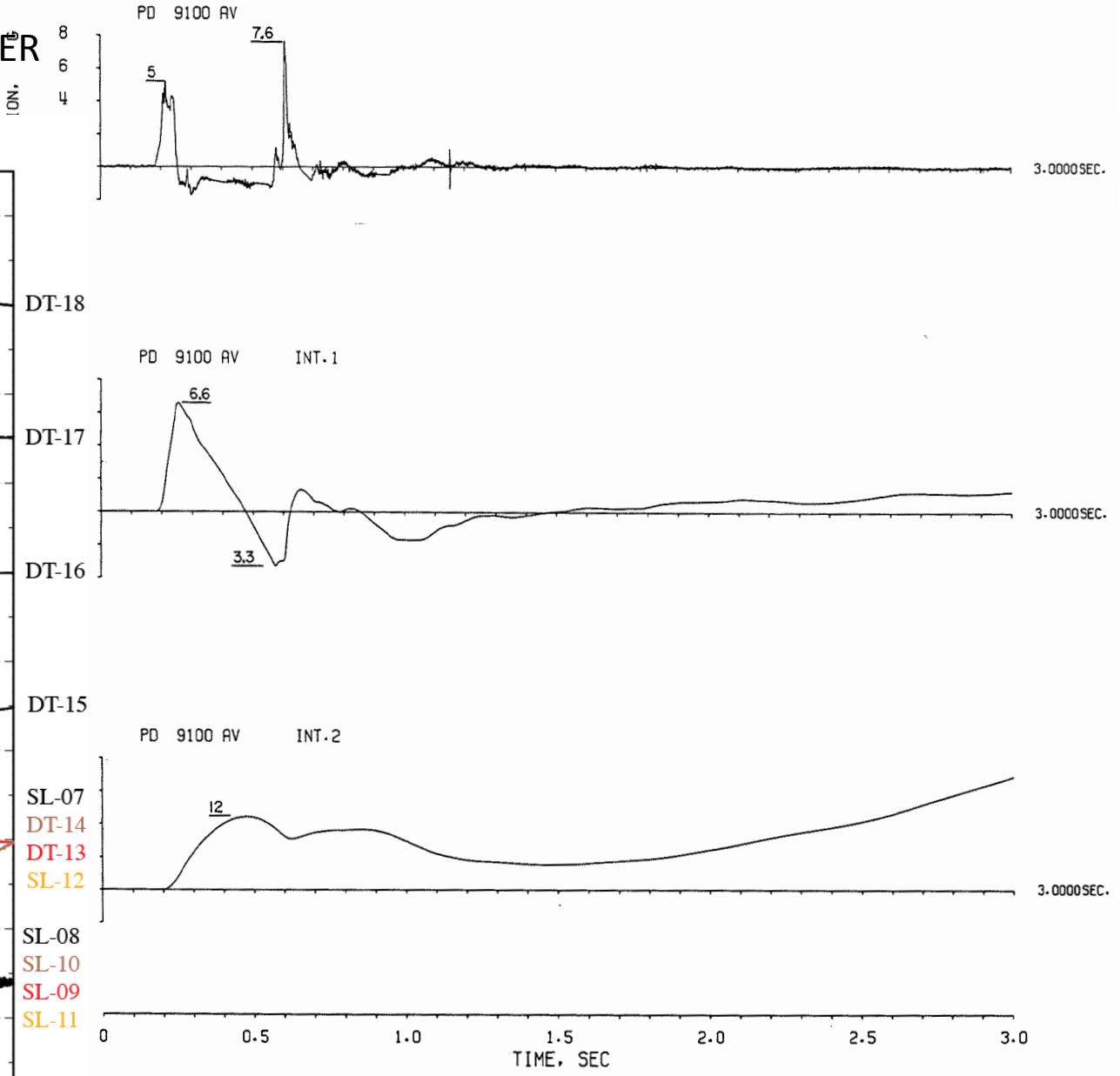

Figure 3.50 Vertical acceleration, velocity, and displacement in trailer park, 1850 feet horizontal range, 1409 feet above the working point.

Comparison with PILEDRIVER

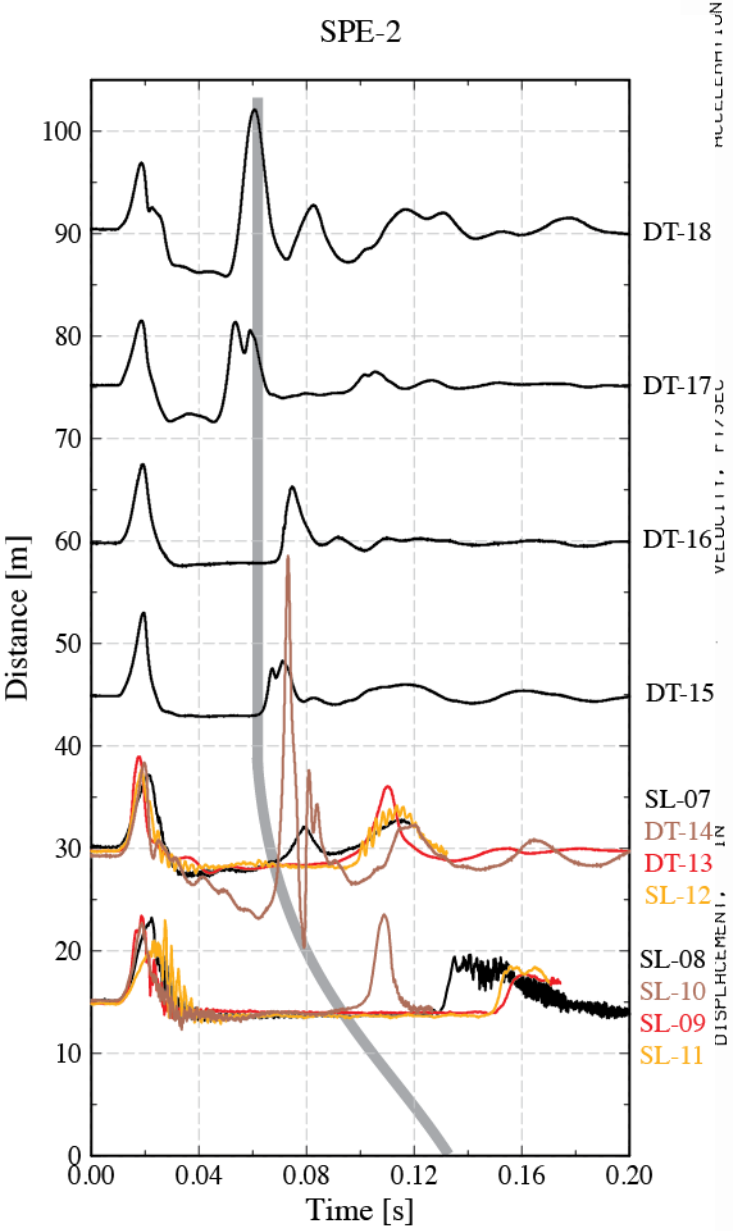

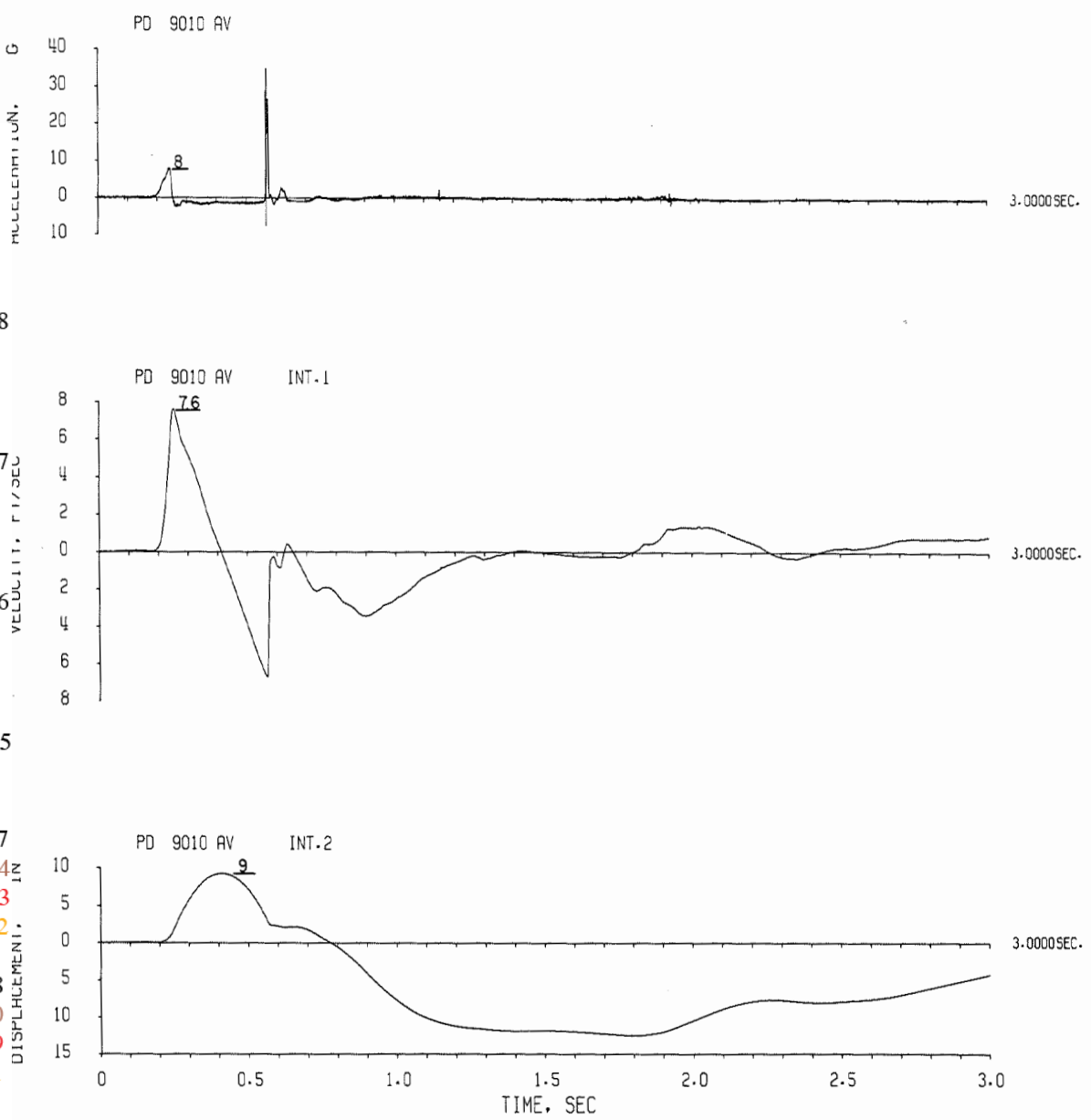

Figure 3.48 Vertical acceleration, velocity, and displacement, 2440 feet horizontal range, 1539 feet above the working point.

Peak GZ velocity

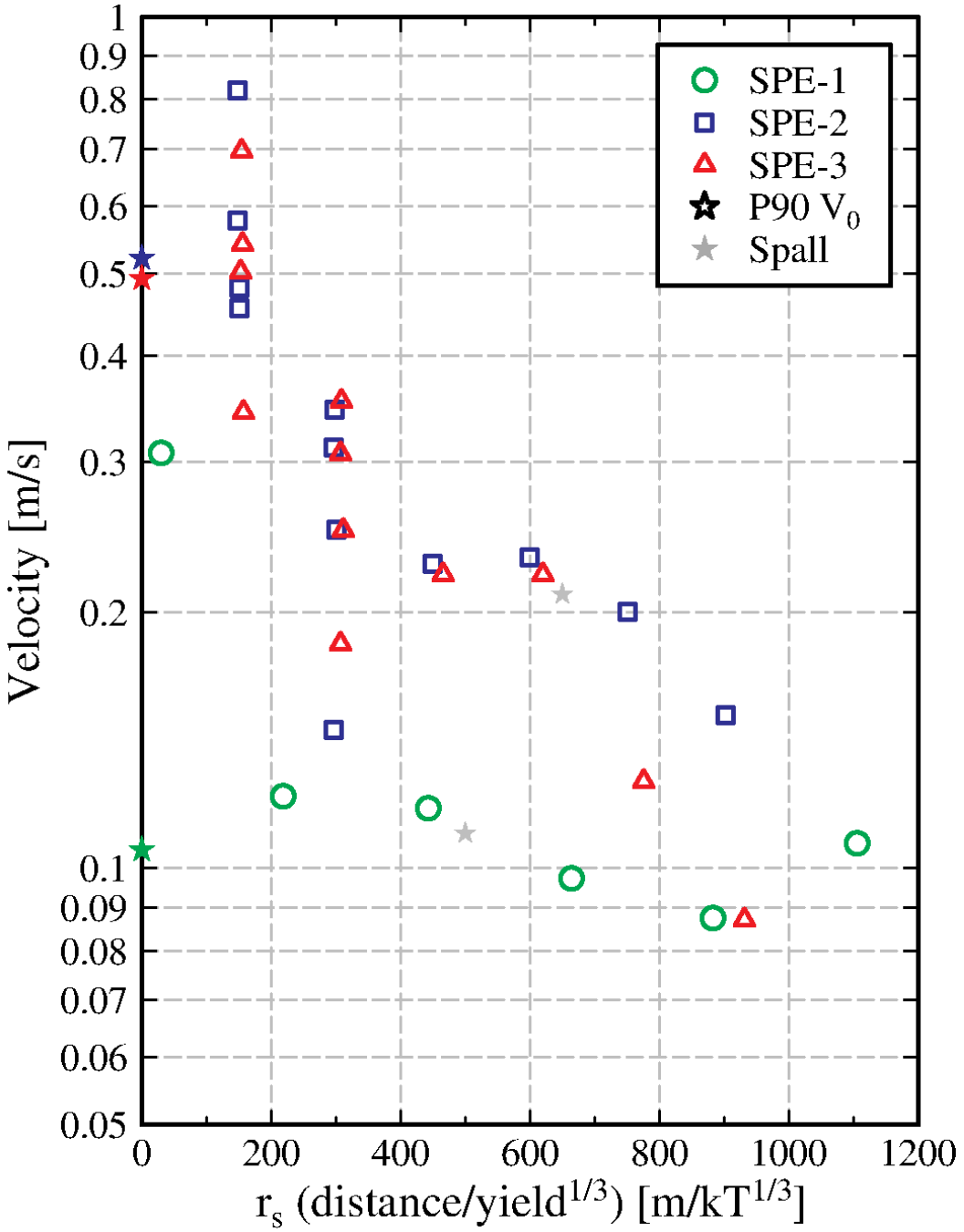

SPE-4 V_0 = 0.05 m/s

Model comparison with SL-10 (15m-NW)

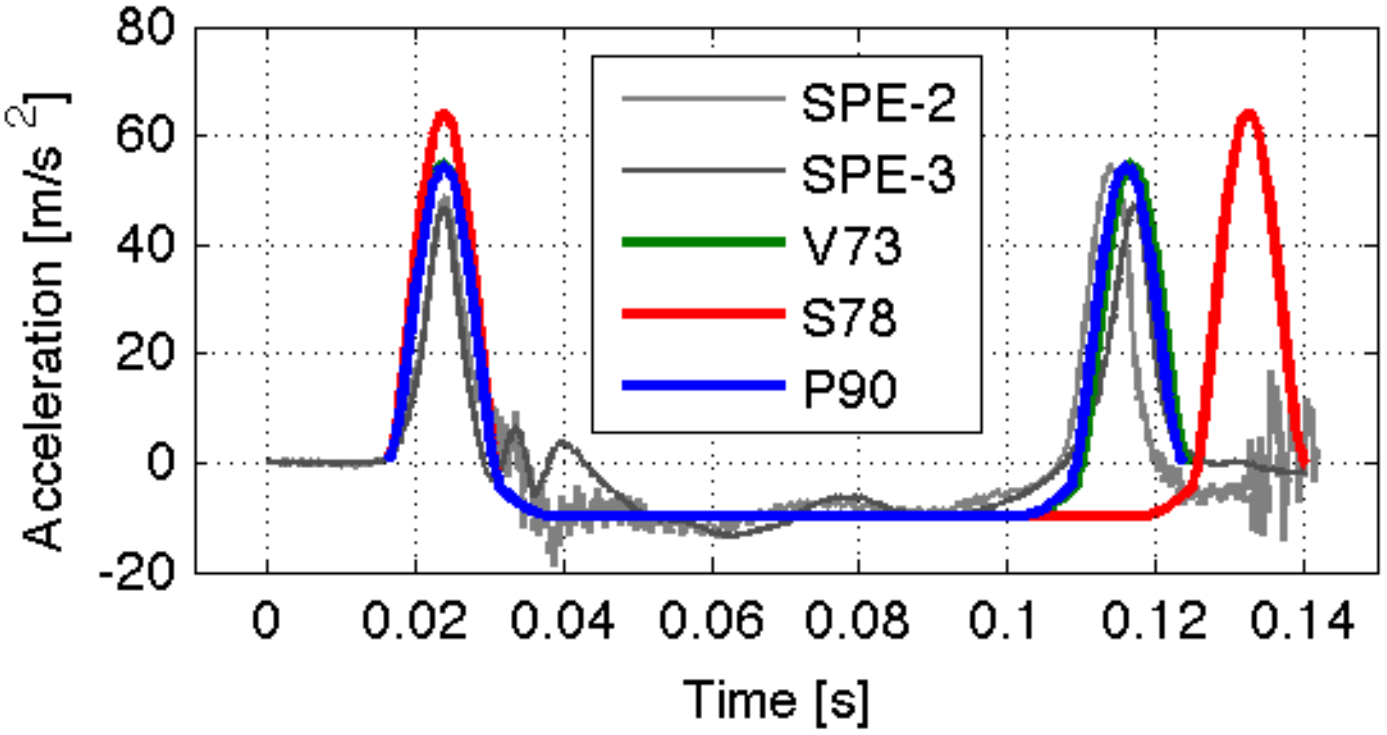

Model	Gap [cm]	Radius [m]	V_0 [cm/s]	Mass [T]	Dwell [ms]	Rise [ms]
V73	1.06	10.00	45.51	2.18	92.9	15.6
S78	1.45	28.72	53.24	24.62	108.7	15.6
P90	1.04	59.39	45.15	75.73	92.2	15.6

Explosion moment and spall force functions

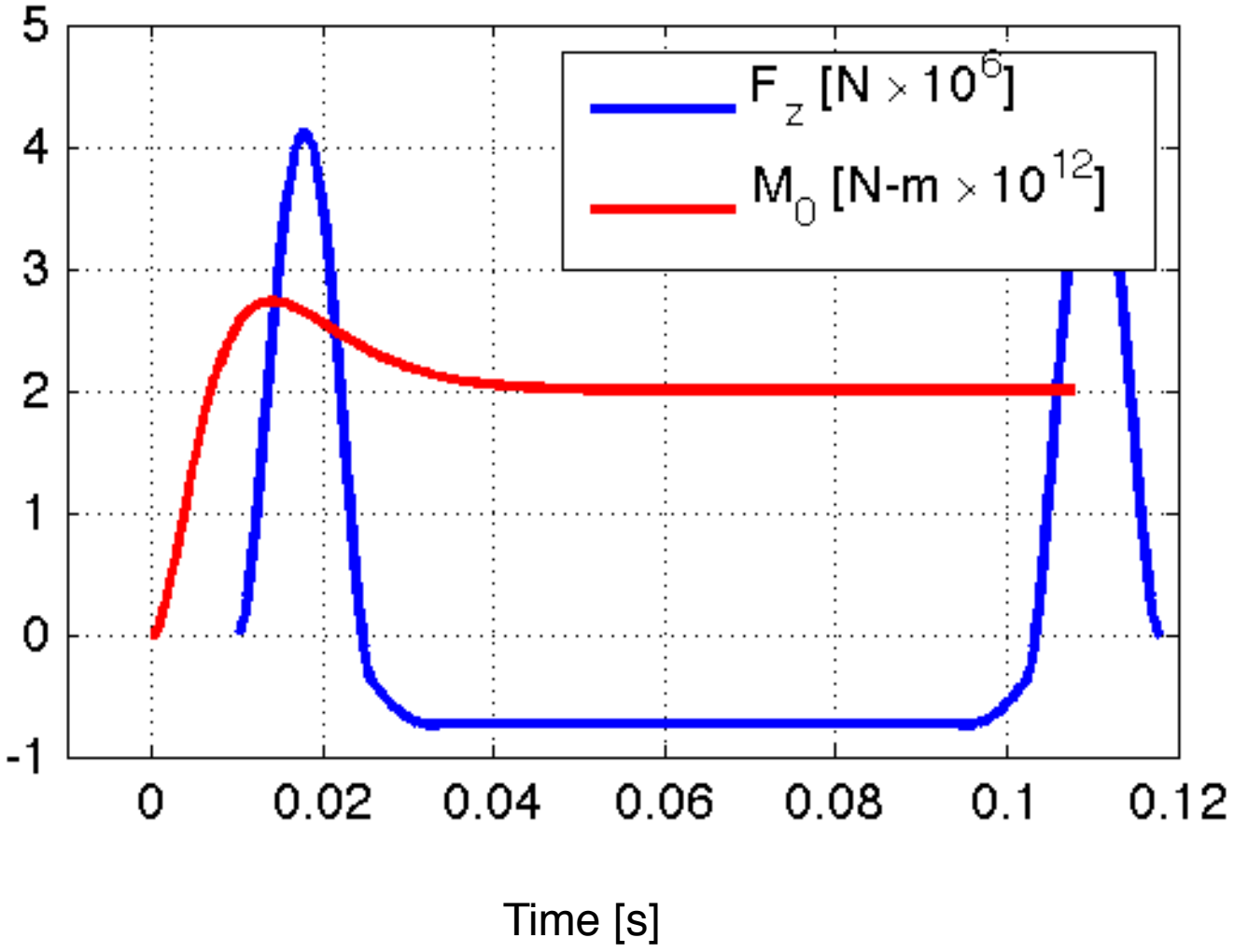

Far-field displacement functions

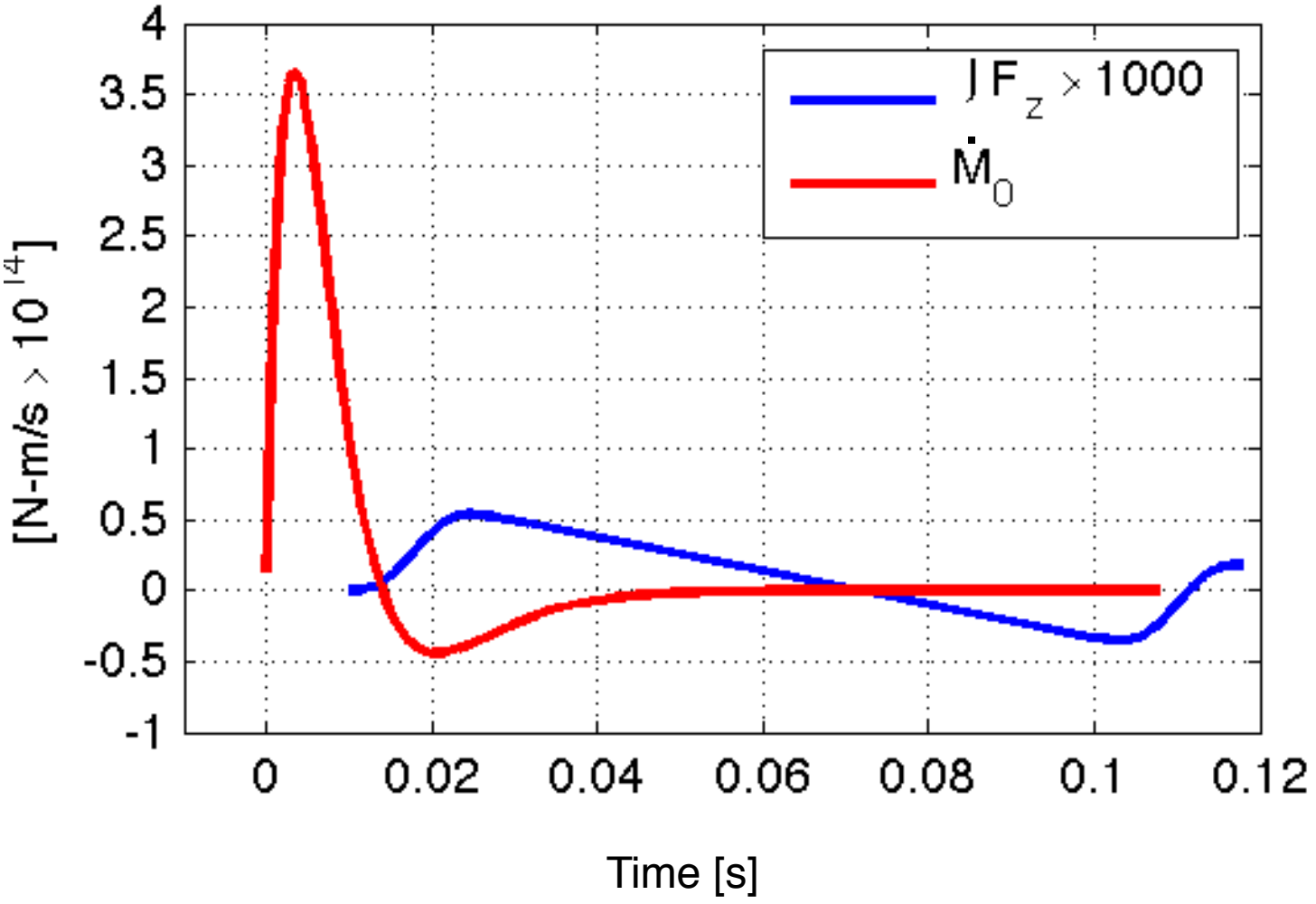

SPE-2/-1 Deconvolution

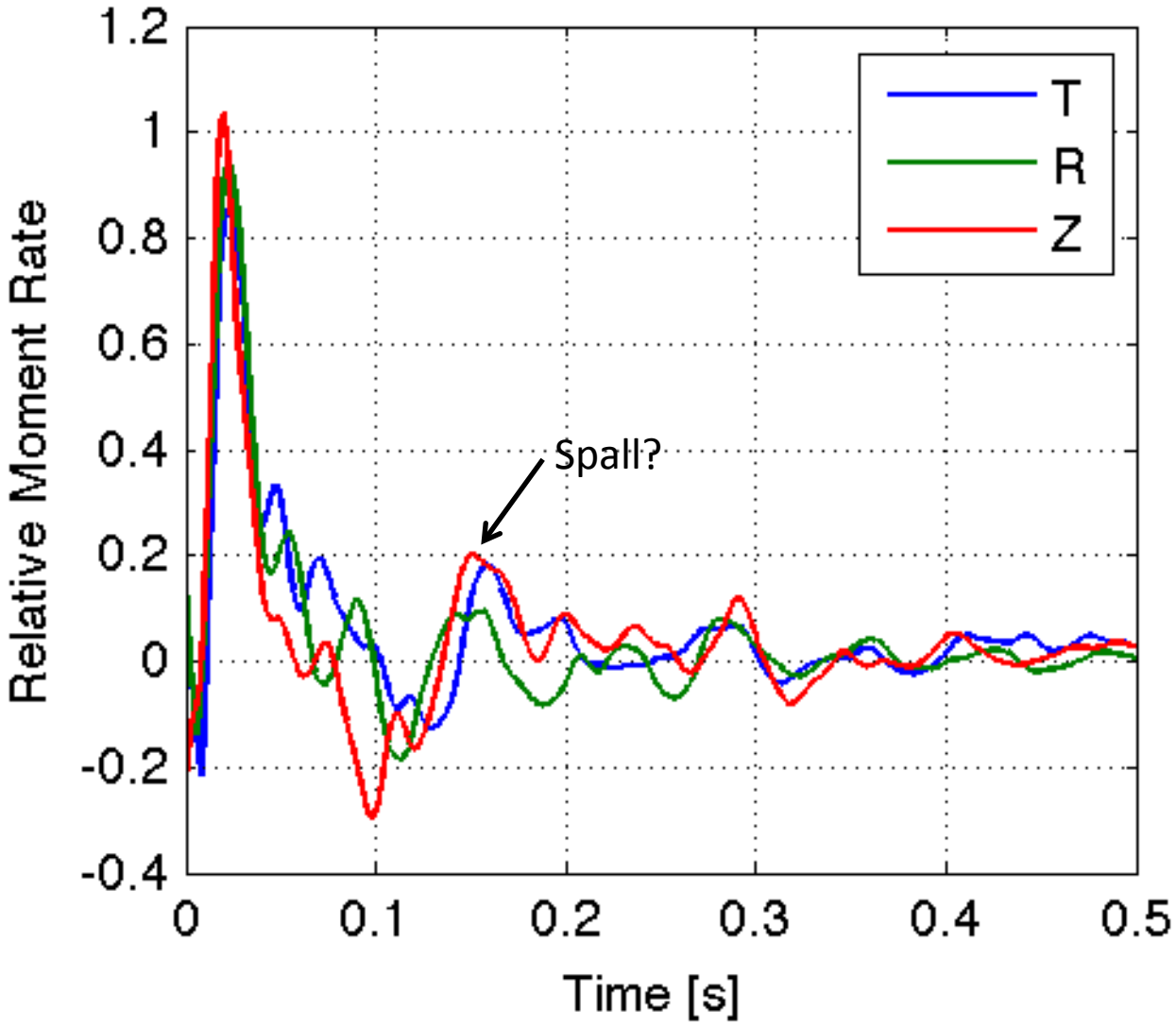

sean@llnl.gov

SPE Signals and Setting: Seismic Amplitudes and Velocity Models

R. J. Mellors, J. Sweeney, W. Walter, S. Ford, E. Matzel, A. Pitarka

Lawrence Livermore National Laboratory

LLNL-PRES-642636

This work was performed under the auspices of the U.S. Department of Energy by Lawrence Livermore National Laboratory under contract DE-AC52-07NA27344. Lawrence Livermore National Security, LLC

Overview

- EM & Aftershocks
  [*Sweeney et al*., 2013]
- Earthquake/explosion differences
  [*Walter et al*., 2013]
- Velocity models [*Matzel and Mellors*, 2013]
- Next steps

Electromagnetic measurements

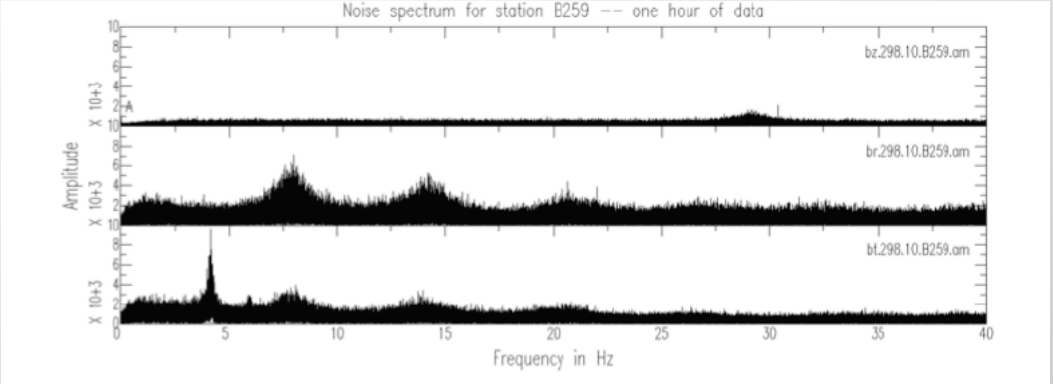

Schumann resonance

Question: Is a low-frequency electromagnetic pulse produced by chemical explosions?

Two three-component magnetometers deployed
[EMI BF-5 magnetometers sampled at 500 Hz; 60 hz notch; measure B field]
SPE2 60 and 90 m
SPE3 25 and 30 m

SPE3

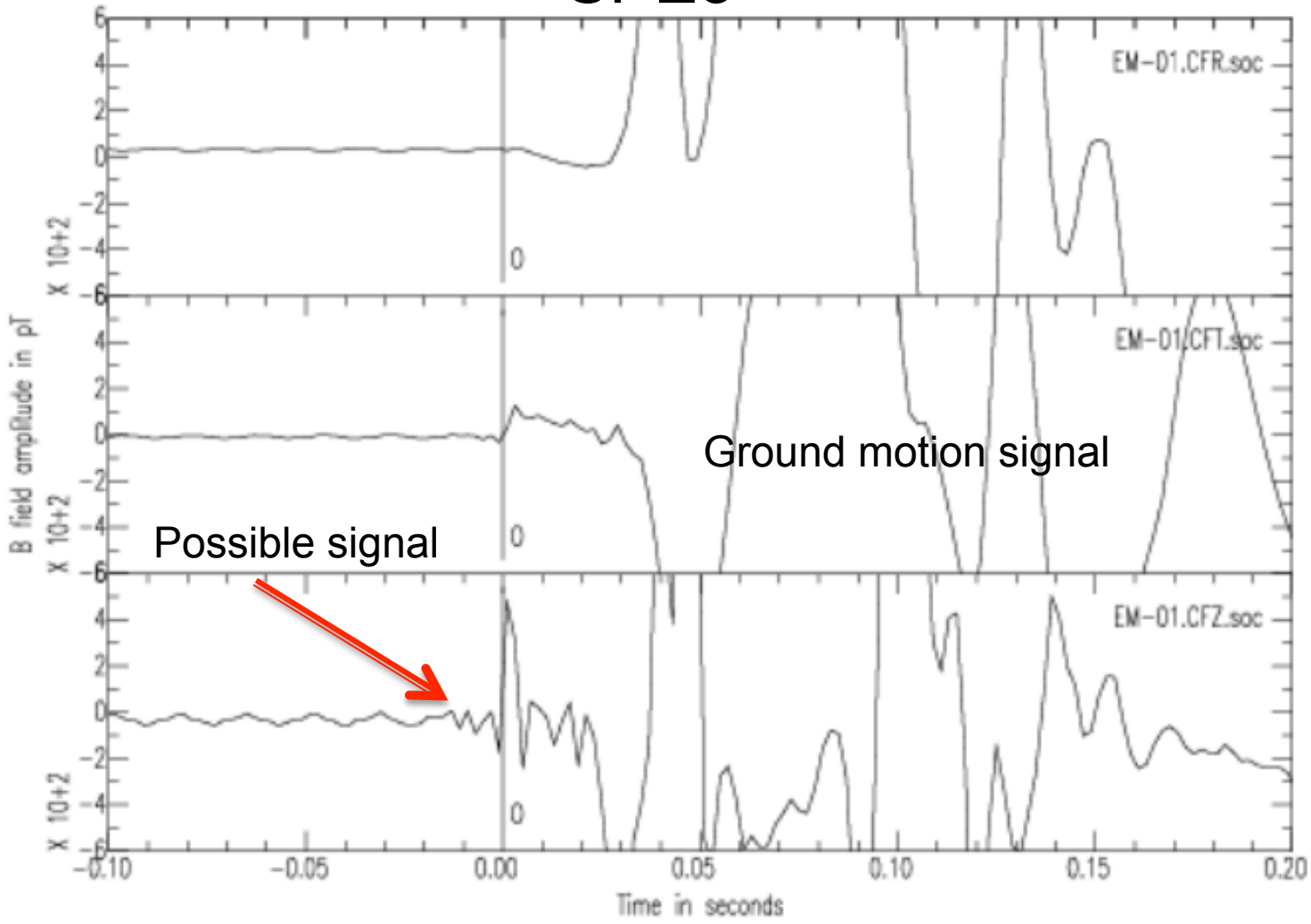

Maybe – SPE 5 and phase II will provide useful constraints

aftershocks

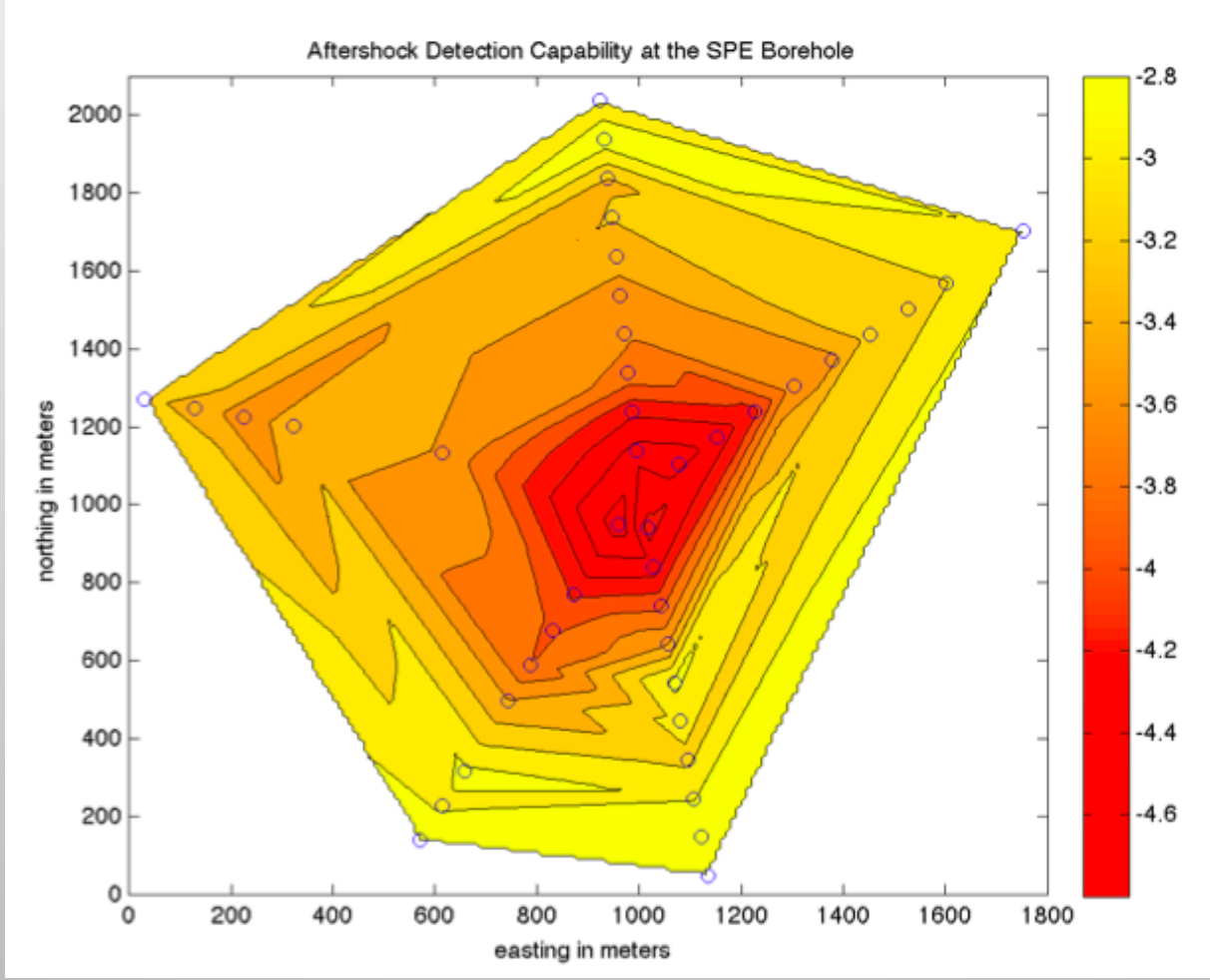

Aftershocks are typical after large underground explosions
None observed for SPE 1, 2, or 3.

Earthquakes and explosions: motivation

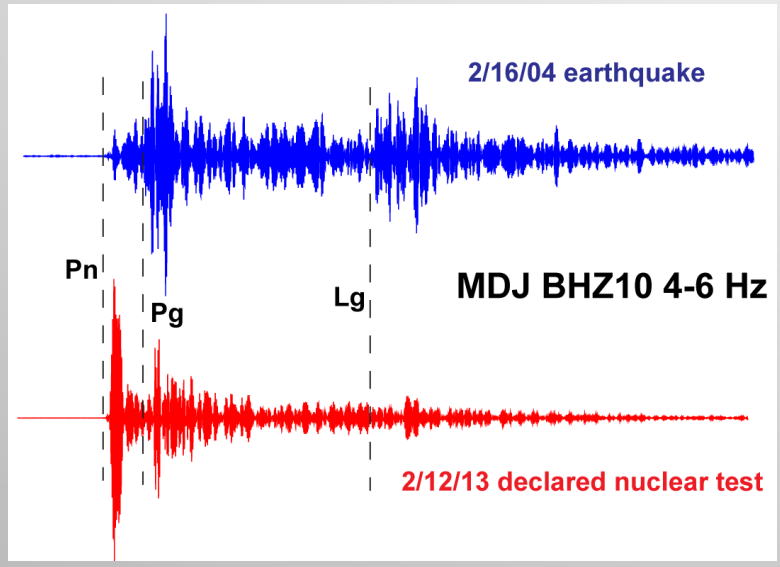

MDAC corrected 4-6 Hz Pn/Lg at MDJ BHZ10

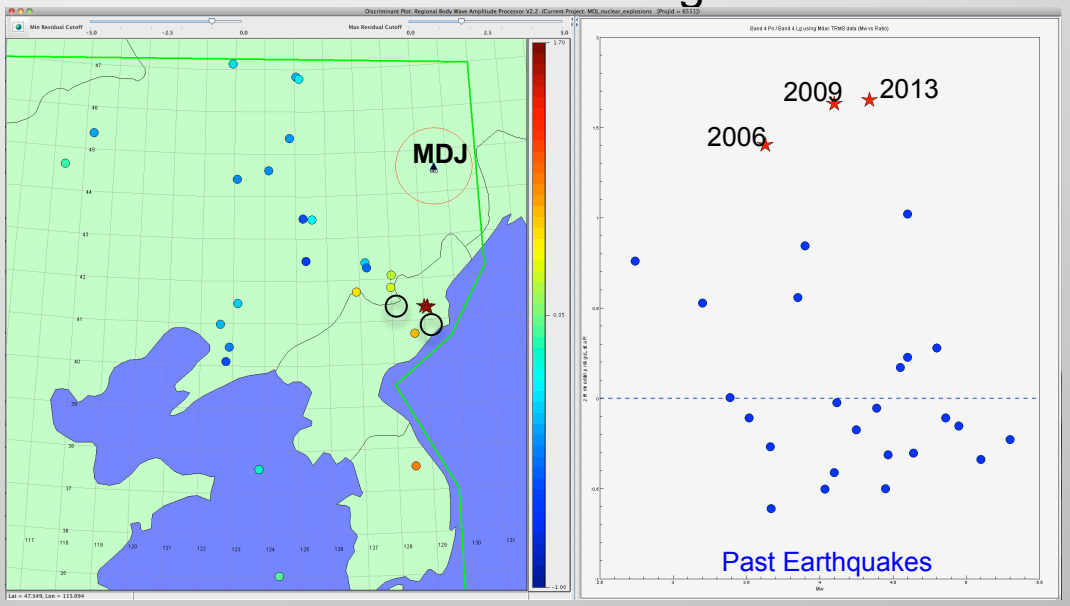

Example of using P and S ratio to discriminate explosions from earthquakes.

Adapted from Walter et al., 2013

In the 1990's we discovered empirically that high-frequency P/S discriminates explosions from earthquakes at all the major test sites

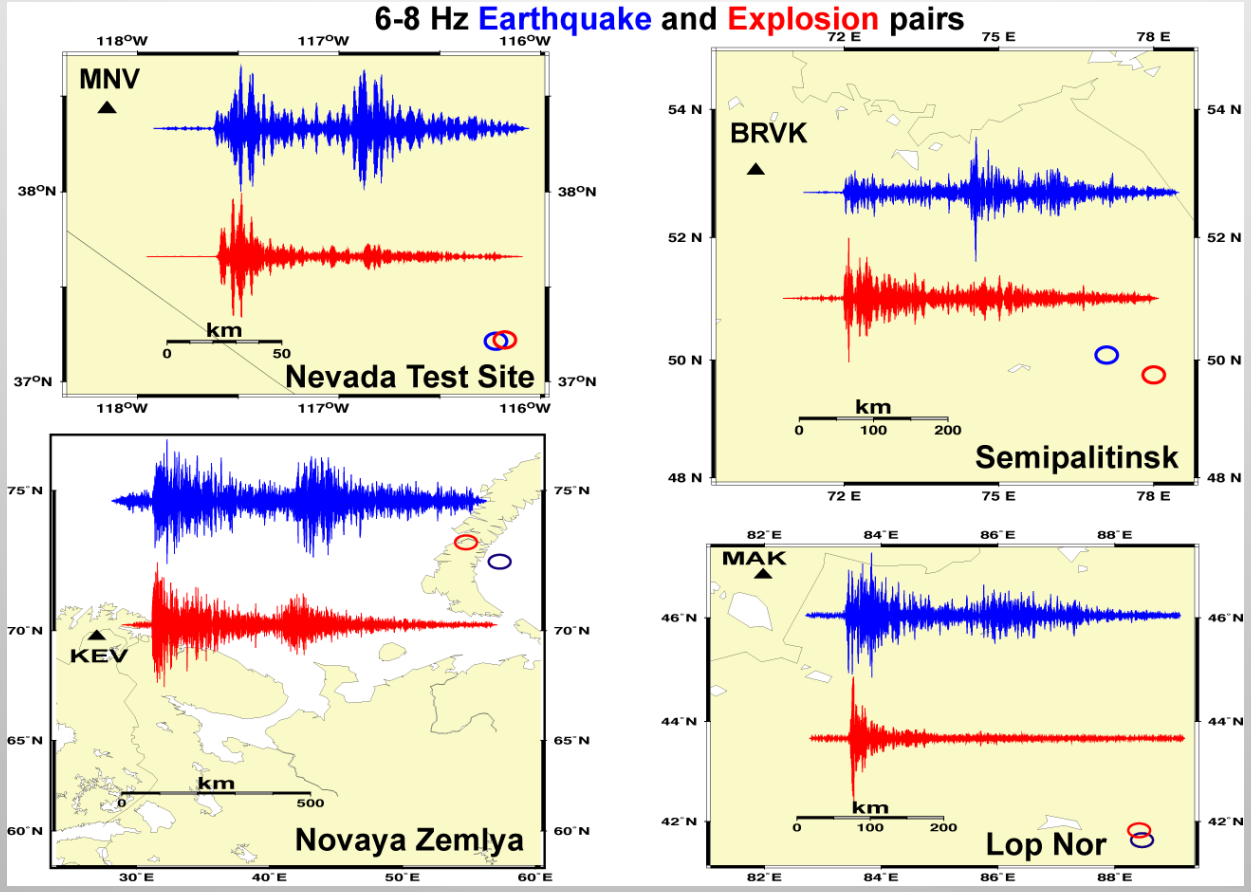

Can we predict the frequencies where P/S discriminates?
Lower frequencies propagate further extending the range of P/S

From Walter et al., 2013

Discrimination at local/regional distances

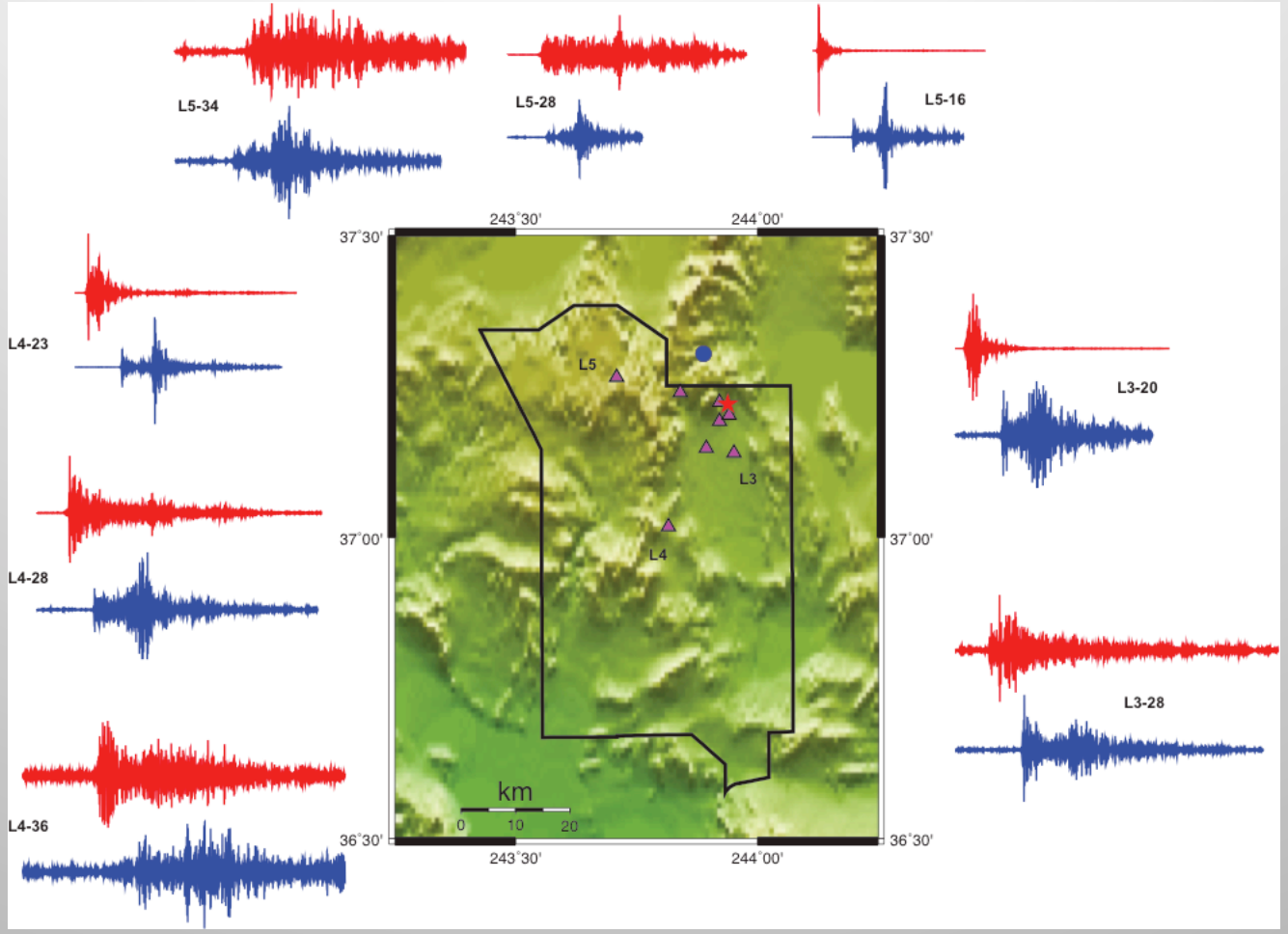

SPE: red Earthquake: blue

From Walter et al., 2013

Local distance P/S may not discriminate explosions from earthquakes without 3D corrections

Note P/S ratio discriminates SPE from nearby earthquake at regional and some local distances as expected.

However at SGV compared to TARNV – appears to be a structural focusing/defocusing effect

Using Source + Path modeling we will test this hypothesis

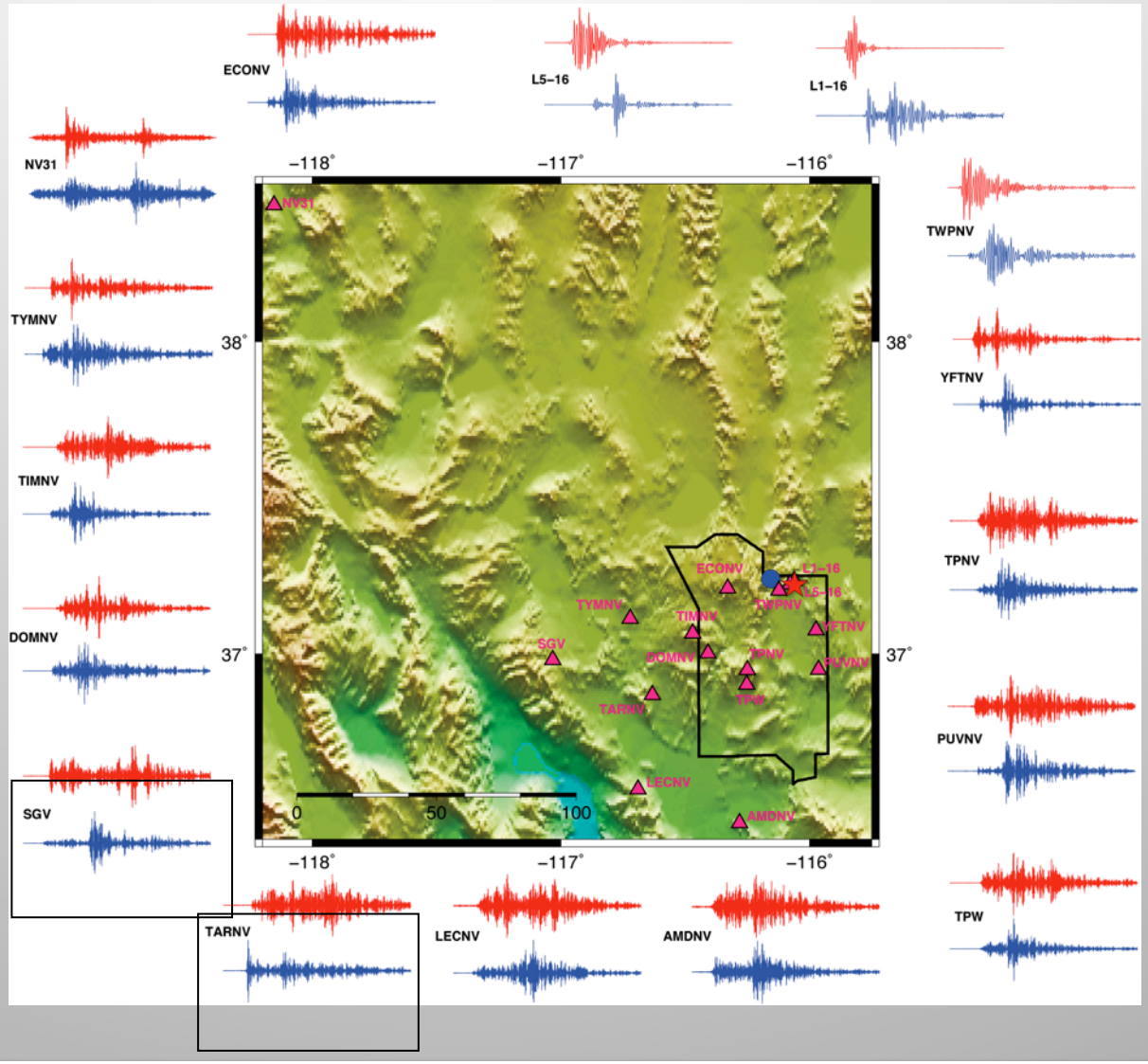

From Walter et al., 2013

Path modeling: Need velocity model

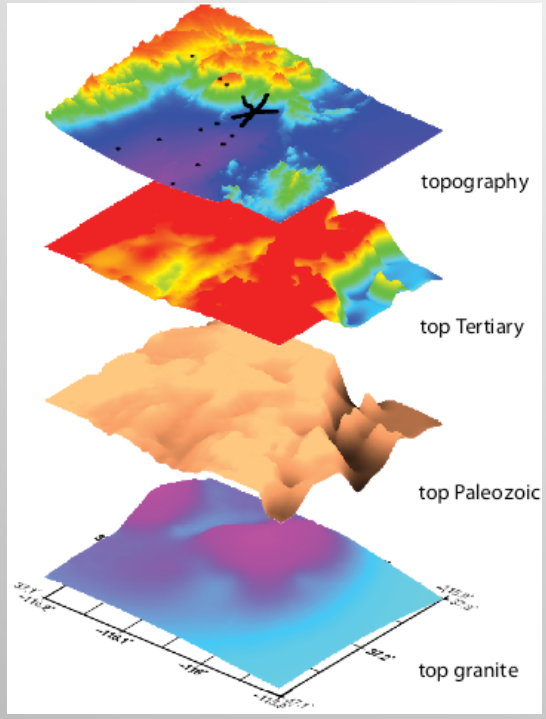

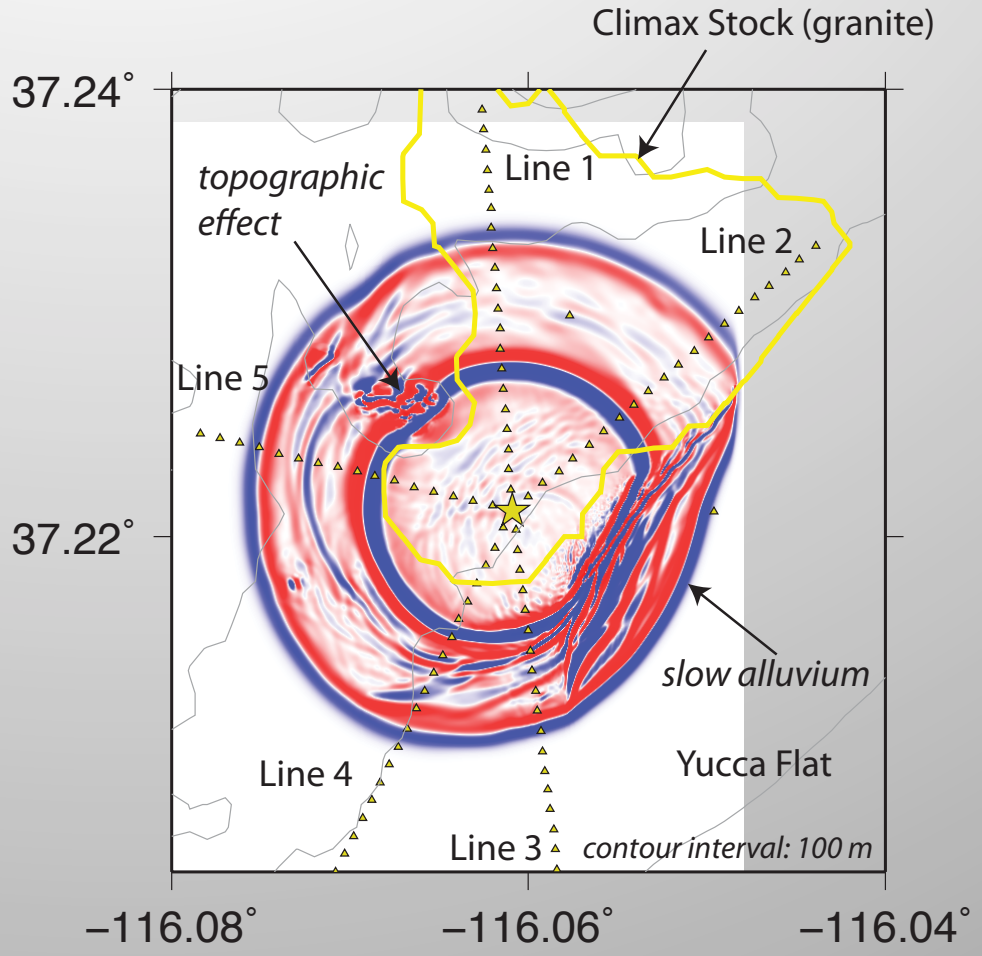

3D WPP finite difference simulation
Simple source representation

Question: How good is the model?

Goals:

- Improve model
- Site characterization
  - Active source
  - Well logs
- Use seismic data
  - Travel times
  - Surface wave dispersion
  - Inversion
  - Noise/coda correlation

Strategy: start with granite and move outward

Needed:
A standard velocity model

1D representation not good enough.

Climax Stock ‘average’ and near borehole profiles

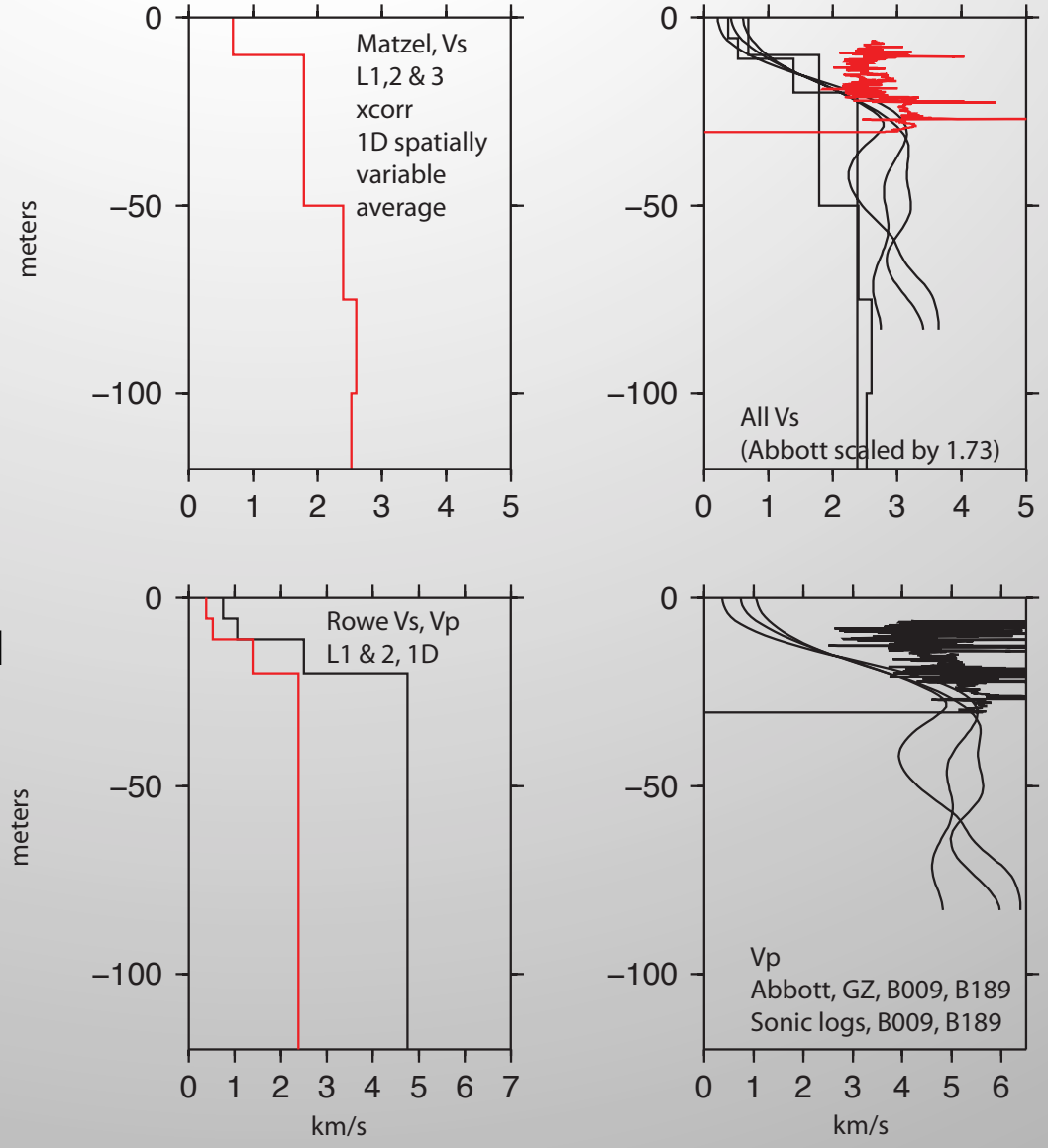

Thanks to C. Rowe, R. Abbott, M. Townsend

geology

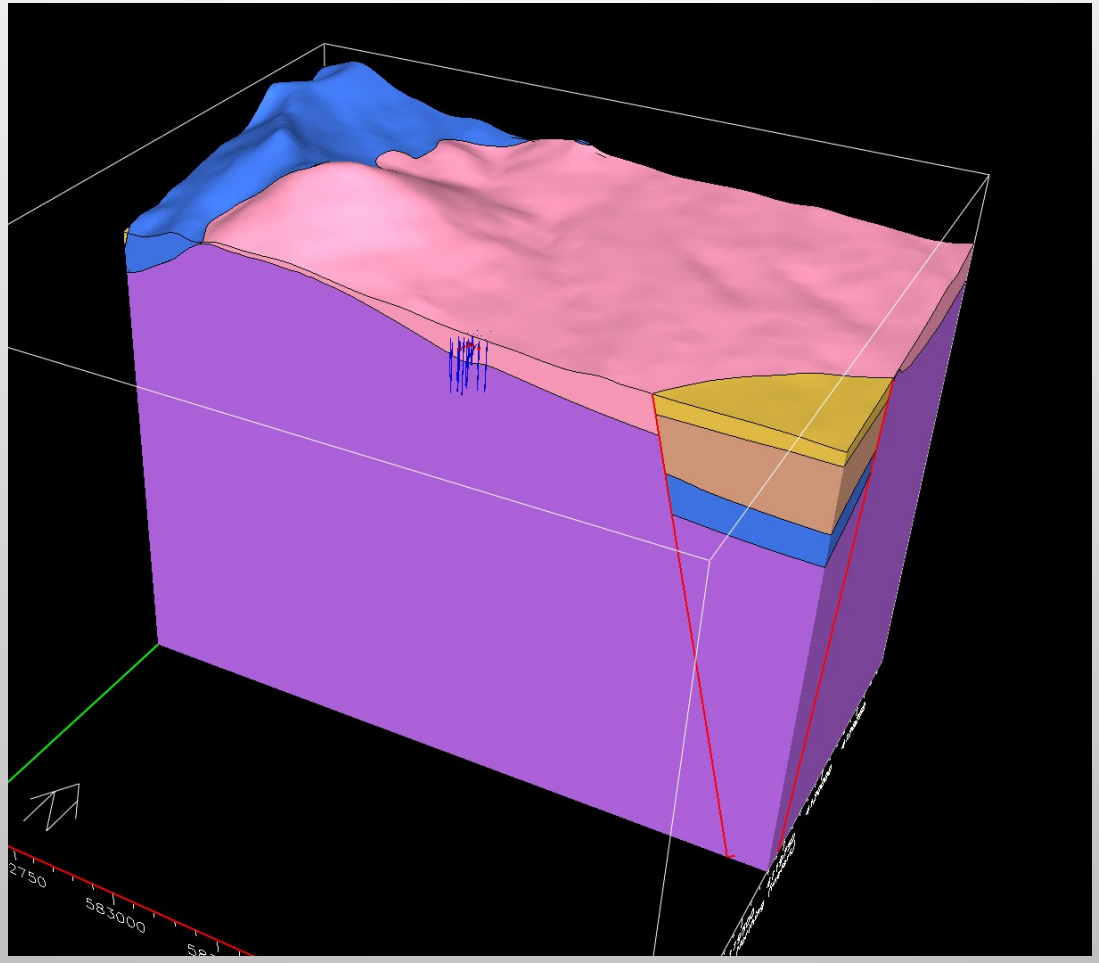

Coda interferometry

- Use shot records from SPE2
- Correlate station with another
- Yields Green's function between stations
- Filter Green's function between 5-10 Hz
- Invert for best-fitting 1D model for each (<5 km) [simulated annealing with FK]
- Combine into 2D profiles along each line

Use absolute value of Green's function

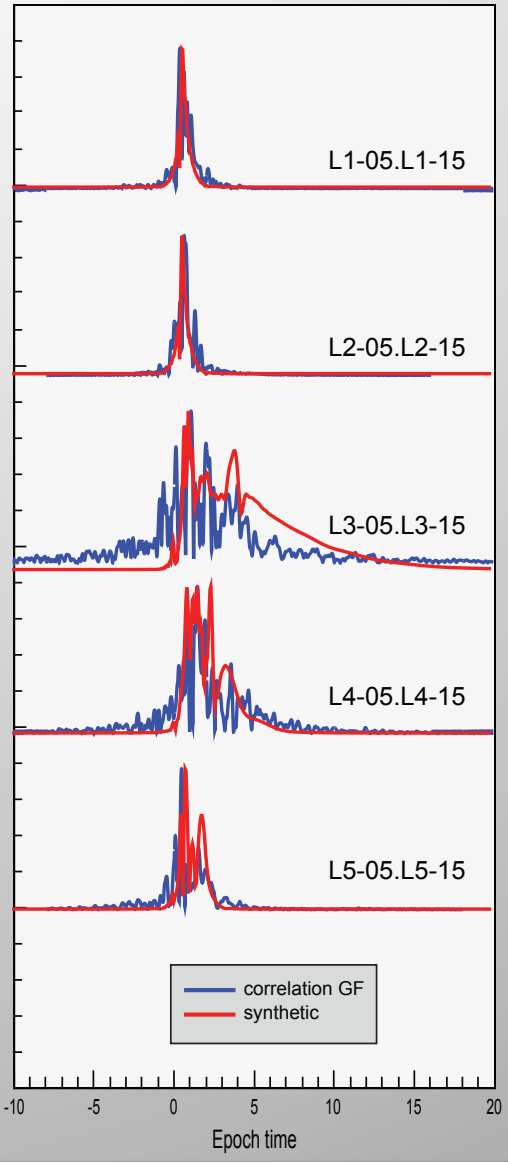

Results

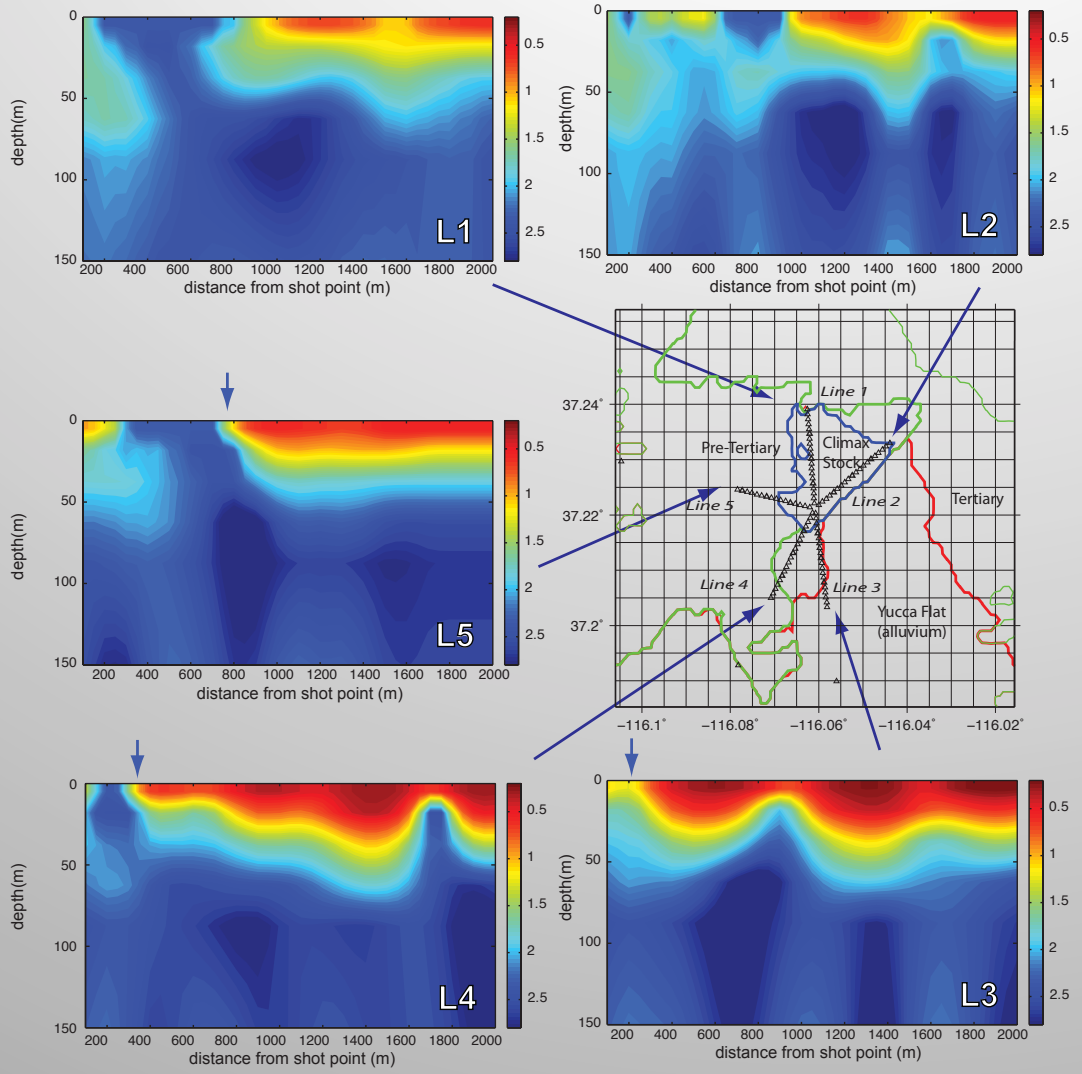

Low velocities along L3, L4
Higher along L1, L2

Velocities at GZ not resolved.

Test model with waveforms

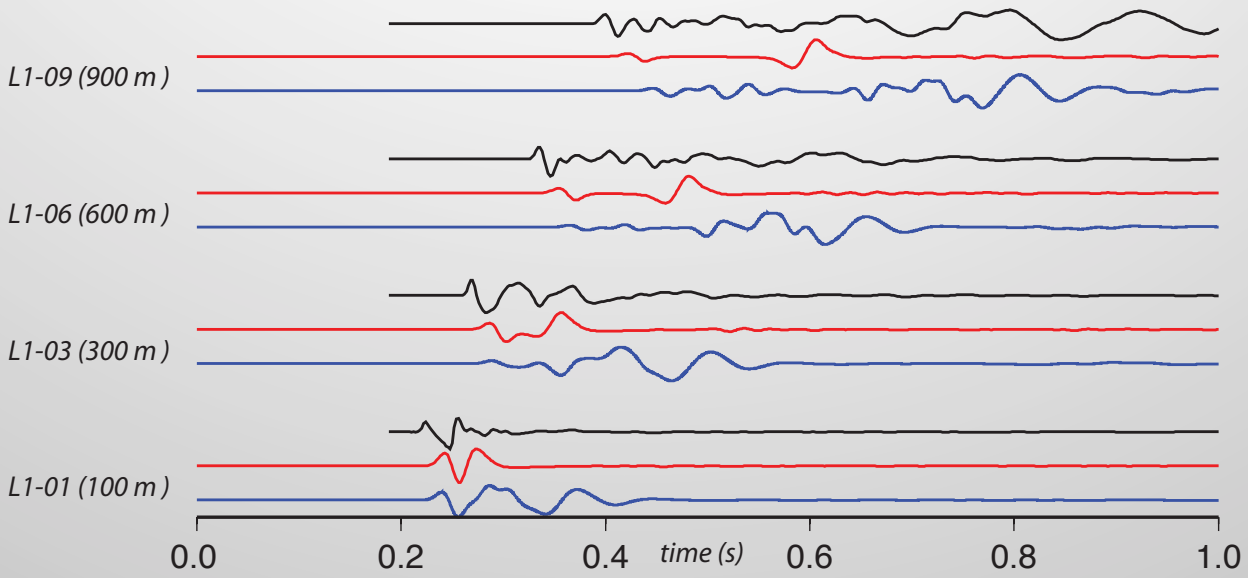

Coda model [2.5 D] travel times delayed w.r.t data
Surface wave generation enhanced.
[geology model here does not include layer]
Need to improve. Use ambient noise.

SPE2 data
geology model
correlation model

Ambient noise correlation

In progress
3 months of high-gain data
All available velocity stations (gs11 and broadbands)
~ 8,000 pairs
Automatically model
Should yield detailed model of region within 2-5 km.

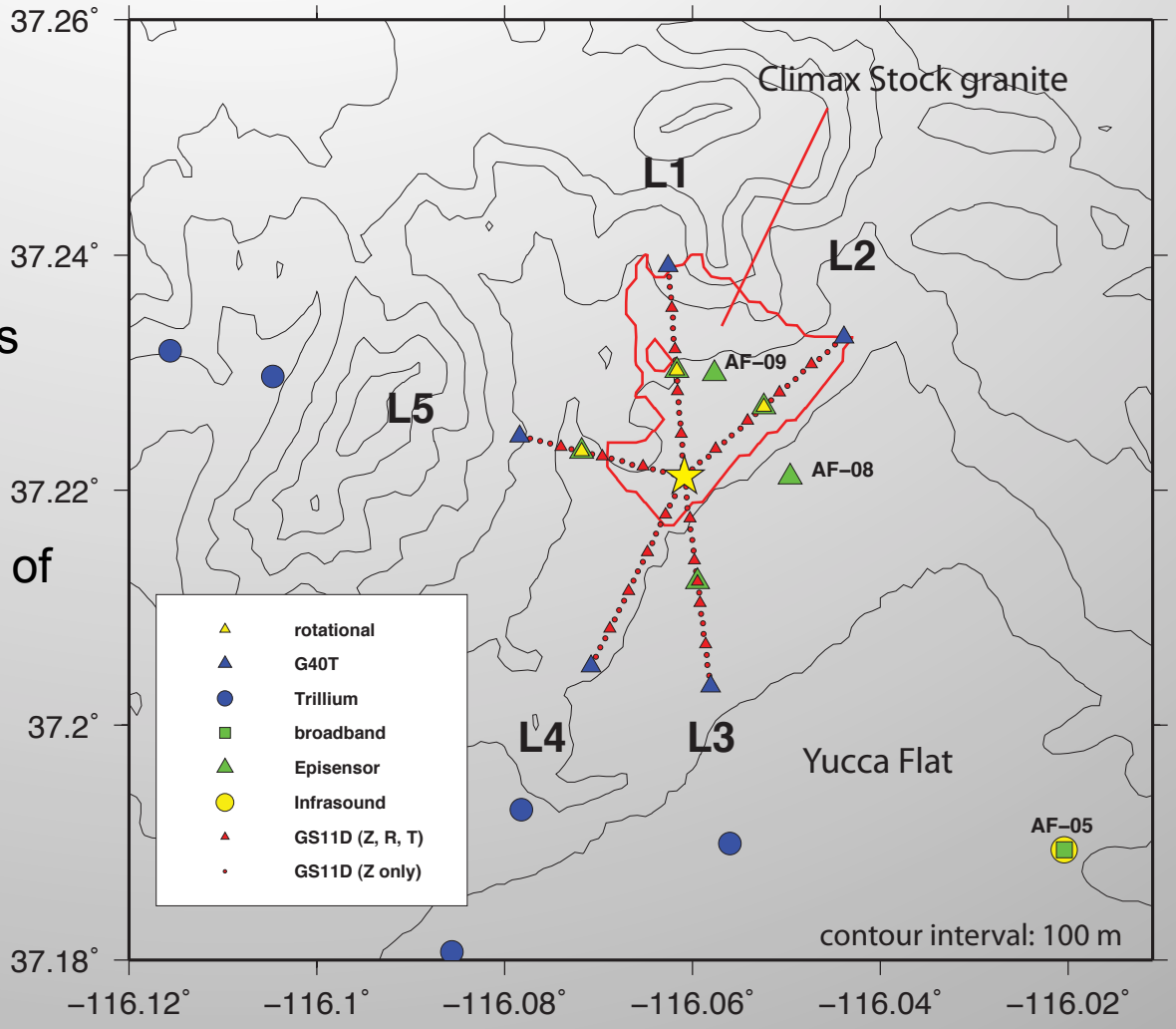

Next steps

- Interferometry appears feasible.
- Ambient noise tomography of all stations (~ 8000 pairs in progress – hope to present at SR/AGU).
- Will yield a 3D velocity model of Climax Stock and northern Yucca Flat.
- Will combine with improved source (e.g. *Vorobiev et al., Pitarka et al.*)
- Should help resolve path effects.

Analysis of Recorded and Simulated Far-Field Ground Motion From the Source Physics Experiment

Arben Pitarka, Robert J. Mellors, Oleg Y. Vorobiev, Ezzedine Souheil,Arthur J. Rodgers, William R. Walter, Tarabay Antoun, Anders Petersson, and Jeff Wagoner.

Lawrence Livermore National Laboratory

State-of Analysis Review Meeting, Las Vegas

August 22, 2013

LLNL-PRES-753593

This work was performed under the auspices of the U.S. Department of Energy by Lawrence Livermore National Laboratory under contract DE-AC52-07NA27344. Lawrence Livermore National Security, LLC

Overview

***Objective**: Improve understanding of the excitation and propagation of seismic waves, especially shear waves, from underground explosions.*

Approach:

- *Simulate near-field ground motion from underground SPE3 explosion using a physics based source model coupled with far-field viscoelastic wave propagation*
- *Compare with observed waveforms from Source Physics Experiment.*
- *Analyze path effects (scattering, topography, and structural variations) at close distances (< 20 km)*

- ***Long-term Goal**: Create a physics-based end-to-end model for monitoring that couples hydrodynamics to elastics and allows for both scenario prediction and detailed analysis of observed signals*

SPE Shots

- Emplaced in granite
- SPE1: 100 kg TNT at 55 m
- SPE2: 1000 kg TNT at 45 m
- SPE3: 1000 kg TNT at 45 m

Sensors

- Array of near-field borehole and surface accelerometers
- Instruments deployed along 5 radial lines out to 20 km
- Mix of short-period and broadband
- Infrasound

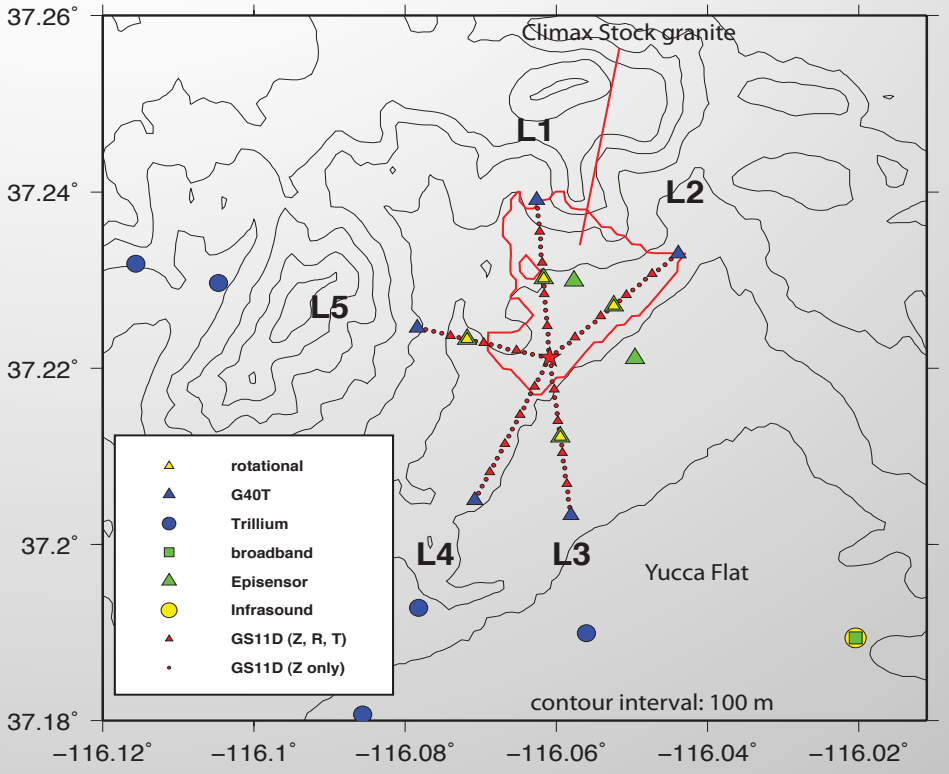

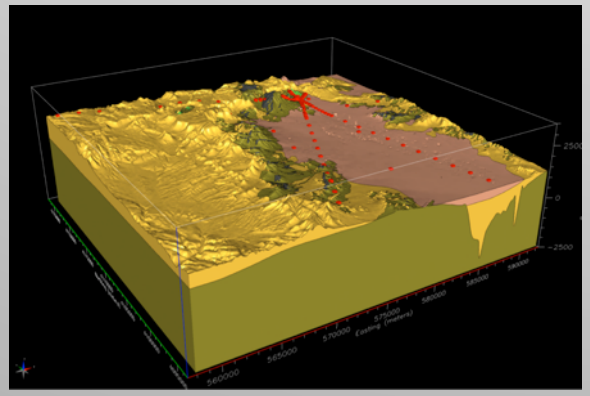

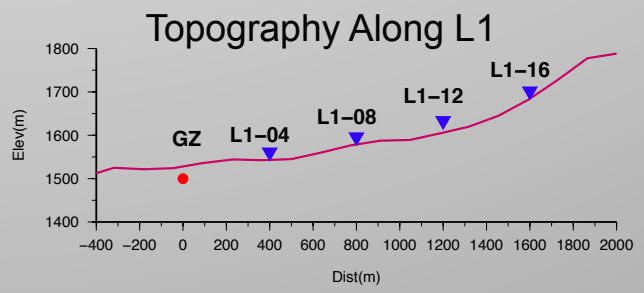

Observed Far-Field Shear Wave Energy

Broad-Band

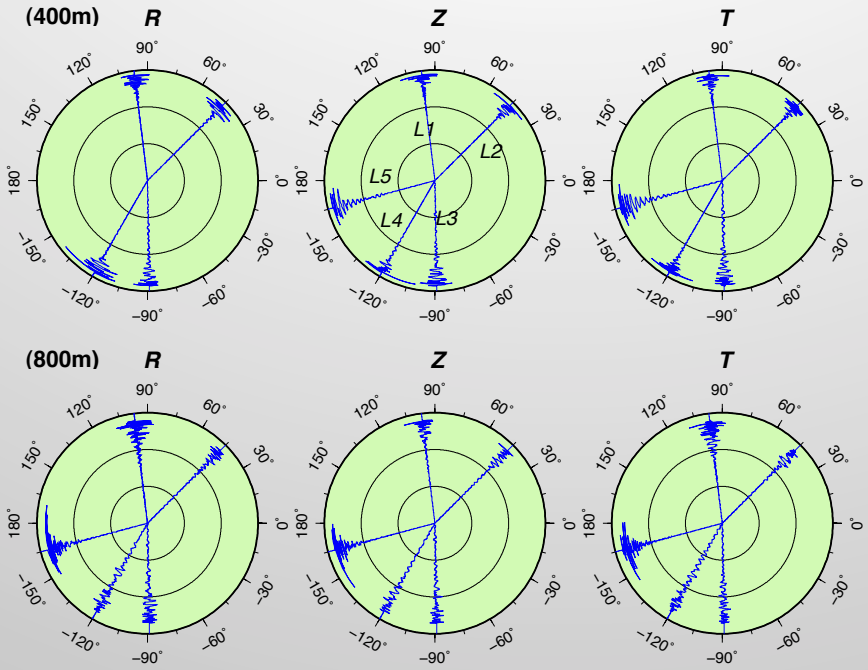

400m

800m

Significant shear wave energy on the tangential component

Causes:

- source effects
- wave propagation effects?
  (structural heterogeneity, surface topography)

FK Analysis Using Small Array Data

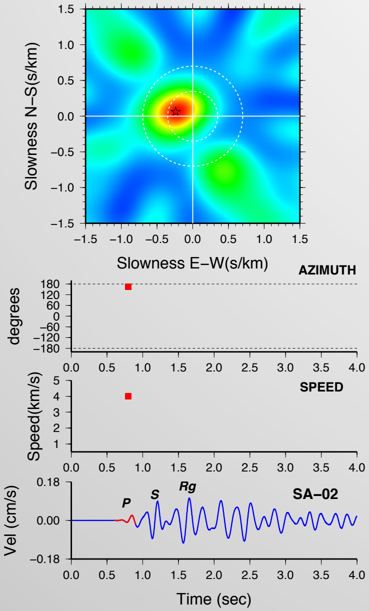

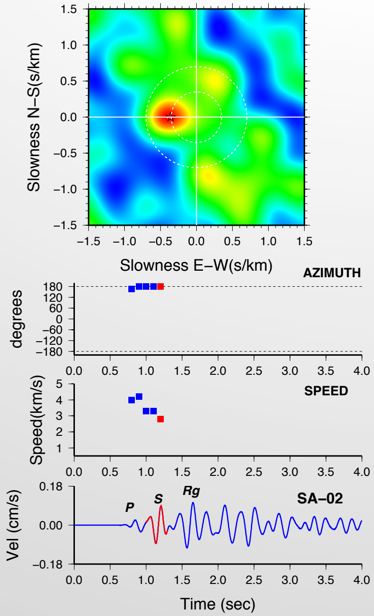

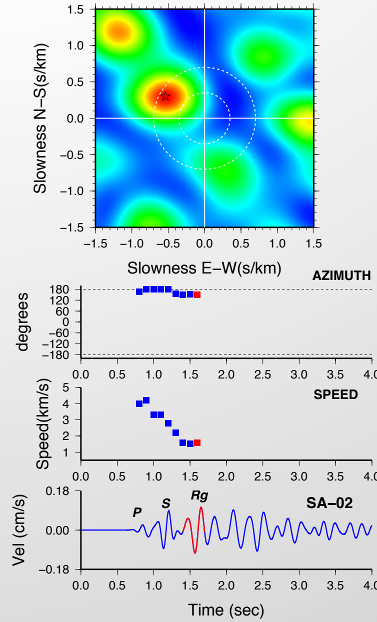

Azimuth

Apparent Velocity

Recorded Motion

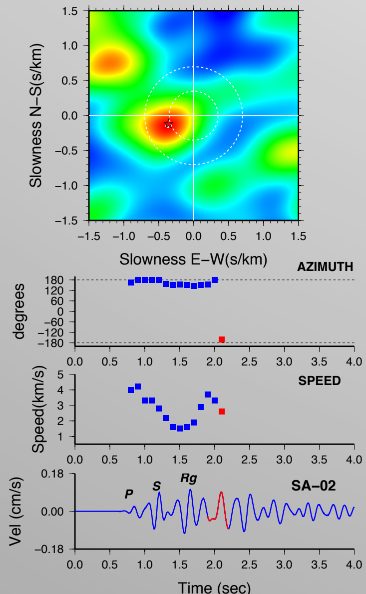

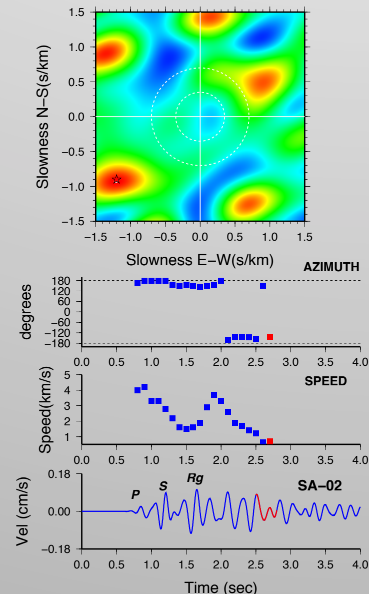

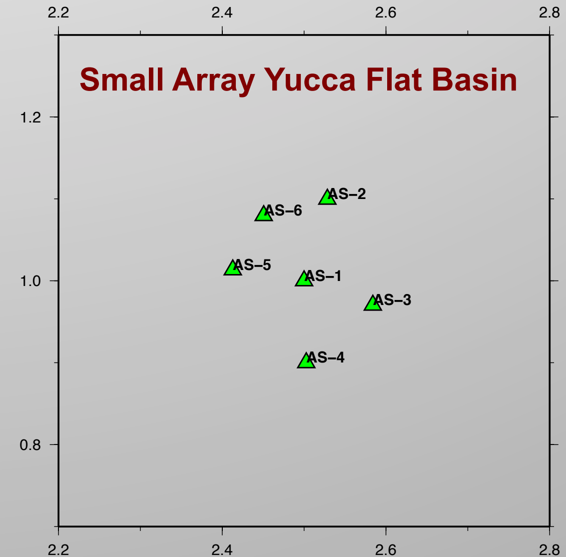

S-waves are produced in the near-field and seem to be consistent with motion on joints

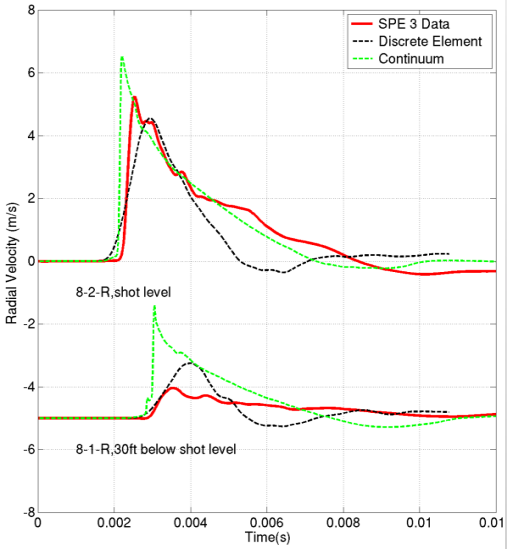

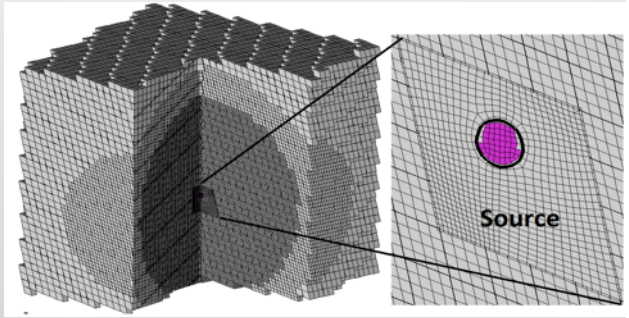

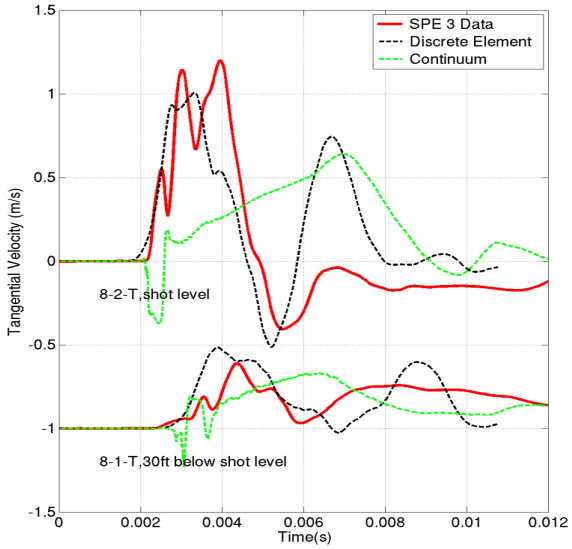

Efforts are underway to improve the quantitative agreement with the near field data and correlate the observed anisotropic behavior to the underlying physical mechanisms

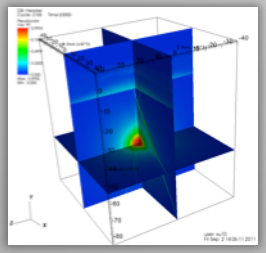

faults & geologic layers

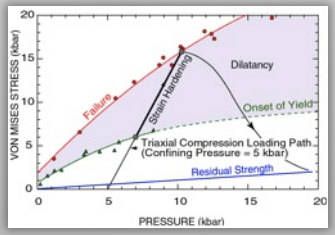

Constitutive behavior of the rock

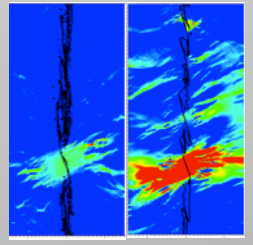

Joint properties

after Vorobiev et al

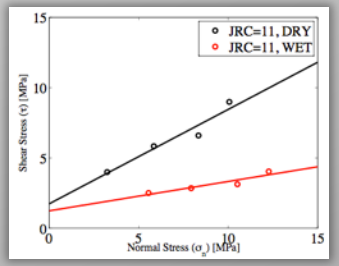

Effect of saturation

Near-Field and Far-Field Coupling

- **One-way coupling** between nonlinear, inelastic near-field and linear, visco-elastic far-field regions using a padding mortar space in 3D.
- **Near-field:** 3D Lagrangian hydrodynamics code with non-linear material response (GEODYN-L)
  - Explosion loading
  - Compressional and tensile failure, yielding, porosity, cavity formation
  - source mortar embedded within finite difference model
- **Far-field: 3D-FDM (WPP)**
  - Driven by interpolated time series from GEODYN model
  - Signals propagated through complex 3D velocity model of geology to distances of 10's of kms
  - Coupling verified and validated.

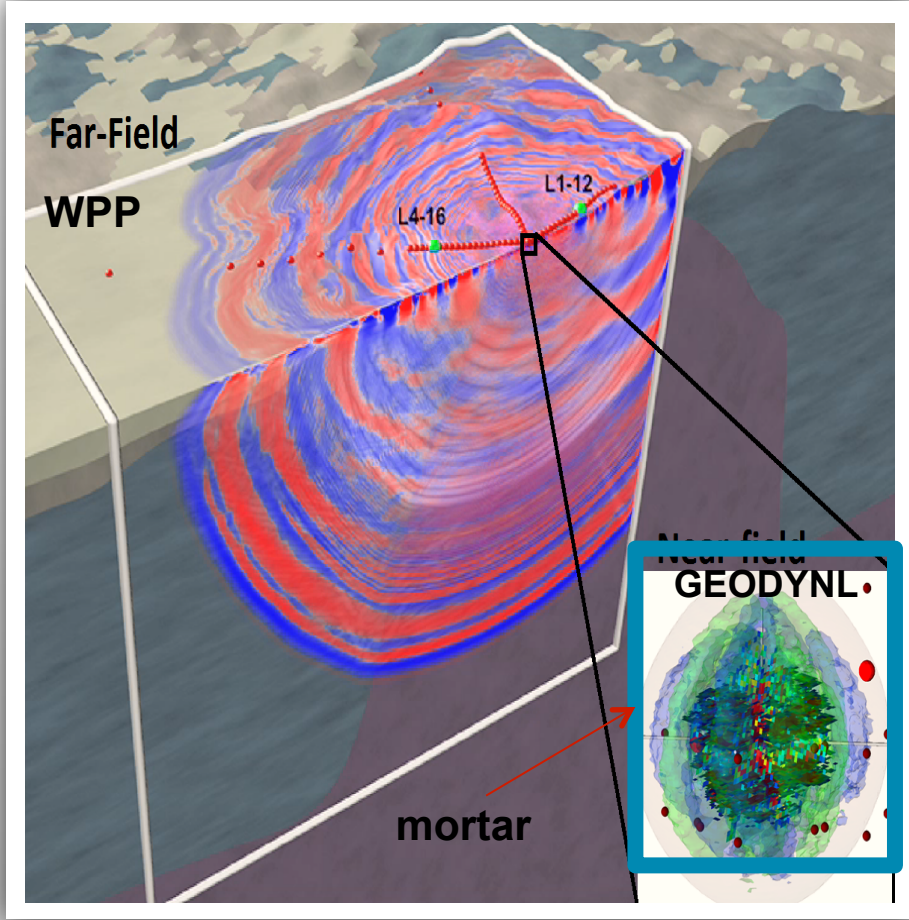

WPP

3D finite-difference code Curvilinear grid for topography, mesh refinement, viscoelastic model .Designed for massively parallel systems

3D Underground Structure

Large Scale Constraints of the 3D Velocity Model

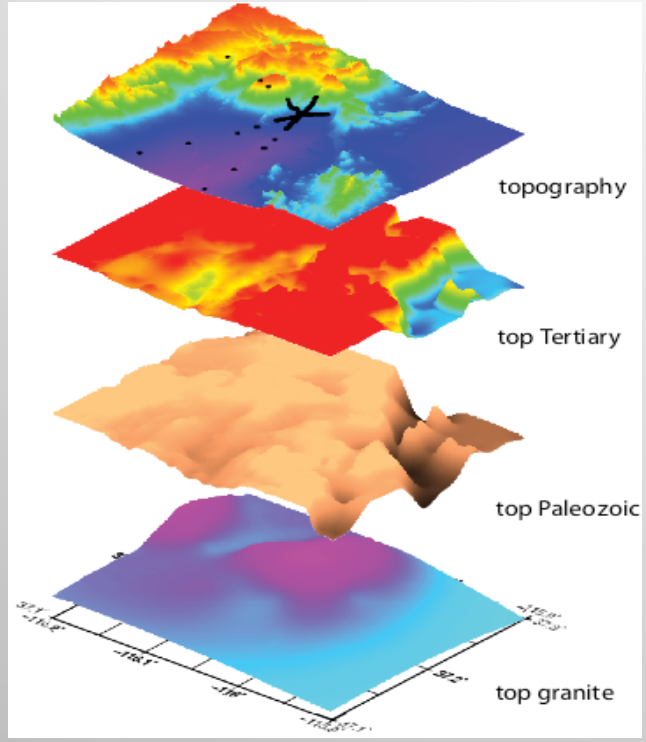

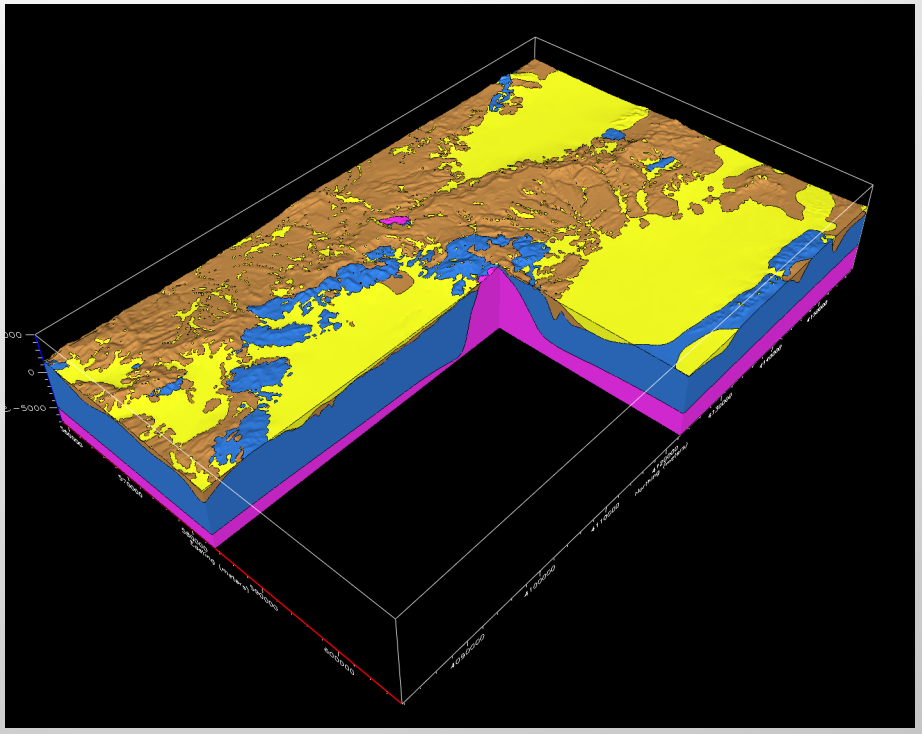

(Wagoner,2012)

3D Model Based on
- Geology
- Surface mapping
- Boreholes
- Geophysical models

Lithology	Vp(km/s)	Vs(km/s)	
Softer Granite	4.34	2.50	H=60m
Granite:	6.20	3.58	no gradient
Paleozoic:	5.60	3.24	small gradient
Tertiary:	4.20	2.42	small gradient
Quaternary:	3.00	1.50	no gradient
Top Quaternary	2.00	0.90	H=80m

Stochastic Small Scale Heterogeneity (l=1km,up 15%)

2.5D Modeling of Shallow Structure in Granite

Coda Interferometry (Matzel et al. 2013 Mellor's talk)

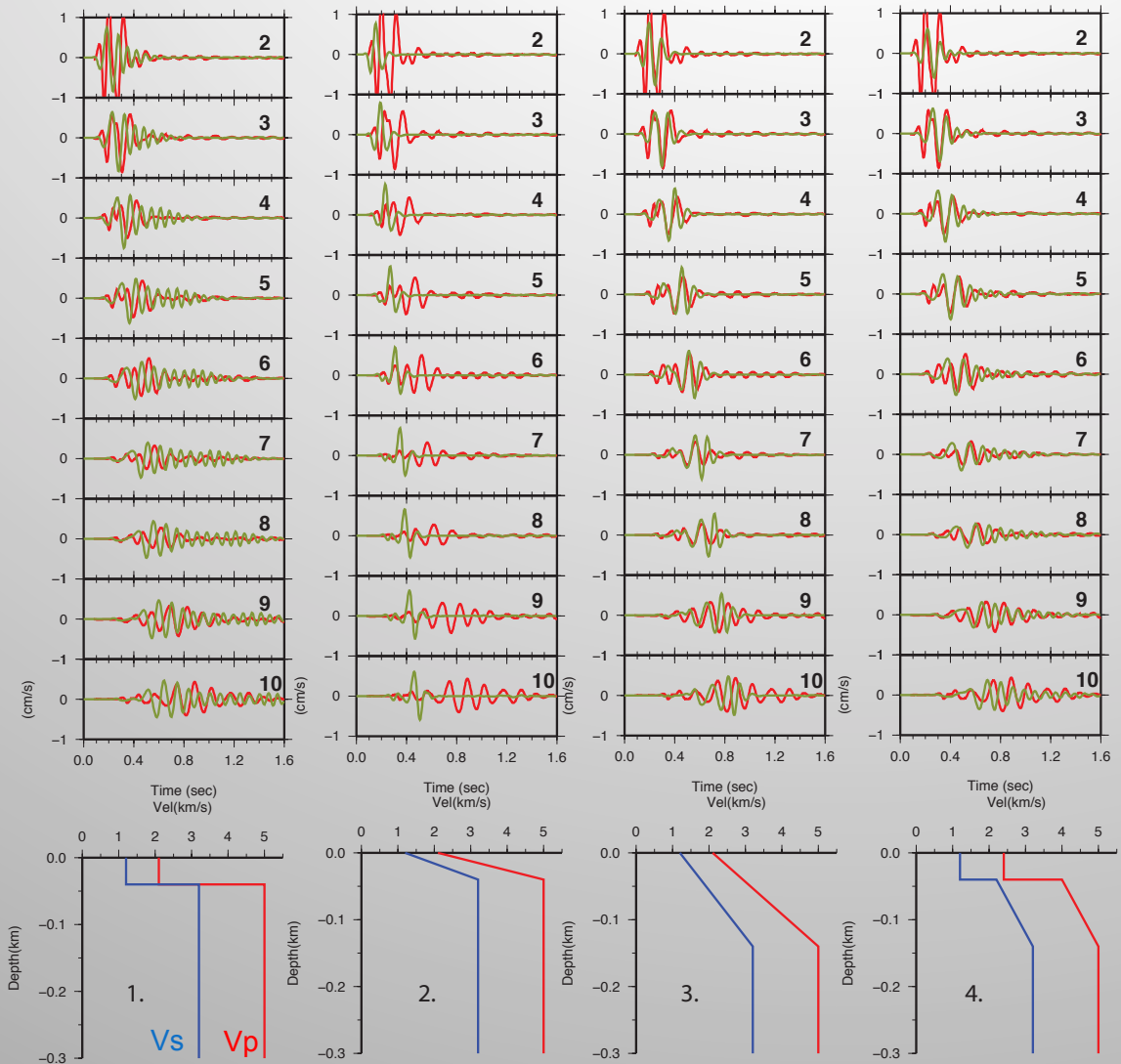

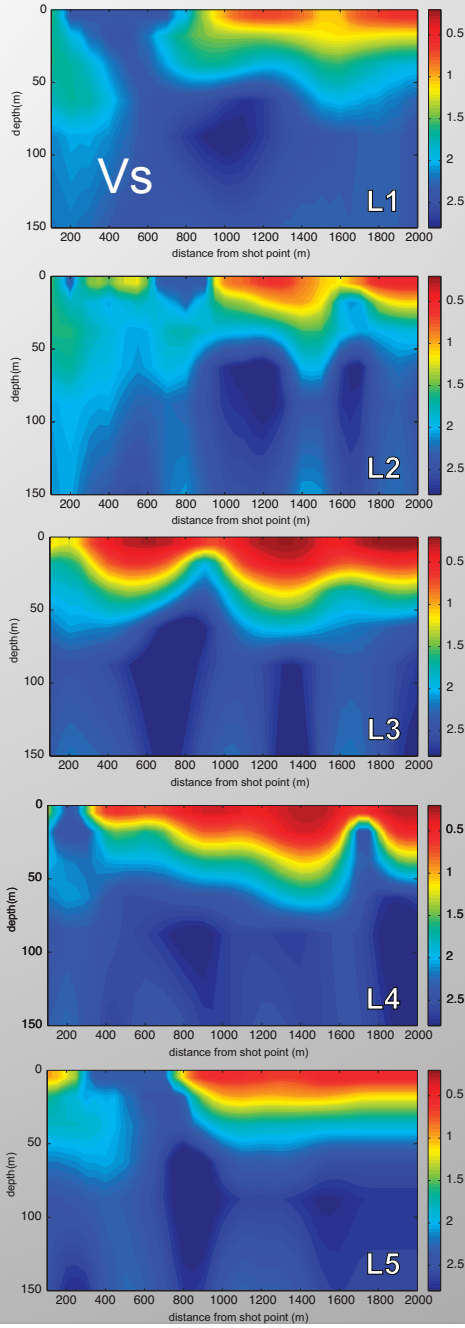

Models of Surface Weathered Layer for L1 (Max Freq 10 Hz)

Small Scale Shallow Variations

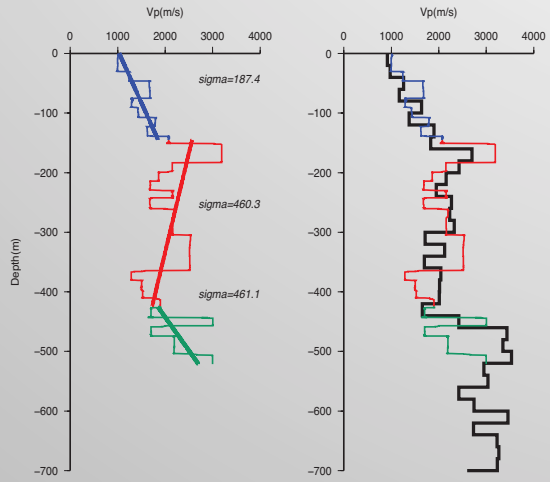

Velocity Model

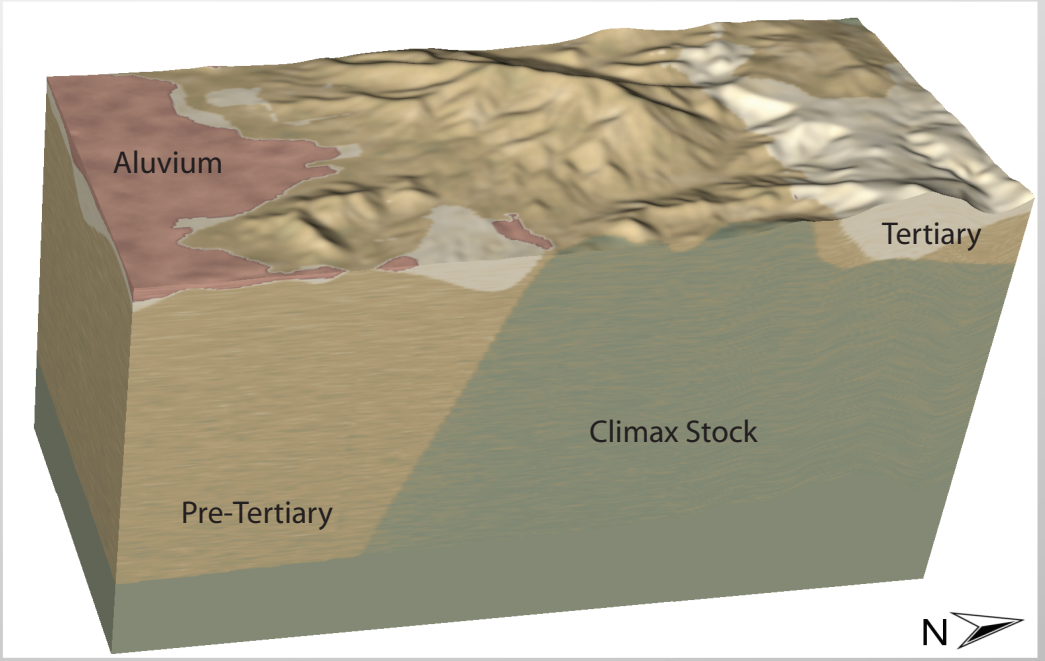

Stochastic Small Scale Heterogeneity
(L=1km,up 15%, Gaussian weighting)

Simulations reveal very complex propagation and clear conversions of P and Rg energy to S-wave energy

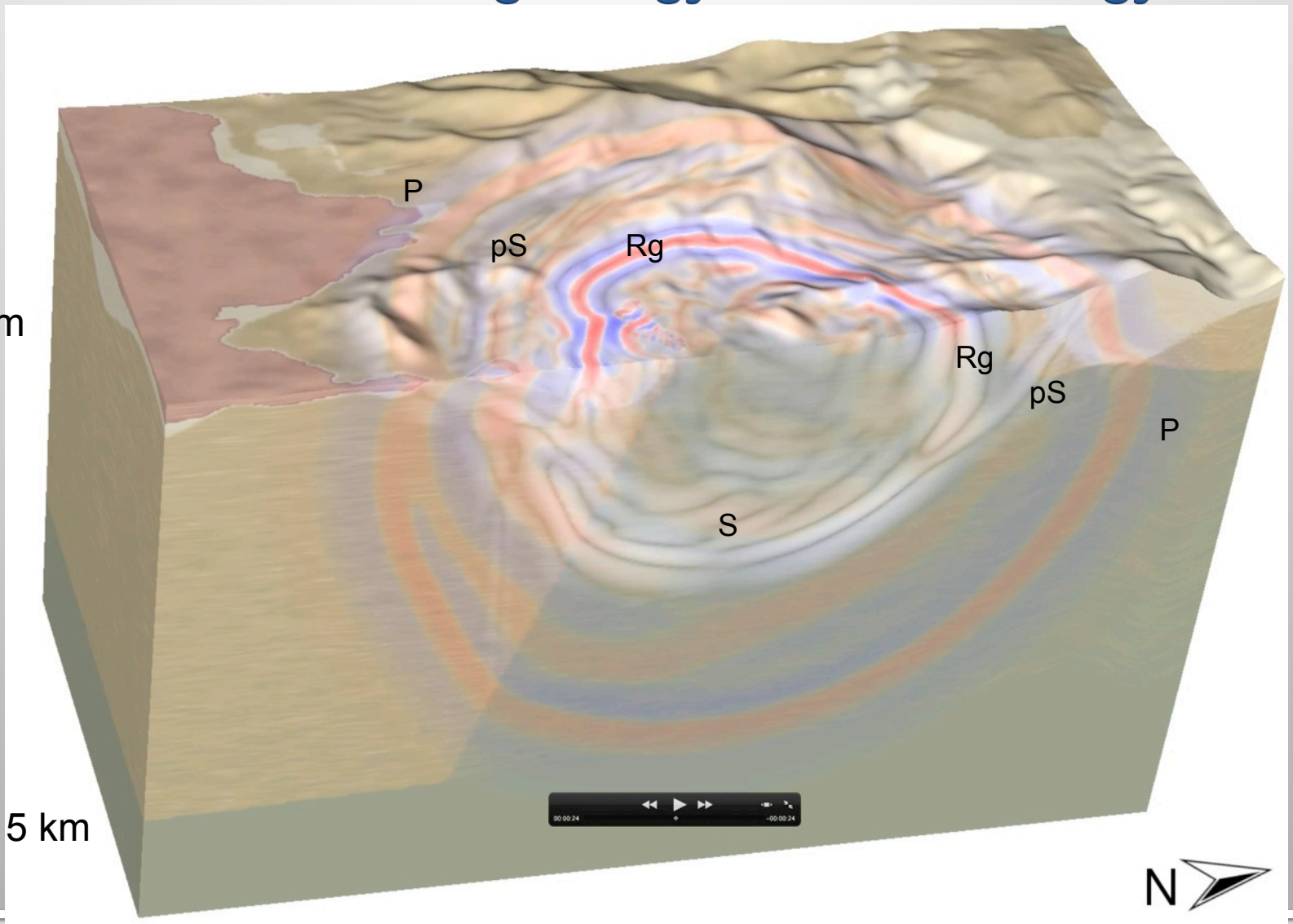

Line 1 Granite

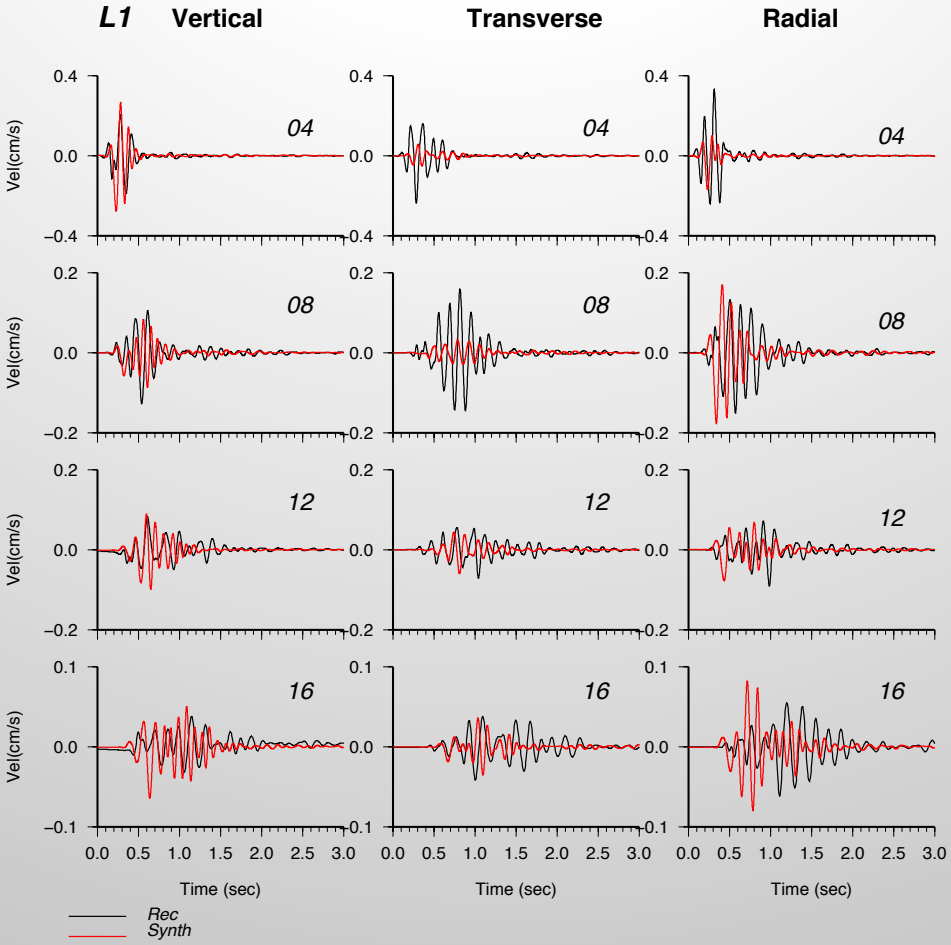

3D Simulation Using Source Coupling
3D Model & Topography
(Max Freq:10Hz)

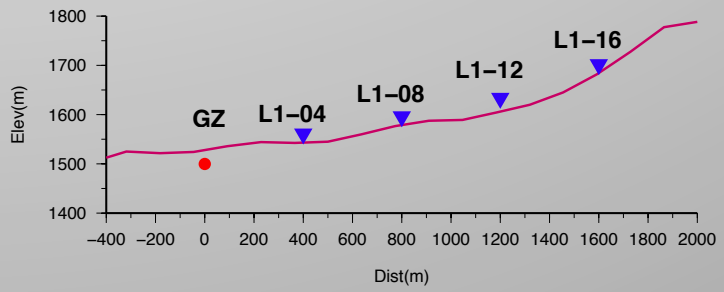

Line 3 Alluvium

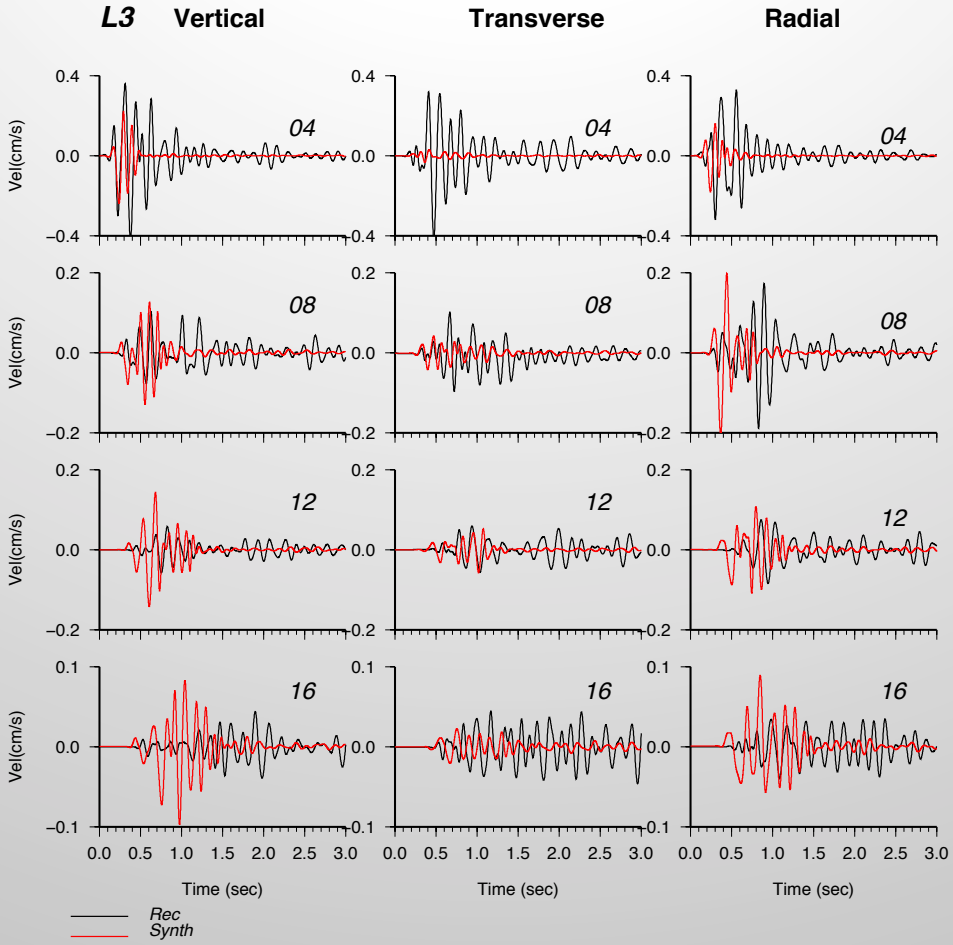

The alluvium structure needs improvements

L1-16 Granite

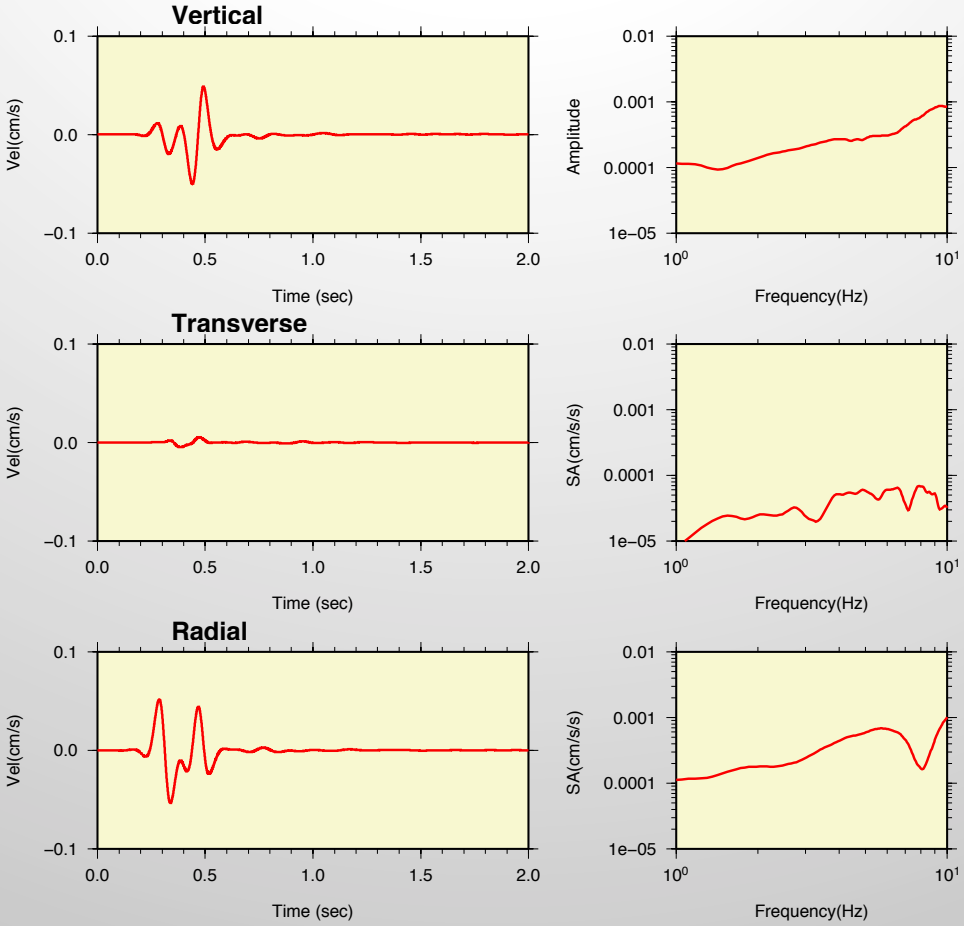

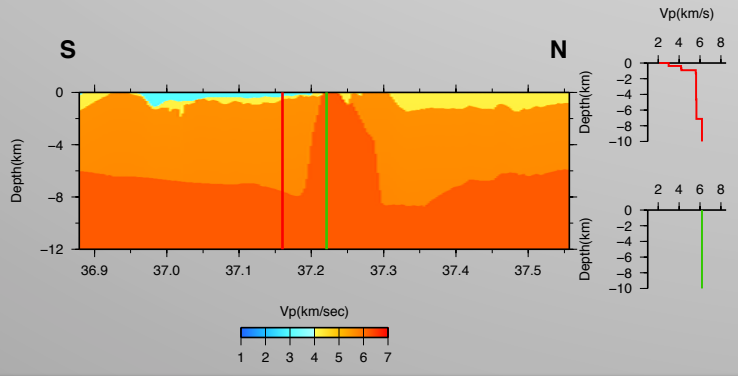

Basic 3D Velocity Model

L1-16

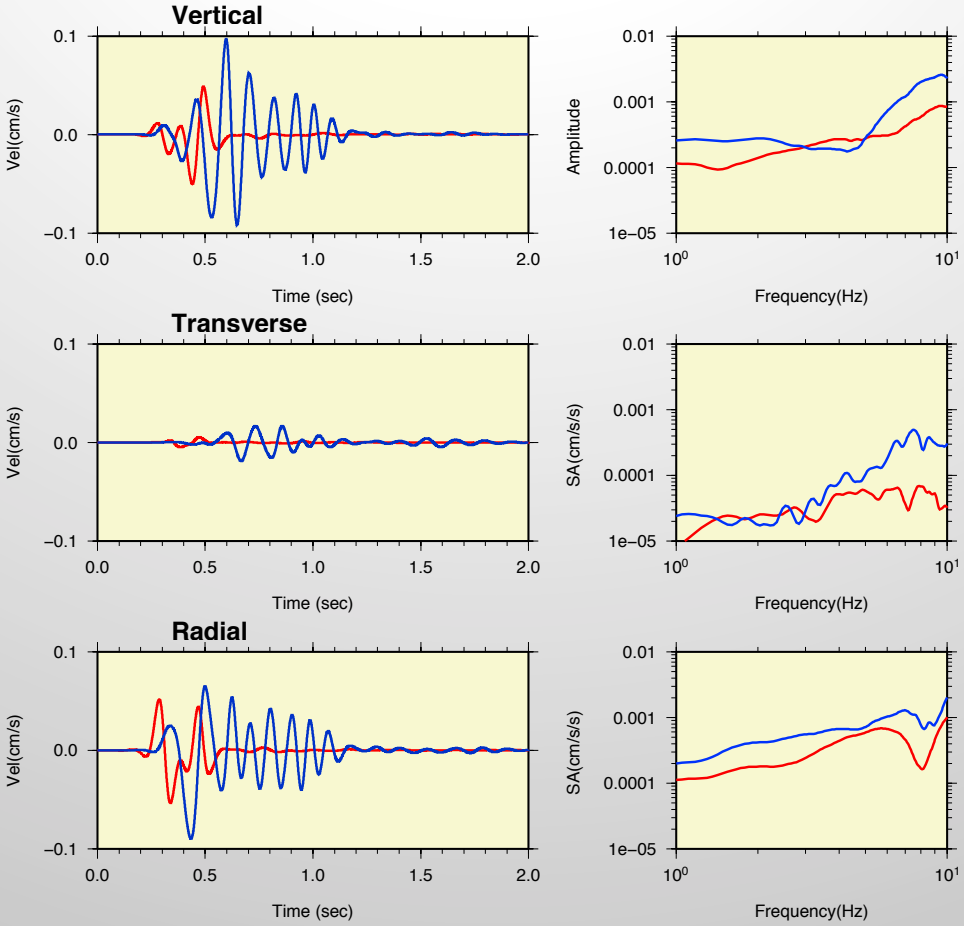

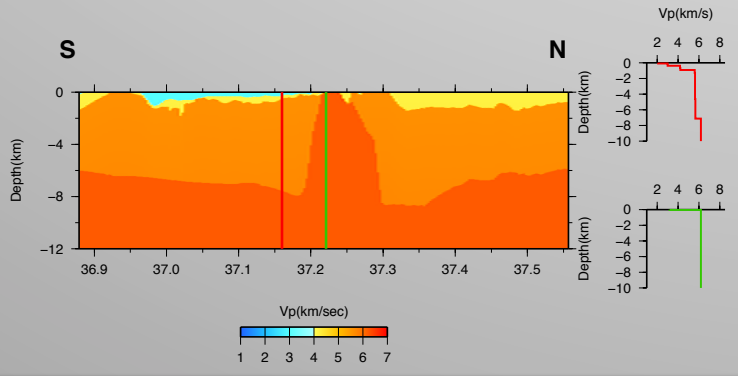

Basic 3D Velocity Model
+ Surface Weathered Layer

Weathered layer increases amplitude and duration

L1-16

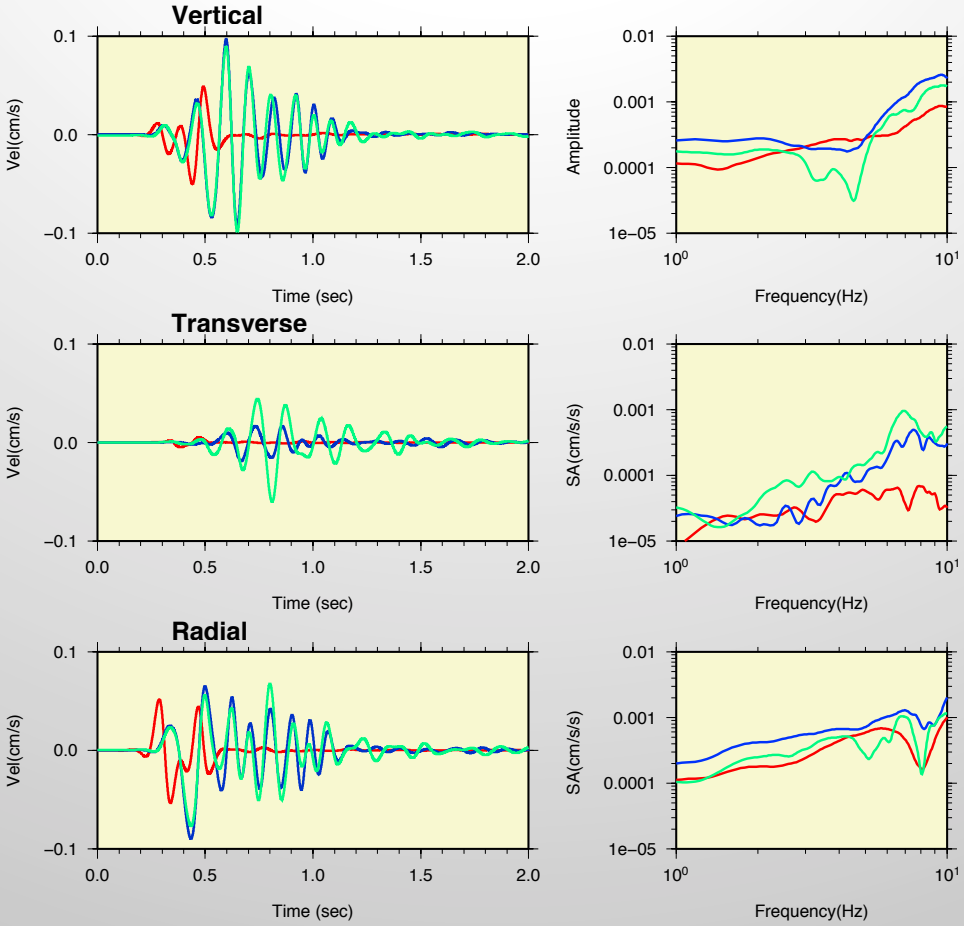

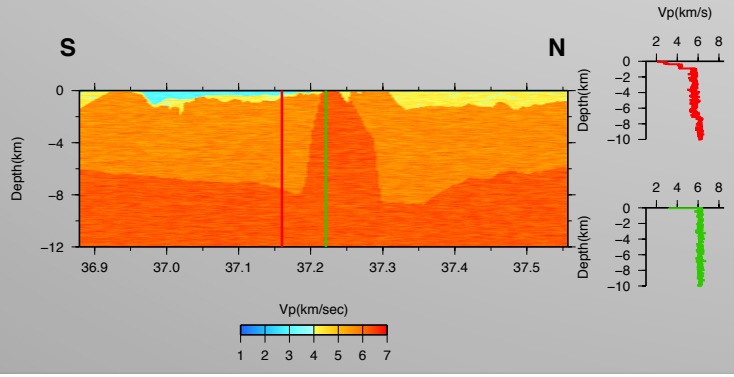

Basic 3D Velocity Model
+ Surface Weathered Layer
+ Topography and Stochastic Heterogeneity (L=1km,up 15%)

Topography and Stochastic Heterogeneity increases amplitude on the transverse component

L3-12 Alluvium

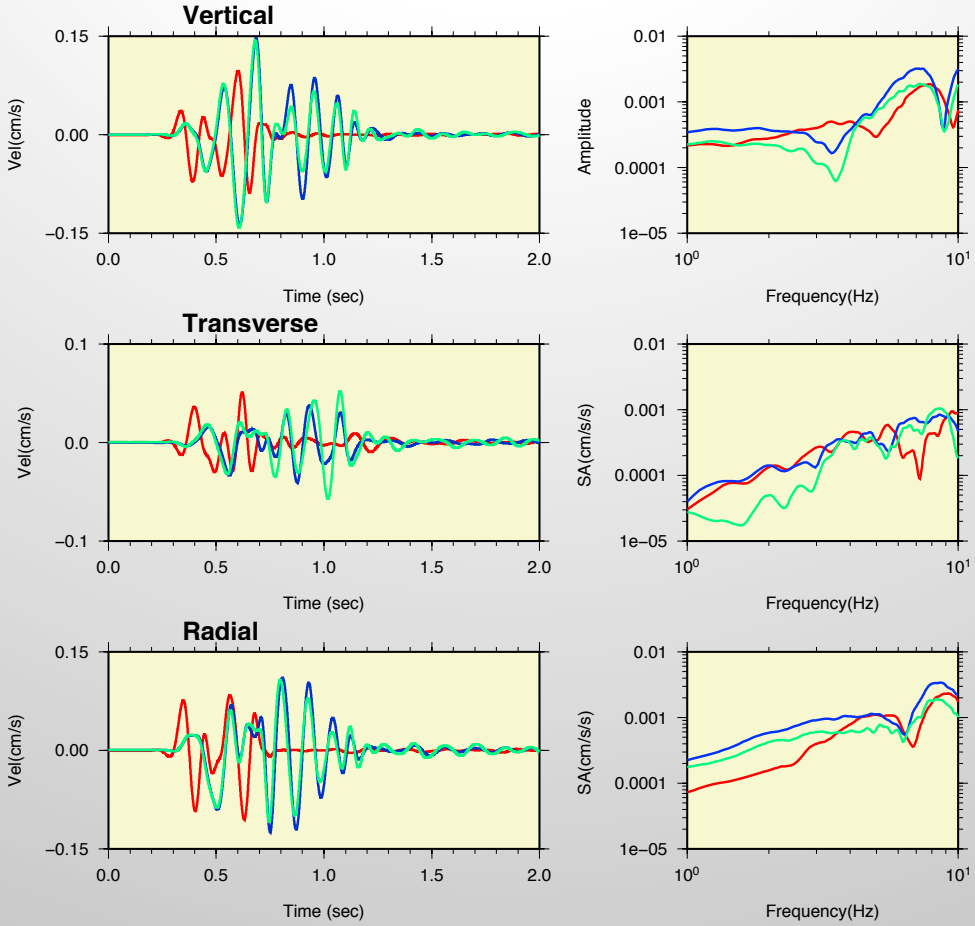

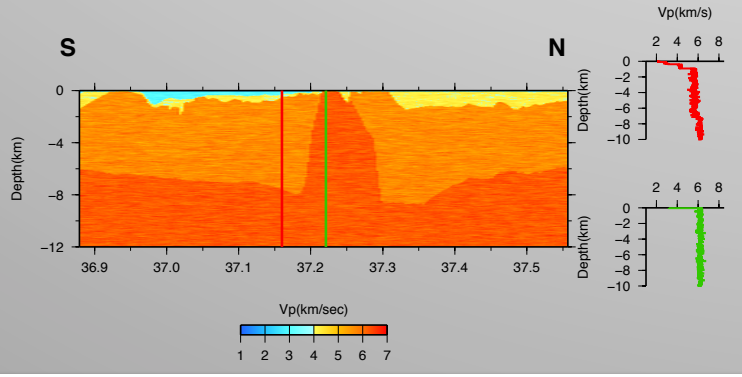

Basic 3D Velocity Model
+ Surface Weathered Layer
+ Topography and Random Variations

Receiver Located 4 km Below the Source

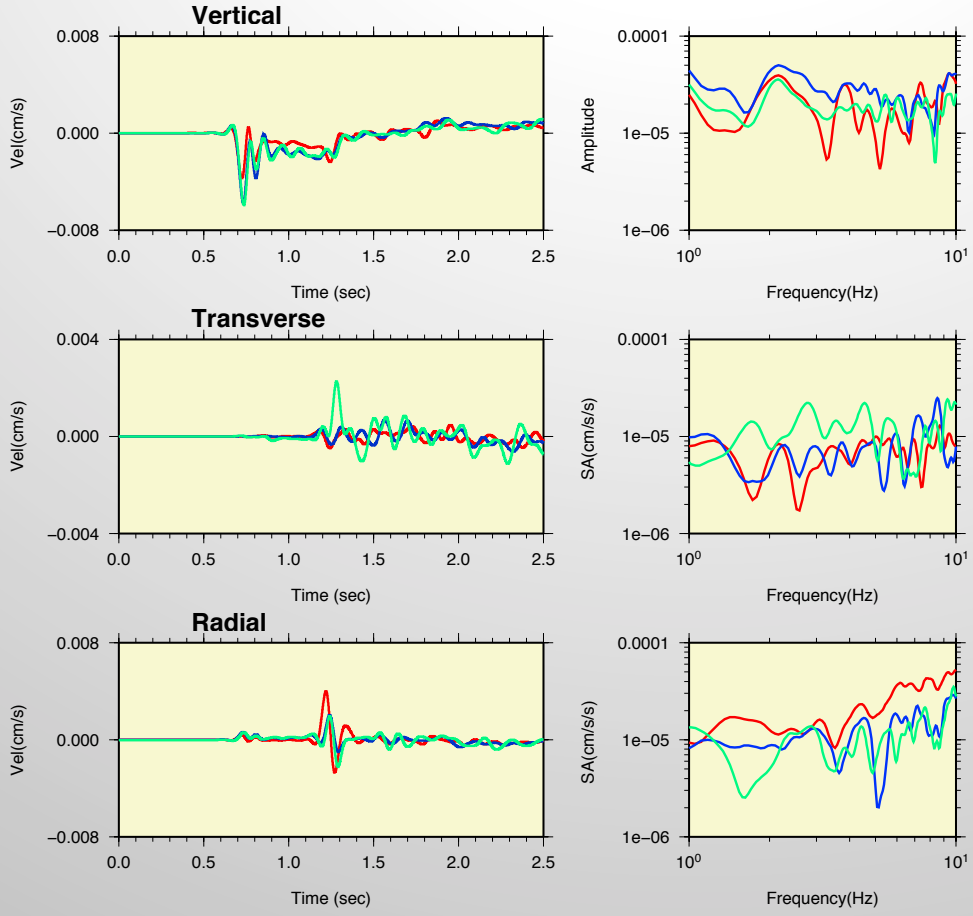

Significant presence of scattering effects local and regional ray paths

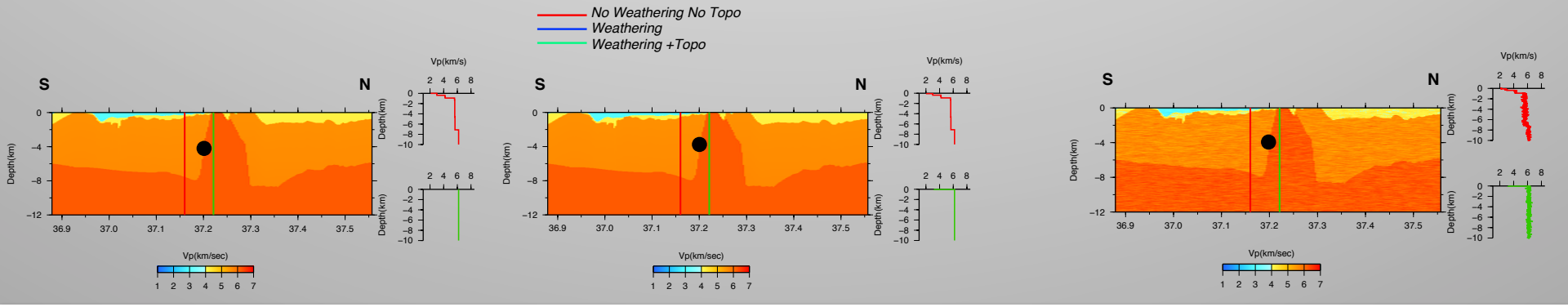

Sensitivity of Far-Field Motion To Source Modeling (Effect of Gravity)

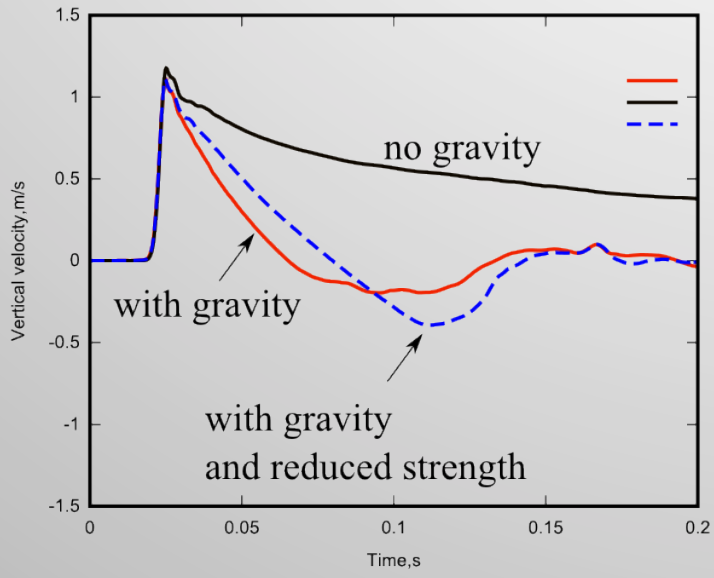

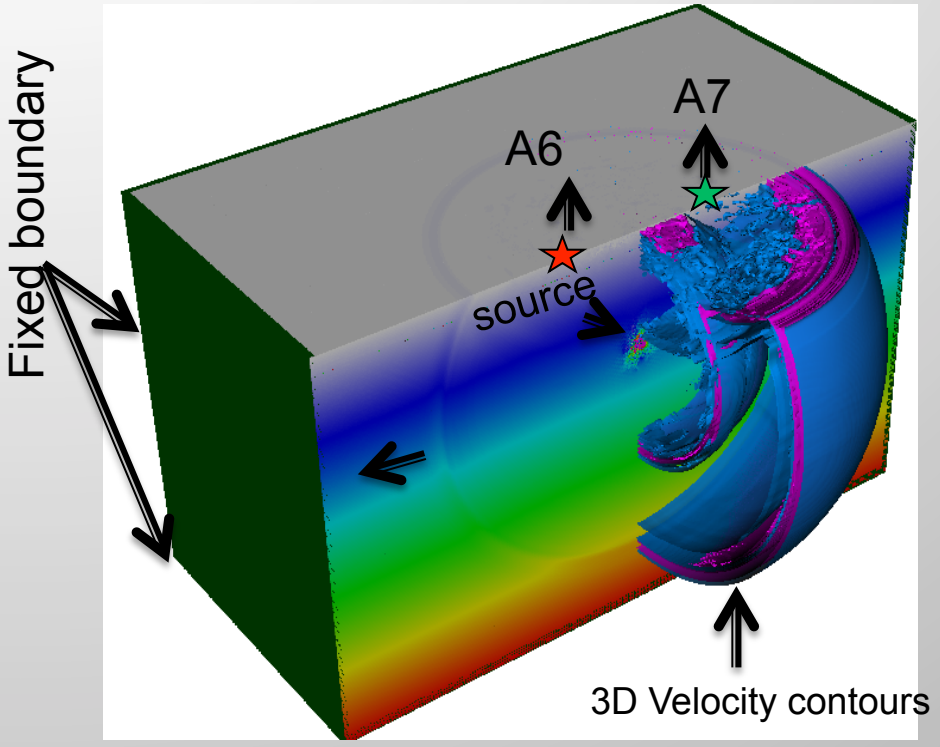

Effects of Gravity

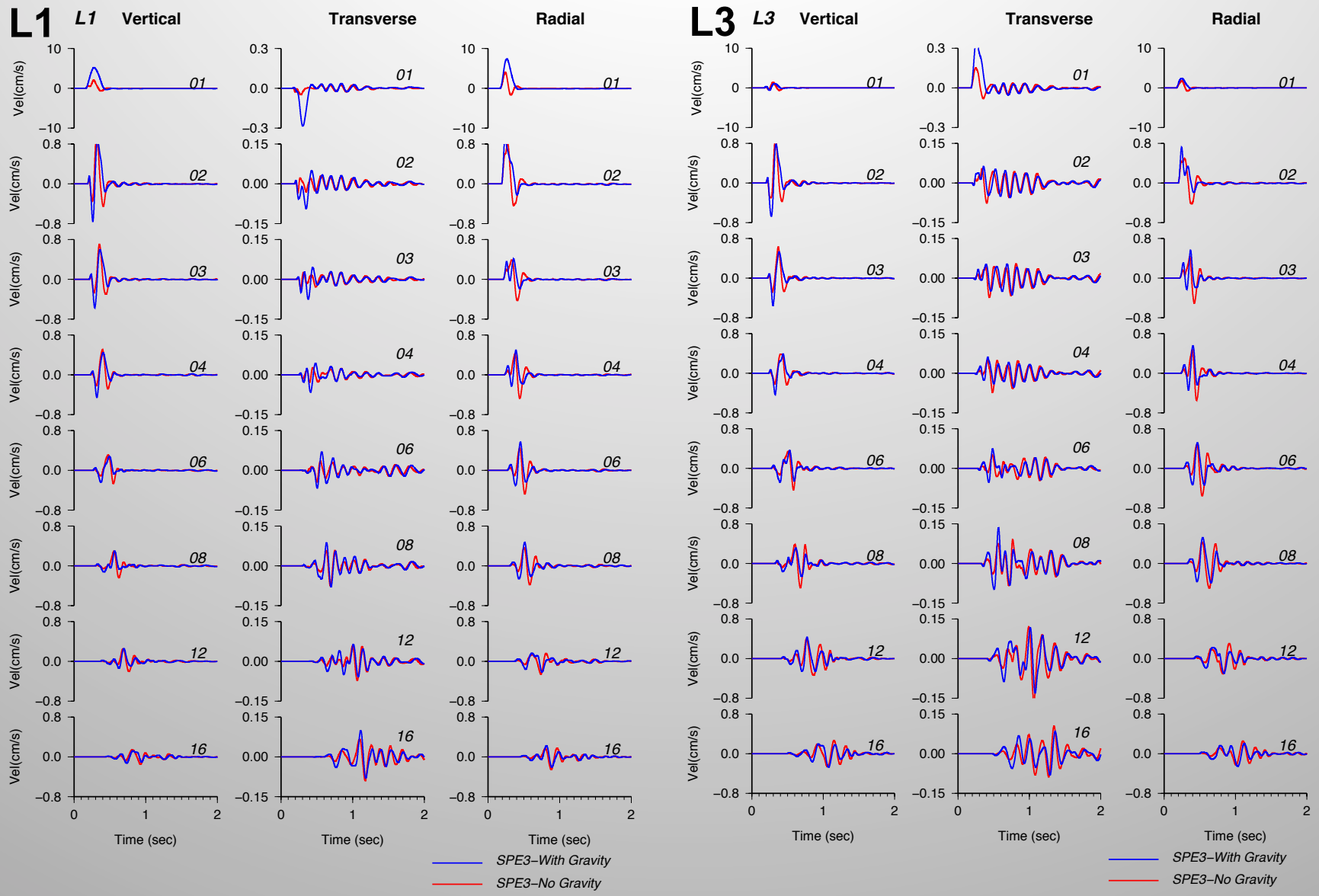

Effects of Gravity Max Freq: 6Hz

Vertical

Transverse

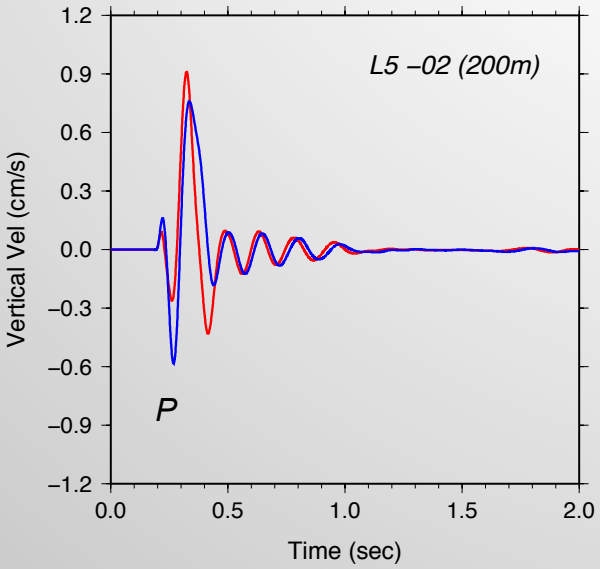

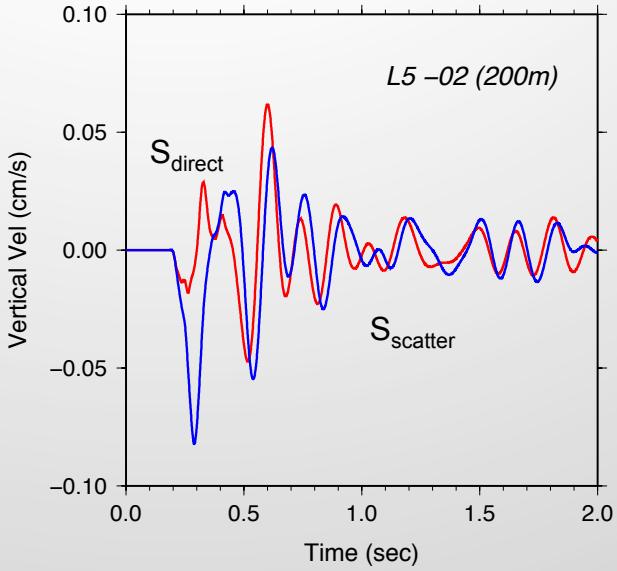

200m

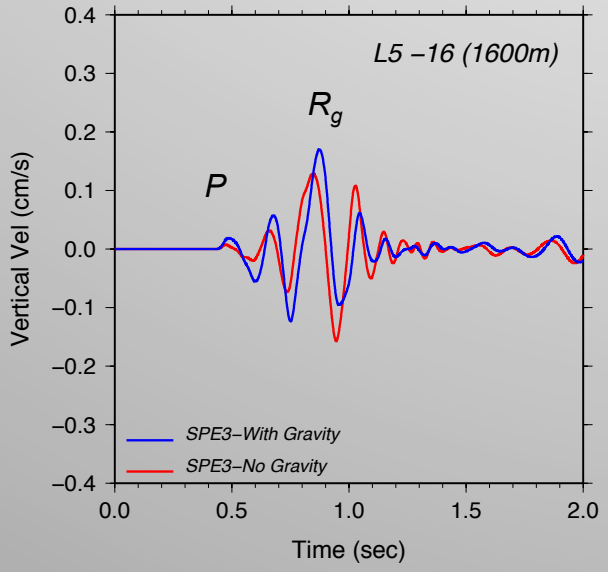

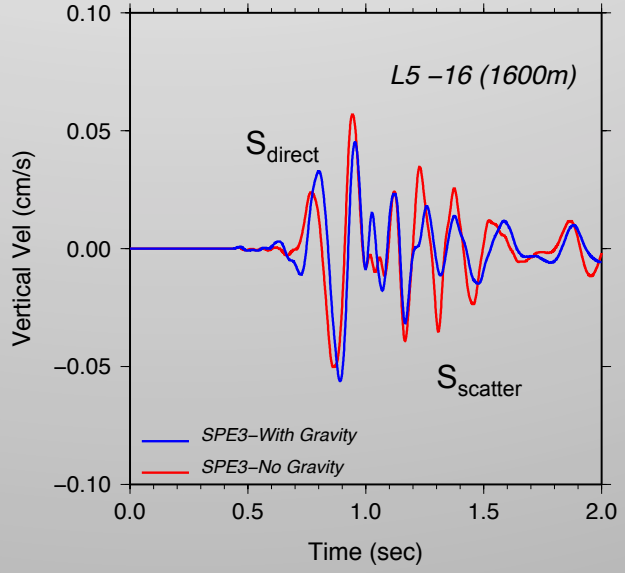

1600m

Sources With Different Equally Probable Joint Network Using Site Fracture Characterization

Model 1 Model 2 Model 3

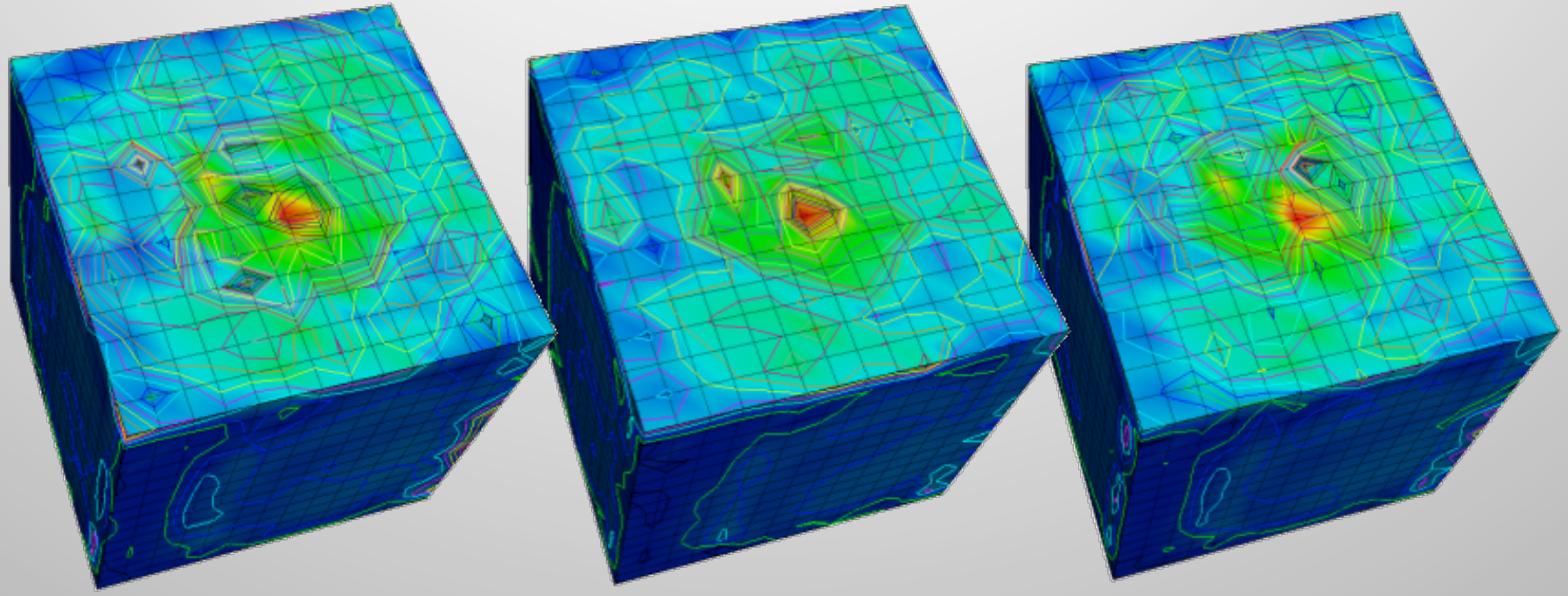

Snapshots of particle velocity amplitude at 10ms, for different sources, computed with 3 different realizations of fracture networks embedded in Geodyn-L.

Effects of Joints Orientation on the Far-Field

Max Freq: 6Hz

Vertical

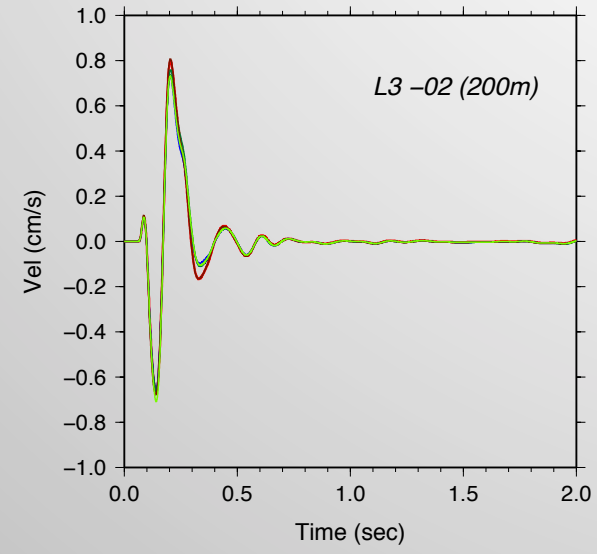

Transverse

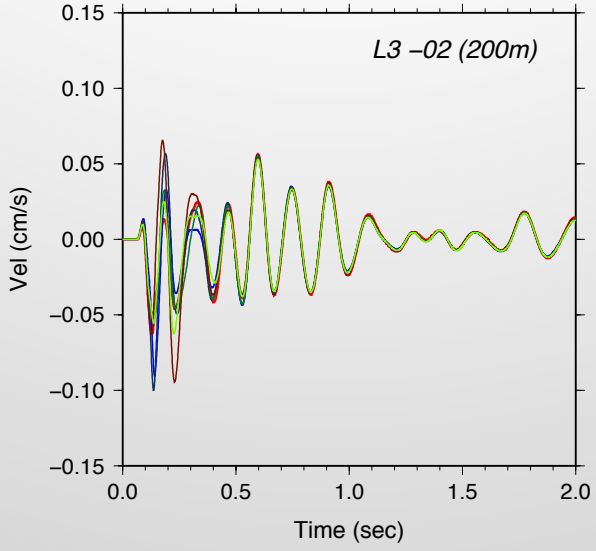

Radial

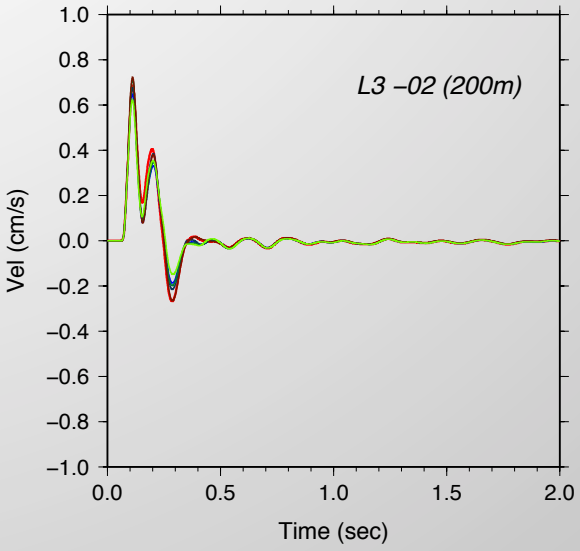

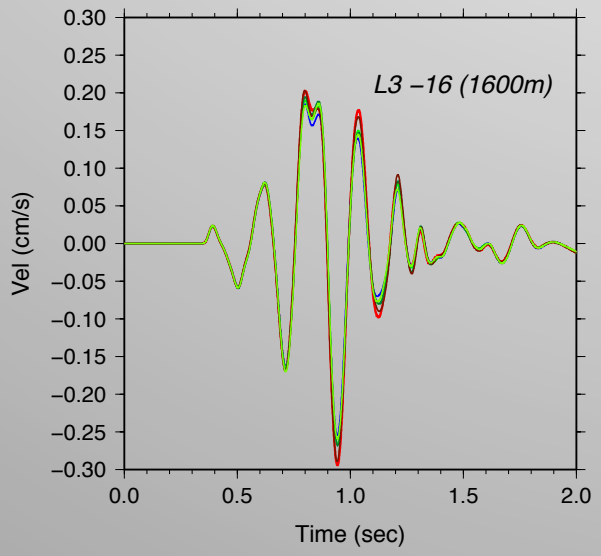

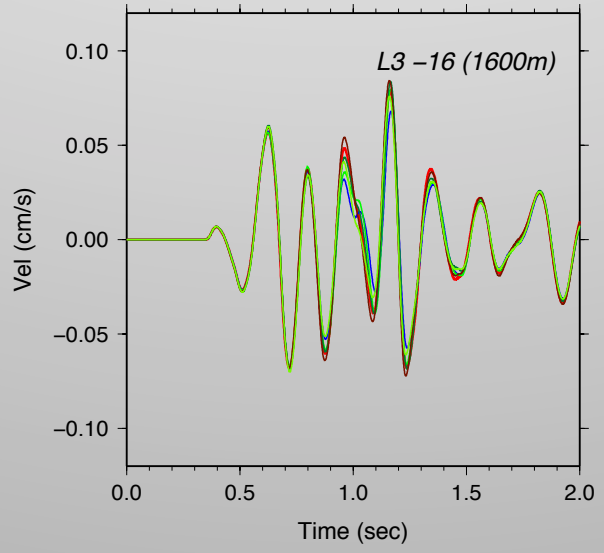

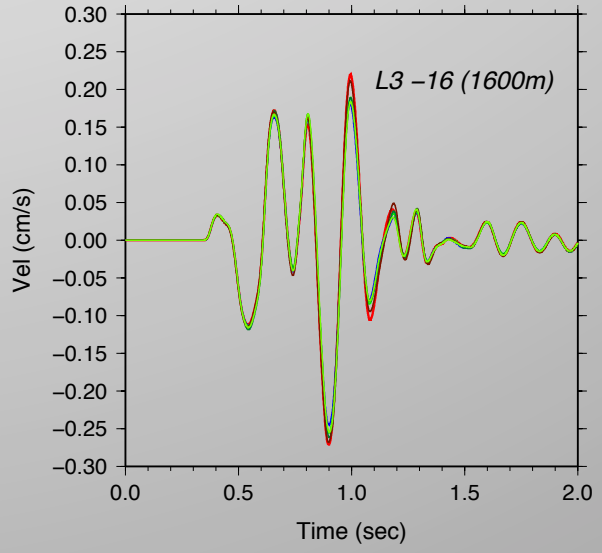

Conclusions

•Coupling of explosion 3D hydrodynamic simulation with anelastic wave propagation modeling improves the quality of simulated waveforms for the SPE

•The combined effects of surface weathered layer, surface topography and small scale structural heterogeneities have a significant impact on creation and amplitude of shear motion during underground explosions

• In addition to shear waves generated at the source, shear waves generated by near-surface structural complexities propagate at local distances. The increase in shear-wave energy could explain why the P/S discriminant for SPE explosions does not work well for some azimuths at local distances.

• Stochastic realizations of joints based on site fracture characterization produce similar shear and compressive far-field ground motion in the modeled frequency range up to 6Hz.

Thank you!

Acknowledgements

Discrete and continuum simulations of near-field ground motion from SPE

Oleg Vorobiev , Souheil Ezzedine,
Eric Herbold, Tarabay Antoun and Lew Glenn

Lawrence Livermore National Laboratory

State of Analysis Review
August 21-22, 2013
Las Vegas

LLNL-PRES-642573
This work was performed under the auspices of the U.S. Department of Energy by Lawrence Livermore National Laboratory under contract DE-AC52-07NA27344. Lawrence Livermore National Security, LLC

What can we learn from near field modeling ?

- ***Shear-wave generation, implications for monitoring***
- ***Role of site characterization***
- ***Role of surface and gravity***
- ***Scalability with yield***
- ***Source model for the far field***

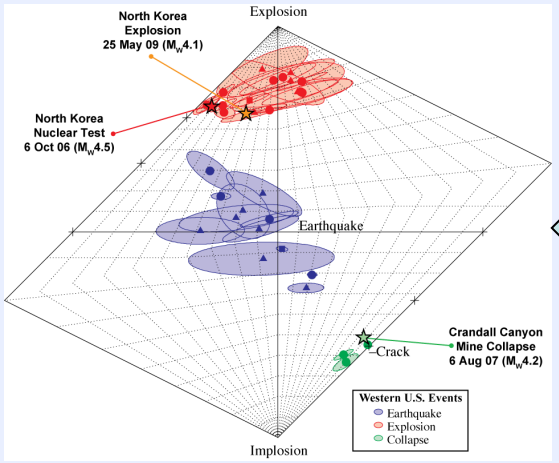

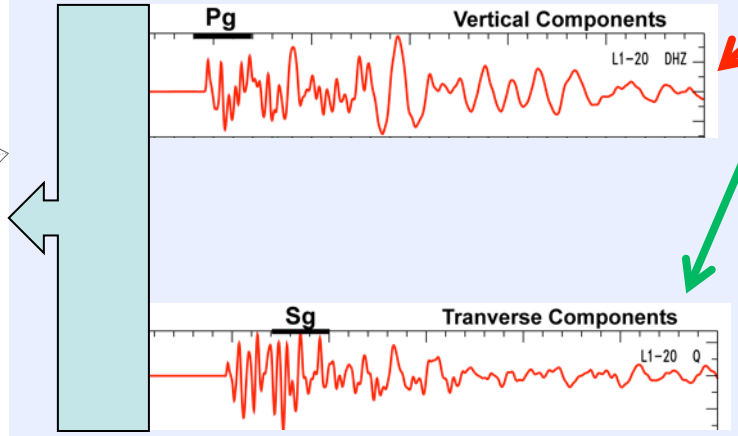

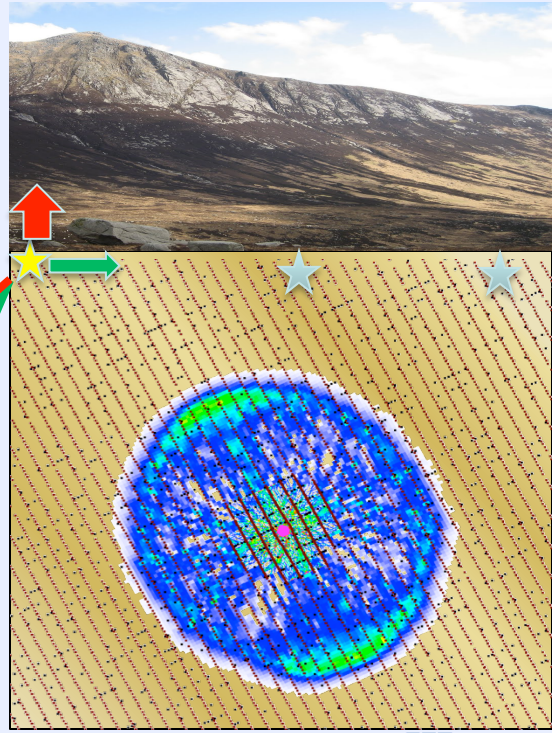

Joints can redirect energy flow from the source

Small scale experiment

Sugar shot (Melzer, 1970)

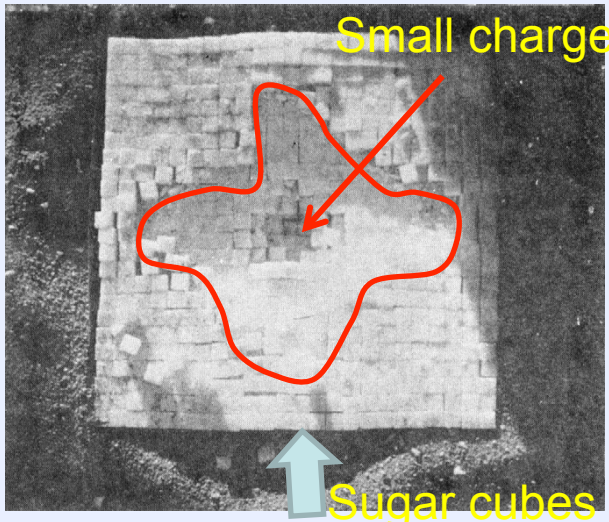

High confinement

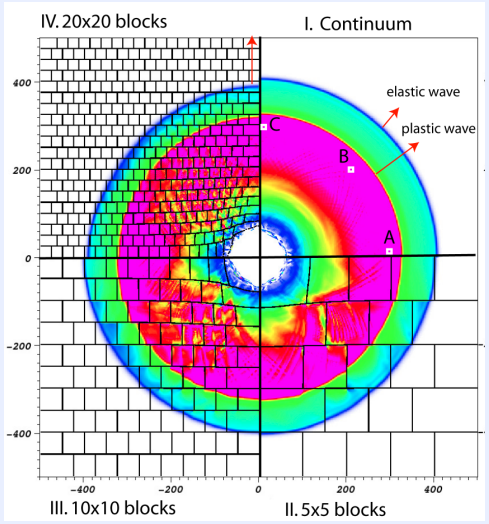

Low confinement

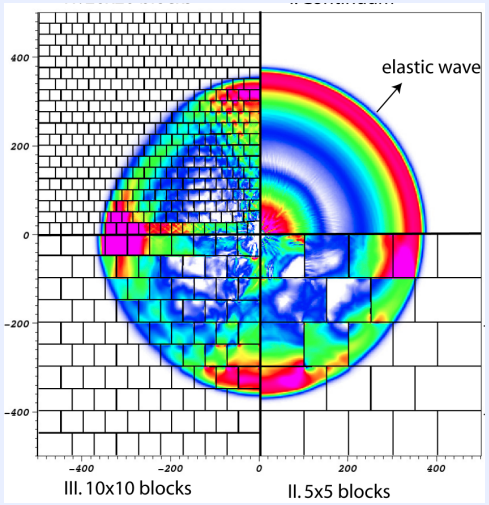

Joint sets at SPE site

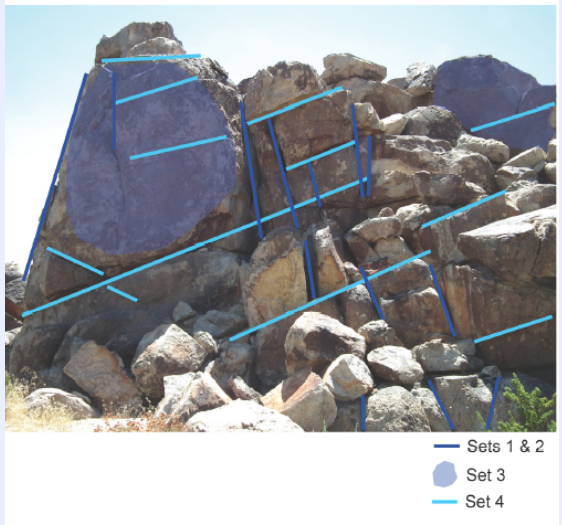

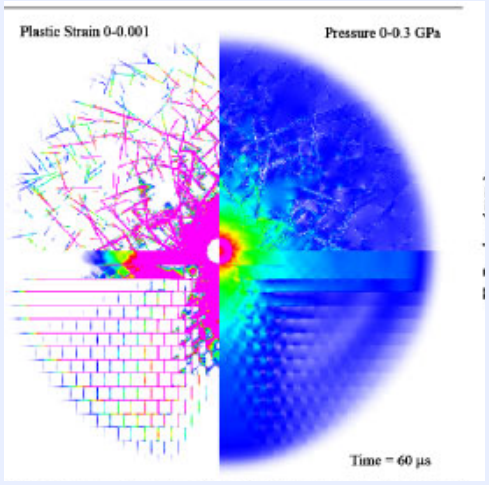

Random joints

Vorobiev, IJNME, 2010

Parallel nonlinear code GEODYN-L is used to model near-source ground motion

Dimensions:

joint aperture ~1 mm
joints spacing ~ 1 m
source size ~1 m
region ~300 m

Computational model:

~20-50 million elements
~100-200 million zones
3240 CPU for 12 hours

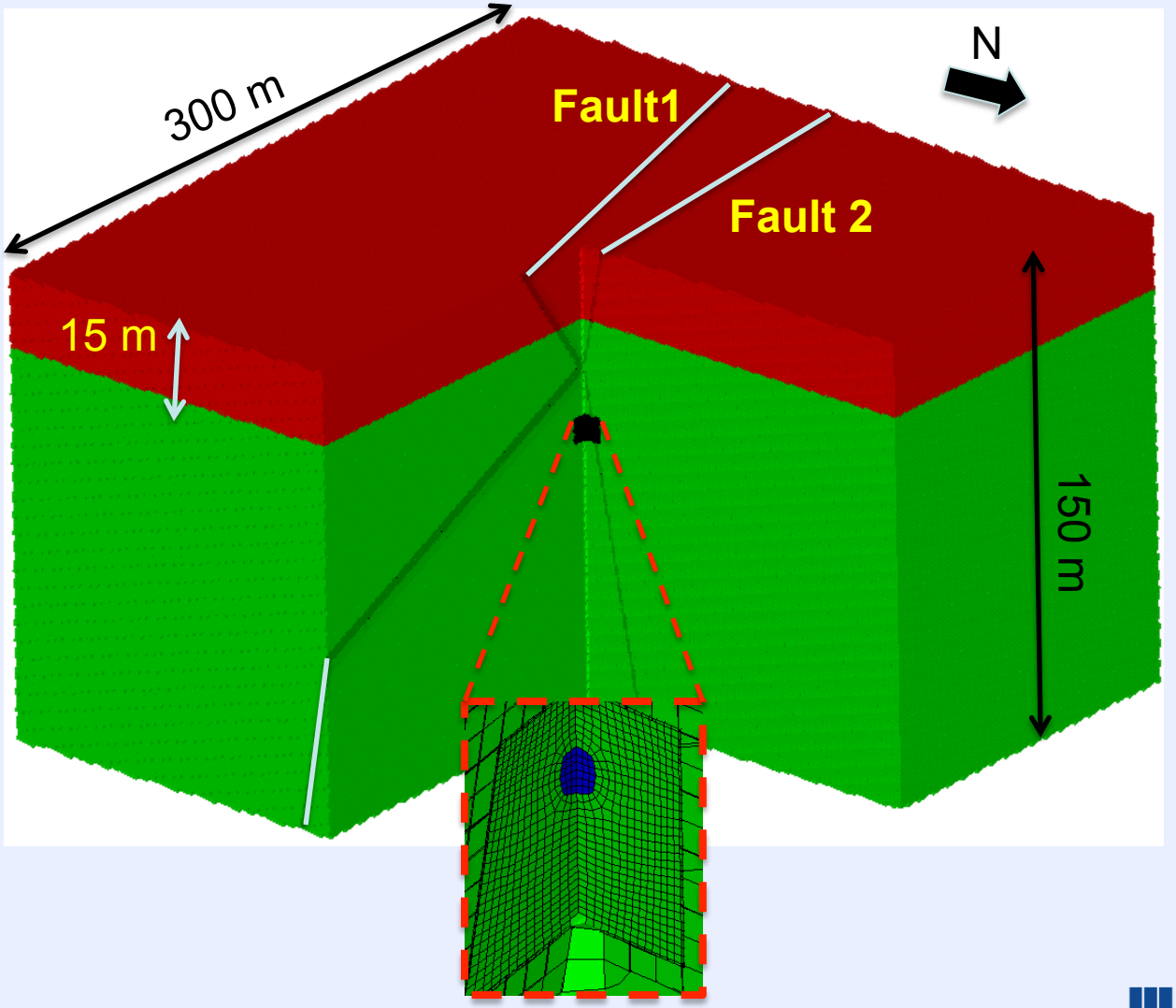

SPE3 discrete model: horizontal shear wave generation

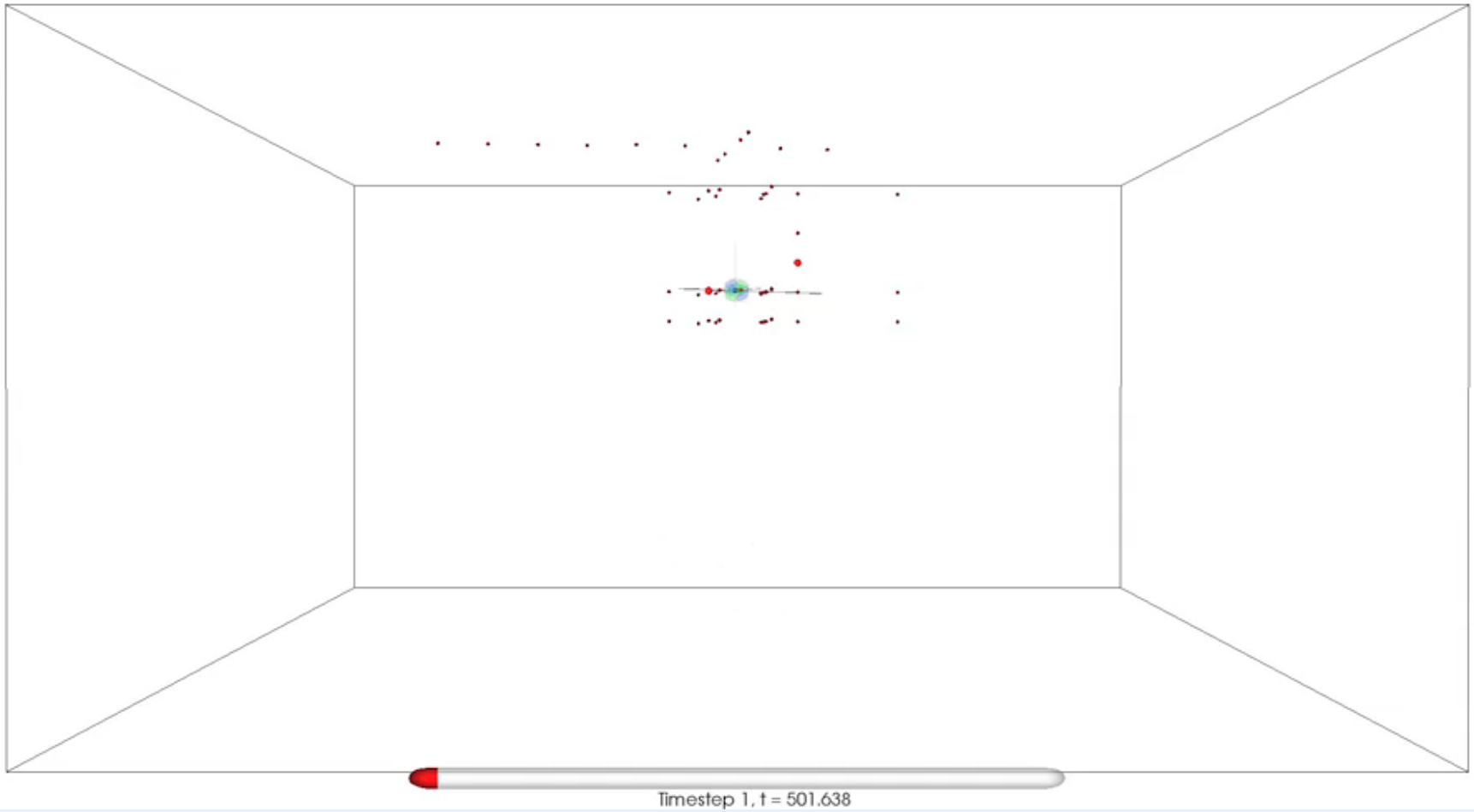

Discrete-continuum simulation of SPE3 using GEODYN-L

Vertical joint sets define polarity of horizontal shear motion

Horizontal shear motion of different polarity

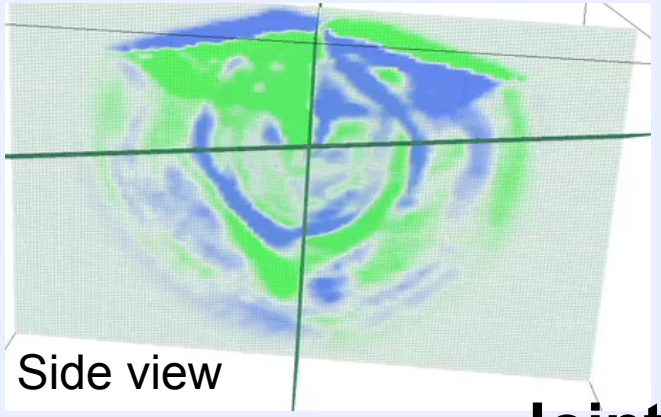

Joint planes

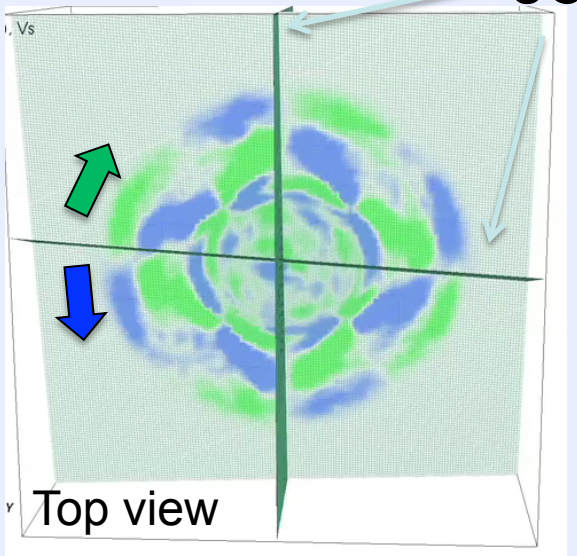

p-wave

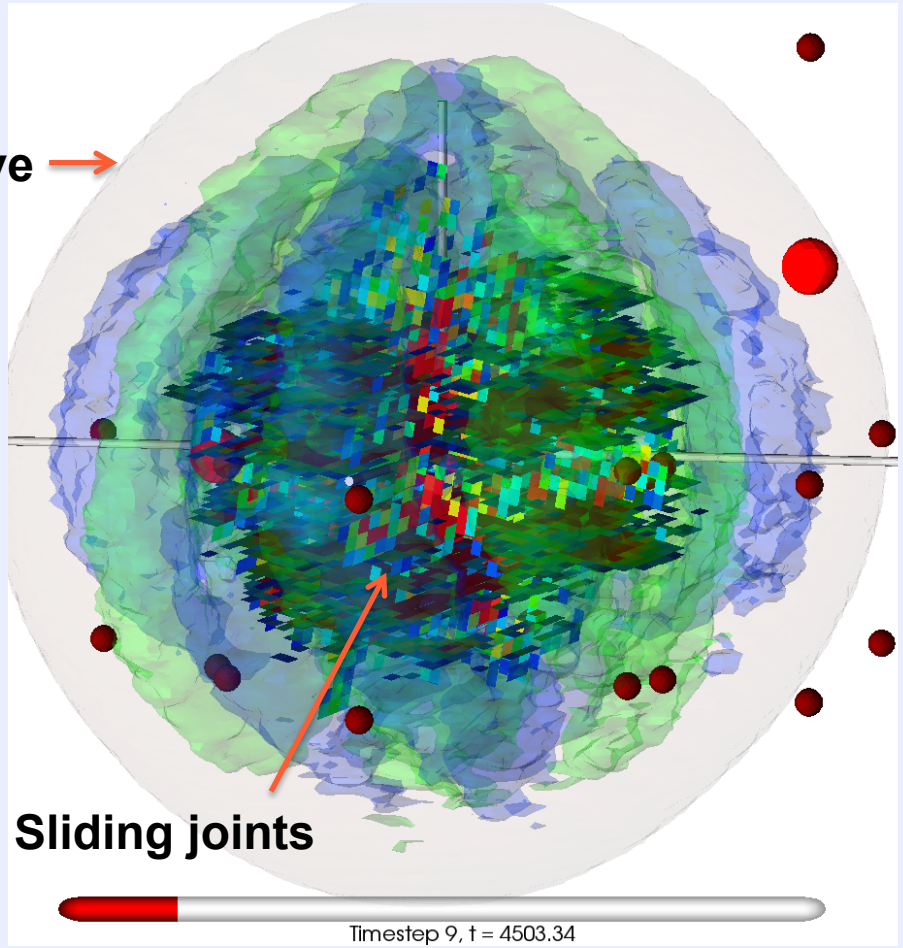

3D discrete model with 3 joint sets : sliding joints produce shear motion

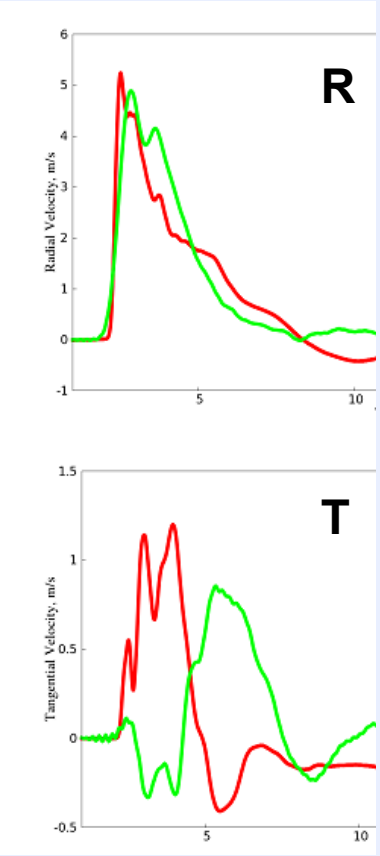

t=2 ms

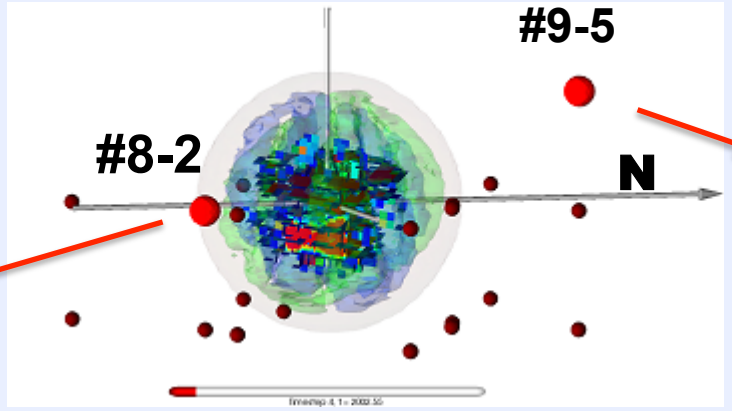

t=20 ms

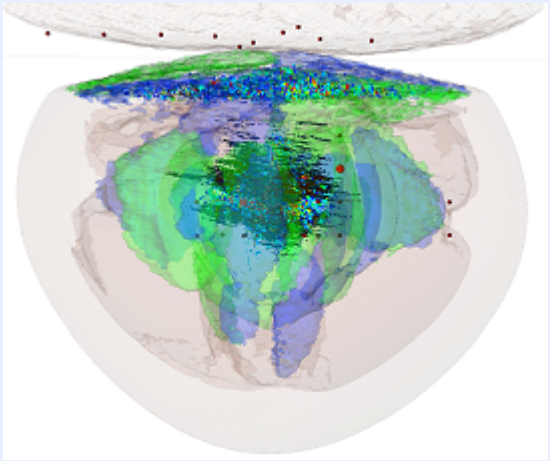

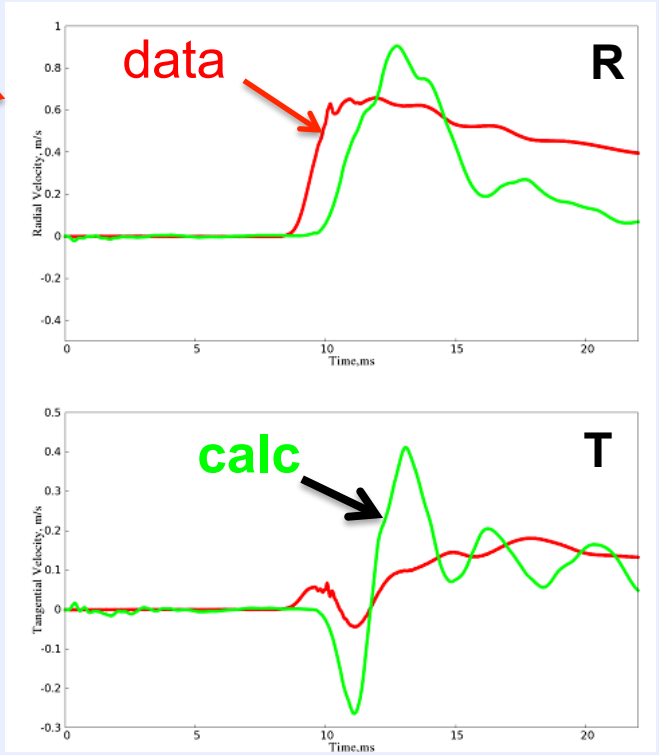

Two vertical joint sets used in calculations cannot explain observed shear motion

#9-2 *located at the source level in normal direction to vertical joint set 1 (which corresponds to high dip angle sets Set-1 and Set-2)*

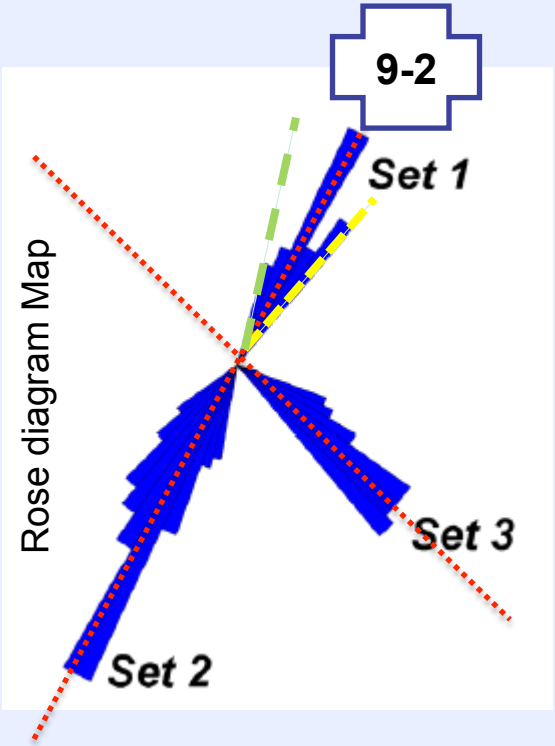

Data vs calculations at 20 m Range

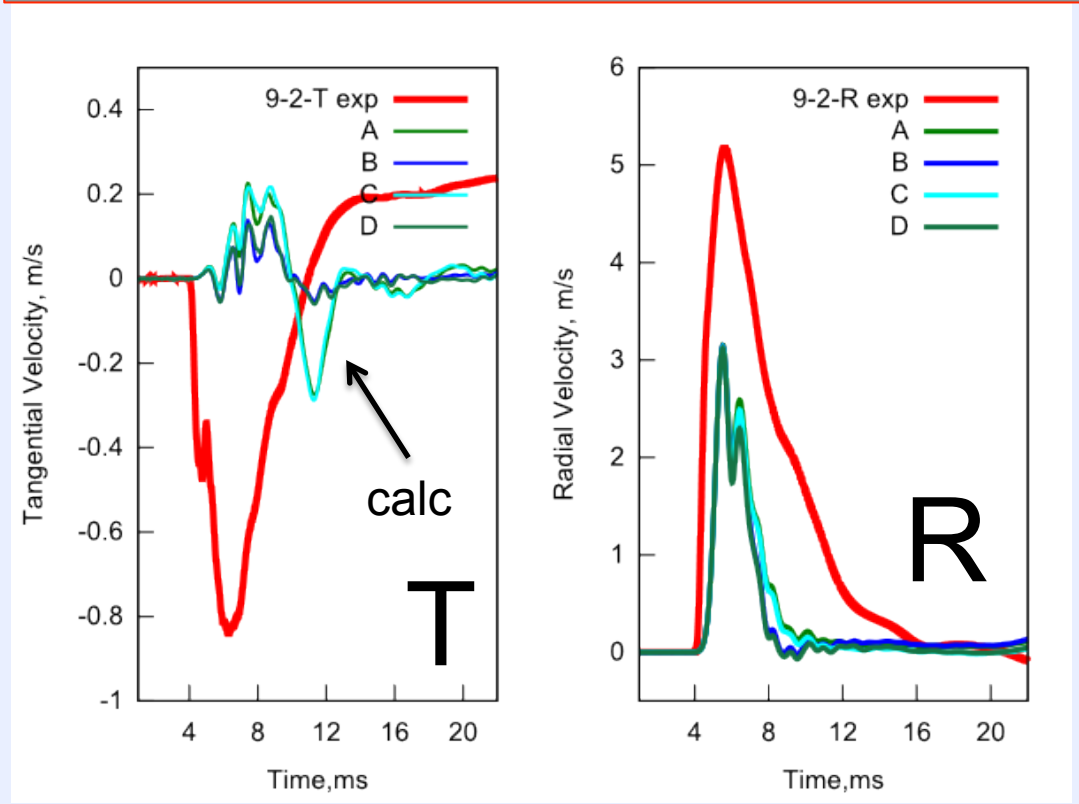

A single vertical joint generates shear motion but not over sufficiently wide azimuth

2D: Motion at 10 and 20 m range for locations oriented at various angles relative to the joint direction:
Joints slide if m > the friction angle

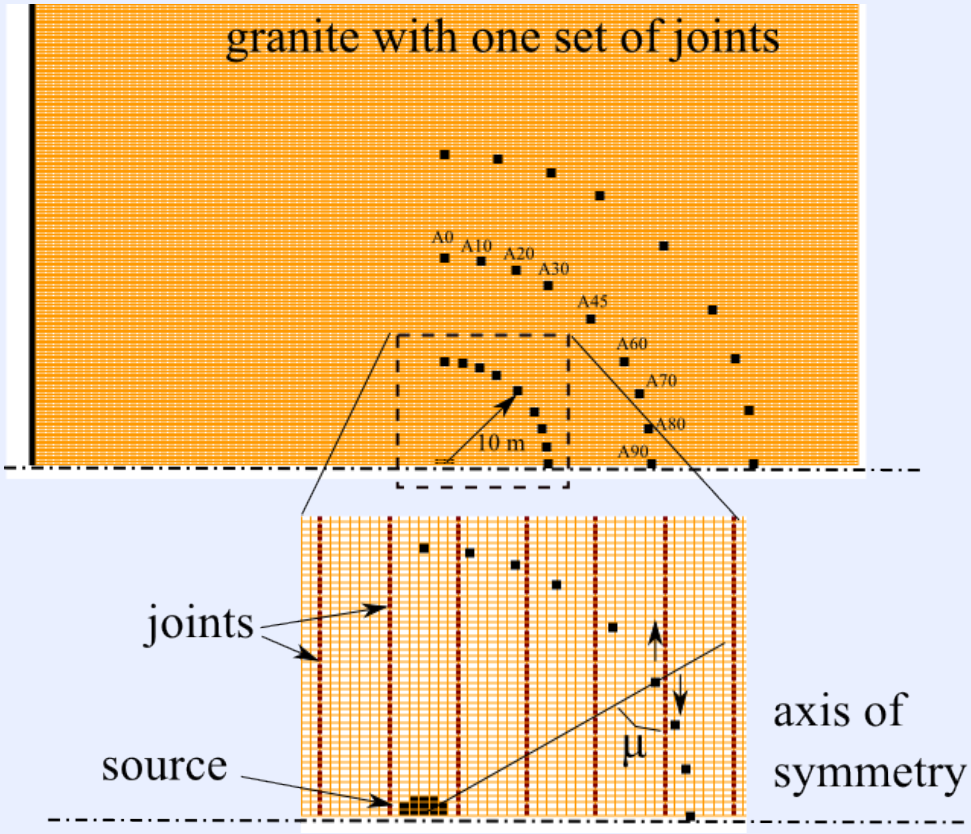

One joint, t=9 ms

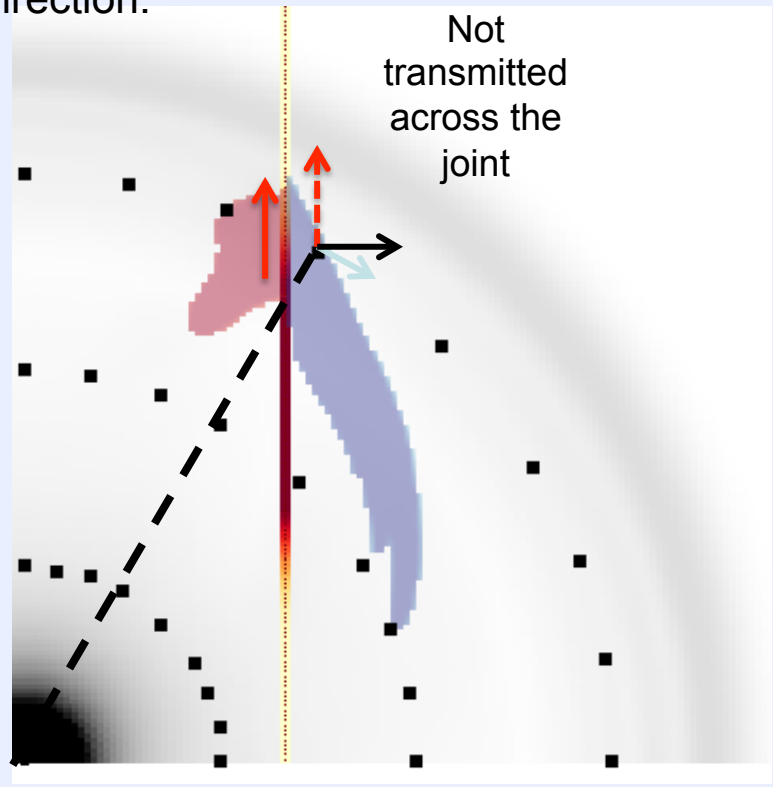

Increasing the number of joints widens the azimuthal region of shear motion

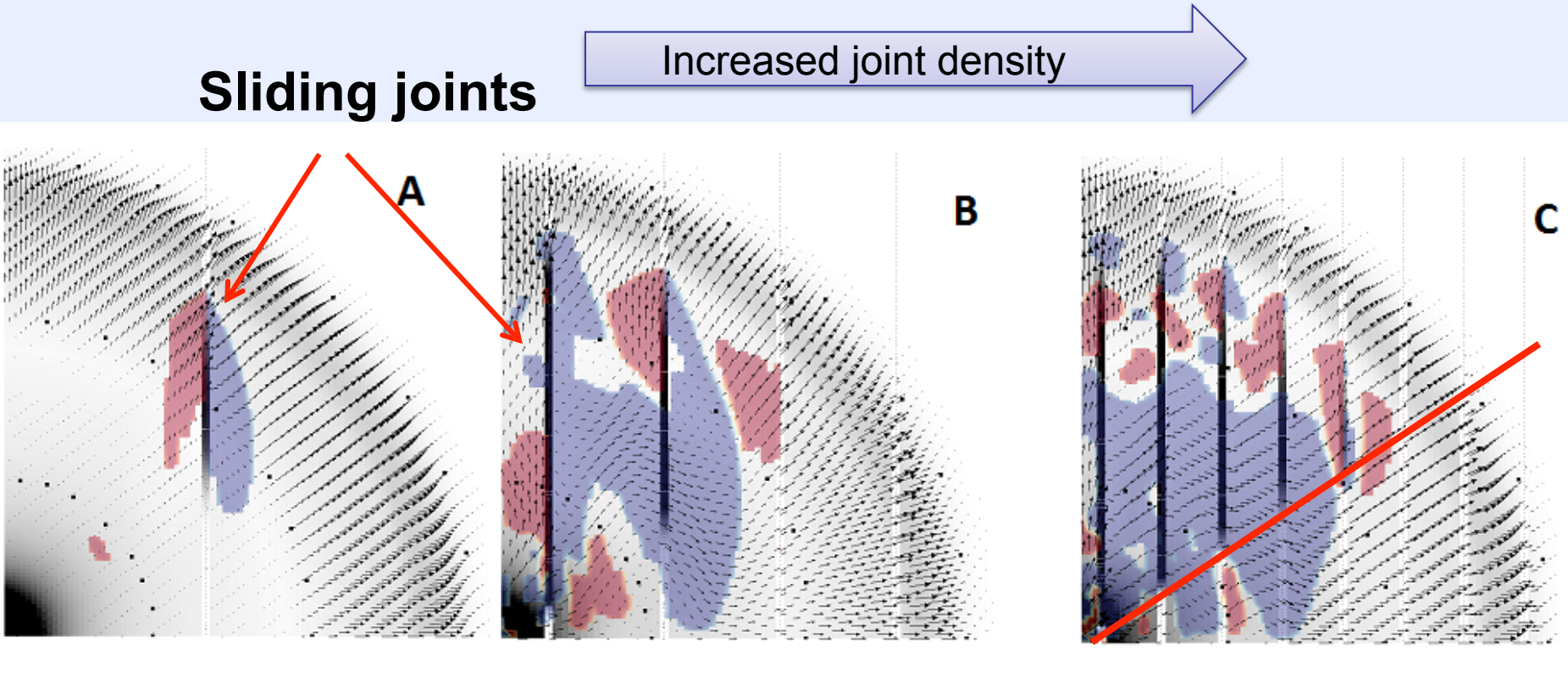

Velocity vectors and tangential velocity directions at 7 ms
Blue clock-wise, red counter-clock-wise.
Friction coefficient=0.6. Slip on the joints is shown in dark grey

The azimuthal region with shear motion also widens with decreasing friction

Friction ~0.4

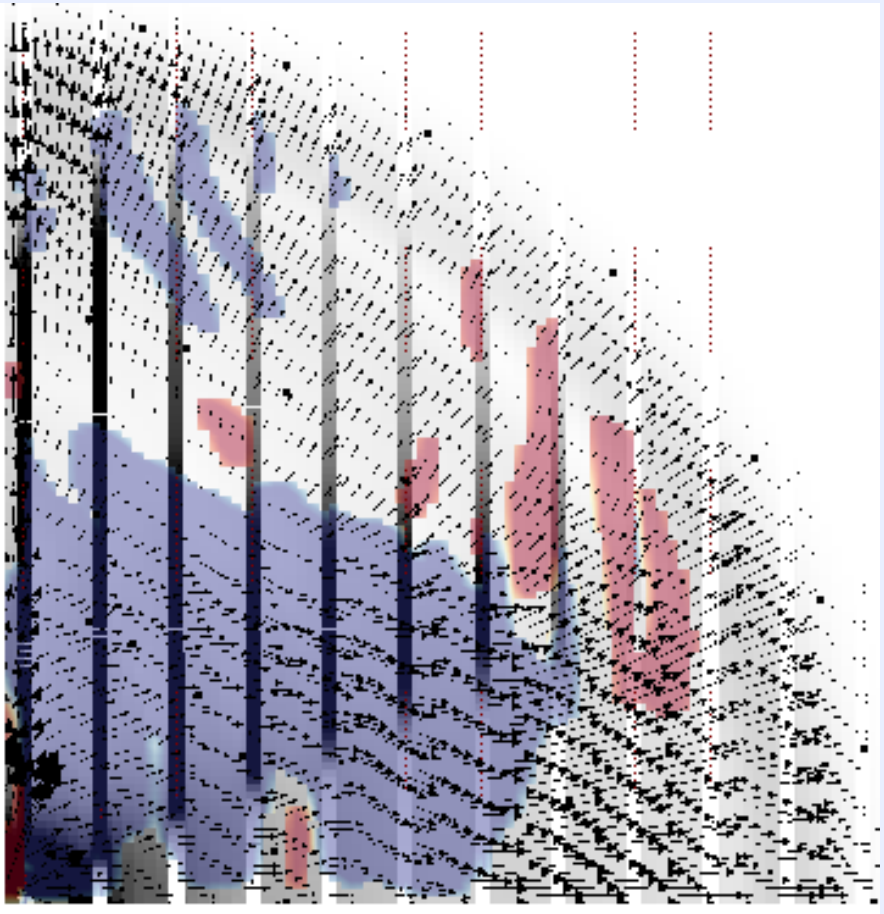

Friction ~0.8

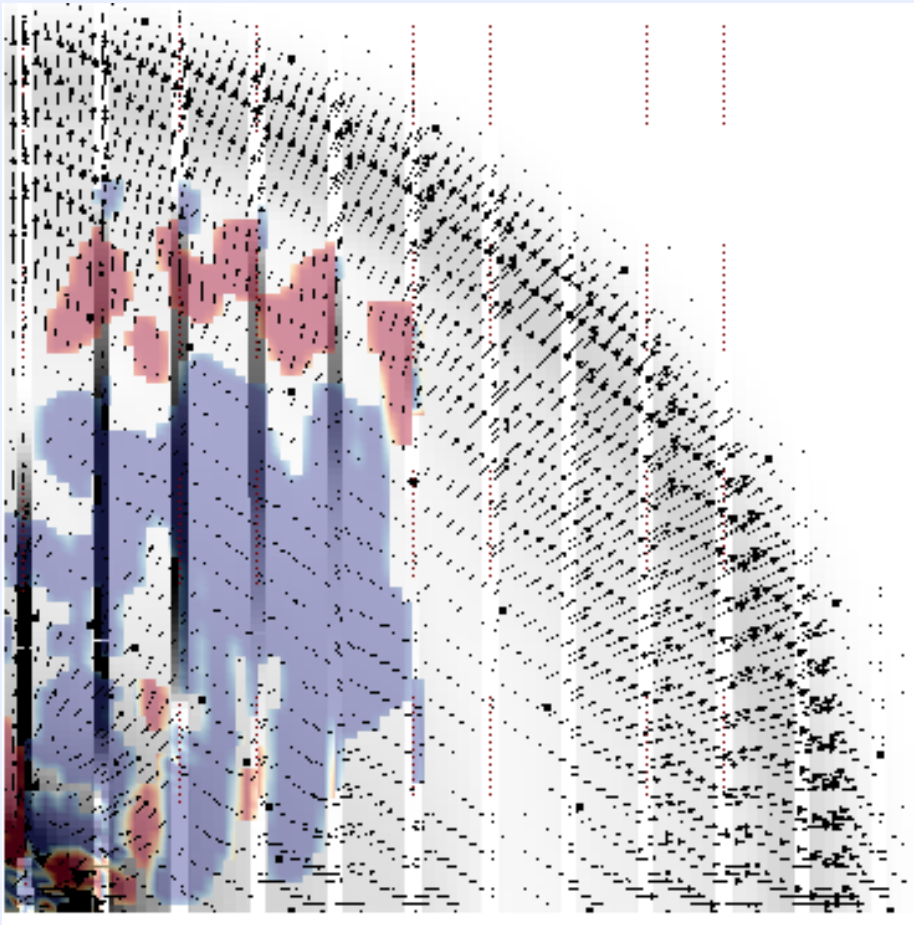

Anomalous high velocity can be explained by various joint properties in the vicinity of that gauge

Assumptions:

#7-2:

joint spacing= 2.5 m

Friction =0.4

Azimuth =30 degrees

#9-2:

Joint spacing = 1.6 m

Friction =0.2

Azimuth= 170 degrees

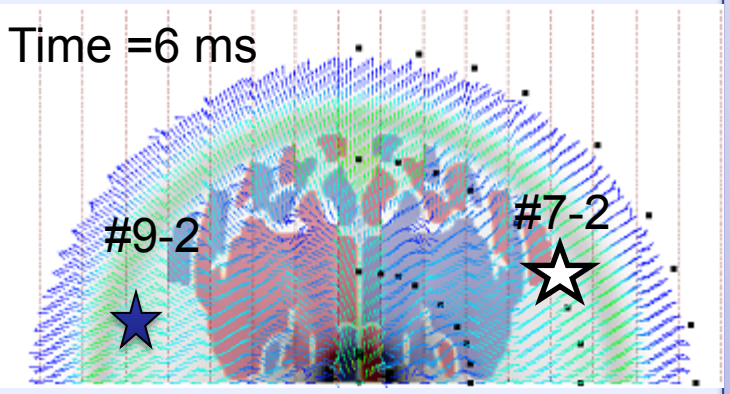

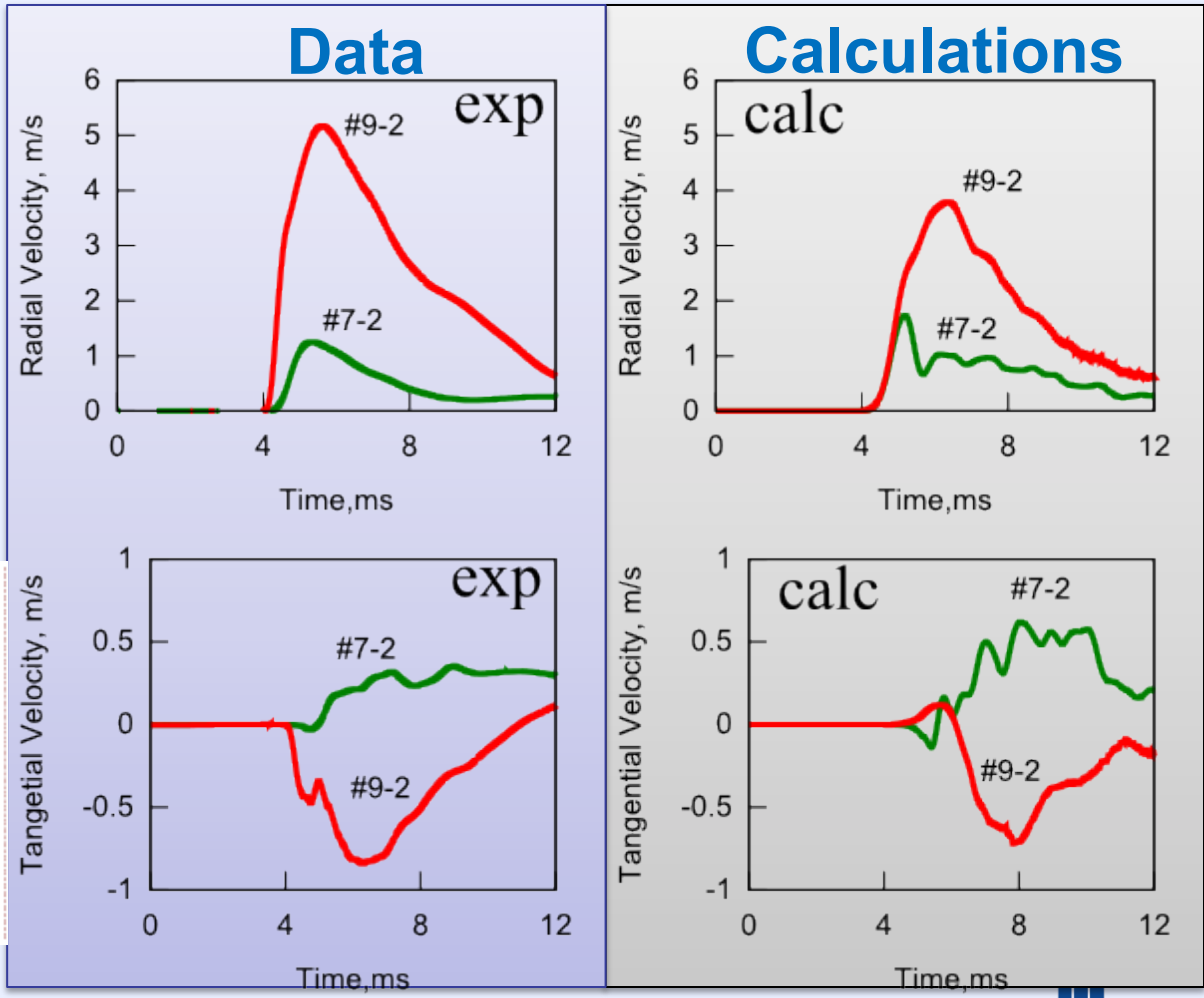

We have employed a continuum joint modeling to study effects of joint orientations and gravity

DISCRETE JOINT

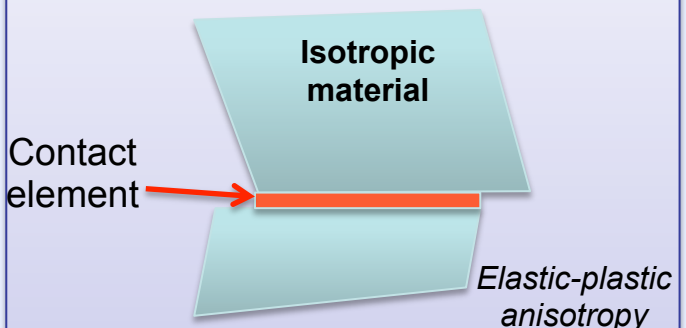

- **Nonlinear normal compliance**
- **Coulomb friction**
- **Valid for large slips and separations**

Bigger domains, more runs

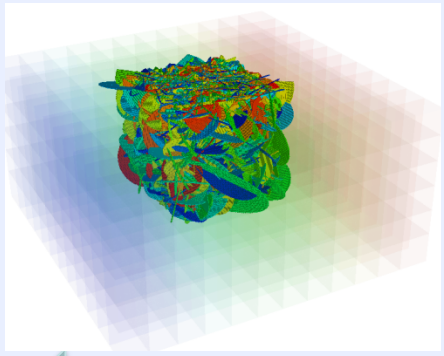

verify

CONTINUUM JOINT

- **No compliance**
- **Coulomb friction**
- **Small deformations**

plastic anisotropy

Both discrete and continuum joint models assume that the joint spacing is bigger than the element size

Discrete and continuum joint methods produce similar results where the flow is controlled by plasticity (2D)

CONTINUUM

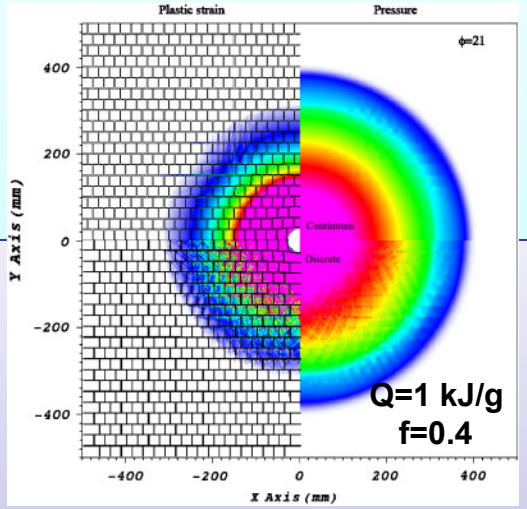

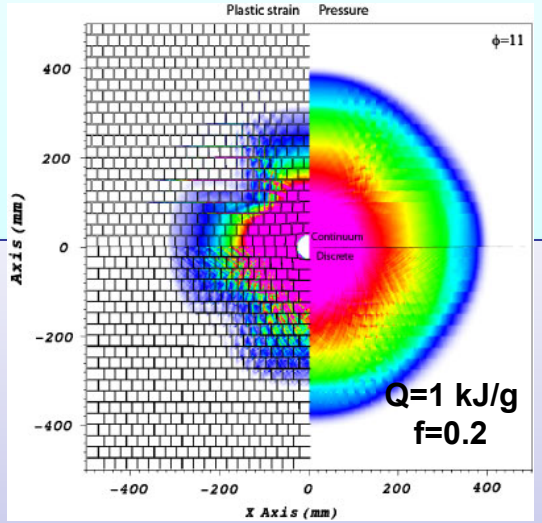

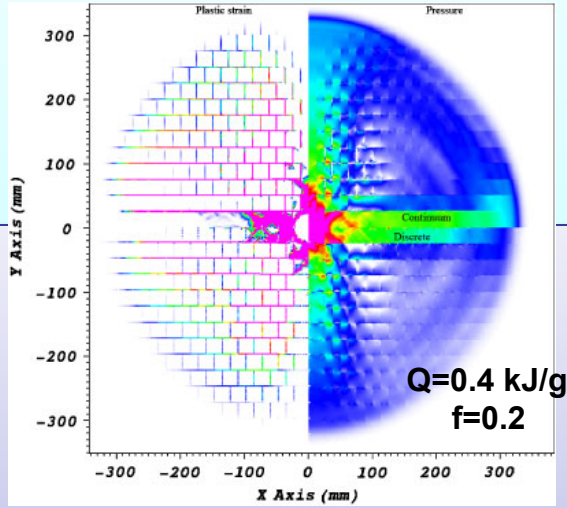

DISCRETE

Discrete and continuum methods show similar results (3D)

Explosion in hard rock with three Cartesian sets of joints

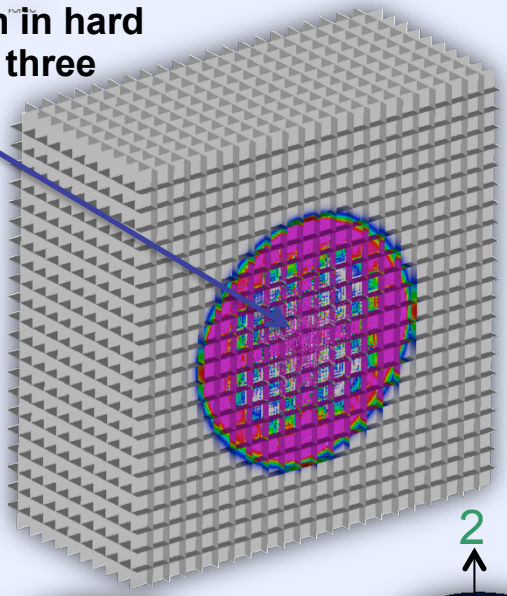

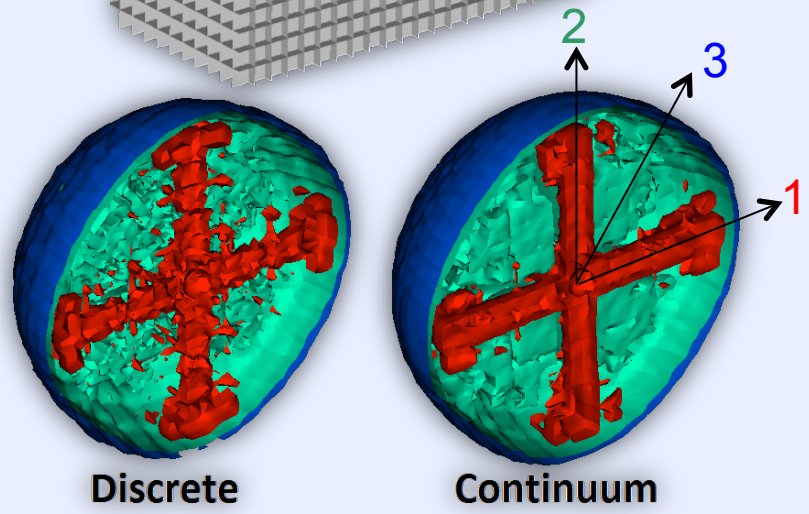

Pressure contours (0-50 MPa)
Joint spacing 1 m, friction ~0.2

Discrete joint representation

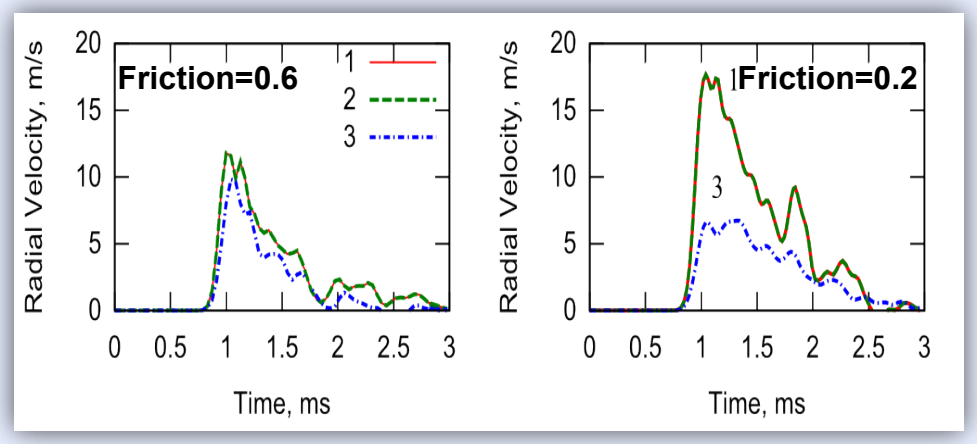

Continuum joint representation

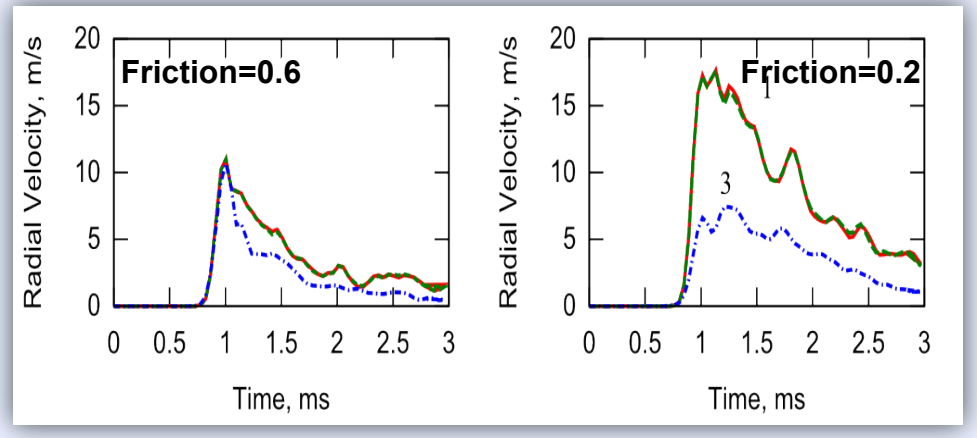

Dependence on joint friction

Material tensile strength affects the vertical velocity calculated at the surface

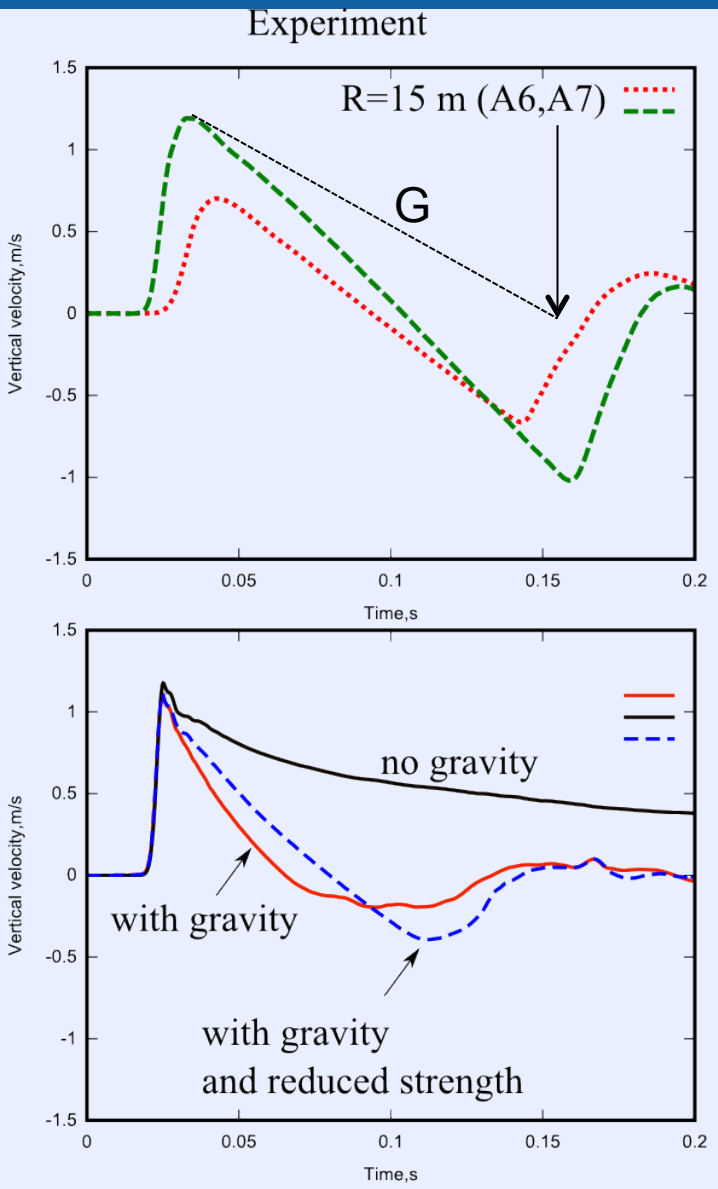

Calculation set up with gravity

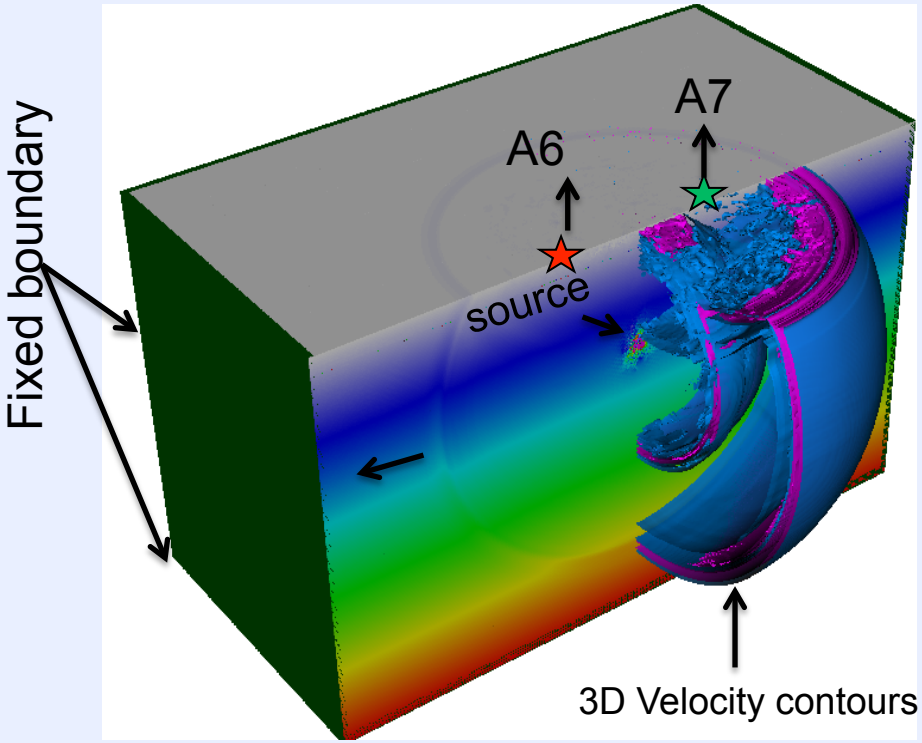

Continuum model with gravity provides reasonable agreement with the surface measurements in SPE3

Continuum joint model, 600mx600mx300m domain, 834 CPU, 6 hours

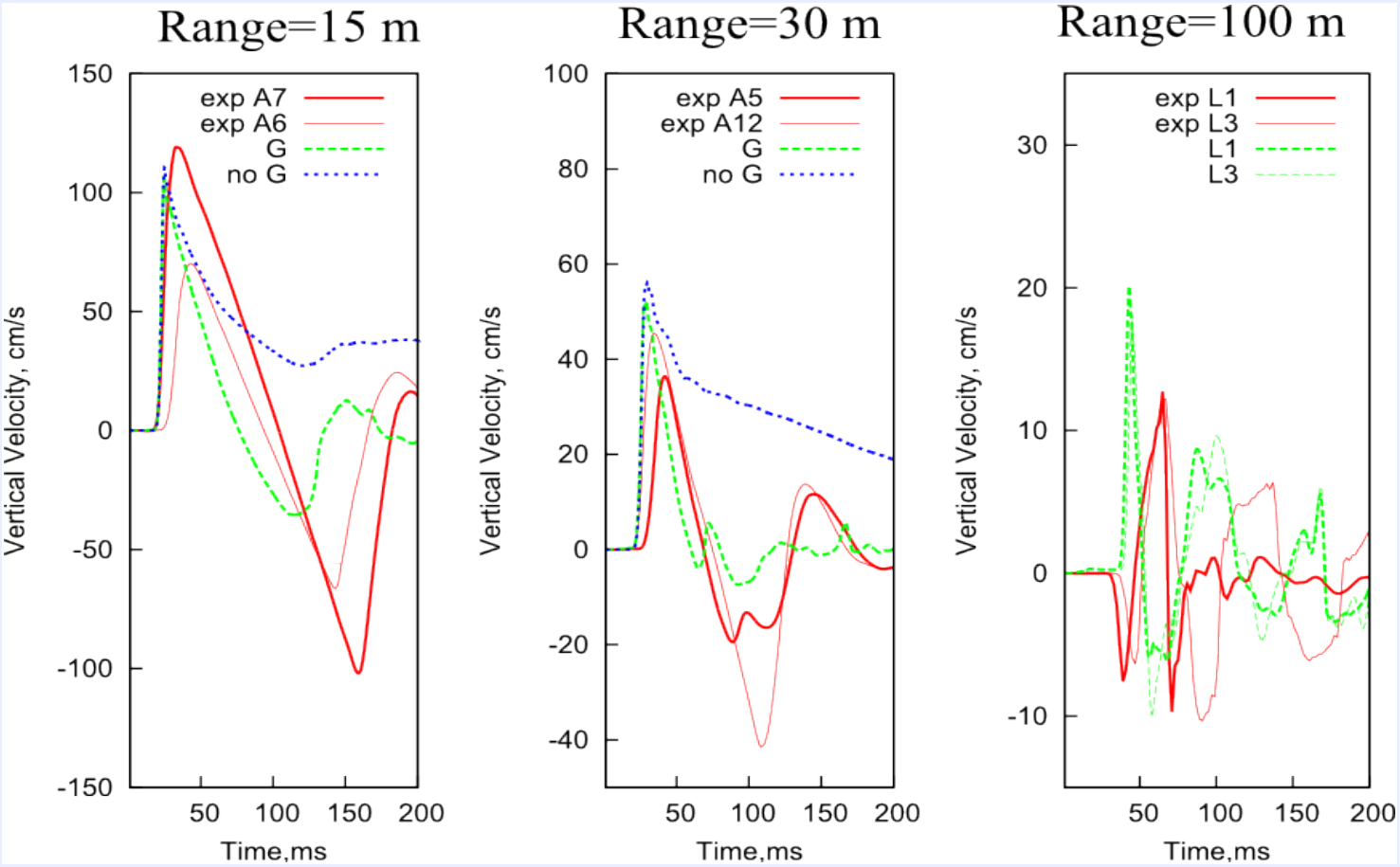

We expect similar near field velocities in SPE4 as in SPE1 with less damage near the surface

Plastic Slip at the joints

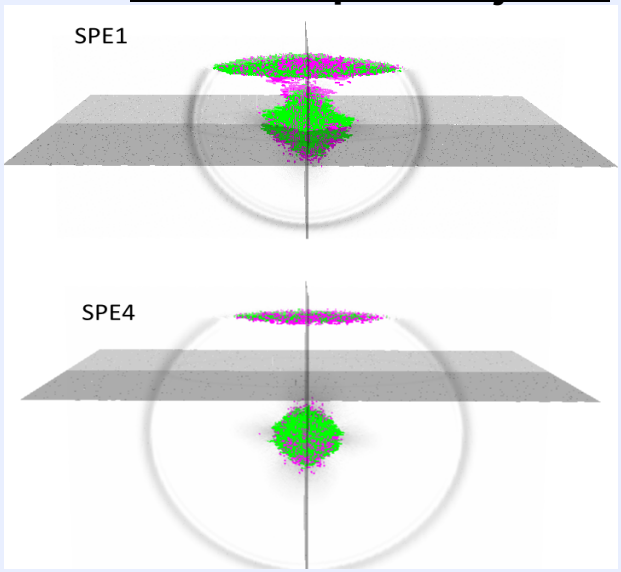

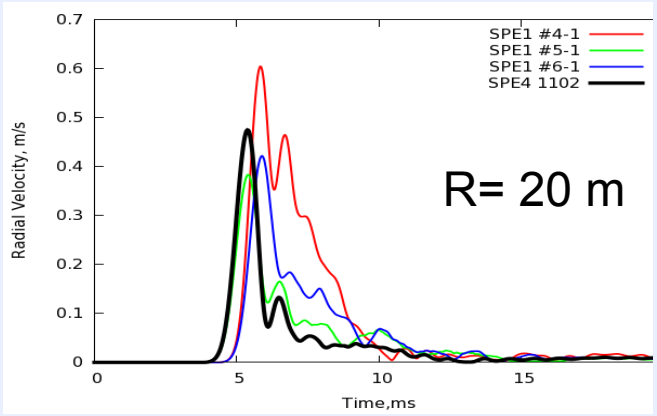

Calculated surface motion (SPE1 vs SPE4) the model is calibrated for SPE3 data first

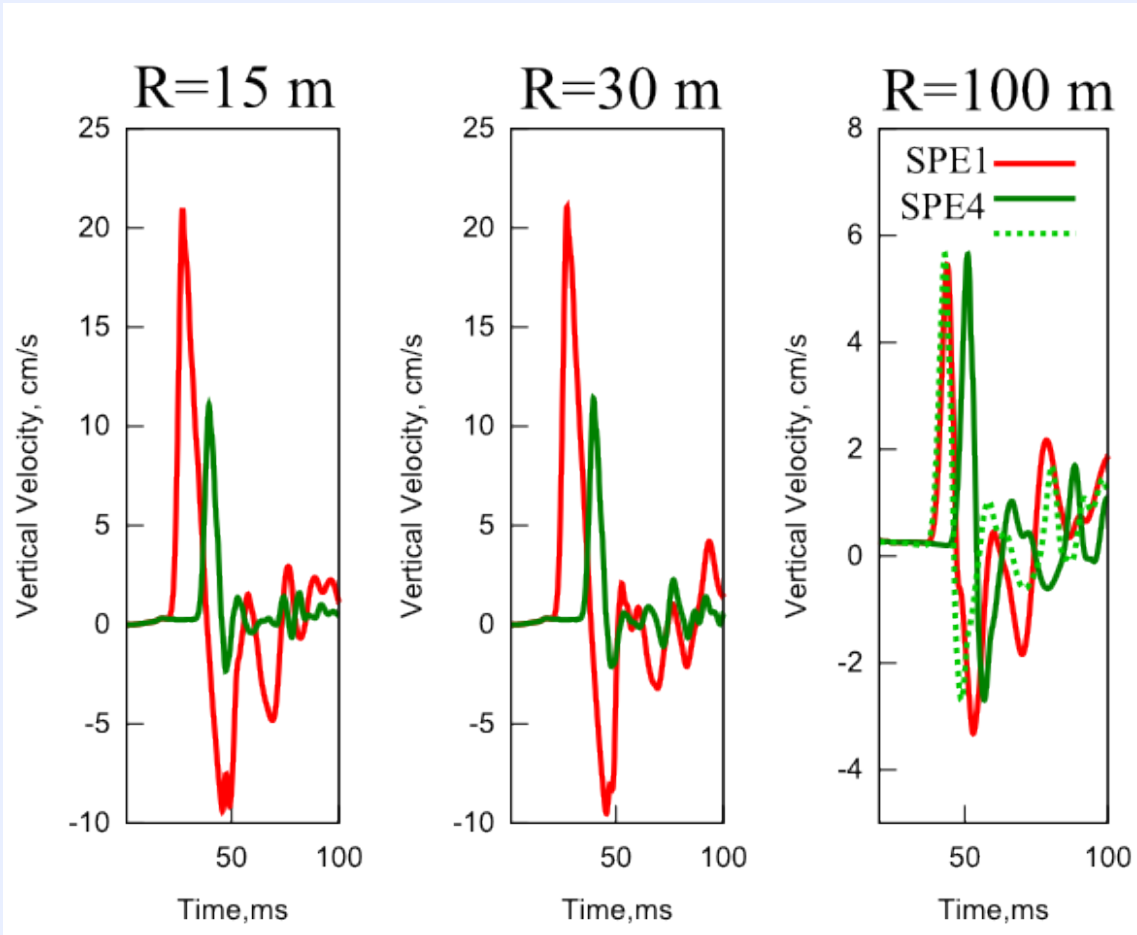

Conclusions

- Vertical Joints can cause significant horizontal motion comparable with that observed in the SPE experiments
- Both joint spacing and friction angle affect the amount of produced shear motion.
- The higher the friction, the shorter and more delayed is the pulse of the shear wave.
- By controlling the joint friction and spacing in a reasonable interval one can describe shear waves that correlate with larger than expected P-wave motion.
- Gravity is important to model the vertical velocity as well as the radial velocity near the surface

Effect of joint friction

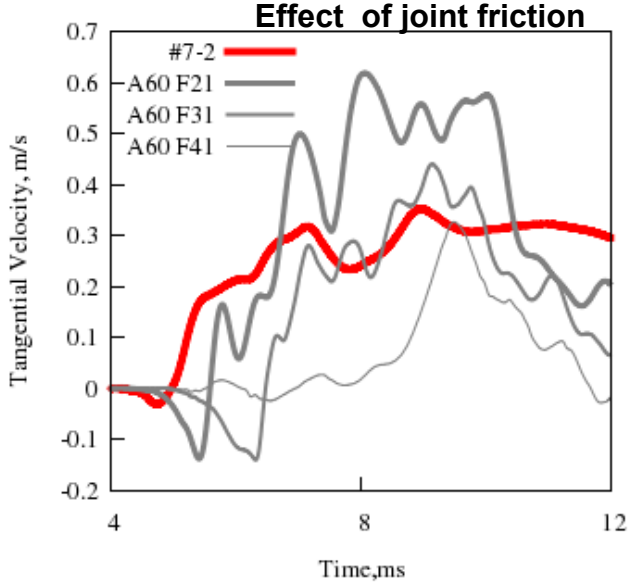

Tangential motion cased by one set of joints

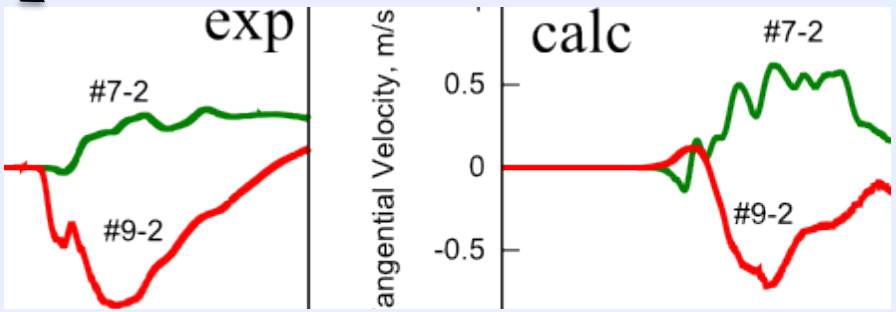

For more information:

Oleg Vorobiev

vorobiev1@llnl.gov

925-423-5151

Auspices

This work was partially performed under the auspices of the U.S. Department of Energy by Lawrence Livermore National Laboratory under Contract DE-AC52-07NA27344.

Disclaimer

Lawrence Livermore
National Laboratory

2D:Transverse and radial motion at 10 and 20 m ranges for 60-70 degree angles

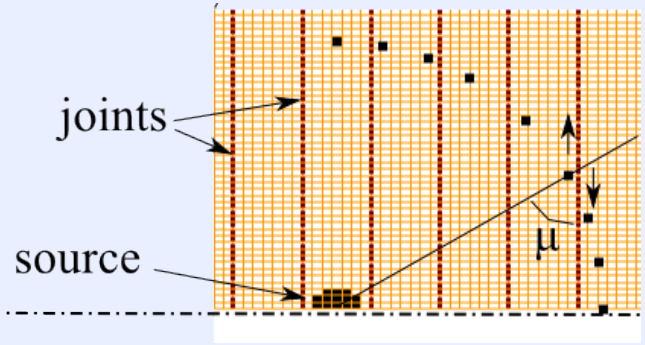

Joint spacing ~2.5 m
Friction angle ~30 deg

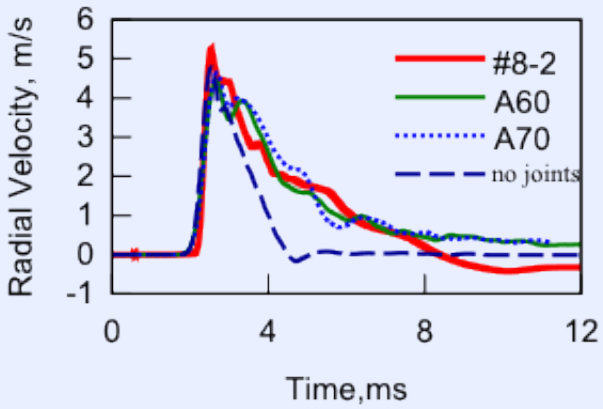

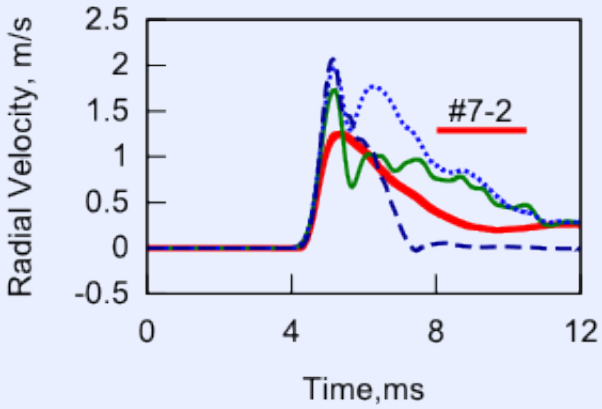

The joints can explain not only tangential motion but also wider radial displacements due to energy redirection (some azimuthal directions will have more and the other ones less energy)

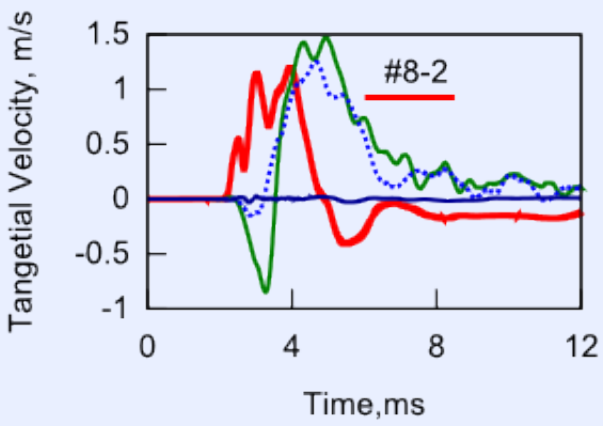

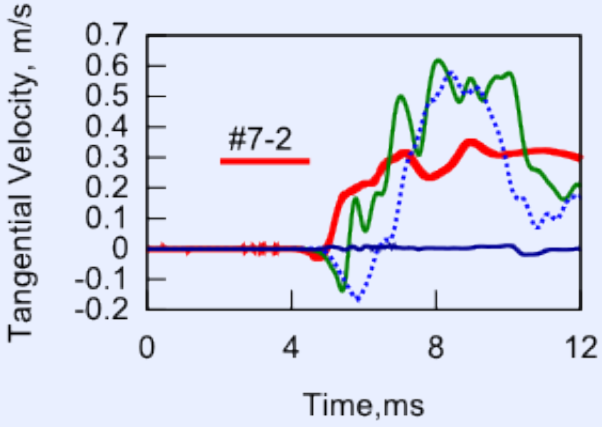

Increasing friction delays the shear motion and makes shear pulse shorter

#7-2, R=20 m

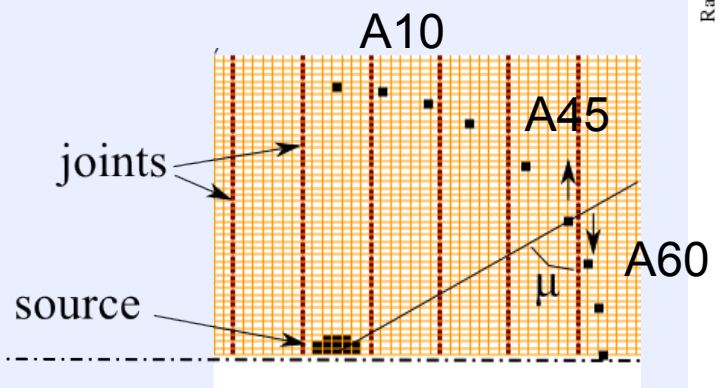

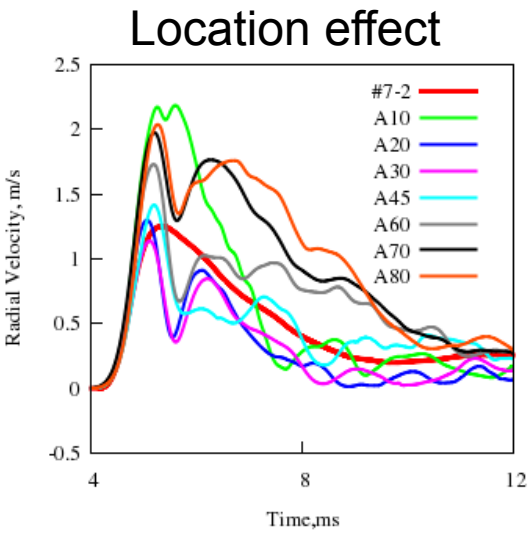

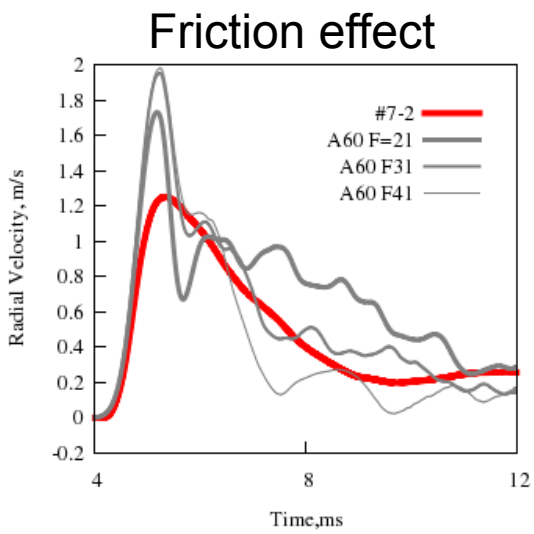

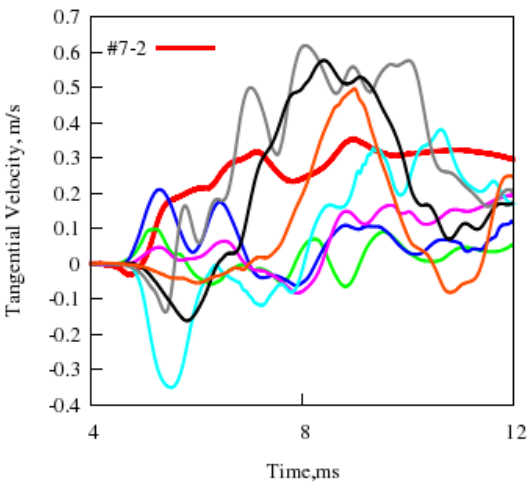

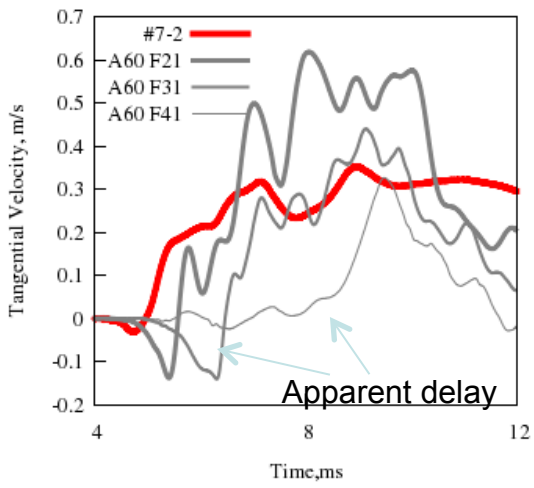

Gravity does not affect velocity histories at R < 20 m

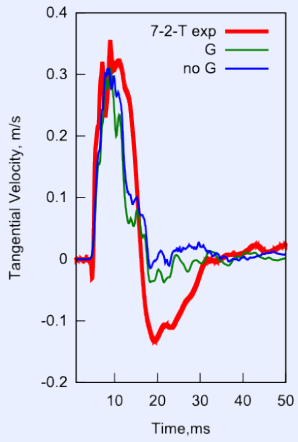

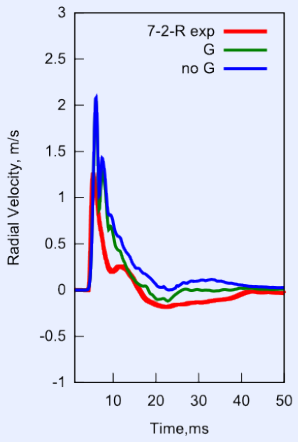

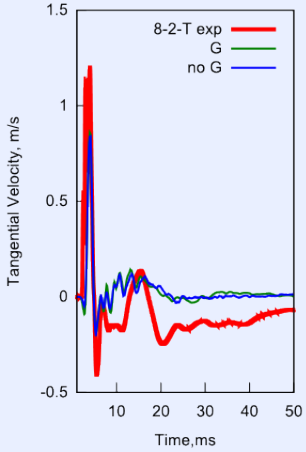

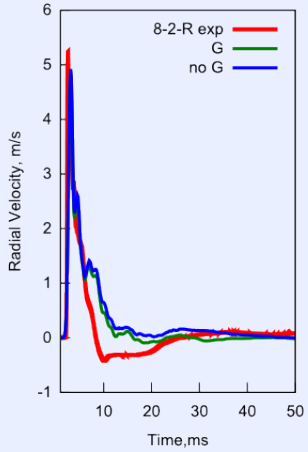

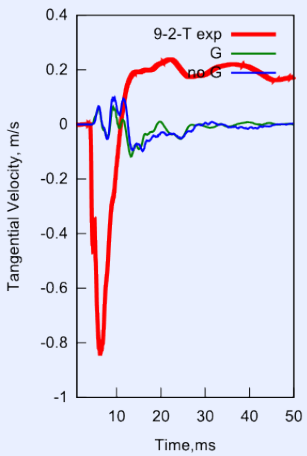

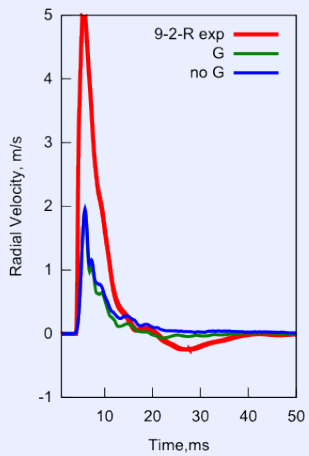

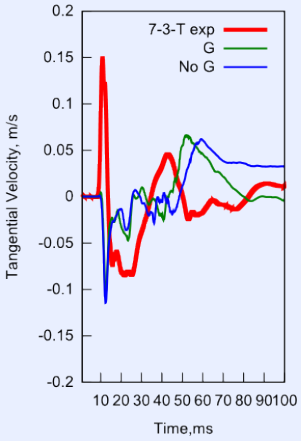

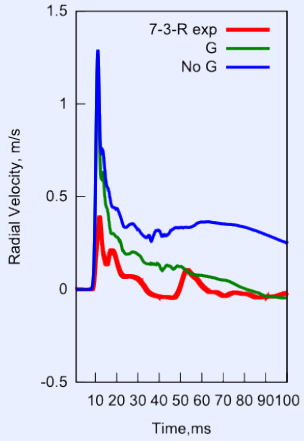

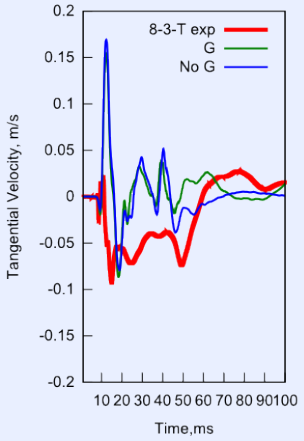

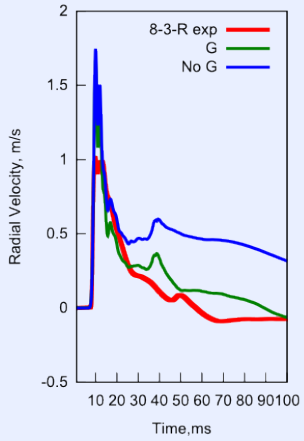

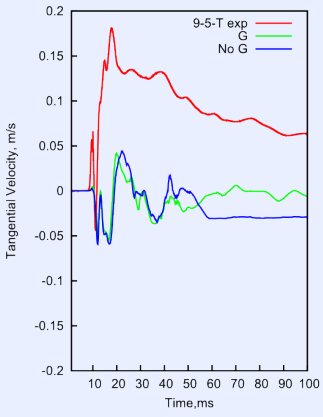

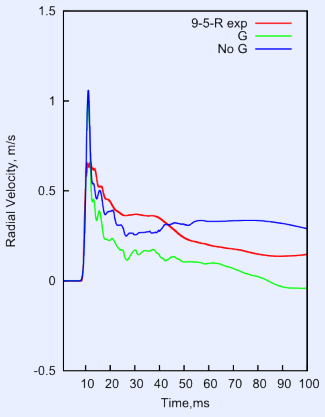

Generation of horizontal shear motion by vertical joints

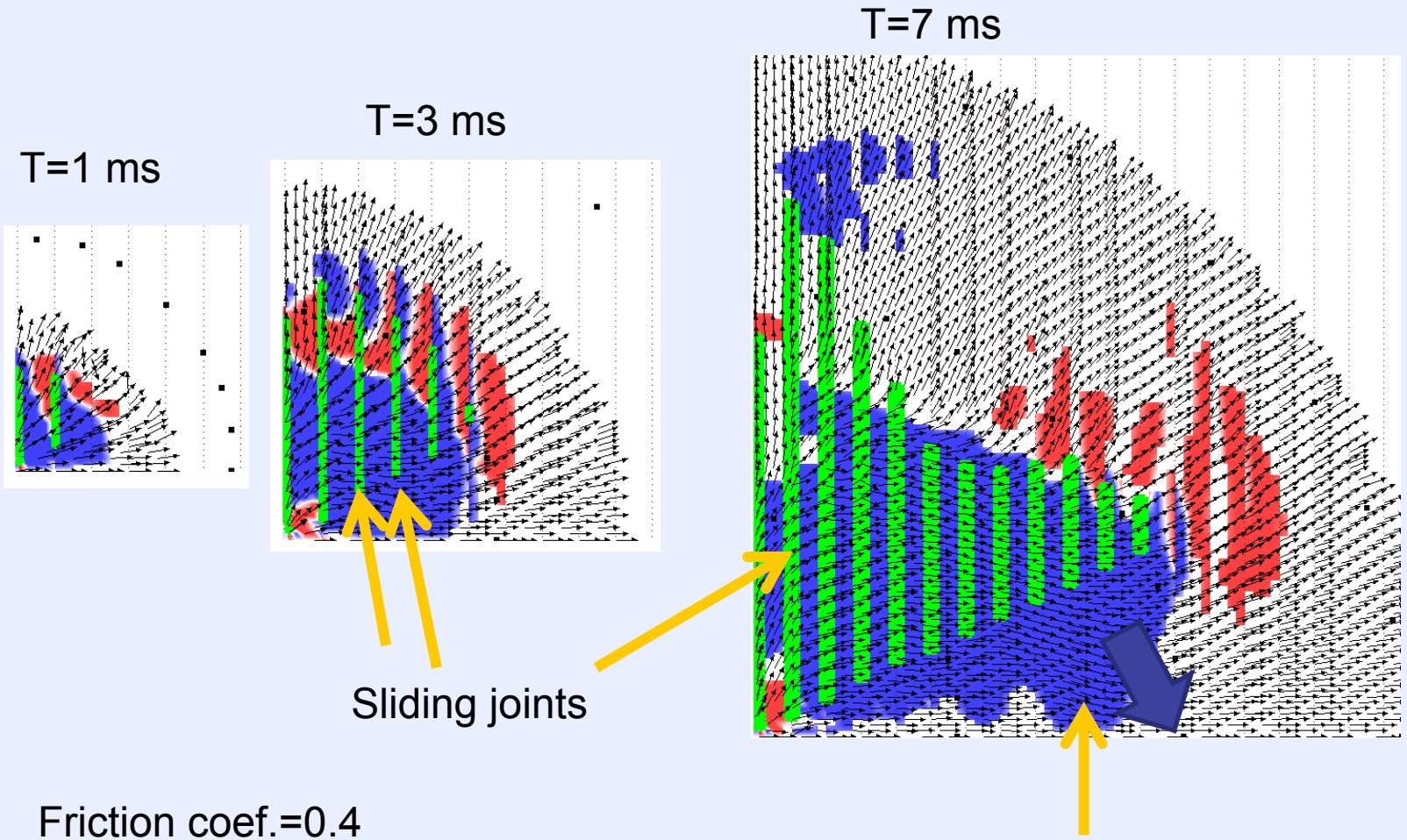

Friction coef.=0.4

Pressure and velocity iso-surfaces for SPE4 explosion simulation (cross-section)

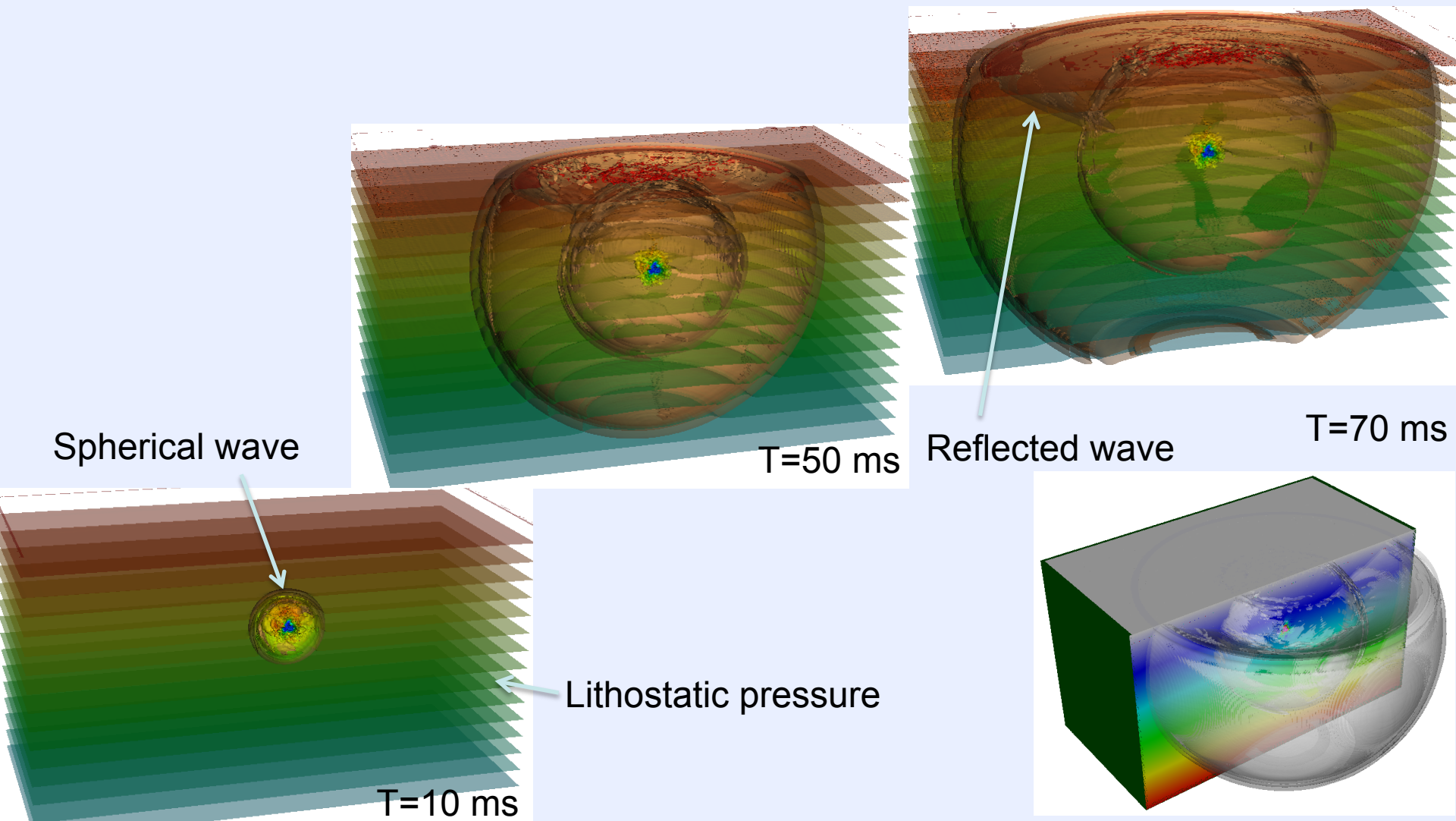

Joint model has been validated for dynamic conditions

Polished joint in Limestone loaded by a shock wave

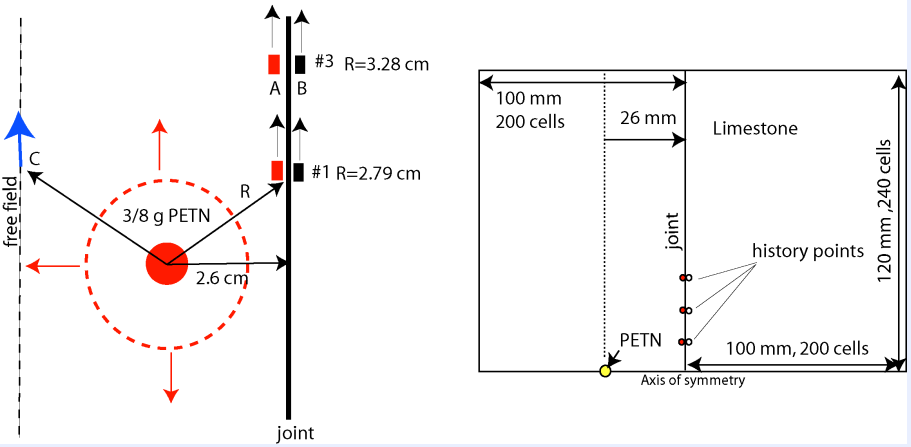

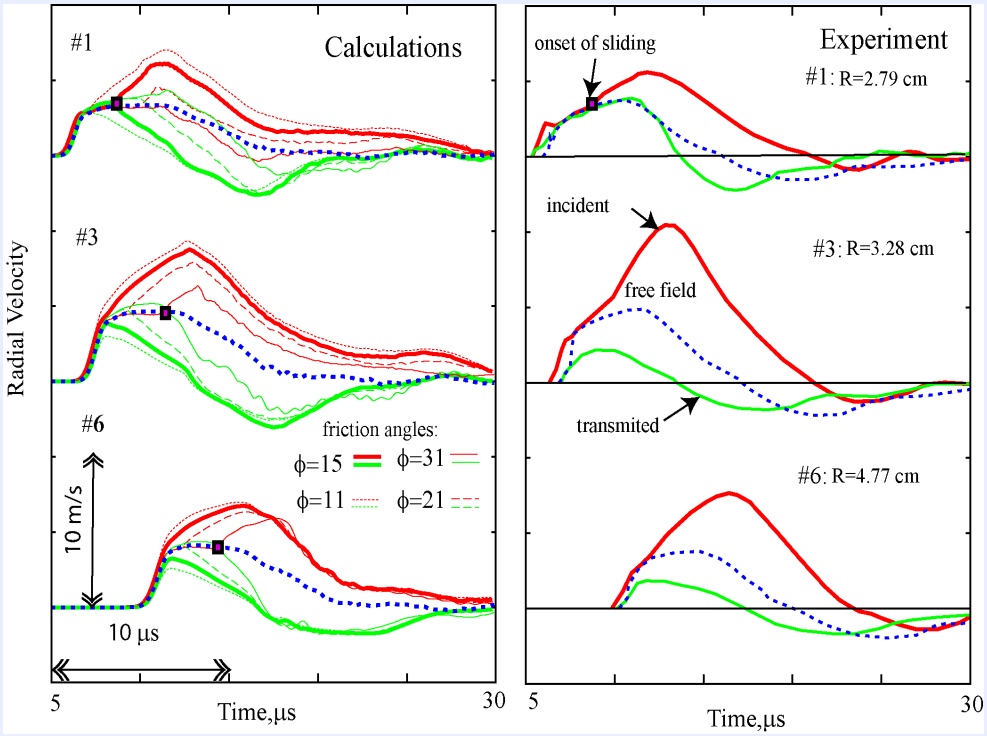

Vorobiev, O.Yu.,(2010),"Discrete and continuum methods for numerical simulations of non-linear wave propagation in discontinuous media", *International Journal for Numerical Methods in Engineering*,83,482-507

Joint model has been validated for quasi-static conditions

Shear test simulation

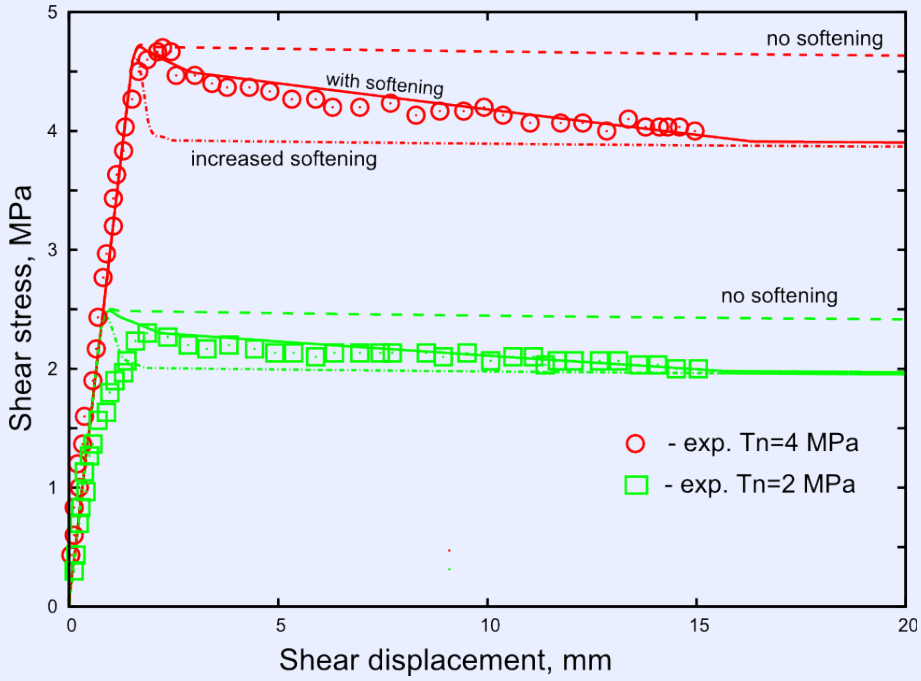

Joint softening effect

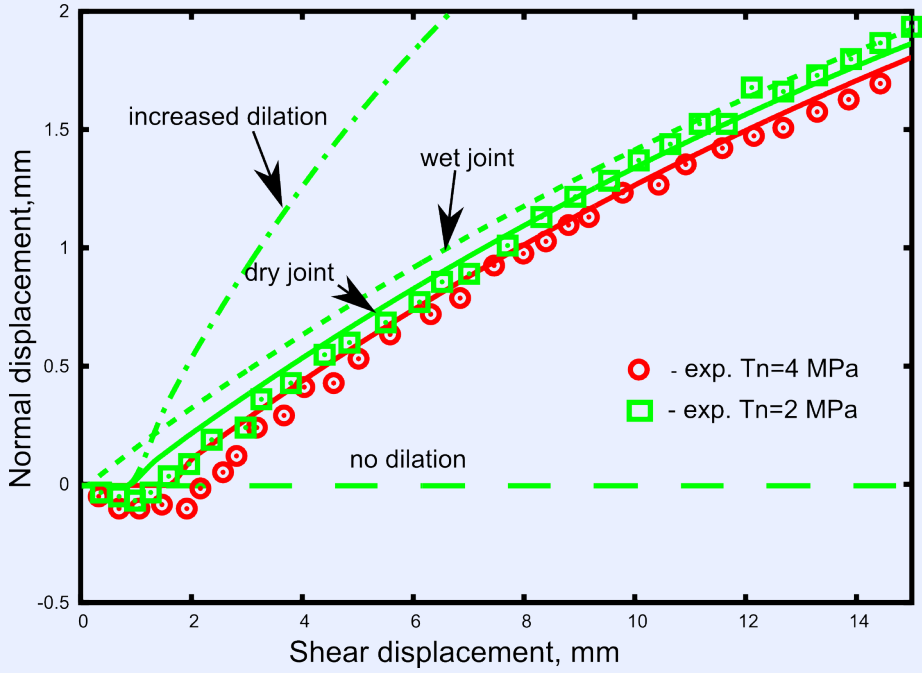

Nonlinear dilatancy